Effects of human neuraminidase and multivalent glycoconjugates on CD22 organization

by

Hanh-Thuc Ton Tran

A thesis submitted in partial fulfillment of the requirements for the degree of

Doctor of Philosophy

Department of Chemistry
University of Alberta

Abstract

The human immune system is a network that is crucial to fight against infections and foreign pathogens. It is divided into innate system, which is the first line of defense, and adaptive immune system, which is more specific. The specificity and long-lasting nature of the adaptive immune system is dependent on the clonal expansion of lymphocytes, T cells and B cells, after exposure to pathogens. However, complications can occur when the adaptive immune system is compromised, leading to conditions such as rheumatoid arthritis, lupus, asthma, and immunodeficiency. Therefore, tight control of these systems is necessary, and cellular receptors are partly responsible for this control. Moreover, understanding how to manipulate the immune system may allow us to develop new therapeutics, or overcome immune-incompatibility in transplantation. In this thesis we explore the use of glycoconjugates to alter the organization of immune receptors. We were interested in studying B cell receptors which recognize glycans, such as the well-known negative regulator of BCR, CD22. Although the function of CD22 is well known, its organization and mechanism are poorly understood. CD22 binds to α2,6-sialosides and is basally masked by cis-ligands on the same cell surface, making interactions with trans-ligands more difficult and require high-affinity ligands. We tested the ability of multivalent displays of CD22 ligands along with and specific antigens to BCR to co-cluster these receptors. We selected B cells expressing BCR which recognize human blood group antigen structures. We observed that these ligands could co-cluster CD22 and BCR on cells.

We also investigated the role of native enzymes in the organization of CD22 receptors on cultured B cells. We hypothesized that neuraminidase (NEU) enzymes, which cleave terminal sialic acids that may act as cis ligands for CD22, could have a role in regulating receptor organization and dynamics. We used confocal microscopy to visualize and quantitate CD22

clustering on individual cells. We confirmed that NEU enzymes had a role in organizing CD22 receptors on the cell membrane, and both NEU1 and NEU3 were found to influence the size and lateral mobility of CD22 clusters.

Preface

Chapter 3 is a collaborative work among members of Dr. Christopher Cairo's group. The glycoconjugates were synthesized by Dr. Gour Dashkhan, and the confocal microscope experiments were performed by Hanh-Thuc Tran. Portions of this work are published in:

Dashkhan, G. C., Tran, H. T., Meloncelli, P. J., Lowary, T. L., West, L. J., and Cairo, C. W. *Bioconjugate Chem*. 2018, 29, 2, 343-362.

Chapter 4 is also a collaborative work among members of Dr. Christopher Cairo's group. The neuraminidase enzymes were made by Cecilia Zou, the mass spectrometry experiment for glycolipid analysis was conducted by Radhika Chakraberty, neuraminidase inhibitors were synthesized by Dr. Tianlin Guo, and other experiments, including confocal microscope, single-particle tracking, western blots, Ca^{2+} flux, were performed by Hanh-Thuc Tran. Portions of this work are included in:

Tran, H-T.; Li, C.; Chakraberty, R.; Cairo, C. W. NEU1 and NEU3 enzymes alter CD22 organization on B cells. *Biophys. Rep.* **2022**, 2(3).

Acknowledgement

Finishing my thesis has been an amazing milestone, which would not have been possible without the support of, encouragement from, and interactions with so many great individuals and groups that I have encountered during my time at the University of Alberta.

First and foremost, I am extremely grateful to my PhD supervisor, Dr. Christopher Cairo. Thank you Dr. Cairo for accepting me into your research group and continuously supporting me throughout my years in graduate school. Your patience and guidance have helped me become a better researcher and person. I am forever indebted to you.

I am extremely thankful for my supervisory committee members, Dr. Ratmir Derda and Dr. Johnathan Veinot, for their support, guidance, and suggestions during my PhD. It was really helpful discussing the status and direction of my research with them.

In addition, I would like to thank my fellow group members, both past and present. You guys always have been available for advice, help, and friendship. I am especially thankful for your help during my early years of graduate school when I desperately needed help to get started with my research. I would like to especially thank Dr. Amran Howlader for his guidance using his extensive knowledge and experience, Radhika Chakraberty for endless mental support and friendship, and Dr. Gour Dashkhan for our collaborative work.

I also would like to thank all the staff in the Department of Chemistry for their assistance over the years: Gareth Lambkin for his guidance and access to his instruments, the Machine Shop staff, Anita Weiler, Dr. Yoram Apelblat, Ryan Lewis. I would also like to thank all the staff at the FlowCore facility and Molecular Biology facility for giving me access to their instruments.

Last but not least, I am grateful for my partner, family and friends' encouragement and mental support during my most difficult times of graduate school when I thought I could not go

any further. I could not be where I am and who I am today without them. I am also thankful for the new friends I have made in graduate school. They have made my time here a lot more enjoyable and unforgettable.

Table of Contents

List of Figures

List of Tables

List of Abbreviations

ADF	Actin depolymerizing factor
ADP	Adenosine diphosphate
AF-488	Alexa fluor 488
AF-647	Alexa fluor 647
AGP	Alpha-1 acidic glycoprotein
APC	Antigen presenting cells
ATP	Adenosine triphosphate
BCR	B-cell receptors
BPA-Neu5Ac	methyl-α-9-*N*-(bipheynyl-4-acetyl)-amino-9-deoxy-Neu5Ac
BPC-Neu5Ac	methyl-α-9-*N*-(bipheynyl-4-carbonyl)-amino-9-deoxy-Neu5Ac
CD20	Cluster of differentiation-20
CD22	Cluster of differentiation-22
CytoD	*Cytochalasin D*
DMSO	Dimethyl sulfoxide
DNP	2,4-dinitrylphenyl
EGF	Epidermal growth factor
ELISA	Enzyme-linked immunoassay
FCS	Fluorescence correlation spectroscopy
FPR	Fluorescence photobleaching recovery
FPS	Frames per second
FRAP	Fluorescence recovery after photobleaching
Gal9	Galectin-9

GH	Glycosyl hydrolase
GPI	Glycosylphosphatidylinositol
GT	Glycosyl transferase
GUV	Giant unilamellar vesicles
HBSS	Hank's balanced salt solution
HRP	Horse radish peroxidase
ICAM-1	Intercellular adhesion molecule-1
IL-6	Interleukin 6
ITAM	Immunoreceptor tyrosine activator
ITIM	Immunoreceptor tyrosine-based inhibitory motif
KD	Knockdown
LacCer	Lactosylceramide
LAMP-1	Lysosome associated membrane protein 1
LatA	*Latrunculin A*
LFA-1	Lymphocyte function-associated antigen-1
LPS	Lipopolysaccharide
LSCM	Laser scanning confocal microscopy
MAL	*Maackia amurensis* lectin
MSD	Mean squared displacement
MTOC	Mitochondrial organizing center
NA	Numerical aperture
NanI	Neuraminidase from *Clostridium perfringens*
NEU	Neuraminidase

NEU1	Neuraminidase 1
NEU2	Neuraminidase 2
NEU3	Neuraminidase 3
NEU4	Neuraminidase 4
PAA	Polyacrylic acid polymer
PALM	Photoactivated localization microscopy
PBS	Phosphate-buffered saline
PFA	Paraformaldehyde
PLL	Poly-L-lysine
PNA	Peanut agglutinin
rGal9	Recombinant galectin-9
scRNA	Scrambled RNA
LC-MS	Liquid chromatography – mass spectrometry
SDS-PAGE	Sodium dodecyl-sulfate polyacrylamide gel electrophoresis
SH2	Src-homology 2
siaAU	Sialidase of *Athrobacter ureafaciens*
Siglec	Sialic-acid binding immunoglobulin-like lectin
SIM	Structured illumination microscopy
SNA	*Sambucus nigra* agglutinin
SPT	Single-particle tracking
STED	Stimulated emission microscopy
STORM	Stochastic optical reconstruction microscopy
TBST	Tris buffered saline with tween (0.1% Tween)

TCR	T-cell receptor
TIR	Total internal reflection
TIRFM	Total internal reflection fluorescence microscope
TTR	Transthyretin

CHAPTER 1. BIOLOGICAL MEMBRANE ORGANIZATION AND CD22 ON THE B CELL MEMBRANE

1.1 BIOLOGICAL MEMBRANES

1.1.1 The fluid mosaic model

Cellular membranes are important not only as a physical barrier, but also for selective permeability, transport, cell recognition, communication, signalling, and attachment. In 1972, Singer and Nicolson proposed the Fluid Mosaic Model of cellular membranes,[1] which stated that biological membranes are dynamic and are composed of a phospholipid bilayer with lipids and proteins embedded within the membranes. The formation of the phospholipid bilayer is thermodynamically driven by non-covalent hydrophilic and hydrophobic interactions; the phospholipids' fatty acid tail groups of both layers turn toward each other, maximizing hydrophobic interactions and sequestering themselves from the aqueous environment while the polar "head" group is exposed to its surrounding. Other components of the cellular membranes, cholesterol, proteins, and lipids are embedded in this bilayer and play important roles in cellular integrity, recognition, and function. Lipids and proteins embedded in biological membranes are fluid; they diffuse freely within the plane of the membrane.[2] Cholesterol lipids are inserted in the bilayer and have an important function in cell membrane permeability, fluidity, and integrity.[3] Incorporation of cholesterol orders lipids and induces phase separation in cellular membranes. These are the concepts of classical fluid mosaic model of biological membranes. In the model, integral proteins diffuse laterally on the cell membrane by simple Brownian diffusion, with size and crowding may influence the diffusion characteristics. While this model partly explains the

behavior of membrane components, it continues to be revised to explain more complex membrane phenomena.

1.1.2 Saffman and Delbruck equation of Brownian motion

In the Singer and Nicolson Fluid Mosaic Model, biological membranes are thought of as a continuous, homogenous, and isotropic solvent with proteins embedded in the membrane governed by simple Brownian motion.[4] The Brownian motion of particles can be described by freely diffusing particles in gas or liquid medium with frequent random bombardments and random fluctuations in positions. The Stokes-Einstein equation (Eq. 1), where D is the diffusion coefficient, k is Botzmann's constant, T is the absolute temperature, η is the viscosity, and r is the radius of the particle, relates the diffusion of a spherical particle to the viscosity of the medium at low Reynold's number, at which the flow is dominated by laminar flow.[5]

$$D = \frac{kT}{6\pi\eta r} \text{ (Eq. 1)}$$

In 1975, Saffman and Delbruck devised an equation to measure the size of an integral membrane protein from its diffusion coefficient (Eq. 2), where D is diffusion, κ_B is Botzmann's constant, T is absolute temperature, η_m is membrane viscosity, h is membrane thickness, L is Saffman-Debruck length (Eq.3), γ is the Euler-Mascheroni constant (0.5772), and η_f is bulk fluid viscosity. From their hydrodynamic model, Saffman and Delbruck suggested that the lateral diffusion of an integral protein is only weakly dependent on the cross-sectional size of an integral membrane protein by a logarithmic relationship.[6]

$$D = \frac{k_B T}{4\pi\eta h}[\ln(\frac{2L}{a}) - \gamma] \text{ (Eq. 2)}$$

$$L = \frac{h\eta_m}{2\eta_f} \text{ (Eq. 3)}$$

In the Saffmnan-Delbruck model, it is assumed that the lipid medium in which these proteins are embedded is continuous and flat over long distances, essentially a two-dimensional medium. However, the cell membrane is a heterogenous medium, which is not perfectly flat or continuous due to multiple factors, including varying sizes of the lipid chains.[7] A number of studies have since tested the Saffman-Delbruck model. These studies have found that the diffusion of an integral protein is dependent on the height of the membrane, where the diffusion is fastest if the hydrophobic region of the protein is similar to the height of the membrane. Moreover, the diffusion of the integral protein was found to fit better to a 1/R relationship, where R is the radius of the protein.[1–3] Therefore, a more comprehensive models which take into account the heterogeneity of biological membranes was needed.

1.1.3 Updated model of biological membranes

The simple model of fluid mosaic model proposed by Singer and Nicolson in 1972 is still useful in describing aspects of biological membranes.[8,9] However, with the emerging techniques for measuring particle diffusion on the membrane, observations of protein diffusion differ from predictions of freely diffusing protein in a mosaic model.[10,11] The first studies on protein diffusion using fluorescence photobleaching recovery (FPR) microscopy[4,5] showed 5- to 50-times slower diffusion rates of proteins in cellular membranes compared to freely diffusing proteins in model membranes, and this was proposed to be due to the presence of hierarchy of membrane organization.[12] Additionally, using the same method, Veatch & Golan's study on band 3 protein on human erythrocyte membrane showed similar results in which the changes in diffusion coefficient of this reversible and it is dependent on the stability of the cytoskeletal structure.[6] They also showed that this method was also useful for studying mobilities of phospholipid and cholesterol on membrane, which were found to depend on the concentration and crowding by

neighboring proteins.[6,7] Kusumi et. al., have proposed three levels of this hierarchy: restrictions by an underlying cytoskeleton structure ("picket and fencing"), raft domains, and dynamic protein complexes.[13] Interestingly, single-particle tracking studies have allowed researchers to determine different modes of protein diffusion including: stationary, simple Brownian diffusion, directed diffusion, confined diffusion, and harmonic-like diffusion modes.[14] Integral proteins reside in these domains temporarily, on average for 25 seconds, and can escape from one domain to another, giving rise to microscopic and macroscopic diffusion coefficients;[15] the microscopic diffusion coefficients measure the rapid free lateral diffusion of proteins within a domain while macroscopic coefficient measures the long-range diffusion of the proteins.[16] The microscopic (D_{micro}) and macroscopic (D_{macro}) diffusions of proteins can be calculated based on mean-square displacement (MSD) equation (**Eq. 4**),[8] in which D is the diffusion coefficient and t is time. For D_{mciro}, MSD measurements of shorter time is taken and α is assumed to be 1, while in D_{macro} calculations the longer segments are used. The residency time of the proteins in compartments depends on their oligomerization state,[17,18] implying the importance of this type of membrane organization for cellular mechanisms. Protein aggregation has been found to depend on the hydrophobic mismatch, protein shape, and membrane curvature.[19] Although the hierarchal-organization model of plasma membranes is still controversial, the model provides enhanced collision and reaction rates, spatial regulation for the collisions, and specialized domains on biological membrane.[20] From these and other studies, it is clear that diffusion in plasma membranes is substantially more complex than the original fluid mosaic model, and it is likely that this complexity is important for the organization, distribution, mobility, and aggregation of integral membrane proteins.

$$MSD = 4Dt^{\alpha} \quad \text{(Eq. 4)}$$

1.1.4 CFG nomenclature

CFG nomenclature is commonly used to represent glycans (Table 1.1). In this nomenclature, same type of sugars have the same shape, specifically, circle represents hexose, square represents *N*-acetylhexosamine, divided square represents hexosamine, triangle represents fucose, and diamond represents acidic sugars. In the same class of sugar, isomers are further differentiated using different colors: yellow for galactose, blue for glucose, green for mannose, and red for fucose. For diamonds of acidic sugars, purple is Neu5Ac, light blue is NeuGc, yellow left segment is Gal, and green right segment is Man.

Name	Symbol	Abbreviation	Structure
Glucose		Glc	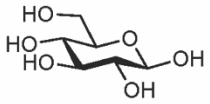
Mannose		Man	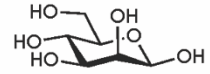
Galactose		Gal	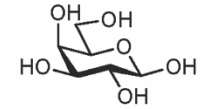
N-acetylglucosamine		GlcNAc	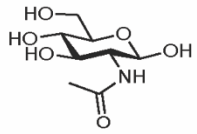
N-acetylmannosamine		ManNAc	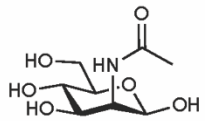
N-acetylgalactosamine		GalNAc	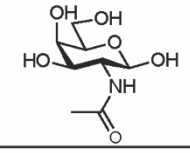
Glucosamine		GlcN	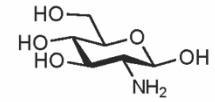
Galactosamine		GalN	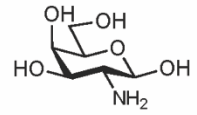
Fucose		Fuc	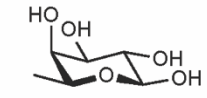
N-acetylneuraminic acid		Neu5Ac	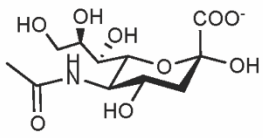

Table 1.1. CFG nomenclature

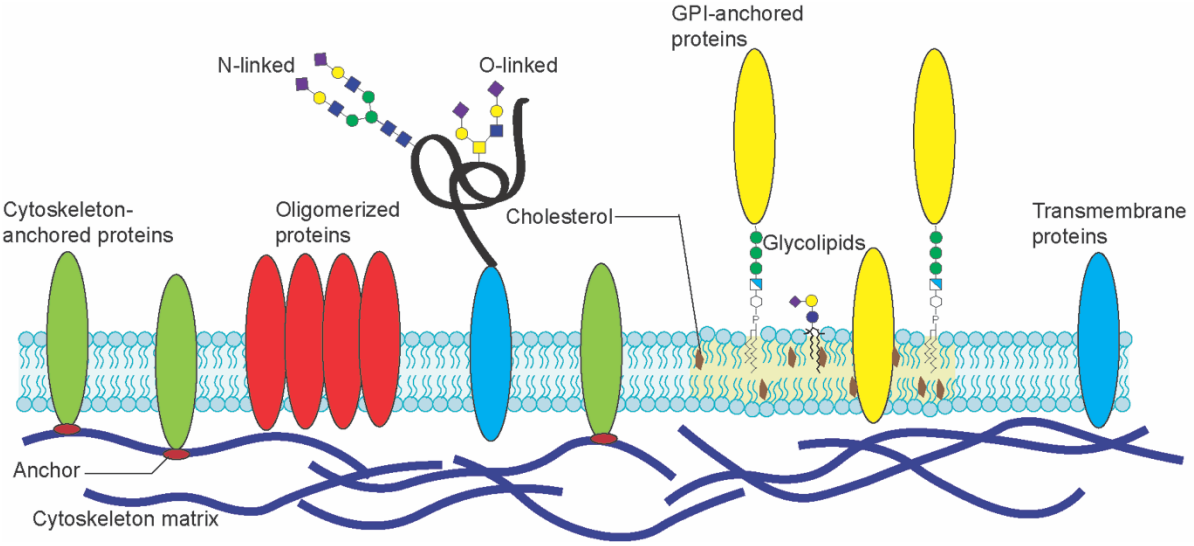

Figure 1.1. A revised model of the plasma membrane. It contains features that influence protein and lipid organization and mobility, including attachment to cytoskeleton (green), oligomerization of proteins (red), residence in membrane domains (yellow), and confinement by other immobile proteins (blue). The glycans were drawn according to the CFG nomenclature.[9,10]

1.1.5 Membrane skeleton-fence model

The cytoskeleton, which underlies and interacts with biological membranes, has important functions in endocytosis, cell division, transport, motility, transmission, adhesion, and cell morphology.[21] The cytoskeleton consists of three major types of proteins: tubulin, actin, and intermediate filaments.[22] Actin is the most dynamic type of filament in the cytoskeleton network, and it exists as globular monomer state (G-actin) or polymer state (F-actin).[23,24] At physiological conditions, G-actin forms a dimer or trimer, which then polymerizes to right-handed helical F-actin with the length of 6-7 μm. F-actin is polarized due to the polarized state of G-actin monomers, with the positive (+) end containing high ATP and undergoing a fast rate of polymerization while the negative (-) end contains high ADP and undergoes disassembly with the help of depolymerizing proteins such as actin-depolymerizing factor (ADF)/cofilin. Actin can form the

actin cortex that is parallel to the plasma membrane (within less than 20 nm, and a thickness ~200 nm).[25,26] The actin cytoskeleton consists of a network of bundles and crosslinked filaments forming a mesh structure. Microtubules are another cytoskeletal structure, which are are larger in diameter and are more stiff as compared to actin. They are composed of α- and β-tubulins,[27] and are seeded by mitochondrial organizing centers (MTOC).[28] Microtubules and actin are linked either indirectly or directly with molecules that interact with both proteins.[29–31] Intermediate filaments are an important component of the cytoskeleton, which have a diameter of around 10 nm and a wide range of protein classes are responsible for forming these filaments; they are α-helix with non-helical structures at both ends.[32,33] Intermediate filaments can orient themselves along the actin and microtubules, and form the mesh network underlying cellular membrane. It is also important to note that other proteins that are not mentioned here are also important in forming cytoskeleton network.

Regulation of membrane and cytoskeleton is tightly controlled by regulatory proteins and adaptor proteins or complexes.[11] For example, spectrin and ankyrin are set of proteins that are associated on the cytoplasmic side of the plasma membrane and are important for tethering proteins and segregation of proteins into functional domains. Spectrins associates with ankyrin through spectrin-binding domain on ankyrin, and ankyrin is linked to a cytoplasmic domain of the membrane protein. Spectrin/ankyrin is involved in organizing specialized membranes; mutations in spectrin genes can lead to dislocations of their binding partners from appropriate sites on the membrane.[12] This complex has been shown to play a role in T-cell receptor (TCR) formation and activation. The spectrin/ankyrin complex directly binds to CD45, a membrane phosphotyrosine phosphatase that regulates TCR activation, which mobilize to T cell surface for activation of TCR.[13] It is also responsible for maintaining CD45-rich microdomains on the cell surface by

tethering the proteins to the underlying cytoskeleton structure. Moreover, the spectrin-ankyrin complex is also known to directly regulate the mobility of CD45 proteins by altering their contact with cytoskeleton.[14] Another example of adaptor protein in cytoskeleton structure is talin. Talin is important for integrins' conformational change that result in higher affinity state and activation that leads to increased adhesion, cell migration, platelet aggregation, and extracellular matrix assembly.[15] Talin associates with integrins and binds to F-actin and actin-binding proteins of the cytoskeleton structure, thus linking the integrin-based extracellular matrix and the cytoskeleton. The lymphocyte function associated antigen-1 (LFA-1) on T cells binds to intercellular adhesion molecule-1 (ICAM-1) and is responsible for T cell migration on endothelial cells.[16] Talin-1 is required for the activation of LFA-1 by regulating their affinity and clustering.[17] In talin-1 defecient T cells, the LFA-1 was shown to alter in polarization, affinity, and LFA-1 rich zones on membrane.[17,18] Thus, in this skeleton-fence model, adaptor proteins which tether integral membrane proteins to the cytoskeleton play crucial roles in their organization and functions.

Diffusion studies that find long-range protein diffusion which was slower than Brownian diffusion have suggested involvement of the cytoskeleton in biological membrane structure .[14,34,35] This slower diffusion was attributed partly to the steric hinderance between cytoplasmic tail of integral membrane proteins and the cytoskeletal meshwork, which has been termed the "picket fence" or "hop-diffusion" models.[19–21] Actin-depolymerizing drugs such as *cytochalasin D* (CytoD) increased the diffusion rate of the proteins while actin-stabilizing drugs such as jasplakinolide increased the residence time within a compartment as determined from mean-squared displacement (MSD).[18,36] Moreover, the diffusion coefficient of proteins within a compartment is comparable to expected Brownian diffusion in a simple lipid bilayer. Lipids are localized on the inner and outer leaflet of the cell membrane, and they undergo a similar pattern of

diffusion to integral membranes, suggesting an indirect influence of the cytoskeleton network on lipids due to immobilized integral proteins. The trapping of integral proteins and lipids depend on the size of the complex, in which at a certain size it is completely trapped within a compartment. Thus, when studying cell membrane components, it is always essential to take the influence of the underlying cytoskeleton network.

Lipid rafts

Our understanding of biological membranes have evolved from the fluid mosaic model, and cellular membranes are now thought to be more complex and have distinct domains that are different from their environment.[37] Lipid domains (also known as "lipid rafts") ordered micro-domains identified on cellular membranes that play a role in protein separation, organization, and signalling.[38] These microdomains are rich in cholesterol and glycosphingolipids. Various membrane proteins segregate into lipid domains, such as glycosylphosphatidylinositol (GPI)-anchored proteins. GPI-linked proteins are linked to a glycan core and a phospholipid tail via phosphoethanolamine linker, or are double-acylated. Phospholipid bilayers can exist in solid phase with ordered acyl chain (So), disordered liquid phase (Ld) with disordered acyl chain, or ordered liquid phase (Lo) with the presence of cholesterol and saturated lipids allowing some degree of ordered acyl chain arrangement.[39–41] The co-existence of Ld and Lo is the principle for non-raft (Ld) and raft (Lo) regions of biological membranes.[42] The lipid raft domains are resistant to detergent extraction and are highly dynamic;[43] the formation of the these lipid microdomains are thought to partially depend on the actin cytoskeleton although more varying mechanisms are also involved in the process.[44,45] Partitioning of proteins into lipid rafts slow their diffusion and increase nanoscale protein-protein collisions.[46,47] It should be noted that lipid raft domains are still controversial and research continues to better define the structure and function of these membrane

components.[48] The presence of these spatially distinct microdomains on cell membrane are particularly important in lymphocytes for their functions.[49,50]

1.1.6 Biophysical methods for studying membrane proteins

The organization and diffusion of membrane proteins are influenced by a number of factors including the presence of microdomains (e.g. lipid rafts), protein-protein interactions, and interactions with the underlying cytoskeleton.[51,52] The study of heterogenous domains and of protein organization and interactions is difficult to achieve due to the diffraction limits of optical techniques.[53] The diffraction of an image is proportional to the wavelength of light and imversely proportional to the numerical aperture of lenses, as described by Abbe diffraction limit (Eq. 4),[22] in which d is the resolvable limit, λ is the wavelength of laser, and NA is the numerical aperture. Moreover, many analyses from fluorescence techniques are not designed for quantitative determinations. One way to visualize the heterogeneity in model membranes is by using giant unilamellar vesicles (GUVs) as a model membrane.[54] This system is useful because one is able to control compositional and environmental factors, however, it is challenging to use these simplified models to study membrane proteins. Thus, a number of methods have been developed to study protein behaviour on intact cell membranes.

$$d = \frac{\lambda}{2NA} \quad \text{(Eq. 4)}$$

Receptors of immune cells that mediate activation and adhesion have been an important focus of many biophysical studies. Lateral mobility of immune cell receptors is complex and can be influenced by a number of factors[55] such as the lateral size of the protein,[56] cytoskeletal barriers,[57-60] the presence of membrane microdomains,[61] and crowding effects.[62] Dynamics and diffusion of membrane proteins can be examined using Fluorescence Recovering after Photobleaching (FRAP, also known as FPR)[12,63,64] and Single Particle Tracking (SPT).[65–67] In

FRAP methods, the protein is fluorescently-labelled and a focused, intense, laser beam is used to bleach one small spot on the cell surface.[4,5,23] The recovery of the spot indicates diffusion of proteins into the spot; the lower intensity recovery is visualized to determine the rate of diffusion.[64] SPT is another biophysical method widely used for studies on protein diffusion. In this method, membrane protein is sparsely labelled by different means including quantum dots, organic dyes, and fluorescent proteins with varying labelling strategies[68]. In SPT experiments, high signal-to-noise ratio is crucial; this is achieved by exciting the fluorophores using evanescent waves emitted from Total Internal Reflection Fluorescence Microscope (TIRFM) when the incident light is totally reflected at its surface. Since evanescent wave intensity decreases exponentially with distance, only the fluorophores within 100 - 200 nm from the surface are excited. Diffusion of the proteins are obtained by taking time-lapse videos, from which trajectories of the particles can be extracted and measured. However, the particle tracking analysis using the videos' frames are challenging due to high particle density, particle motion heterogeneity, temporary particle disappearance, and particle merging and splitting. Besides using low levels of fluorophores, the linear assignment problem mathematical framework can address these issues.[69] In this algorithm, the particles from each frame are detected, localized, and linked to particles in the consecutive frames to form frame-to-frame tracks, which are then analyzed for gap closing and merging.

Another aspect of membrane proteins that is important for their functions is clustering, however, its study is hindered by the diffraction limit. Many statistics of protein clustering have been highly qualitative due to this reason. Confocal fluorescence microscopy is a useful technique since they are readily available at low cost, are versatile, and have simple sample preparation and instrument setup.[70] Confocal microscopes are superior compared to widefield microscopes for this purpose owing to its capability in eliminate out-of-focus light. This way, only the fluorophores on

one focal plane can be excited, making it practical to study membrane proteins. However, these data are often treated qualitativly.[71-74] Several studies have aimed to develop quantitative methods for studying protein clustering. For example, in one study, quantification of immunoblot was utilized to study clustering of IRE1α proteins.[75] This method is challenging for quantitative analyses due to the high level of background and technical demands of the method. Super-resolution microscopy techniques have also been used for years and been increasing in popularity because they are capable of bypassing the diffraction limits imposed by light scattering in other microscopy techniques.[76,77] Despite highly resolved images from these techniques, they require rigorous optimization for sample preparation, advanced instrument set-ups, and complex image processing.[78–80] Moreover, super-resolution techniques require usage of fixed cells and due to the time-consuming nature of these experiments, it is not always possible to obtain large amount of data to perform statistical analyses. Therefore, using TIRF microscopy for diffusion and confocal microscopy for diffusion and analyses of receptor organization, respectively, may be more useful.

1.2 B CELL IMMUNE RECEPTORS

1.2.1 B Cell Receptor signaling

B cells, which arise from stem cells in the bone marrow, are an important component of the adaptive immune system providing specific immunity towards antigens.[81] Many receptors on the B cell membrane mediate these functions, and B-cell receptors (BCRs) are responsible for recognizing and binding to antigens and eliciting immune responses.[82,83] BCRs are composed of antigen-binding Ig domain and Ig-α and Ig-β sheaths that contain immunoreceptor tyrosine activator (ITAM) motifs (Figure 2). B cells respond to both soluble and membrane-bound antigens on antigen presenting cells (APCs), and upon binding to specific antigens, BCRs ligate and ITAM domains get phosphorylated by Lyn and induce cellular responses such as antibody production as

well as survival, differentiation, and proliferation of memory B cells. Lipid rafts may play a role in B cell activation and formation of BCR activation complex.[84,85]

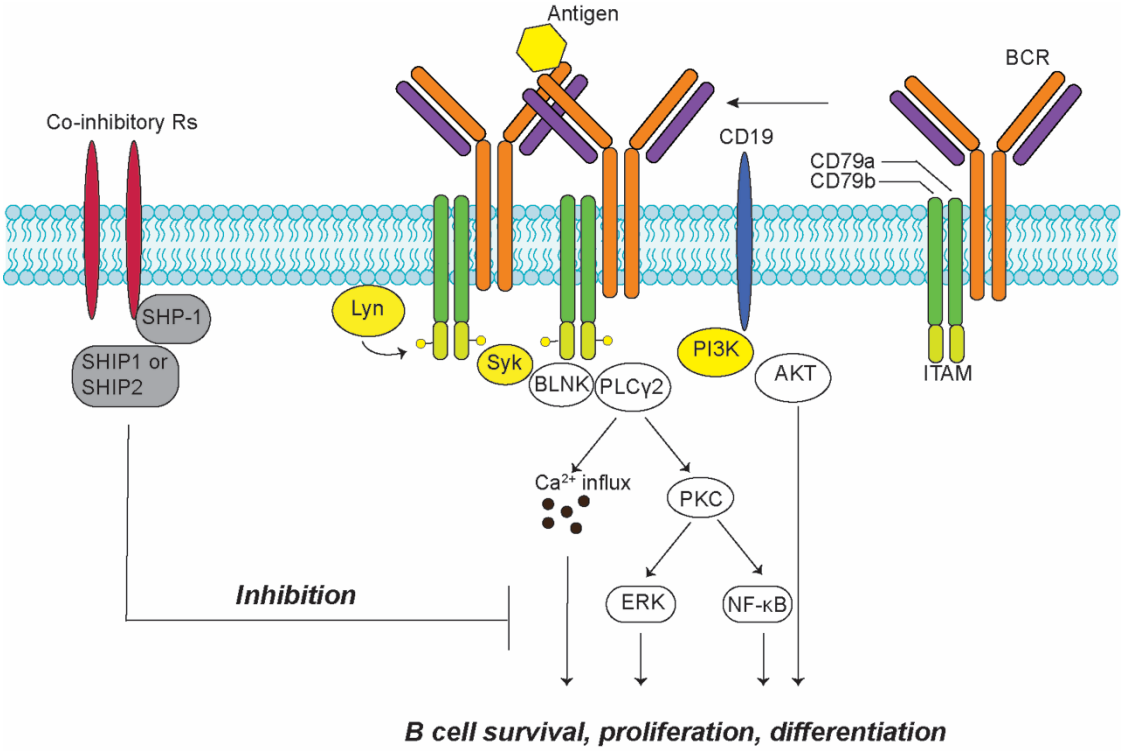

Figure 1.2. B cell response upon binding to antigens. BCRs consist of immunoreceptor (orange and purple) and signal transduction domains, co-receptors CD79a and CD79b (green). Once BCR binds to a specific antigen (yellow), the ITAM motif (yellow-green) is phosphorylated (small yellow circles attached to BCR) by Lyn, which then recruits the signalling complex that induces cellular response.

BCRs organization and mobility are heavily influenced by cytoskeletal network[86,87] (Figure 1.3). BCRs are believed to be organized in pre-formed nanoclusters on cell membranes. These BCRs in nanoclusters have restrained mobility due to boundaries formed by erzin and actin cytoskeletal network. Upon antigen binding, actin detaches from the cell membrane and transiently increases in depolymerization, leading to faster diffusion of BCRs and BCR nanoclusters coalesce to form larger microclusters and move to one pole of the cell or to the point of cell contact. The

formation of BCR microcluster were suggested to be dependent on Cμ4 domain of the BCR. Actin polymerization then occurs near one pole of B cells, near the BCR microclusters. Thus, cytoskeletal reorganization is important in BCR organization and function. Indeed, when B cells were treated with treated with latrunculin A, a cytoskeleton disruptor, resulted in increased BCR clustering and B cell activity, while jasplakinolide treatment, an actin stabilizing agent, inhibited BCR clustering.[88,89] Interestingly, CD45 has been found to be excluded from these microclusters, suggesting they place crucial role in regulating B cell responses.[89] Additionally, CD19 has also been suggested to be crucial in B cell signaling in response to antigen binding.

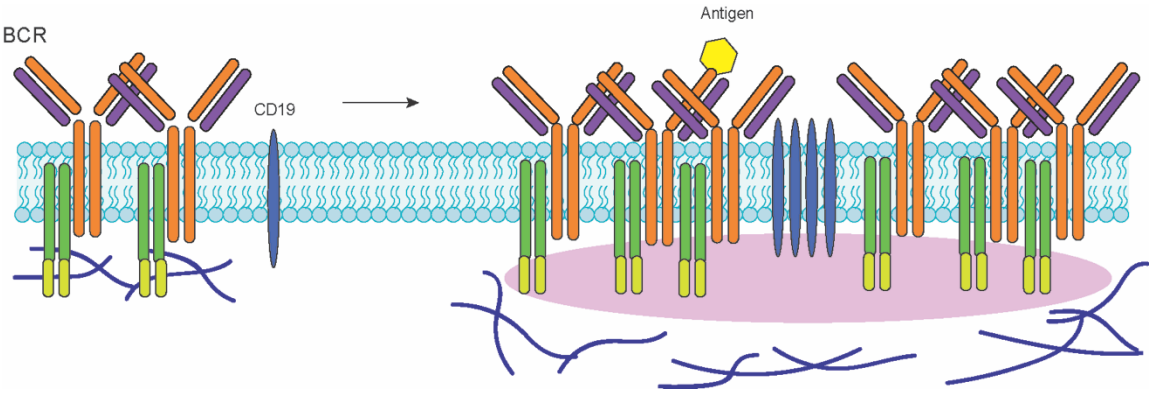

Figure 1.3. Influence of cytoskeleton on BCR organization. Figure adapted from Mattila et al., 2012. Upon antigen binding, actin depolymerizes and BCR diffusion increases to form larger BCR clusters that are fenced by reorganized actin cytoskeleton structure (dark blue curved lines) that is formed around these BCR nanoclusters.

1.2.2 Autoimmune diseases

Given the importance of B cells in immune response, as might be expected, misregulation of B cell response is linked to numerous immune disorders. Since adaptive immunity is acquired from gene translocation mutations,[90] autoimmunity can emerge when regulatory mechanisms fail. Autoimmune diseases result from a number of mechanisms, such as production of autoantibodies

that recognize and bind to self-antigens, damaging or destroying organs or receptors,[91-93] increasing infections, disrupting the balance between effector T cells and Treg, and antigen mimicry. For example, rheumatoid arthritis is an autoimmune disease in which the immune system attacks joint tissues, causing damage in the joints throughout the body.[94,95] Although it is unclear whether dysregulation is caused by aberrant T cell or B cell activity, B cells have been used as target for drug development to regulate the activity of B cells,[96] reducing adverse effects of immune diseases. B cell dysregulation is also responsible for other immune disorders including systemic lupus erythematosus,[97–99] Sjogren's syndrome,[100,101] diabetes,[102] and multiple sclerosis.[103-105] Interestingly, it has been widely suggested that B-cell intrinsic signals can function to promote autoimmunity by skewing naïve B cell repertoire and T-dependent and T-independent activation of extrafollicular B cells.[106]

B cells are widely targeted for autoimmune disease treatments. Rituximab is a B-cell depleting antibody used to treat B cell lymphomas,[107] and recently, it was discovered that this antibody is also effective against rheumatoid arthritis. Rituximab targets CD20, which is a glycoprotein expressed on B cells; coating of B cells with this antibody leads to depletion of B cells using an antibody-dependent mechanism.[108,109] Some studies find that IL-6 producing B cells were depleted following rituximab treatment in mice, which is significant for a number of autoimmune diseases that have elevated levels of this group of B cells, such as autoimmune encephalomyelitis and multiple sclerosis.[110] Interestingly, this antibody has also shown degrees of efficacy towards other autoimmune diseases.

1.2.3 Co-receptors of BCR

Since dysregulation in B cell response can lead to adverse conditions, tight regulation is required which can be achieved by the presence of inhibitory and activatory co-receptors on B cell

membrane. Several co-receptors of BCR have been described, examples include CD28, F*c*γRIIb, PD-1, CD72, and CD22.[111,112] Inhibitory co-receptors share structural and functional similarities; they contain one or more immunoreceptor tyrosine-based inhibitory motifs (ITIM) that have consensus amino acid sequence of (Ile/Val/Leu/Ser)-X-Tyr-X-X-(Leu/Val). When ITIM comes in proximity to immunoreceptor tyrosine-based activatory motifs (ITAM), such as the one present on BCR, they get phosphorylated by tyrosine kinase *lyn* and recruit src-homology 2 (SH2) containing phosphatases such as SHP-1, SHP-2, SHIP, and SHIP2.

Co-receptors play crucial roles in tight regulation of B cell responses in order to avoid autoimmune diseases described above. For example, F*c*γRIIb is an inhibitory co-receptors on B cells that bind to IgG complexed with soluble antigens or on cell membrane and its cross-linking with BCR lead to inhibition of B cell activation through Fc of BCR.[113,114] Murine models deficient in F*c*γRIIb showed elevated humoral responses following immunizations and are more likely to develop inducible autoimmunity.[115] More recently, CD19 has been found to be essential for B cell activation. CD19 is recruited to BCR microclusters upon antigen binding and is believed to be important for B cell spreading, leading to more recruitment of signaling molecules such as Syk and Vav to the cell contact. Indeed, CD19 - deficient mice were found to be unable to recognize membrane-bound antigens.

1.3 THE CD22 RECEPTOR

1.3.1 CD22 Function

CD22 (or Siglec-2) is a sialic acid-binding immunoglobulin-like lectin (SigLec) that is a negative co-receptor of BCRs.[116] The receptor was originally found as sialoadhesion molecule on B cells.[117] CD22 expression is specific to the B cell lineage; they are expressed on pre- and immature B cells, and maximum expression is found on mature B cells while lower expression

was detected on plasma B cells. The extracellular domain of CD22 adopts a rigid rod-like structure that comprises of seven Ig domains and the amino-terminal is responsible for ligand binding.[118] The intracellular domain of CD22 is made up of two immunoreceptor tyrosine inhibitory motifs (ITIMs) that contain six tyrosine residues, three of which are phosphorylated upon antigen binding.[119] Upon binding to antigens displaying CD22 specific ligands, α2,6-sialosides, they crosslink with BCRs to modulate B cell activity. Crosslinking of CD22 recruits *src* family protein tyrosine kinase, *Lyn*, to phosphorylate the ITIM motifs of CD22 molecules, which then recruits SH-2 domain containing phosphatase SHP-1 to de-phosphorylate BCR, dampening B cell activity.[120] The phosphorylation of CD22 receptors are crucial for their function as B cells in mice with Y2,5,6F showed no binding of SHP-1 to CD22, leading to increased B cell response.[121] The importance of CD22 receptors in regulating B cell activity was demonstrated in mice with the CD22 gene deleted, which showed heightened B cell activation and a high level of autoantibody production.[122] CD22 has also been shown to interact with plasma membrane Ca^{2+} ATPase to remove Ca^{2+}, further inhibiting the B cell response.[123,124] Interestingly, high-affinity ligands for CD22 were found to be downregulated in germinal center (GC) B-cells, and this is believed to be important in B cell selection in GCs.[125-127] Recently, CD22 was suggested to be important in regulating TI-2 antigens by regulating B-1b cells.[128] The specificity and mechanism of CD22 receptors is important for differentiating between self- and non-self-antigens, as human glycans are capped with terminal sialic acids while sialic acid expression is limited in pathogenic organisms.

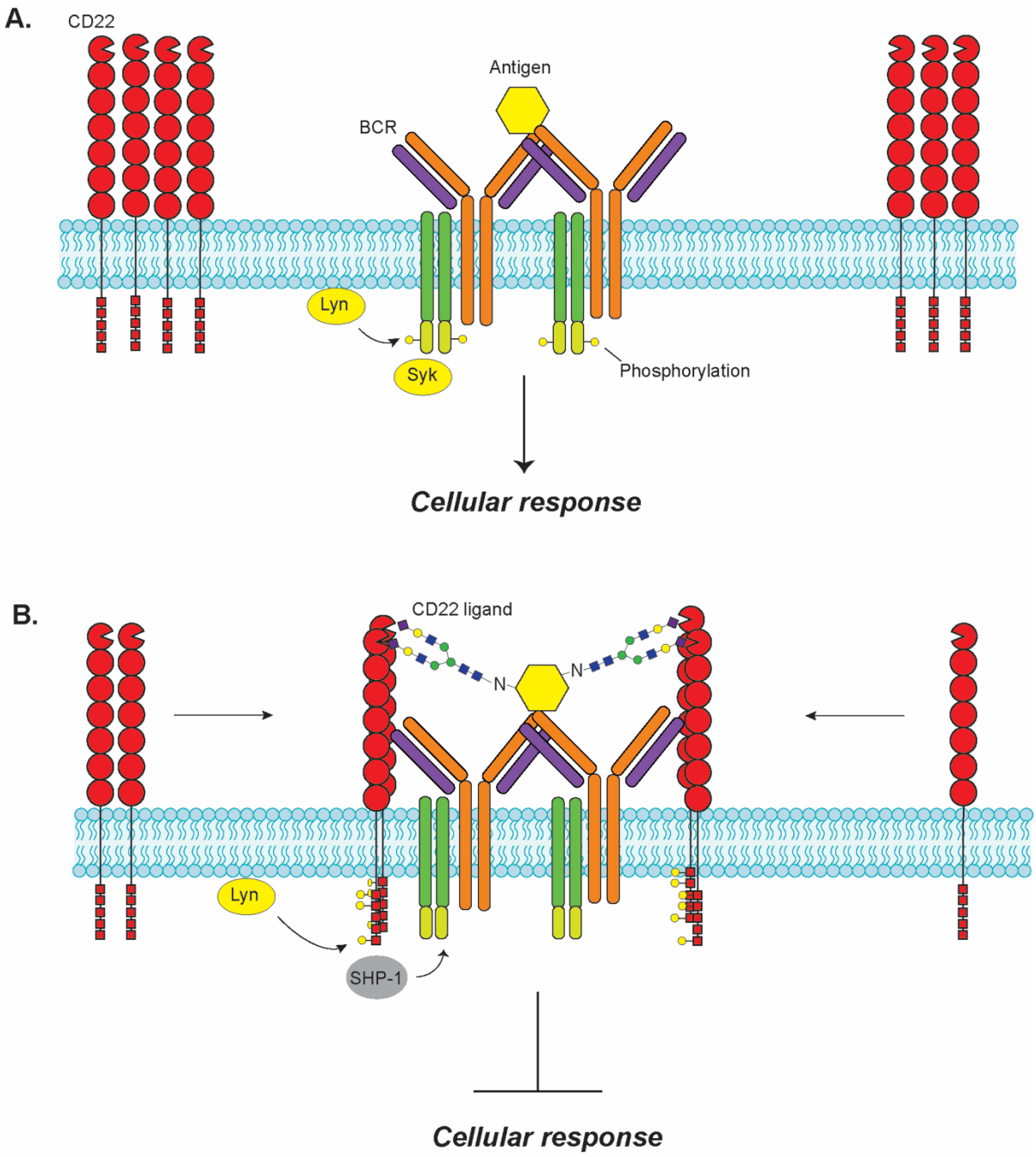

Figure 1.4. Inhibition of B cell response by CD22 co-receptors. (A) When no CD22 ligand is present, cellular response upon BCR binding to antigen is induced. (B) Presentation of a CD22 ligand-containing antigen to BCR results in CD22 co-clustering, and the ITIM domain of CD22 is phosphorylated by Lyn, recruiting SHP-1 to de-phosphorylate BCR and inhibit B cell response.

1.3.2 CD22 cis-ligands

CD22 receptors are masked by cis-interactions with other glycans, which are on the same cell, on B cell membrane. Using a biotinylated acrylamide probe substituted with α2,6-sialyllactose, it was found that this probe had no activity against CD22-positive B cells or Epstein Barr Virus transformed lymphoblasts, but it was active when surface sialosides were reduced by enzymatic or periodate treatment.[129] Among many binding partners on the B cell surface, the most prominent binding partners of CD22 were found to be CD22 and CD45, and this protein was found to be important for CD22's function in modulating B cell signaling. The extracellular domain of CD45 is believed to be responsible for interactions of CD45 and CD22, and mice lacking the extracellular domain of CD45 showed B cells' hypoactivity similar to R120E mutant B cells.[130] The masking of CD22 on the cell membrane is important for their role in regulating B cell activity as disrupting these interactions have shown aberrant cell activation. In one study, B cells from mice with R120E CD22, in which it was mutated at the ligand binding site, showed increased co-clustering with BCRs, significantly lower Ca^{2+} mobilization,[131] and overall hypoactivity of B cells, which was similar to B cells from mice deficient in ST6Gal I which makes CD22 ligands. On the other hand, when mice were deficient in both ST6Gal and CD22, the B cell activation was restored. Recently, another protein on B cells, galectin-9, was also found play a role in association of CD22 and BCR, and galectin-9 deficient B cells showed elevated B cell response due to the lack of this association.[132] CD22 expression was found to be affected by a newly identified binding partner of CD22, cullin 3,[133] which works to internalize CD22 receptors upon B cell activation. Together, these studies elegantly showed the importance of CD22 cis-ligands on the B cell surface.

1.3.3 CD22 trans-ligands

The inhibition of B cell activity by CD22 requires the cross-linking of CD22 and BCR by trans-ligands, suggesting unmasking of CD22 is required. Binding of siglecs to their ligands are generally weak, but cis-interactions are difficult to overcome due to their high local concentration. Although binding of CD22 to sialoside probes required treatment with enzyme or periodate,[130] it was shown that masking of CD22 receptors did not interfere with receptor binding to trans ligands on neighbouring cells and distribution to the cell-cell contact using immunofluorescence microscopy.[134,135] Furthermore, high-affinity probes have been developed using different scaffolds to inhibit B cell activity. Synthetic multivalent CD22 ligands on a polymer scaffold failed to bind to CD22, however, the addition of BCR-specific antigen, 2,4-dinitrylphenyl (DNP), to the polymer led to binding of the probe on the cell surface.[136] This probe also inhibited the Ca^{2+} mobilization into the cells as examined using flow cytometry. Liposomes are another popular scaffold for CD22 high-affinity ligands. Nanoparticle liposomes decorated with BCR antigens and CD22 ligands induced apoptosis and tolerance of B cells towards T cell-dependent antigens in vitro,[137] as well as in-vivo.[8] Since CD22 is an endocytic receptor, it was shown in another study that antigenic liposomes carrying CD22 ligands were bound to the receptors and endocytosed.[138] Another type of scaffold that has been utilized in developing CD22 trans-ligands is synthetic multivalent glycoconjugates.[139]

CD22 has been a therapeutic target for autoimmune diseases and B cell malignancies due to their specific B-cell restrictive expression and B cell inhibition function. For this purpose, several antibody-based inhibitors have been developed. Modified sialosides have been discovered as high-affinity inhibitors of CD22.[140] Kelm et. al., developed high-affinity CD22 ligands that have substitution at C-9 position of sialic acid to improve low-affinity natural ligands.[141] When the C-9

position of sialic acid was substituted with biphenyl-4-carbonyl (methyl-α-9-*N*-(bipheynyl-4-carbonyl)-amino-9-dexoy-Neu5Ac, or BPC-Neu5Ac) or biphenyl-4-acetyl (methyl-α-9-*N*-(bipheynyl-4-acetyl)-amino-9-dexoy-Neu5Ac, or BPA-Neu5Ac), with the former being able to increase inhibitory potential as measured by IC_{50}, selectively inhibited staining of CD22, and increased IgM-stimulated B cell signalling. In another study, 9-*N*-*m*-phenoxybenzamide-Neu5Fc (MPB-Neu5Fc) was discovered as a high-affinity ligand for CD22.[142] These discoveries led to development of high-affinity CD22 probes for therapeutic targeting. For instance, bi- and tri-valent N-glycan scaffolds bearing these sialic acid analogs were developed that increased the affinity by 1,500-fold and were sufficiently bound to hCD22, endocytosed, and delivered toxins inside the cells.[143] Moreover, liposomal nanoparticles displaying BPC-Neu5Ac that are loaded with a chemotherapy medication doxorubixin were bound and endocytosed into model B cell lymphoma to extend its life, and effectively killed malignant B cells obtained from blood samples of patients suffering from B cell malignancies.[144]

1.3.4 CD22 organization on the B cell membrane

Although CD22 function is well studied, their organization on the cell membrane and the biophysical mechanism for their clustering and association with IgM are not clearly understood. CD22 is known to form clusters on the B cell membrane due to homotypic interactions. The ectodomain of CD22 has 12 N-glycosylation site, and mutation of five of these sites were associated with increased clustering of CD22 and attenuated B cell response.[145] In their study, Wasim et al., also found that treatment of B cells with recombinant Galectin-9 (rGal9), which mediates the association of CD22 with BCR to inhibit B cell signalling, decreased CD22 clustering and their association with BCR, and did not change the level of CD22 phosphorylation, suggesting that N-glycosylation sites are important for Gal9-mediated BCR inhibition by CD22. Wasim et al.

suggested that the role of Gal9 in mediating the CD22 and BCR association can be the result of Gal9 binding to glycans on CD22 molecules or on CD45, which is a well-known CD22 cis-ligand. This is consistent with a crystal structure of CD22 which suggested that the extracellular domain is tilted and rigid, optimal for competing binding with flexible carbohydrates on neighbouring glycoproteins and trans-ligands presented on antigen-presenting cells.[111] CD22 receptors are surveillance molecules that regulate B cell response, so an understanding of the mechanisms that regulate their cluster formation and diffusion to sites of cell-cell contact or BCR in the presence of self-antigens is important.

The cytoskeleton is important in BCR mobility and signalling and disruption of this structure led to heightened B-cell response. One study found that CD22 has no contact with the cytoskeleton,[24] and only cis-interactions were proposed to be important to diffusion and clustering. Specifically, in CD45-deficient B cells, CD22 clustering increased while the diffusion decreased, and this was reversed with sialidase treatment. They suggested that the organization of CD22 on B-cell membrane is controlled by binding to the cis-ligand, CD45, acting as the spacer between CD22 molecules. The proposal that CD22 is not influenced by cytoskeletal interactions is puzzling considering multiple studies find it has interactions with CD45 as its major cis-ligand. CD45 is well known to have direct contact with the cytoskeleton via the spectrin-ankyrin complex.[146–147] Thus, direct or indirect interaction with the cytoskeleton could regulate CD22 organization.

1.4 HUMAN NEURAMINIDASE ENZYMES

Sialidases, or neuraminidases, are enzymes that are responsible for cleaving terminal sialic acids and that modify the glycosylation content of cells.[148] They are glycosyl hydrolases (GH) in humans are classified as GH33,[149] which encompasses non-viral neuraminidases. There are 4 different isoenzymes of human neuraminidases, each differ in their substrate selectivity,

specificity, and subcellular localization.[150] Despite their differences, they share similarities in having an Arg triad, Asp boxes, and RIP motifs. Moreover, human sialidases are exo-sialidases, in which catalysis of sialic acid hydrolysis occurs via an acid/base double displacement mechanism. NEU enzymes are proposed to have a role in regulating immune responses.[151-153] The fact that NEU isoenzymes are membrane-associated may suggest an influence on membrane receptors. Since human sialidases play important roles in cellular functions, protein organization, malignancy, and immunity, it is interesting to study how they may influence the CD22 organization on B cells, which in turn may alter B cell activity. We briefly review the features of the four human NEU isoenzymes, and their relevance to B cell function, below.

1.4.1 NEU1

Human NEU1 enzymes have been found to localize to lysosomes, the plasma membrane, and exocytotic and endocytic vesicles.[154,155] NEU1 is selective towards α2,3-linked terminal sialic acids on glycoproteins. The expression of NEU1 on the cell membrane was detected in activated lymphocytes, neutrophils, and monocytes.[156] Unlike other human NEU isoforms, the association with lysosomal protective coat cathepsin A and β-galatosidase is required for NEU1 activation.[157–159] Deficiency of NEU1 enzymes lead to an autosomal recessive disorder, sialidosis, which is a metabolic disease that causes accumulation of NEU1 substrates, namely sialylglycoproteins.[160,161] Galactosialidosis is a neurodegenerative disease caused by secondary deficiency of NEU1 from cathepsin A deficiency.[156,162,163]

Aside from its catabolic function, NEU1 is involved in other cellular signalling pathways. For example, NEU1 modulates lysosomal exocytosis.[164,165] Lysosomal exocytosis is the process where the lysosome fuses with plasma membrane and releases its contents. This process is important in immunity, secretions, and plasma membrane repair in fibroblasts. NEU1 deficiency

led to increased protease and glycosidase secretion, and expression of highly-sialylated lysosome associated membrane protein 1 (LAMP-1). Thus, it is thought that NEU1 modulates lysosomal exocytosis partly through sialylation of LAMP-1 receptors. Additionally, the NEU1 enzyme is implicated in migration, invasion, and adhesion of cancer cells.[166] It is known that cancer cells have elevated levels of sialylated glycoproteins and glycolipids,[167] and altered NEU levels in all 4 isoenzymes have been detected. The overexpression of NEU1 decreased the metastastatic ability of the B12 melanoma and HT-29 colon cancer cells.[168] Since NEU1 expression on the plasma membrane is increased during activation of lymphocytes, neutrophils, and macrophages, downregulation of these enzymes lead to retarded cellular activation of immune cells, possibly by regulation sialylation of siglecs' ligands on cell surface.

1.4.2 NEU2

Human NEU2 was first identified and characterized using cDNA of human skeletal muscle. NEU2 enzymes are found in the cytosol, and unlike other human NEU isoforms, they are not membrane-associated. The X-ray crystal structure of NEU2 showed a six-bladed β-propeller in the active site. NEU2 has broad activity across glycoproteins and glycolipids and is active at neutral pH of 7. Using quantitative real-time PCR, expression of NEU2 was found to be low or undetectable in all tissues, with some exceptions in placenta and testis.[169] In their study, they also found that PC-3 prostate cancer cell line was the only cancer cell line among many they tested that exhibited upregulation of NEU2, and an another study found the high enzyme activity is only detectable during cell differentiation induced by growth factors.[170] NEU2 upregulation was also found to involve in myoblast differentiation in C2C12 immortalized mouse myoblast cell line.[171]

1.4.3 NEU3

The human NEU3 enzyme was identified and characterized from cDNA of bovine brain.[172] It is located on chromosome 11 at q 13.5, and contains a putative transmembrane helix and share 78% sequence similarity with other NEU isoforms. Additionally, this sialidase was determined to be integral membrane, in which the cytosol domain is S-acylated.[29] NEU3 is a retaining exo-sialidase;[173] and a plasma membrane-bound enzyme selective towards gangliosides at optimal pH of 4.5 with some activity at neutral pH.

Several studies have examined the roles of NEU3 in cellular function. For example, NEU3 overexpression increased skeletal muscle cells resistance to hypoxia by stimulating epidermal growth factor (EGF) receptors and inhibit apoptosis.[174] Additionally, it was recently found that NEU3 modifies glycosylation, clustering, expression, and binding of lymphocyte function-associated molecule 1 (LFA-1) receptors to intercellular adhesion molecules (ICAMs) on cell membrane.[175] LFA-1 is an integrin responsible to cell-cell adhesion in T cell activation.[176] Moreover, NEU3 expression is modulated by sp1/sp3 transcription factors which in turn regulate other protein expressions.[177] NEU3 has also been shown be implicated in autoimmune diseases. For example, the ratio of sialyltransferase and NEU3 enzymes correlated with disease activity in patients with systemic lupus erythematosus and rheumatoid arthritis.

Upregulation of NEU3 is consistently seen in many types of malignancy.[178] For example, increased levels of NEU3 were detected in cancer cells. This is thought to increase the lactosylceramide (LacCer), which is a by-product of NEU3 activity, leading to inhibition of apoptosis and programmed cell death.[179] Additionally, detected increased NEU3 expression in renal cell carcinomas was linked to increased interleukin-6 (IL-6) expression, which was found to suppress apoptosis and promote motility of cancer cells.[180] The suppression of apoptosis was

observed with Neu3 siRNA treatment in cancer cells, and overexpression of the enzymes elevated cellular apoptosis, likely due to changes in glycolipid content.[181] Overexpression of IL-6 caused by NEU3 upregulation has also been linked to a positive feedback loop in pulmonary fibrosis, where *Neu3*$^{-/-}$ showed resistance in induced lung inflammation compared to wild-type.[182]

1.4.4 NEU4

Human NEU4 is the most recently discovered isoenzyme of hNEU.[183] NEU4 activity is optimal at an acidic pH of 4.5. It is broadly expressed and has specificity towards oligosaccharides, glycoproteins, and glycolipids. Two isoforms of human NEU4 have been identified, short and long forms that differ in the presence of 12 amino acid sequence and the N-terminus, and they seem to have similar specificities but different tissue expression and subcellular localization.[184] Both short and long forms of NEU4 are localized to the membrane, and additionally, it was found that long form is also associated with mitochondria and short form with endoplasmic reticulum.[185,186] Thus, the N-terminal amino acid sequence is believed to be responsible for mitochondrial localization of the long form enzyme.

Similar to other hNEU isoenzymes, NEU4 is important in cellular processes and several human diseases. For instance, NEU4 is involved in postnatal brain development by modulation of gangliosides.[187] Overexpression of NEU4 in sialidosis and galactosialidosis patients showed clearance of accumulated sialylated glycoconjugates in lysosomes.[188] NEU4 is also involved in cancer cell survival and progression. It is overexpressed in glioblastoma cells and its inhibition led to lower cell survival.[189] On the other hand, NEU4 is down-regulated in colon cancer cells through inhibition of apoptosis by desialylation of glycoproteins.[190]

1.5 HYPOTHESIS AND OBJECTIVES

The recognition of glycoconjugates by CD22 can temper the immune response through negative regulation of BCR. Previous studies have developed multivalent conjugates that act to mimic glycosylated antigens which were combined with haptens that interact with BCR. These conjugates demonstrated that the combination of these components (a BCR antigen and a CD22 ligand) could be used to induce co-clustering. In this thesis we set out to test the ability of synthetic glycans to act as BCR antigens in this process, and the influence of changes to cellular glycosylation on CD22 clustering.

In Chapter 2, we develop a method to quantify changes in clustering of CD22 receptors on the B cell membrane. Many studies of receptor clustering on cellular membranes have been qualitative or require special sample preparation and instrumental setups to perform superresolution analysis. Our method uses standard confocal microscopy to quantify changes in receptor clustering.

In Chapter 3, we used our analysis of receptor clustering to analyze changes in CD22 receptor organization on a glycan-antigen recognizing B cell line (A-BCL). These cells express a BCR complex that recognizes A-type I and A-type II blood group antigens. We used bi-functional multivalent conjugates bearing BCR specific antigens and CD22 ligands. It is known that high-affinity CD22 ligands are required to overcome cis interactions of CD22 with other glycoproteins on the cell surface. We investigated whether bi-functional multivalent glycoconjugates could overcome these interactions with a glycan antigen. This study provides insight into important features on CD22 ligands in order to regulate B cell activity.

Sialosides play a critical role as cis-ligands in the maintenance of CD22 organization, and thus have a role in regulating BCR activity. We considered that the NEU enzymes are an important

regulator of sialoside homeostasis on B cells and could therefore influence CD22 and BCR function through changes to membrane glycans. We hypothesized that changes in glycosylation of cell surface components (glycoproteins and glycolipids) by NEU enzymes could alter CD22 organization, leading to changes in B cell activation. An understanding of how NEU enzymes influence B cell activation could suggest strategies to manipulate B cell activation in disease. In Chapter 4, we investigated changes in CD22 organization on the B cell membrane due to NEU enzyme activity. CD22 receptors are present as clusters on B cell membrane, however, what controls their organization is not well understood. We employed cytoskeletal disruptors, NEU enzymes, and NEU enzyme inhibitors to study whether the cytoskeleton or changes in sialosides influences clustering and diffusion on the membrane. Additionally, we investigated whether NEU enzymes have any effects on B cell activity.

Finally, in Chapter 5 we present a summary and future outlook on the role of human NEU in regulation of immunity are discussed.

REFERENCES

(1) Singer, S. J.; Nicolson, G. L. The Fluid Mosaic Model of the Structure of Cell Membranes. *Science* **1972**, *175* (4023), 720–731. https://doi.org/10.1126/science.175.4023.720.

(2) Lenaz, G. Lipid Fluidity and Membrane Protein Dynamics. *Biosci. Rep.* **1987**, *7* (11), 823–837. https://doi.org/10.1007/BF01119473.

(3) Yang, S.-T.; Kreutzberger, A. J. B.; Lee, J.; Kiessling, V.; Tamm, L. K. The Role of Cholesterol in Membrane Fusion. *Chem. Phys. Lipids* **2016**, *199*, 136–143. https://doi.org/10.1016/j.chemphyslip.2016.05.003.

(4) Kusumi, A.; Nakada, C.; Ritchie, K.; Murase, K.; Suzuki, K.; Murakoshi, H.; Kasai, R. S.; Kondo, J.; Fujiwara, T. Paradigm Shift of the Plasma Membrane Concept from the Two-Dimensional Continuum Fluid to the Partitioned Fluid: High-Speed Single-Molecule Tracking of Membrane Molecules. *Annu. Rev. Biophys. Biomol. Struct.* **2005**, *34* (1), 351–378. https://doi.org/10.1146/annurev.biophys.34.040204.144637.

(5) Edward, J. T. Molecular Volumes and the Stokes-Einstein Equation. *J. Chem. Educ*. **1970**, 47(4), 261.

(6) Saffman, P. G.; Delbruck, M. Brownian Motion in Biological Membranes. *Proc. Natl. Acad. Sci.* **1975**, *72* (8), 3111–3113. https://doi.org/10.1073/pnas.72.8.3111.

(7) Gambin, Y.; Lopez-Esparza, R.; Reffay, M.; Sierecki, E.; Gov, N. S.; Genest, M.; Hodges, R. S.; Urbach, W. Lateral Mobility of Proteins in Liquid Membranes Revisited. *Proc. Natl. Acad. Sci.* **2006**, *103* (7), 2098–2102. https://doi.org/10.1073/pnas.0511026103.

(8) Nicolson, G. L. Update of the 1972 Singer-Nicolson Fluid-Mosaic Model of Membrane Structure. 14.

(9) Nicolson, G. L. The Fluid—Mosaic Model of Membrane Structure: Still Relevant to Understanding the Structure, Function and Dynamics of Biological Membranes after More than 40years. *Biochim. Biophys. Acta* **1838**, 16.

(10) Jacobson, K.; Sheets, E.; Simson, R. Revisiting the Fluid Mosaic Model of Membranes. *Science* **1995**, *268* (5216), 1441–1442. https://doi.org/10.1126/science.7770769.

(11) Goñi, F. M. The Basic Structure and Dynamics of Cell Membranes: An Update of the Singer–Nicolson Model. *Biochim. Biophys. Acta BBA - Biomembr.* **2014**, *1838* (6), 1467–1476. https://doi.org/10.1016/j.bbamem.2014.01.006.

(12) Jacobson, K.; Derzko, Z.; Wu, E.-S.; Hou, Y.; Poste, G. Measurement of the Lateral Mobility of Cell Surface Components in Single Living Cells by Fluorescence Recovery after Photobleaching. *J. Supramol. Struct.* **1976**, *5* (4), 565–576. https://doi.org/10.1002/jss.400050411.

(13) Kusumi, A.; Fujiwara, T. K.; Chadda, R.; Xie, M.; Tsunoyama, T. A.; Kalay, Z.; Kasai, R. S.; Suzuki, K. G. N. Dynamic Organizing Principles of the Plasma Membrane That Regulate Signal Transduction: Commemorating the Fortieth Anniversary of Singer and Nicolson's Fluid-Mosaic Model. **2012**, 39.

(14) Kasumi, A.; Sako, Y. Cell Surface Organization by the Membrane Cytoskeleton. *Curr. Opin. Cell Biol.* **1996**, *8*, 566–574.

(15) Murase, K.; Fujiwara, T.; Umemura, Y.; Suzuki, K.; Iino, R.; Yamashita, H.; Saito, M.; Murakoshi, H.; Ritchie, K.; Kusumi, A. Ultrafine Membrane Compartments for Molecular Diffusion as Revealed by Single Molecule Techniques. *Biophys. J.* **2004**, *86* (6), 4075–4093. https://doi.org/10.1529/biophysj.103.035717.

(16) Vaz, W. L.; Almeida, P. F. Microscopic versus Macroscopic Diffusion in One-Component Fluid Phase Lipid Bilayer Membranes. *Biophys. J.* **1991**, *60* (6), 1553–1554. https://doi.org/10.1016/S0006-3495(91)82190-7.

(17) Paladino, S.; Sarnataro, D.; Pillich, R.; Tivodar, S.; Nitsch, L.; Zurzolo, C. Protein Oligomerization Modulates Raft Partitioning and Apical Sorting of GPI-Anchored Proteins. *J. Cell Biol.* **2004**, *167* (4), 699–709. https://doi.org/10.1083/jcb.200407094.

(18) Ritchie, K.; Iino, R.; Fujiwara, T.; Murase, K.; Kusumi, A. The Fence and Picket Structure of the Plasma Membrane of Live Cells as Revealed by Single Molecule Techniques (Review). *Mol. Membr. Biol.* **2003**, *20* (1), 13–18. https://doi.org/10.1080/0968768021000055698.

(19) Parton, D. L.; Klingelhoefer, J. W.; Sansom, M. S. P. Aggregation of Model Membrane Proteins, Modulated by Hydrophobic Mismatch, Membrane Curvature, and Protein Class. *Biophys. J.* **2011**, *101* (3), 691–699. https://doi.org/10.1016/j.bpj.2011.06.048.

(20) Kusumi, A.; Suzuki, K. G. N.; Kasai, R. S.; Ritchie, K.; Fujiwara, T. K. Hierarchical Mesoscale Domain Organization of the Plasma Membrane. *Trends Biochem. Sci.* **2011**, *36* (11), 604–615. https://doi.org/10.1016/j.tibs.2011.08.001.

(21) Hohmann, T.; Dehghani, F. The Cytoskeleton - a Complex Interacting Meshwork. *Cells.* **2019**, 8(4), 362.

(22) Birchmeier, W. Cytoskeleton Structure and Function. *Trends Biochem. Sci.* **1984**, *9* (4), 192–195. https://doi.org/10.1016/0968-0004(84)90137-3.

(23) Hartwig, J. H.; DeSisto, M. The Cytoskeleton of the Resting Human Blood Platelet: Structure of the Membrane Skeleton and Its Attachment to Actin Filaments. *J. Cell Biol.* **1991**, *112* (3), 407–425. https://doi.org/10.1083/jcb.112.3.407.

(24) Ono, S. Mechanism of Depolymerization and Severing of Actin Filaments and Its Significance in Cytoskeletal Dynamics. In *International Review of Cytology*; Elsevier, 2007; Vol. 258, pp 1–82. https://doi.org/10.1016/S0074-7696(07)58001-0.

(25) Clark, A. G.; Dierkes, K.; Paluch, E. K. Monitoring Actin Cortex Thickness in Live Cells. *Biophys. J.* **2013**, *105* (3), 570–580. https://doi.org/10.1016/j.bpj.2013.05.057.

(26) Chugh, P.; Clark, A. G.; Smith, M. B.; Cassani, D. A. D.; Dierkes, K.; Ragab, A.; Roux, P. P.; Charras, G.; Salbreux, G.; Paluch, E. K. Actin Cortex Architecture Regulates Cell Surface Tension. *Nat. Cell Biol.* **2017**, *19* (6), 689–697. https://doi.org/10.1038/ncb3525.

(27) Downing, K. H.; Nogales, E. Tubulin and Microtubulue Structure. *Curr. Opin. Cell Biol.* **1998**, *10*, 16–22.

(28) Kimble, M.; Kuriyama, R. Functional Components Of Microtubule-Organizing Centers. In *International Review of Cytology*; Elsevier, 1992; Vol. 136, pp 1–50. https://doi.org/10.1016/S0074-7696(08)62049-5.

(29) Dogterom, M.; Koenderink, G. H. Actin–Microtubule Crosstalk in Cell Biology. *Nat. Rev. Mol. Cell Biol.* **2019**, *20* (1), 38–54. https://doi.org/10.1038/s41580-018-0067-1.

(30) Goode, B. L.; Drubin, D. G.; Barnes, G. Functional Cooperation between the Microtubule and Actin Cytoskeletons. *Curr. Opin. Cell Biol*. **2000**, 12(1), 63-71.

(31) Rodriguez, O. C.; Schaefer, A. W.; Mandato, C. A.; Forscher, P.; Bement, W. M.; Waterman-Storer, C. M. Conserved Microtubule–Actin Interactions in Cell Movement and Morphogenesis. *Nat. Cell Biol.* **2003**, *5* (7), 599–609. https://doi.org/10.1038/ncb0703-599.

(32) Steinert, P. M.; Steven, A. C.; Roop, D. R. The Molecular Biology of Intermediate Filaments. *Cell* **1985**, *42* (2), 411–419. https://doi.org/10.1016/0092-8674(85)90098-4.

(33) Chang, L.; Goldman, R. D. Intermediate Filaments Mediate Cytoskeletal Crosstalk. *Nat. Rev. Mol. Cell Biol.* **2004**, *5* (8), 601–613. https://doi.org/10.1038/nrm1438.

(34) Kusumi, A.; Sako, Y.; Yamamoto, M. Confined Lateral Diffusion of Membrane Receptors as Studied by Single Particle Tracking (Nanovid Microscopy). Effects of Calcium-Induced Differentiation in Cultured Epithelial Cells. *Biophys. J.* **1993**, *65* (5), 2021–2040. https://doi.org/10.1016/S0006-3495(93)81253-0.

(35) Meilhac, N.; Le Guyader, L.; Salomé, L.; Destainville, N. Detection of Confinement and Jumps in Single-Molecule Membrane Trajectories. *Phys. Rev. E* **2006**, *73* (1), 011915. https://doi.org/10.1103/PhysRevE.73.011915.

(36) Fujiwara, T.; Ritchie, K.; Murakoshi, H.; Jacobson, K.; Kusumi, A. Phospholipids Undergo Hop Diffusion in Compartmentalized Cell Membrane. *J. Cell Biol.* **2002**, *157* (6), 1071–1082. https://doi.org/10.1083/jcb.200202050.

(37) Mukherjee, S.; Maxfield, F. R. MEMBRANE DOMAINS. *Annu. Rev. Cell Dev. Biol.* **2004**, *20* (1), 839–866. https://doi.org/10.1146/annurev.cellbio.20.010403.095451.

(38) Lindner, R.; Naim, H. Y. Domains in Biological Membranes. *Exp. Cell Res.* **2009**, *315* (17), 2871–2878. https://doi.org/10.1016/j.yexcr.2009.07.020.

(39) Feigenson, G. W. Phase Diagrams and Lipid Domains in Multicomponent Lipid Bilayer Mixtures. *Biochim. Biophys. Acta BBA - Biomembr.* **2009**, *1788* (1), 47–52. https://doi.org/10.1016/j.bbamem.2008.08.014.

(40) Korlach, J.; Schwille, P.; Webb, W. W.; Feigenson, G. W. Characterization of Lipid Bilayer Phases by Confocal Microscopy and Fluorescence Correlation Spectroscopy. *Proc. Natl. Acad. Sci.* **1999**, *96* (15), 8461–8466. https://doi.org/10.1073/pnas.96.15.8461.

(41) Wan, C.; Kiessling, V.; Tamm, L. K. Coupling of Cholesterol-Rich Lipid Phases in Asymmetric Bilayers. *Biochemistry* **2008**, *47* (7), 2190–2198. https://doi.org/10.1021/bi7021552.

(42) Niemela, P. S.; Ollila, S.; Hyvonen, M. T.; Kattunen, M.; Vattulainen, I. Assessing the Nature of Lipid Raft Membranes. *PLOS Comp. Biol*. **2007**, 3(2), 34.

(43) Chamberlain, L. H. Detergents as Tools for the Purification and Classification of Lipid Rafts. *FEBS Lett.* **2004**, *559* (1–3), 1–5. https://doi.org/10.1016/S0014-5793(04)00050-X.

(44) Dinic, J.; Ashrafzadeh, P.; Parmryd, I. Actin Filaments Attachment at the Plasma Membrane in Live Cells Cause the Formation of Ordered Lipid Domains. *Biochim. Biophys. Acta BBA - Biomembr.* **2013**, *1828* (3), 1102–1111. https://doi.org/10.1016/j.bbamem.2012.12.004.

(45) Owen, D. M.; Magenau, A.; Williamson, D.; Gaus, K. The Lipid Raft Hypothesis Revisited - New Insights on Raft Composition and Function from Super-Resolution Fluorescence Microscopy. *BioEssays* **2012**, *34* (9), 739–747. https://doi.org/10.1002/bies.201200044.

(46) Owen, D. M.; Williamson, D. J.; Magenau, A.; Gaus, K. Sub-Resolution Lipid Domains Exist in the Plasma Membrane and Regulate Protein Diffusion and Distribution. *Nat. Commun.* **2012**, *3* (1), 1256. https://doi.org/10.1038/ncomms2273.

(47) Nicolau, D. V.; Burrage, K.; Parton, R. G.; Hancock, J. F. Identifying Optimal Lipid Raft Characteristics Required To Promote Nanoscale Protein-Protein Interactions on the Plasma Membrane. *Mol. Cell. Biol.* **2006**, *26* (1), 313–323. https://doi.org/10.1128/MCB.26.1.313-323.2006.

(48) Shaw, A. S. Lipid Rafts: Now You See Them, Now You Don't. *Nat. Immunol.* **2006**, *7* (11), 1139–1142. https://doi.org/10.1038/ni1405.

(49) Yi, J.; Balagopalan, L.; Nguyen, T.; McIntire, K. M.; Samelson, L. E. TCR microclusters form spatially segregated domains and sequentially assemble in calcium- dependent kinetic steps. *Nat. Comm.* **2019**, 10(277).

(50) Maity, P.C .; Yang, J.; Klaesener, K.; Reth, M. The nanoscale organization of the B lymphocyte membrane. *Biochimica et Biophys. Acta*. **2015**, 1853, 830-840.

(51) Duncan, A. L.; Reddy, T.; Koldsø, H.; Hélie, J.; Fowler, P. W.; Chavent, M.; Sansom, M. S. P. Protein Crowding and Lipid Complexity Influence the Nanoscale Dynamic

Organization of Ion Channels in Cell Membranes. *Sci. Rep.* **2017**, *7* (1), 16647. https://doi.org/10.1038/s41598-017-16865-6.

(52) Koldsø, H.; Sansom, M. S. P. Organization and Dynamics of Receptor Proteins in a Plasma Membrane. *J. Am. Chem. Soc.* **2015**, *137* (46), 14694–14704. https://doi.org/10.1021/jacs.5b08048.

(53) Lommerse, P. H. M.; Spaink, H. P.; Schmidt, T. In Vivo Plasma Membrane Organization: Results of Biophysical Approaches. *Biochim. Biophys. Acta BBA - Biomembr.* **2004**, *1664* (2), 119–131. https://doi.org/10.1016/j.bbamem.2004.05.005.

(54) Bagatolli, L. A. To See or Not to See: Lateral Organization of Biological Membranes and Fluorescence Microscopy. *Biochim. Biophys. Acta BBA - Biomembr.* **2006**, *1758* (10), 1541–1556. https://doi.org/10.1016/j.bbamem.2006.05.019.

(55) Cairo, C. W.; Golan, D. E. T Cell Adhesion Mechanisms Revealed by Receptor Lateral Mobility. *Biopolymers* **2008**, *89* (5), 409–419. https://doi.org/10.1002/bip.20898.

(56) Ramadurai, S.; Holt, A.; Krasnikov, V.; van den Bogaart, G.; Killian, J. A.; Poolman, B. Lateral Diffusion of Membrane Proteins. *J. Am. Chem. Soc.* **2009**, *131* (35), 12650–12656. https://doi.org/10.1021/ja902853g.

(57) Auth, T.; Gov, N. S. Diffusion in a Fluid Membrane with a Flexible Cortical Cytoskeleton. *Biophys. J.* **2009**, *96* (3), 818–830. https://doi.org/10.1016/j.bpj.2008.10.038.

(58) Saha, S.; Lee, I.-H.; Polley, A.; Groves, J. T.; Rao, M.; Mayor, S. Diffusion of GPI-Anchored Proteins Is Influenced by the Activity of Dynamic Cortical Actin. *Mol. Biol. Cell* **2015**, *26* (22), 4033–4045. https://doi.org/10.1091/mbc.E15-06-0397.

(59) Koppel, D. E.; Sheetz, M. P.; Schindler, M. Matrix Control of Protein Diffusion in Biological Membranes. *Proc. Natl. Acad. Sci.* **1981**, *78* (6), 3576–3580. https://doi.org/10.1073/pnas.78.6.3576.

(60) Gómez-Llobregat, J.; Buceta, J.; Reigada, R. Interplay of Cytoskeletal Activity and Lipid Phase Stability in Dynamic Protein Recruitment and Clustering. *Sci. Rep.* **2013**, *3* (1), 2608. https://doi.org/10.1038/srep02608.

(61) Lenne, P.-F.; Wawrezinieck, L.; Conchonaud, F.; Wurtz, O.; Boned, A.; Guo, X.-J.; Rigneault, H.; He, H.-T.; Marguet, D. Dynamic Molecular Confinement in the Plasma Membrane by Microdomains and the Cytoskeleton Meshwork. *EMBO J.* **2006**, *25* (14), 3245–3256. https://doi.org/10.1038/sj.emboj.7601214.

(62) Javanainen, M.; Martinez-Seara, H.; Metzler, R.; Vattulainen, I. Diffusion of Integral Membrane Proteins in Protein-Rich Membranes. *J. Phys. Chem. Lett.* **2017**, *8* (17), 4308–4313. https://doi.org/10.1021/acs.jpclett.7b01758.

(63) Braeckmans, K.; Peeters, L.; Sanders, N. N.; De Smedt, S. C.; Demeester, J. Three-Dimensional Fluorescence Recovery after Photobleaching with the Confocal Scanning

Laser Microscope. *Biophys. J.* **2003**, *85* (4), 2240–2252. https://doi.org/10.1016/S0006-3495(03)74649-9.

(64) Axelrod, D.; Koppel, D. E.; Schlessinger, J.; Elson, E.; Webb, W. W. Mobility Measurement by Analysis of Fluorescence Photobleaching Recovery Kinetics. *Biophys. J.* **1976**, *16* (9), 1055–1069. https://doi.org/10.1016/S0006-3495(76)85755-4.

(65) Qian, H.; Sheetz, M. P.; Elson, E. L. Single Particle Tracking. Analysis of Diffusion and Flow in Two-Dimensional Systems. *Biophys. J.* **1991**, *60* (4), 910–921. https://doi.org/10.1016/S0006-3495(91)82125-7.

(66) Saxton, M. J. Single-Particle Tracking: The Distribution of Diffusion Coefficients. *Biophys. J.* **1997**, *72* (4), 1744–1753. https://doi.org/10.1016/S0006-3495(97)78820-9.

(67) Saxton, M. J.; Jacobson, K. SINGLE-PARTICLE TRACKING:Applications to Membrane Dynamics. *Annu. Rev. Biophys. Biomol. Struct.* **1997**, *26* (1), 373–399. https://doi.org/10.1146/annurev.biophys.26.1.373.

(68) Alcor, D.; Gouzer, G.; Triller, A. Single-Particle Tracking Methods for the Study of Membrane Receptors Dynamics. *Eur. J. Neurosci.* **2009**, *30* (6), 987–997. https://doi.org/10.1111/j.1460-9568.2009.06927.x.

(69) Jaqaman, K.; Loerke, D.; Mettlen, M.; Kuwata, H.; Grinstein, S.; Schmid, S. L.; Danuser, G. Robust Single-Particle Tracking in Live-Cell Time-Lapse Sequences. *Nat. Methods* **2008**, *5* (8), 695–702. https://doi.org/10.1038/nmeth.1237.

(70) Wilson, T. Resolution and Optical Sectioning in the Confocal Microscope: PROPERTIES OF THE FLUORESCENT CONFOCAL MICROSCOPE. *J. Microsc.* **2011**, *244* (2), 113–121. https://doi.org/10.1111/j.1365-2818.2011.03549.x.

(71) Bugaj, L. J.; Choksi, A. T.; Mesuda, C. K.; Kane, R. S.; Schaffer, D. V. Optogenetic Protein Clustering and Signaling Activation in Mammalian Cells. *Nat. Methods*. **2013**, 10(3).

(72) Chichili, G. R. Clustering of Membrane Raft Proteins by the Actin Cytoskeleton. *J. Biol. Chem*. **2007**, *282* (50), 10.

(73) Tkachenko, E. Clustering Induces Redistribution of Syndecan-4 Core Protein into Raft Membrane Domains. *J. Biol. Chem*. **2002**, 277(22), 19946-19951.

(74) Wallrabe, H.; Elangovan, M.; Burchard, A.; Periasamy, A.; Barroso, M. Confocal FRET Microscopy to Measure Clustering of Ligand-Receptor Complexes in Endocytic Membranes. *Biophys. J.* **2003**, *85* (1), 559–571. https://doi.org/10.1016/S0006-3495(03)74500-7.

(75) Belyy, V.; Tran, N.-H.; Walter, P. Quantitative Microscopy Reveals Dynamics and Fate of Clustered IRE1α. *Proc. Natl. Acad. Sci.* **2020**, *117* (3), 1533–1542. https://doi.org/10.1073/pnas.1915311117.

(76) Galbraith, C. G.; Galbraith, J. A. Super-Resolution Microscopy at a Glance. *J. Cell Sci.* **2011**, *124* (10), 1607–1611. https://doi.org/10.1242/jcs.080085.

(77) Schermelleh, L.; Ferrand, A.; Huser, T.; Eggeling, C.; Sauer, M.; Biehlmaier, O.; Drummen, G. P. C. Super-Resolution Microscopy Demystified. *Nat. Cell Biol.* **2019**, *21* (1), 72–84. https://doi.org/10.1038/s41556-018-0251-8.

(78) Durisic, N. Quantitative Super-Resolution Microscopy: Pitfalls and Strategies for Image Analysis. *Curr. Opin. Chem. Biol.* **2014**, 20, 22-28.

(79) Fornasiero, E. F.; Opazo, F. Super-resolution Imaging for Cell Biologists. *Bioessays*. **2015**, 37(4), 436-451.

(80) Lambert, T. J.; Waters, J. C. Navigating Challenges in the Application of Superresolution Microscopy. *J. Cell Biol*. **2017**, 216(1), 53-63.

(81) Hardy, R. R.; Hayakawa, K. B cell development pathways. *Annu. Rev. Immunol.* **2001**, *19* (1), 595–621. https://doi.org/10.1146/annurev.immunol.19.1.595.

(82) Guo, B.; Kato, R. M.; Garcia-Lloret, M.; Wahl, M. I.; Rawlings, D. J. Engagement of the Human Pre-B Cell Receptor Generates a Lipid Raft–Dependent Calcium Signaling Complex. *Immunity* **2000**, *13* (2), 243–253. https://doi.org/10.1016/S1074-7613(00)00024-8.

(83) Reth, M.; Hombach, J.; Wienands, J.; Campbell, K. S.; Chien, N.; Justement, L. B.; Cambier, J. C. The B-Cell Antigen Receptor Complex. *Immunol. Today* **1991**, *12* (6), 196–201. https://doi.org/10.1016/0167-5699(91)90053-V.

(84) Gupta, N.; DeFranco, A. L. Visualizing Lipid Raft Dynamics and Early Signaling Events during Antigen Receptor-Mediated B-Lymphocyte Activation□V. *Mol. Biol. Cell* **2003**, *14* (2), 432–444. https://doi.org/www.molbiolcell.org/cgi/doi/10.1091/mbc.02– 05– 0078.

(85) Saeki, K. The B Cell-Specific Major Raft Protein, Raftlin, Is Necessary for the Integrity of Lipid Raft and BCR Signal Transduction. *EMBO J.* **2003**, *22* (12), 3015–3026. https://doi.org/10.1093/emboj/cdg293.

(86) Mattila, P. K.; Batista, F. D.; Treanor, B. Dynamics of the actin cytosketon mediates receptor cross talk: An emerging concept in tuning receptor signaling. *J. Cell Biol*. **2016**, 212 (3), 267-180.

(87) Treanor, B.; Depoli, D.; Gonzalez-Granja, A.; Barral, P.; Weber, M.; Dushek, O.; Bruckbauer, A.; Batista, F. The Membrane Skeleton Controls Diffusion Dynamics and Signaling through the B Cell Receptor. *Immunity*. **2010**, 32, 187-199.

(88) Song, W.; Liu, C.; Upadhyaya, A. The pivotal position of the actin cytoskeleton in the initiation and regulation of B cell receptor activation. *Biochim. Biophysic. Acta.* **2014**, 1838, 569-578.

(89) Treanor, B. B-cell receptor: from resting state to activate. *Immunol*. **2012**, 136, 21-27.

(90) Bonilla, F. A.; Oettgen, H. C. Adaptive Immunity. *J. Allergy Clin. Immunol.* **2010**, *125* (2), S33–S40. https://doi.org/10.1016/j.jaci.2009.09.017.

(91) Lleo, A.; Invernizzi, P.; Gao, B.; Podda, M.; Gershwin, M. E. Definition of Human Autoimmunity — Autoantibodies versus Autoimmune Disease. *Autoimmun. Rev.* **2010**, *9* (5), A259–A266. https://doi.org/10.1016/j.autrev.2009.12.002.

(92) Naparstekt, Y. The Role of Autoantibodies in Autoimmune Disease. *Ann. Rev. Immunol*. **1993**, 11(1), 79-104.

(93) Scofield, R. H. Autoantibodies as Predictors of Disease. *THE LANCET* **2004**, *363*, 3.

(94) Firestein, G. S. Evolving Concepts of Rheumatoid Arthritis. *Nature* **2003**, *423* (6937), 356–361. https://doi.org/10.1038/nature01661.

(95) McInnes, I. B. The Pathogenesis of Rheumatoid Arthritis. *N. Engl. J. Med.* **2011**, 15.

(96) Edwards, J. C. W.; Szechinski, J.; Emery, P.; Shaw, T. Efficacy of B-Cell–Targeted Therapy with Rituximab in Patients with Rheumatoid Arthritis. *N. Engl. J. Med.* **2004**, 10.

(97) Grammer, A. C.; Lipsky, P. E. B Cell Abnormalities in systemic lupus erythematosus. *Arthritis Res. Ther.* **2003**, *5*, S22. https://doi.org/10.1186/ar1009.

(98) Kozyrev, S. V.; Abelson, A.-K.; Wojcik, J.; Zaghlool, A.; Linga Reddy, M. V. P.; Sanchez, E.; Gunnarsson, I.; Svenungsson, E.; Sturfelt, G.; Jönsen, A.; Truedsson, L.; Pons-Estel, B. A.; Witte, T.; D'Alfonso, S.; Barizzone, N.; Danieli, M. G.; Gutierrez, C.; Suarez, A.; Junker, P.; Laustrup, H.; González-Escribano, M. F.; Martin, J.; Abderrahim, H.; Alarcón-Riquelme, M. E. Functional Variants in the B-Cell Gene BANK1 Are Associated with Systemic Lupus Erythematosus. *Nat. Genet.* **2008**, *40* (2), 211–216. https://doi.org/10.1038/ng.79.

(99) Yurasov, S.; Wardemann, H.; Hammersen, J.; Tsuiji, M.; Meffre, E.; Pascual, V.; Nussenzweig, M. C. Defective B Cell Tolerance Checkpoints in Systemic Lupus Erythematosus. *J. Exp. Med.* **2005**, *201* (5), 703–711. https://doi.org/10.1084/jem.20042251.

(100) Royer, B.; Cazals-Hatem, D.; Sibilia, J.; Agbalika, F.; Cayuela, J.-M.; Soussi, T.; Maloisel, F.; Clauvel, J.-P.; Brouet, J.-C.; Mariette, X. Lymphomas in Patients With Sjögren's Syndrome Are Marginal Zone B-Cell Neoplasms, Arise in Diverse Extranodal and Nodal Sites, and Are Not Associated With Viruses. *Blood* **1997**, *90* (2), 766–775. https://doi.org/10.1182/blood.V90.2.766.

(101) Shen, L.; Gao, C.; Suresh, L.; Xian, Z.; Song, N.; Chaves, L. D.; Yu, M.; Ambrus, J. L. Central Role for Marginal Zone B Cells in an Animal Model of Sjogren's Syndrome. *Clin. Immunol.* **2016**, *168*, 30–36. https://doi.org/10.1016/j.clim.2016.04.008.

(102) Chen, M.-P.; Chung, F.-M.; Chang, D.-M.; Tsai, J. C.-R.; Huang, H.-F.; Shin, S.-J.; Lee, Y.-J. Elevated Plasma Level of Visfatin/Pre-B Cell Colony-Enhancing Factor in Patients with Type 2 Diabetes Mellitus. *J. Clin. Endocrinol. Metab.* **2006**, *91* (1), 295–299. https://doi.org/10.1210/jc.2005-1475.

(103) Cepok, S.; Rosche, B.; Grummel, V.; Vogel, F.; Zhou, D.; Sayn, J.; Sommer, N.; Hartung, H.-P.; Hemmer, B. Short-Lived Plasma Blasts Are the Main B Cell Effector Subset during the Course of Multiple Sclerosis. *Brain* **2005**, *128* (7), 1667–1676. https://doi.org/10.1093/brain/awh486.

(104) Kinnunen, T.; Chamberlain, N.; Morbach, H.; Cantaert, T.; Lynch, M.; Preston-Hurlburt, P.; Herold, K. C.; Hafler, D. A.; O'Connor, K. C.; Meffre, E. Specific Peripheral B Cell Tolerance Defects in Patients with Multiple Sclerosis. *J. Clin. Invest.* **2013**, *123* (6), 2737–2741. https://doi.org/10.1172/JCI68775.

(105) Li, R.; Rezk, A.; Miyazaki, Y.; Hilgenberg, E.; Touil, H.; Shen, P.; Moore, C. S.; Michel, L.; Althekair, F.; Rajasekharan, S.; Gommerman, J. L.; Prat, A.; Fillatreau, S.; Bar-Or, A.; on behalf of the Canadian B cells in MS Team. Proinflammatory GM-CSF–Producing B Cells in Multiple Sclerosis and B Cell Depletion Therapy. *Sci. Transl. Med.* **2015**, *7* (310), 310ra166-310ra166. https://doi.org/10.1126/scitranslmed.aab4176.

(106) Rawlings, D. J.; Metzler, G.; Wray-Dutra, M.; Jackson, S. W. Altered B cells signaling and autoimmunity. *Immunol*. **2017**, 17, 421-436.

(107) Reff, M.; Carner, K.; Chambers, K.; Chinn, P.; Leonard, J.; Raab, R.; Newman, R.; Hanna, N.; Anderson, D. Depletion of B Cells in Vivo by a Chimeric Mouse Human Monoclonal Antibody to CD20. *Blood* **1994**, *83* (2), 435–445. https://doi.org/10.1182/blood.V83.2.435.435.

(108) Hamaguchi, Y.; Xiu, Y.; Komura, K.; Nimmerjahn, F.; Tedder, T. F. Antibody Isotype-Specific Engagement of Fcγ Receptors Regulates B Lymphocyte Depletion during CD20 Immunotherapy. *J. Exp. Med.* **2006**, *203* (3), 743–753. https://doi.org/10.1084/jem.20052283.

(109) Uchida, J.; Hamaguchi, Y.; Oliver, J. A.; Ravetch, J. V.; Poe, J. C.; Haas, K. M.; Tedder, T. F. The Innate Mononuclear Phagocyte Network Depletes B Lymphocytes through Fc Receptor–Dependent Mechanisms during Anti-CD20 Antibody Immunotherapy. *J. Exp. Med.* **2004**, *199* (12), 1659–1669. https://doi.org/10.1084/jem.20040119.

(110) Barr, T. A.; Shen, P.; Brown, S.; Lampropoulou, V.; Roch, T.; Lawrie, S.; Fan, B.; O'Connor, R. A.; Anderton, S. M.; Bar-Or, A.; Fillatreau, S.; Gray, D. B Cell Depletion Therapy Ameliorates Autoimmune Disease through Ablation of IL-6–Producing B Cells. *J. Exp. Med.* **2012**, *209* (5), 1001–1010. https://doi.org/10.1084/jem.20111675.

(111) Nitschke, L. The Role of CD22 and Other Inhibitory Co-Receptors in B-Cell Activation. *Curr. Opin. Immunol.* **2005**, *17* (3), 290–297. https://doi.org/10.1016/j.coi.2005.03.005.

(112) Pritchard, N. R.; Smith, K. G. C. B Cell Inhibitory Receptors and Autoimmunity. *Immunology* **2003**, *108* (3), 263–273. https://doi.org/10.1046/j.1365-2567.2003.01592.x.

(113) Brooks, D. G.; Qiu, W. Q.; Luster, A. D.; Ravetch, J. V. Structure and Expression of Human IgG FcRII(CD32). Functional Heterogeneity Is Encoded by the Alternatively Spliced Products of Multiple Genes. *J. Exp. Med.* **1989**, *170* (4), 1369–1385. https://doi.org/10.1084/jem.170.4.1369.

(114) Tridandapani, S.; Kelley, T.; Pradhan, M.; Cooney, D.; Justement, L. B.; Coggeshall, K. M. Recruitment and Phosphorylation of SH2-Containing Inositol Phosphatase and Shc to the B-Cell Fc Gamma Immunoreceptor Tyrosine-Based Inhibition Motif Peptide Motif. *Mol. Cell. Biol.* **1997**, *17* (8), 4305–4311. https://doi.org/10.1128/MCB.17.8.4305.

(115) Ondee, T.; Surawut, S.; Taratummarat, S.; Hirankarn, N.; Palaga, T.; Pisitkun, P.; Pisitkun, T.; Leelahavanichkul, A. Fc Gamma Receptor IIB Deficient Mice: A Lupus Model with Increased Endotoxin Tolerance-Related Sepsis Susceptibility. *Shock* **2017**, *47* (6), 743–752. https://doi.org/10.1097/SHK.0000000000000796.

(116) Nitschke, L.; Carsetti, R.; Ocker, B.; Köhler, G.; Lamers, M. C. CD22 Is a Negative Regulator of B-Cell Receptor Signalling. *Curr. Biol.* **1997**, *7* (2), 133–143. https://doi.org/10.1016/S0960-9822(06)00057-1.

(117) Tedder, T. F.; Tuscano, J.; Sato, S.; Kehrl, J. H. CD22, A B LYMPHOCYTE–SPECIFIC ADHESION MOLECULE THAT REGULATES ANTIGEN RECEPTOR SIGNALING *. *Annu. Rev. Immunol.* **1997**, *15* (1), 481–504. https://doi.org/10.1146/annurev.immunol.15.1.481.

(118) Ereño-Orbea, J.; Sicard, T.; Cui, H.; Mazhab-Jafari, M. T.; Benlekbir, S.; Guarné, A.; Rubinstein, J. L.; Julien, J.-P. Molecular Basis of Human CD22 Function and Therapeutic Targeting. *Nat. Commun.* **2017**, *8* (764), 1–11. https://doi.org/10.1038/s41467-017-00836-6.

(119) Otipoby, K. L.; Draves, K. E.; Clark, E. A. CD22 Regulates B Cell Receptor-Mediated Signals via Two Domains That Independently Recruit Grb2 and SHP-1. *J. Biol. Chem.* **2001**, *276* (47), 44315–44322. https://doi.org/10.1074/jbc.M105446200.

(120) Doody, G.; Justement, L.; Delibrias, C.; Matthews, R.; Lin, J.; Thomas, M.; Fearon, D. A Role in B Cell Activation for CD22 and the Protein Tyrosine Phosphatase SHP. *Science* **1995**, *269* (5221), 242–244. https://doi.org/10.1126/science.7618087.

(121) Clark, E. A.; Giltiay, N. CD22: A Regulator of Innate and Adaptive B Cell Responses and Autoimmunity. *Frontiers in Immunol*. **2018**, 2235 (9).

(122) O'Keefe, T. L.; Williams, G. T.; Davies, S. L.; Neuberger, M. S. Hyperresponsive B Cells in CD22-Deficient Mice. *Science* **1996**, *274* (5288), 798–801. https://doi.org/10.1126/science.274.5288.798.

(123) Chen, J.; McLean, P. A.; Neel, B. G.; Okunade, G.; Shull, G. E.; Wortis, H. H. CD22 attenuates calcium signaling by potentiating plasma membrane calcium-ATPase activity. *Nat. Immunol*. **2004**, 6(5), 651-657.

(124) Chen, J.; Wang, H.; Xu, W.; Wei, S.; Li, H. J.; Mei, Y.; Li, Y.; Wang, Y. *Oncotarget*. **2016**. 35(7). 56129-56146.

(125) Enterina, J. R.; Jung, J.; Macauley, M. S. Coordinated roles for glycans in regulating the inhibitory function of CD22 on B cells. *Biomed. J*. **2019**, 42, 218-232.

(126) Meyer, S. J.; Steffensen, M.; Acs, A.; Wesenburger, T.; Wadewitz, C.; Winkler, T. H.; Nitschke, L. *J. Immunol*. **2021**, 207(4), 1018-1032.

(127) Enterina, J. R.; Sarkar, S.; Streith, L.; Jung, J.; Arlian, B. M.; Meyer, S. J.; Takematsu, H.; Xiao, C.; Baldwin, T. A.; Nitschke, L.; Shlomchick, M. J.; Paulson, J. C.; Macauley, M. S. *Cell Reports*. **2022**, 38(11), 110512.

(128) Hass, K. M.; Johnson, K. L.; Phipps, J. P.; Do, C. CD22 promotes B-1b Cell Responses to T Cell-Independent Type 2 Antigens. *J. Immunol*. **2018**, 200, 1671-1681.

(129) Razi, N.; Varki, A. Masking and Unmasking of the Sialic Acid-Binding Lectin Activity of CD22 (Siglec-2) on B Lymphocytes. *Proc. Natl. Acad. Sci.* **1998**, *95* (13), 7469–7474. https://doi.org/10.1073/pnas.95.13.7469.

(130) Coughlin, S.; Noviski, M.; Mueller, J. L.; Chuwonpad, A.; Raschke, W.; Weiss, A.; Zikherman, J. An extracatalytic function of CD45 in B cells is mediated by CD22. *PNAS*. **2015**, 112(47), E6515-E6524.

(131) Muller, J.; Obermeier, I.; Wohner, M.; Brandl, C.; Mrotzek, S.; Angermuller, S.; Maity, P. C.; Reth, M.; Nitschke, L. CD22 Ligand-Binding and Signaling Domains Reciprocally Regulate B-Cell Ca2+ Signaling. *Proc. Natl. Acad. Sci.* **2013**, *110* (30), 12402–12407. https://doi.org/10.1073/pnas.1304888110.

(132) Cao, A.; Alluqmani, N.; Buhari, F. H. M.; Wasim, L.; Smith, L. K.; Quaile, A.; Shannon, M.; Hakim, Z.; Furmli, H.; Owen, D. M.; Savchenko, A.; Treanor, B. Galectin-9 binds IgM-BCR to regulate B cell siganlling. *Nat. Comm*. **2018**, 9, 3288.

(133) Meyer, S. J.; Boser, A.; Korn, M. A.; Koller, C.; Bertocci, B.; Reimann, L.; Warscheid, B.; Nitschke, L. Cullin 3 Is Crucial for Pro-B Cell Proliferation, Interacts with CD22, and Controls CD22 Internalization on B cells. *J. Immunol*. **2020**, 204, 3360-3374.

(134) Collins, B. E.; Smith, B. A.; Bengtson, P.; Paulson, J. C. Ablation of CD22 in Ligand-Deficient Mice Restores B Cell Receptor Signaling. *Nat. Immunol.* **2006**, *7* (2), 8.

(135) Macauley, M.; Paulson, J. Siglecs induce tolerance to cell surface antigens by BIM-dependent deletion of the antigen-reactive B cells. *J. Immunol*. **2014**, 193(9), 4312-4321.

(136) Collins, B. E.; Blixt, O.; DeSieno, A. R.; Bovin, N.; Marth, J. D.; Paulson, J. C. Masking of CD22 by Cis Ligands Does Not Prevent Redistribution of CD22 to Sites of Cell Contact. *Proc. Natl. Acad. Sci.* **2004**, *101* (16), 6104–6109. https://doi.org/10.1073/pnas.0400851101.

(137) Courtney, A. H.; Puffer, E. B.; Pontrello, J. K.; Yang, Z.-Q.; Kiessling, L. L. Sialylated Multivalent Antigens Engage CD22 *in Trans* and Inhibit B Cell Activation. *Proc. Natl. Acad. Sci.* **2009**, *106* (8), 2500–2505. https://doi.org/10.1073/pnas.0807207106.

(138) Macauley, M. S.; Pfrengle, F.; Rademacher, C.; Nycholat, C. M.; Gale, A. J. Antigenic Liposomes Displaying CD22 Ligands Induce Antigen-Specific B Cell Apoptosis. *J. Clin. Invest.* **2013**, *123* (7), 3074–3083. https://doi.org/10.1172/JCI69187.

(139) Chen, W. C.; Sigal, D. S.; Saven, A.; Paulson, J. C. Targeting B Lymphoma with Nanoparticles Bearing Glycan Ligands of CD22. *Leuk. Lymphoma* **2012**, *53* (2), 208–210. https://doi.org/10.3109/10428194.2011.604755.

(140) Daskhan, G. C.; Tran, H.-T. T.; Meloncelli, P. J.; Lowary, T. L.; West, L. J.; Cairo, C. W. Construction of Multivalent Homo- and Heterofunctional ABO Blood Group Glycoconjugates Using a Trifunctional Linker Strategy. *Bioconjug. Chem.* **2018**, *29* (2), 343–362. https://doi.org/10.1021/acs.bioconjchem.7b00679.

(141) Büll, C.; Heise, T.; Adema, G. J.; Boltje, T. J. Sialic Acid Mimetics to Target the Sialic Acid–Siglec Axis. *Trends Biochem. Sci.* **2016**, *41* (6), 519–531. https://doi.org/10.1016/j.tibs.2016.03.007.

(142) Kelm, S.; Gerlach, J.; Brossmer, R.; Danzer, C.-P.; Nitschke, L. The Ligand-Binding Domain of CD22 Is Needed for Inhibition of the B Cell Receptor Signal, as Demonstrated by a Novel Human CD22-Specific Inhibitor Compound. *J. Exp. Med.* **2002**, *195* (9), 1207–1213. https://doi.org/10.1084/jem.20011783.

(143) Rillahan, C. D.; Macauley, M. S.; Schwartz, E.; He, Y.; McBride, R.; Arlian, B. M.; Rangarajan, J.; Fokin, V. V.; Paulson, J. C. Disubstituted Sialic Acid Ligands Targeting Siglecs CD33 and CD22 Associated with Myeloid Leukaemias and B Cell Lymphomas. *Chem. Sci.* **2014**, *5* (6), 2398. https://doi.org/10.1039/c4sc00451e.

(144) Peng, W.; Paulson, J. C. CD22 Ligands on a Natural *N* -Glycan Scaffold Efficiently Deliver Toxins to B-Lymphoma Cells. *J. Am. Chem. Soc.* **2017**, *139* (36), 12450–12458. https://doi.org/10.1021/jacs.7b03208.

(145) Chen, W. C.; Completo, G. C.; Sigal, D. S.; Crocker, P. R.; Saven, A.; Paulson, J. C. In Vivo Targeting of B-Cell Lymphoma with Glycan Ligands of CD22. *Blood* **2010**, *115* (23), 4778–4786. https://doi.org/10.1182/blood-2009-12- 257386.

(146) Wasim, L.; Buhari, F. H. M.; Yoganathan, M.; Sicard, T.; Ereño-Orbea, J.; Julien, J.-P.; Treanor, B. N-Linked Glycosylation Regulates CD22 Organization and Function. *Front. Immunol.* **2019**, *10*, 699. https://doi.org/10.3389/fimmu.2019.00699.

(147) Cambi, A.; Lidke, D. S. Nanoscale Membrane Organization: Where Biochemistry Meets Advanced Microscopy. *ACS Chem. Biol.* **2012**, *7* (1), 139–149. https://doi.org/10.1021/cb200326g.

(148) Cairo, C. W.; Das, R.; Albohy, A.; Baca, Q. J.; Pradhan, D.; Morrow, J. S.; Coombs, D.; Golan, D. E. Dynamic Regulation of CD45 Lateral Mobility by the Spectrin-Ankyrin Cytoskeleton of T Cells. *J. Biol. Chem.* **2010**, *285* (15), 11392–11401. https://doi.org/10.1074/jbc.M109.075648.

(149) Lokeshwar, V. B.; Bourguignon, L. Y. Tyrosine Phosphatase Activity of Lymphoma CD45 (GP180) Is Regulated by a Direct Interaction with the Cytoskeleton. *J. Biol. Chem.* **1992**, *267* (30), 21551–21557. https://doi.org/10.1016/S0021-9258(19)36645-1.

(150) Pradhan, D.; Morrow, J. S. The Spectrin-Ankyrin Skeleton Controls CD45 Surface Display and Interleukin-2 Production. *Immunity* **2002**, *17* (3), 303–315. https://doi.org/10.1016/S1074-7613(02)00396-5.

(151) Roggentin, P.; Schauer, R.; Hoyer, L. L.; Vimr, E. R. The Sialidase Superfamily and Its Spread by Horizontal Gene Transfer. *Mol. Microbiol.* **1993**, *9* (5), 915–921. https://doi.org/10.1111/j.1365-2958.1993.tb01221.x.

(152) Cantarel, B. L.; Coutinho, P. M.; Rancurel, C.; Bernard, T.; Lombard, V.; Henrissat, B. The Carbohydrate-Active EnZymes Database (CAZy): An Expert Resource for Glycogenomics. *Nucleic Acids Res.* **2009**, *37* (Database issue), D233–D238. https://doi.org/10.1093/nar/gkn663.

(153) Miyagi, T.; Yamaguchi, K. Mammlian Sialidases: Physiological and Pathological Roles in Cellular Functions. *Glycobiology* **2012**, *22* (7), 880–896. https://doi.org/10.1093/glycob/cws057.

(154) Pshezhetsky, A. V.; Richard, C.; Michaud, L.; Igdoura, S.; Wang, S.; Elsliger, M.-A.; Qu, J.; Leclerc, D.; Gravel, R.; Dallaire, L.; Potier, M. Cloning, Expression and Chromosomal Mapping of Human Lysosomal Sialidase and Characterization of Mutations in Sialidosis. *Nat. Genet.* **1997**, *15* (3), 316–320. https://doi.org/10.1038/ng0397-316.

(155) Gee, K.; Kozlowski, M.; Kumar, A. Tumor Necrosis Factor-Alpha Induces Functionally Active Hyaluronan-Adhesive CD44 by Activating Sialidase through P38 Mitogen-Activated Protein Kinase in Lipopolysaccharide-Stimulated Human Monocytic Cells. *J. Biol. Chem.* **2003**, *278* (39), 37275–37287.

(156) Liang, F.; Seyrantepe, V.; Landry, K.; Ahmad, R.; Ahmad, A.; Stamatos, N. M.; Pshezhetsky, A. V. Monocyte Differentiation Up-Regulates the Expression of the Lysosomal Sialidase, Neu1, and Triggers Its Targeting to the Plasma Membrane via Major Histocompatibility Complex Class II-Positive Compartments. *J. Biol. Chem.* **2006**, *281* (37), 27526–27538. https://doi.org/10.1074/jbc.M605633200.

(157) Nan, X.; Carubelli, I.; Stamatos, N. M. Sialidase Expression in Activated Human T Lymphocytes Influences Production of IFN-γ. *J. Leukoc. Biol.* **2007**, *81* (1), 284–296. https://doi.org/10.1189/jlb.1105692.

(158) Liang, F.; Seyrantepe, V.; Landry, K.; Ahmad, R.; Ahmad, A.; Stamatos, N. M.; Pshezhetsky, A. V. Monocyte Differentiation Up-Regulates the Expression of the Lysosomal Sialidase, Neu1, and Triggers Its Targeting to the Plasma Membrane via Major Histocompatibility Complex Class II-Positive Compartments. *J. Biol. Chem.* **2006**, *281* (37), 27526–27538. https://doi.org/10.1074/jbc.M605633200.

(159) Nan, X.; Carubelli, I.; Stamatos, N. M. Sialidase Expression in Activated Human T Lymphocytes Influences Production of IFN-γ. *J. Leukoc. Biol.* **2007**, *81* (1), 284–296. https://doi.org/10.1189/jlb.1105692.

(160) Bonten, E. J.; Campos, Y.; Zaitsev, V.; Nourse, A.; Waddell, B.; Lewis, W.; Taylor, G.; d'Azzo, A. Heterodimerization of the Sialidase NEU1 with the Chaperone Protective Protein/Cathepsin A Prevents Its Premature Oligomerization. *J. Biol. Chem.* **2009**, *284* (41), 28430–28441. https://doi.org/10.1074/jbc.M109.031419.

(161) Luu, A. R.; Wong, C.; Agrawal, V.; Wise, N.; Handyside, B.; Lo, M. J.; Pacheco, G.; Felix, J. B.; Giaramita, A.; d'Azzo, A.; Vincelette, J.; Bullens, S.; Bunting, S.; Christianson, T. M.; Hague, C. M.; LeBowitz, J. H.; Yogalingam, G. Intermittent Enzyme Replacement Therapy with Recombinant Human β-Galactosidase Prevents Neuraminidase 1 Deficiency. *J. Biol. Chem.* **2020**, *295* (39), 13556–13569. https://doi.org/10.1074/jbc.RA119.010794.

(162) Wang, D.; Zaitsev, S.; Taylor, G.; d'Azzo, A.; Bonten, E. Protective Protein/Cathepsin A Rescues N-Glycosylation Defects in Neuraminidase-1. *Biochim. Biophys. Acta BBA - Gen. Subj.* **2009**, *1790* (4), 275–282. https://doi.org/10.1016/j.bbagen.2009.01.006.

(163) Pattison, S.; Pankarican, M.; Rupar, C. A.; Graham, F. L.; Igdoura, S. A. Five Novel Mutations in the Lysosomal Sialidase Gene (*NEU1*) in Type II Sialidosis Patients and Assessment of Their Impact on Enzyme Activity and Intracellular Targeting Using Adenovirus-Mediated Expression. *Hum. Mutat.* **2004**, *23* (1), 32–39. https://doi.org/10.1002/humu.10278.

(164) Seyrantepe, V.; Poupetova, H.; Froissart, R.; Zabot, M.-T.; Maire, I.; Pshezhetsky, A. V. Molecular Pathology of NEU1 Gene in Sialidosis. *Hum. Mutat.* **2003**, *22* (5), 343–352. https://doi.org/10.1002/humu.10268.

(165) de Geest, N. Systemic and Neurologic Abnormalities Distinguish the Lysosomal Disorders Sialidosis and Galactosialidosis in Mice. *Hum. Mol. Genet.* **2002**, *11* (12), 1455–1464. https://doi.org/10.1093/hmg/11.12.1455.

(166) Zhou, X.-Y.; Willemsen, R.; Berry, G. T.; Strisciuglio, P.; Andria, G. Molecular and Biochemical Analysis of Protective Protein/Cathepsin A Mutations: Correlation with Clinical Severity in Galactosialidosis. 11.

(167) Annunziata, I.; Patterson, A.; Helton, D.; Hu, H.; Moshiach, S.; Gomero, E.; Nixon, R.; d'Azzo, A. Lysosomal NEU1 Deficiency Affects Amyloid Precursor Protein Levels and Amyloid-β Secretion via Deregulated Lysosomal Exocytosis. *Nat. Commun.* **2013**, *4* (1), 2734. https://doi.org/10.1038/ncomms3734.

(168) Yogalingam, G.; Bonten, E. J.; van de Vlekkert, D.; Hu, H.; Moshiach, S.; Connell, S. A.; d'Azzo, A. Neuraminidase 1 Is a Negative Regulator of Lysosomal Exocytosis. *Dev. Cell* **2008**, *15* (1), 74–86. https://doi.org/10.1016/j.devcel.2008.05.005.

(169) Hou, G.; Liu, G.; Yang, Y.; Li, Y.; Yuan, S.; Zhao, L.; Wu, M.; Liu, L.; Zhou, W. Neuraminidase 1 (NEU1) Promotes Proliferation and Migration as a Diagnostic and Prognostic Biomarker of Hepatocellular Carcinoma. *Oncotarget* **2016**, *7* (40), 64957–64966. https://doi.org/10.18632/oncotarget.11778.

(170) Adamczyk, B.; Tharmalingam, T.; Rudd, P. M. Glycans as Cancer Biomarkers. *Biochim. Biophys. Acta BBA - Gen. Subj.* **2012**, *1820* (9), 1347–1353. https://doi.org/10.1016/j.bbagen.2011.12.001.

(171) Uemura, T.; Shiozaki, K.; Yamaguchi, K.; Miyazaki, S.; Satomi, S.; Kato, K.; Sakuraba, H.; Miyagi, T. Contribution of Sialidase NEU1 to Suppression of Metastasis of Human Colon Cancer Cells through Desialylation of Integrin B4. **2009**, 28, 1218-1229.

(172) Koseki, K.; Wada, T.; Hosono, M.; Hata, K.; Yamaguchi, K.; Nitta, K.; Miyagi, T. Human Cytosolic Sialidase NEU2-Low General Tissue Expression but Involvement in PC-3 Prostate Cancer Cell Survival. *Biochem. Biophys. Res. Commun.* **2012**, *428* (1), 142–149. https://doi.org/10.1016/j.bbrc.2012.10.028.

(173) Fanzani, A.; Colombo, F.; Giuliani, R.; Preti, A.; Marchesini, S. Cytosolic Sialidase Neu2 Upregulation during PC12 Cells Differentiation. *FEBS Lett.* **2004**, *566* (1–3), 178–182. https://doi.org/10.1016/j.febslet.2004.03.115.

(174) Fanzani, A.; Giuliani, R.; Colombo, F.; Zizioli, D.; Presta, M.; Preti, A.; Marchesini, S. Overexpression of Cytosolic Sialidase Neu2 Induces Myoblast Differentiation in C2C12 Cells. *FEBS Lett.* **2003**, *547* (1–3), 183–188. https://doi.org/10.1016/S0014-5793(03)00709-9.

(175) Monti, E.; Bassi, M. T.; Papini, N.; Riboni, M.; Manzoni, M.; Venerando, B.; Croci, G.; Preti, A.; Ballabio, A.; Tettamanti, G.; Borsani, G. Identification and Expression of NEU3, a Novel Human Sialidase Associated to the Plasma Membrane. *Biochem. J*. **2000**, 349(1), 343-351.

(176) Albohy, A.; Li, M. D.; Zheng, R. B.; Zou, C.; Cairo, C. W. Insight into Substrate Recognition and Catalysis by the Human Neuraminidase 3 (NEU3) through Molecular Modeling and Site-Directed Mutagenesis. *Glycobiology* **2010**, *20* (9), 1127–1138. https://doi.org/10.1093/glycob/cwq077.

(177) Scaringi, R.; Piccoli, M.; Papini, N.; Cirillo, F.; Conforti, E.; Bergante, S.; Tringali, C.; Garatti, A.; Gelfi, C.; Venerando, B.; Menicanti, L.; Tettamanti, G.; Anastasia, L. NEU3

Sialidase Is Activated under Hypoxia and Protects Skeletal Muscle Cells from Apoptosis through the Activation of the Epidermal Growth Factor Receptor Signaling Pathway and the Hypoxia-Inducible Factor (HIF)-1α. *J. Biol. Chem.* **2013**, *288* (5), 3153–3162. https://doi.org/10.1074/jbc.M112.404327.

(178) Howlader, Md. A.; Li, C.; Zou, C.; Chakraberty, R.; Ebesoh, N.; Cairo, C. W. Neuraminidase-3 Is a Negative Regulator of LFA-1 Adhesion. *Front. Chem.* **2019**, *7*, 791. https://doi.org/10.3389/fchem.2019.00791.

(179) Dustin, M. L.; Springer, T. A. T-Cell Receptor Cross-Linking Transiently Stimulates Adhesiveness through LFA-1. *Nature* **1989**, *341* (6243), 619–624. https://doi.org/10.1038/341619a0.

(180) Yamaguchi, K.; Koseki, K.; Shiozaki, M.; Shimada, Y.; Wada, T.; Miyagi, T. Regulation of Plasma-Membrane-Associated Sialidase NEU3 Gene by Sp1/Sp3 Transcription Factors. *Biochem. J.* **2010**, *430* (1), 107–117. https://doi.org/10.1042/BJ20100350.

(181) Miyagi, T.; Wada, T.; Yamaguchi, K. Roles of Plasma Membrane-Associated Sialidase NEU3 in Human Cancers. *Biochim. Biophys. Acta BBA - Gen. Subj.* **2008**, *1780* (3), 532–537. https://doi.org/10.1016/j.bbagen.2007.09.016.

(182) Kakugawa, Y.; Wada, T.; Yamaguchi, K.; Yamanami, H.; Ouchi, K.; Sato, I.; Miyagi, T. Up-Regulation of Plasma Membrane-Associated Ganglioside Sialidase (Neu3) in Human Colon Cancer and Its Involvement in Apoptosis Suppression. *Proc. Natl. Acad. Sci.* **2002**, *99* (16), 10718–10723. https://doi.org/10.1073/pnas.152597199.

(183) Ueno, S.; Saito, S.; Wada, T.; Yamaguchi, K.; Satoh, M.; Arai, Y.; Miyagi, T. Plasma Membrane-Associated Sialidase Is Up-Regulated in Renal Cell Carcinoma and Promotes Interleukin-6-Induced Apoptosis Suppression and Cell Motility. *J. Biol. Chem.* **2006**, *281* (12), 7756–7764. https://doi.org/10.1074/jbc.M509668200.

(184) Wada, T.; Hata, K.; Yamaguchi, K.; Shiozaki, K.; Koseki, K.; Moriya, S.; Miyagi, T. A Crucial Role of Plasma Membrane-Associated Sialidase in the Survival of Human Cancer Cells. *Oncogene* **2007**, *26* (17), 2483–2490. https://doi.org/10.1038/sj.onc.1210341.

(185) Karhadkar, T. R.; Chen, W.; Gomer, R. H. Attenuated Pulmonary Fibrosis in Sialidase-3 Knockout (*Neu3* $^{-/-}$) Mice. *Am. J. Physiol.-Lung Cell. Mol. Physiol.* **2020**, *318* (1), L165–L179. https://doi.org/10.1152/ajplung.00275.2019.

(186) Monti, E.; Bassi, M. T.; Bresciani, R.; Civini, S.; Croci, G. L.; Papini, N.; Riboni, M.; Zanchetti, G.; Ballabio, A.; Preti, A.; Tettamanti, G.; Venerando, B.; Borsani, G. Molecular Cloning and Characterization of NEU4, the Fourth Member of the Human Sialidase Gene Family. *Genomics* **2004**, *83* (3), 445–453. https://doi.org/10.1016/j.ygeno.2003.08.019.

(187) Seyrantepe, V.; Landry, K.; Trudel, S.; Hassan, J. A.; Morales, C. R.; Pshezhetsky, A. V. Neu4, a Novel Human Lysosomal Lumen Sialidase, Confers Normal Phenotype to Sialidosis and Galactosialidosis Cells. *J. Biol. Chem.* **2004**, *279* (35), 37021–37029. https://doi.org/10.1074/jbc.M404531200.

(188) Bigi, A.; Morosi, L.; Pozzi, C.; Forcella, M.; Tettamanti, G.; Venerando, B.; Monti, E.; Fusi, P. Human Sialidase NEU4 Long and Short Are Extrinsic Proteins Bound to Outer Mitochondrial Membrane and the Endoplasmic Reticulum, Respectively. *Glycobiology* **2010**, *20* (2), 148–157. https://doi.org/10.1093/glycob/cwp156.

(189) Yamaguchi, K.; Hata, K.; Koseki, K.; Shiozaki, K.; Akita, H.; Wada, T.; Moriya, S.; Miyagi, T. Evidence for Mitochondrial Localization of a Novel Human Sialidase (NEU4). *Biochem. J.* **2005**, *390* (1), 85–93. https://doi.org/10.1042/BJ20050017.

(190) Seyrantepe, V.; Canuel, M.; Carpentier, S.; Landry, K.; Durand, S.; Liang, F.; Zeng, J.; Caqueret, A.; Gravel, R. A.; Marchesini, S.; Zwingmann, C.; Michaud, J.; Morales, C. R.; Levade, T.; Pshezhetsky, A. V. Mice Deficient in Neu4 Sialidase Exhibit Abnormal Ganglioside Catabolism and Lysosomal Storage. *Hum. Mol. Genet.* **2008**, *17* (11), 1556–1568. https://doi.org/10.1093/hmg/ddn043.

(191) Silvestri, I.; Testa, F.; Zappasodi, R.; Cairo, C. W.; Zhang, Y.; Lupo, B.; Galli, R.; Di Nicola, M.; Venerando, B.; Tringali, C. Sialidase NEU4 Is Involved in Glioblastoma Stem Cell Survival. *Cell Death Dis.* **2014**, *5* (8), e1381–e1381. https://doi.org/10.1038/cddis.2014.349.

(192) Yamanami, H.; Shiozaki, K.; Wada, T.; Yamaguchi, K.; Uemura, T.; Kakugawa, Y.; Hujiya, T.; Miyagi, T. Down-Regulation of Sialidase NEU4 May Contribute to Invasive Properties of Human Colon Cancers. *Cancer Sci.* **2007**, *98* (3), 299–307. https://doi.org/10.1111/j.1349-7006.2007.00403.x.

CHAPTER 2. QUANTIFYING MEMBRANE RECEPTOR CLUSTERING ON B CELLS USING CONFOCAL MICROSCOPY

2.1 INTRODUCTION

The fluid mosaic model proposed by Singer and Nicolson envisions the cell membrane as a fluid-like phospholipid bilayer in which proteins and lipids are embedded.[1] Membrane proteins have many important functions for signalling and transport, and are critical targets for pharmaceutical agents.[2–4] The distribution of membrane proteins in the membrane is dynamic[5–7] and is influenced by factors including lipid composition,[8,9] lipid raft microdomains,[10,11] binding partners, and interaction with the underlying cytoskeleton. The dynamic organization of membrane proteins is important for their cellular functions and signalling processes. For example, B cell receptors (BCRs) crosslink with one another upon engagement of specific antigens, leading to phosphorylation of the cell receptor and immune response.[12,13] The activation of B cell receptor can be modulated by numerous co-receptors present on the membrane.[14] For instance, CD22 receptors are negative regulators of BCRs and the co-engagement of these receptors is crucial for their functions.[15,16] CD22 itself forms homotypic clusters through interactions of its lectin domain with glycans of other CD22 receptors. These clusters of CD22 diffuse to loci close to BCRs on the membrane, leading to CD22's phosphorylation on the cytoplasmic tail to de-phosphorylate and inhibit BCRs. Despite the importance of organization of membrane proteins for their function, it is challenging to quantify the distribution of specific receptors on the cell membrane due to the diffraction limit, background fluorescence, and the variability of cell and membrane topology.[17,18]

Single-molecule techniques have emerged to improve spatial and temporal resolution of fluorescence microscopy for the purpose of understanding dynamics and interaction of membrane proteins.[29,30] Fluorescence Correlation Spectroscopy (FCS) focuses the light within the volume of approximately 10^{-15} L and measures fluorescence fluctuations.[31] Fluctuations in fluorescence is due to the fluorophores moving in and out of the excitation volume or changing fluorescence emission, allowing for the analyses of density and diffusion of single molecules on the cell surface with low amounts of fluorophores. Since the illumination depth in this technique is thicker than the cell membrane, this technique has a high level of background. This limitation can be overcome by reducing the thickness of illumination which can be achieved by two-photon excitation[32] and total internal reflection (TIR).[33] The former technique uses pulses of infrared photons and only those fluorophores that absorb two photons concurrently are excited (at 2λ). This effectively eliminates the background fluorescence since the number of photons received by fluorophores is highest at the focal point and exponentially decreases with distance away from the focus. However, the use of two-photon illumination decreases the resolution due to the larger wavelength.[29] TIR Fluorescence (TIRF) microscopy achieves a high signal to noise ratio by exciting the fluorophores using evanescent wave.[34] This is a low intensity standing wave that is formed by total reflection of the incident light above a critical angle; it allows for illumination of only the fluorophores near the focal point which can be adjusted by changing the incident angle. Although these single-molecule techniques are useful for understanding dynamics and mechanisms of membrane proteins, TIRF microscopy is limited to visualization within 150 nm of the coverslip,[35] which may not be representative of the clustering characteristics of the proteins, therefore, a fluorescence method that allows imaging at greater depth may be desired.

Laser Scanning Confocal Microscopy (LSCM) is an imaging technique to improve optical resolution. This technique uses a pinhole as a physical barrier to block out-of-focus signal to allow imaging at one single focal plane.[19] As most of the signal is eliminated by the pinhole to increase the resolution, high intensity light and long exposure are required to compensate for the decreased signal. As a result, this technique may not be suitable for imaging of live cells and tissues to observe fast dynamics. However, since LCSM is useful for imaging and studying membrane proteins on fixed cells; it can give information on organization of proteins on the membrane on a thin optical section due to the absence of fluorescence signal from other planes and reduction of background. There are many examples of studies on membrane proteins using confocal microscopy for imaging and analysis, but they are heavily qualitative,[20–23] or their quantifications are complex, are arbitrary, or are not statistically significant.[24–28] Clustering, crowding, and interactions of membrane receptors are crucial for cellular processes, therefore, a robust method for quantitative analysis is needed to statistically study the proteins' characteristics such as cluster size and receptor numbers.

Super-resolution imaging has become a valuable method for visualization of protein localization in live cells below the diffraction limit, which is the spreading of light wave and is proportional the wavelength of light and to the numerical aperture of the objective. There are multiple strategies for super-resolution imaging which include stimulated emission microscopy (STED),[36] structured illumination microscopy (SIM),[37] stochastic optical reconstruction microscopy (STORM),[38] and photoactivated localization microscopy (PALM).[39] Although these techniques overcome the diffraction limit, they may require special reagents and sample preparation, long imaging times, and complicated analysis. On the other hand, confocal microscope techniques only requires simple sample preparation that is similar to that for wide-

field microscope, allowing us to obtain more data for quantitative analyses. Thus, depending on the purpose of the experiment, confocal microscope may be a more straightforward approach that is sufficient to obtain the information needed.

2.2 MATERIALS AND METHODS

Herein, we present a confocal microscope experiment to study and analyze the organization of CD22 receptors on B cell membrane. As mentioned above, clustering of CD22 receptors is crucial for their function as negative co-receptors of BCRs. However, the studies on CD22 receptors have been qualitative[40,41] or use super-resolution microscopes with complex analysis methods.[17,42] We were interested in developing a method whereby it is simple to perform and statistically meaningful data are collected and formed. To do this, we optimized the conditions for fixing, staining, and imaging of the receptors. We devised an imaging method using confocal microscopy to visualize the membrane receptors with high signal-to-noise ratio. We used the taken images to detect, analyzed, and statistically compared these receptors for their clustering characteristics. Using this method, we were able to quantify number and size of the clusters on cell membrane.

2.2.1 Culturing A-BCL cells

A-BCL cells[43] were thawed and seeded at the density of 10^5 cells/mL in 12 well plates (Corning., Inc) in R10 media supplemented with fresh glutamax and β-mercaptoethanol at a final concentration of 1%. Plates were kept in a humidified incubator at 37 °C and 5% CO_2. Every two days, the media were replaced. The cells were subcultured when the density reached 10^5 cells/mL as measure by hemocytometer using Trypan Blue. The cells at passage numbers between 3 and 7 were used to imaging and analyses.

2.2.2 Flow cytometry for staining and expression of receptors

A-BCL cells were prepared and grown as described above. To confirm the expression of CD22 and BCR cells were stained and quantified by flow cytometry. One million cells were spun and washed three times with phosphate buffered saline (PBS) by spinning at 300 x g for 15 min. Cells were fixed with 1% paraformyldehyde (PFA) on ice for 20 min. Fixed cells were washed three times with PBS and re-suspended in 1 mL PBS, then treated with antibodies against specific surface antigens conjugated to fluorophores (1 μg/mL mouse anti-CD22 antibody-AF647; 1 μg/mL mouse anti-CD22 antibody (clone HIB22, BD Pharmingen); 1 μg/mL rabbit anti-human IgM-AF488; or 1 μg/mL rabbit anti-human IgM) for one hour at room temperature. For indirect staining, samples were washed with PBS and stained with goat anti-mouse IgG (polyclonal, Sigma-Aldrich) conjugated with Alexa Fluor 647 and goat anti-rabbit IgG (polyclonal, Invitrogen) conjugated with Alexa Fluor 543 secondary antibodies for one hour at room temperature. Cells were then washed 3 times and re-suspended in PBS buffer. Cells were analyzed for receptor staining and expression using BD Accuri C6 (BD Biosciences).

2.2.3 Transmitted microscopy

A-BCL cells were prepared and grown as described above. For transmitted imaging, 2 X 10^6 cells were washed and treated with 2% glutaraldehyde for 20 minutes, 40 minutes, or 3 hours, or with 4% PFA for 20 minutes or 40 minutes, or 100% or 50% cold acetone for 10 minutes. The cells were washed three times and re-suspended in PBS. The fixed cells were then transferred to 24-well plates (Corning, Inc.,) loaded with 12 mm circular coverglass slides pre-treated with 0.001% Poly-L-Lysine (PLL) and spun at 300 x g for 15 min. Cover glass slides with samples were washed, mounted onto microscopy slides with PBS, and sealed with Cytoseal 60. Samples were imaged on a laser scanning confocal microscope (Olympus IX81) at 60X.

2.2.4 One-color confocal microscopy

A-BCL cells were prepared and grown as described above. For single-color fluorescence microscopy experiments, 2 x10^6 cells were washed and treated with 25 ng mL^{-1} of the indicated sample on ice for 1 h, then fixed using 1% PFA on ice for 20 min. Samples were treated with 1 μL mL^{-1} mouse anti-human IgM (clone IM260, Abcam) or mouse anti-human CD22 (clone HIB22, BD Pharmingen) at 4 °C overnight, washed, and stained with goat anti-mouse IgG (polyclonal, Sigma-Aldrich) conjugated with Alexa Flour 647 at room temperature for 1 h. The loading of the fluorophores was approximately 2 dye per protein as determined by spectrophotometry. After washing, samples were transferred to 24-well plates (Corning, Inc.) loaded with 12 mm circular cover glass slides pre-treated with 0.001% poly-L-lysine and spun at 300 x g for 15 min. Cover glass slides with samples were washed, mounted onto microscopy slides with Slowfade Antifade (Thermo Fisher), and sealed with Cytoseal 60. Samples were imaged on a laser scanning confocal microscope (Olympus IX81) at 60X. Ten cells from each condition were chosen for analysis based on transmitted and fluorescence images, in which each image was subjected to similar thresholding levels, and each cluster was analyzed using the particle analysis function on ImageJ. The area of a single-pixel in these images was 0.053 μm^2. The areas of each cluster from the analyses were plotted using beanplot in the R statistical package.[107] Analysis of the means and Student's t-test were performed in Graphpad Prism.

2.3 RESULTS AND DISCUSSIONS

2.3.1 Fixatives

In order to accurately visualize membrane proteins, it is important to employ a mild fixing method that ensures the suspension of cellular processes with minimal disruption of membrane integration, cell morphology, or protein structures.[44,45] Proteins on biological membrane are

dynamic and mobile, and diffusion is dependent on number of factors such as size, interactions with cytoskeletal proteins, protein crowding,[46,47] clustering, and compartmentalizations.[28,48] Quantification of membrane receptor distribution using this strategy requires that receptor diffusion in the membrane (lateral mobility) be arrested. The ideal fixing conditions may vary for individual cell lines and conditions, hence optimizing this parameter in sample preparation prior to obtaining data is crucial. A range of fixatives have been used for imaging research, classes include cross-linking agents, dehydrating agents, and oxidizing agents. Cross-linking agents including formaldehyde and glutaraldehyde which form covalent bonds between amino acids of cellular proteins, creating a rigid structure within cells;[49] dehydrating fixatives such as ethanol, methanol, and acetone disrupt hydrophobic interactions leading to the denaturing and proteins and aggregation.[50] We investigated some of these fixatives at different concentrations and duration of fixation. As shown in **Figure 1**, fixing A-BCL cells with 4% paraformaldehyde (PFA) disrupted cells' integration even after 20 min, while 2% glutaraldehyde allowed cells to retain their shapes even after 2 h. Fixing by dehydration using 100% cold acetone for 10 min also retained cell morphology, but some cells showed shrinkage; decreasing the concentration of cold acetone to 1:1 acetone:methanol improved this effect. From our results, we concluded that PFA was too harsh for A-BCL cells and glutaraldehyde or acetone were better choices. However, since acetone dehydrates phospholipids and disrupts hydrophobic interactions, it may not be an optimal fixative for studying membrane proteins. Hence, we proposed to use 2% glutaradehyde as our fixative in future optimizations, given this type of fixative does not give rise to any complications that may affect our results.

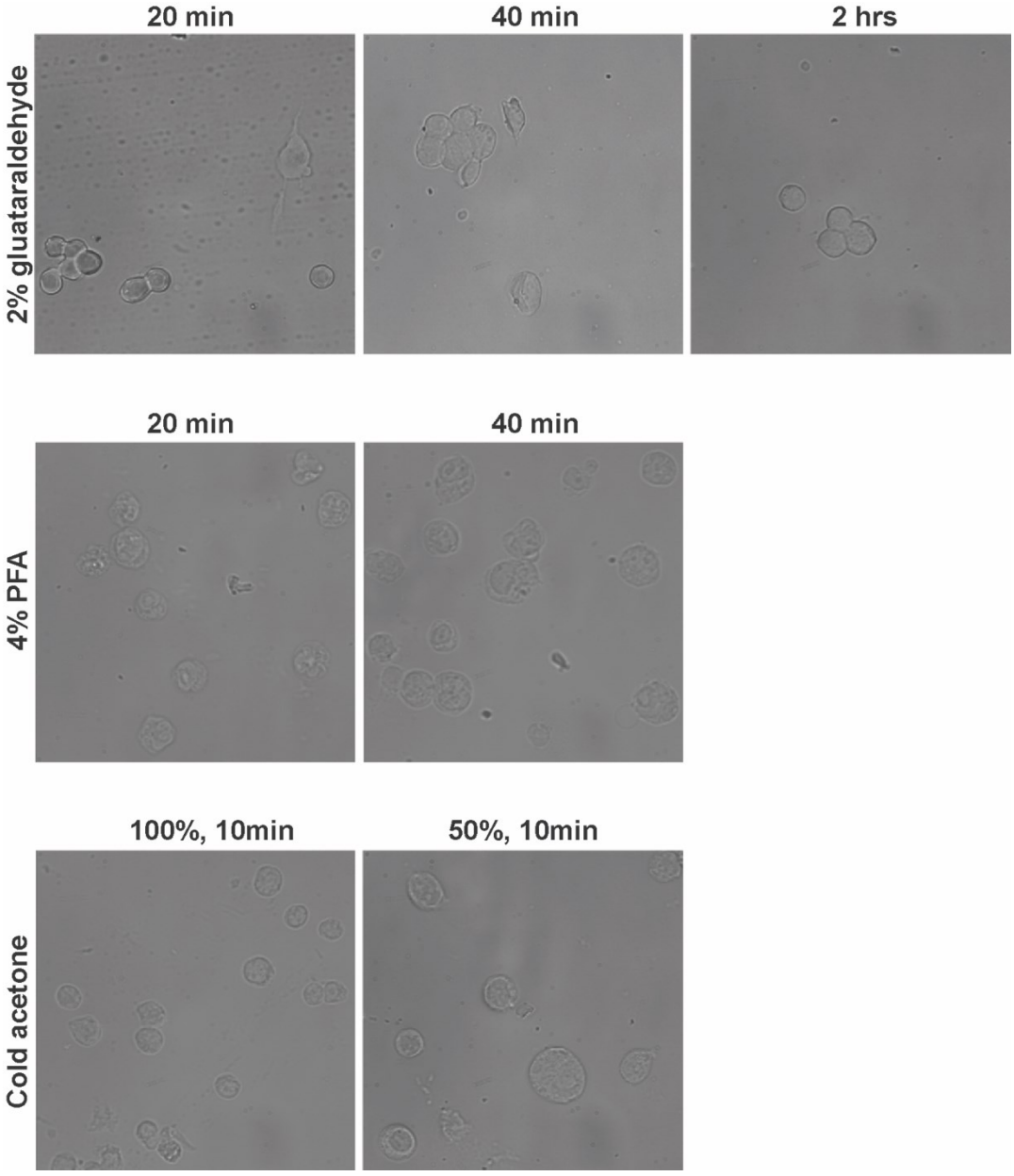

Figure 2.1. Bright-field microscope images of A-BCL cells. A-BCL cells were washed and treated with the indicated conditions as fixatives. The cells were then washed and imaged using fluorescence microscope and cells were inspected for their size and morphology.

2.3.2 Antigen staining

Immunofluorescence staining is an important step in visualization, detection, and localization of proteins. Staining of the cellular proteins can be direct using only primary antibody

or indirect using both primary and secondary antibodies. As shown in **Figure 2.2A**, preliminary images of CD22 staining using only primary antibody (anti-CD22 conjugated with Alexa Flour 488, AF488), did not yield membrane staining. Instead, the staining looked like artifacts due to air bubbles formed when preparing the slides (**Figure 2.2A, left**). In another case, the staining gave signals as small fragments (**Figure 2.2A, right**), possibly due to disruption of the cells in preparation. Based on these observations, we repeated stating with extra precautions, by reducing the duration and speed of centrifugation and number of washes, and careful avoidance of air bubbles during slide preparation. **Figure 2.2B** shows staining of cells which included intracellular staining for CD22, a result of endocytosis of primary antibodies. In order to avoid this issue, we repeated the staining at 4 °C, which is known to slow endocytosis (**Figure 2.2C**).

Using a similar method, we performed two-color immunofluorescence where B cell receptor (BCR) was also stained using anti-IgM conjugated with TRITC (**Figure 2.3A**). However, these channels could not resolve and bleed-through seemed to occur, as there is substantial overlap between BCR and CD22 stains, thus we switched the fluorophore on anti-IgM antibody to Alexa Fluor 647 (AF647) and lowered the laser intensity in the green channel (**Figure 2.3B**), but this caused the CD22 signal to become very weak. We suspected autofluorescence was responsible for our observations. Some studies have examined the autofluorescence when using cross-linking fixatives and found that glutaraldehyde generally has more autofluorescence compared to PFA.[51,52] Indeed, when we imaged A-BCL cells without anti-CD22-AF488 primary antibody, signals were observed in the green channel only (**Figure 2.3C**). The presence of this autofluorescence could potentially impede our ability to image and analyse protein organization. In order to circumvent this, PFA was used as fixative reagent; only a low concentration of 1% was used as this fixative was harsh on A-BCL cells as observed in our previous study. However, low levels of

autofluorescence still occurred. We checked the expression of the proteins on A-BCL cell membrane using flow cytometry (**Figure 2.4A**). Direct staining of CD22 receptors did not significantly shift the fluorescence and the population of the unstained cells was bimodal in A-BCL cells but not Raji cells. These observations suggested autofluorescence was present for A-BCL cells and the receptors were either absent on the cell membrane or direct staining was not sufficient. We used the secondary antibody conjugated to AF488 and observed significant shift in population with higher fluorescence intensity (**Figure 2.4B**). From our results, we decided to proceed with future experiments by indirect staining using secondary antibody and stain CD22 receptors using Alexa Flour 647 (AF647) and BCR by Alexa Flour 555 (AF555) to avoid autofluorescence. Additionally, Anti-fade was also employed to increase signal to noise ratio and to reduce photobleaching for better images.

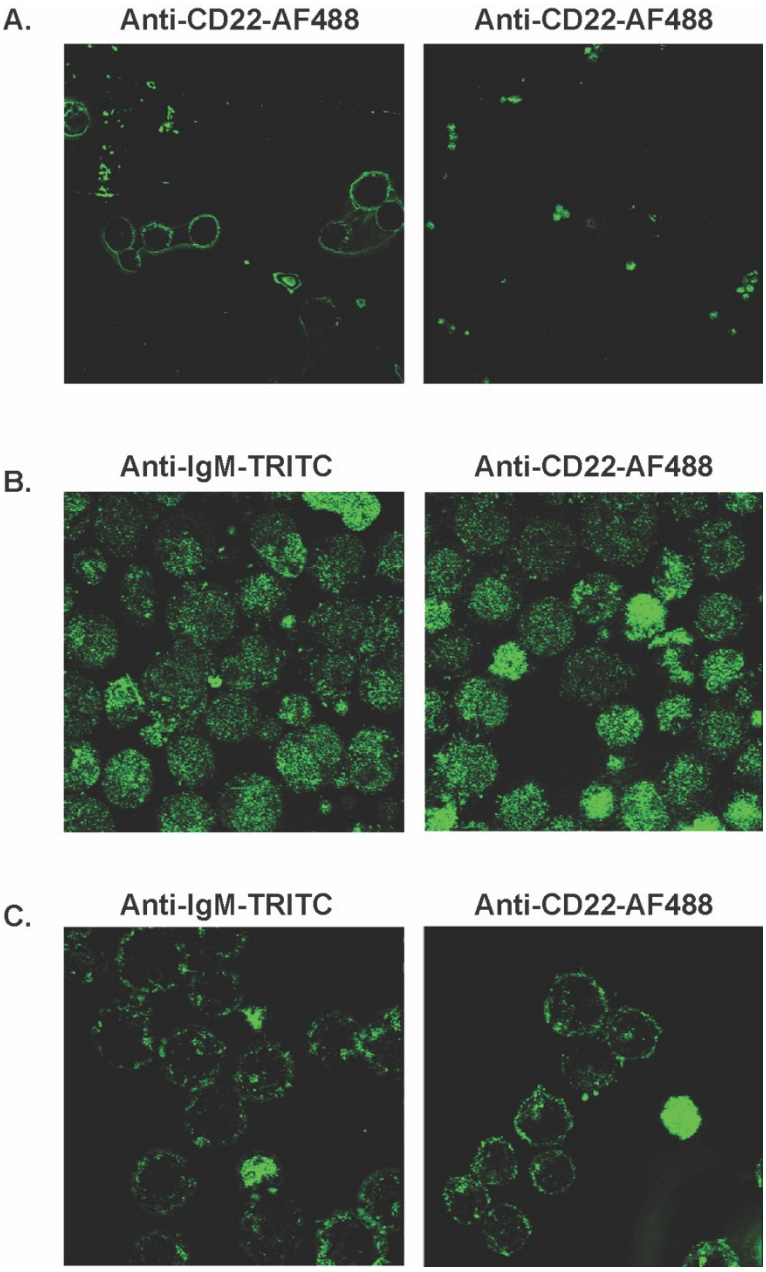

Figure 2.2. One-color direct staining of IgM and CD22 receptors. A-BCL cells were washed and stained with anti-CD22-AF488 or anti-IgM-TRITC for one hour on ice and fixed using 2% glutaraldehyde for 2 hours. The cells were attached to PLL-treated coverslips and transferred to microscopy slides, which were imaged using confocal microscopy. (A) and (B) staining was performed at room temperature, in which (A) showed artifacts in the image while (B) showed intracellular staining. (C) staining was performed at 4 °C.

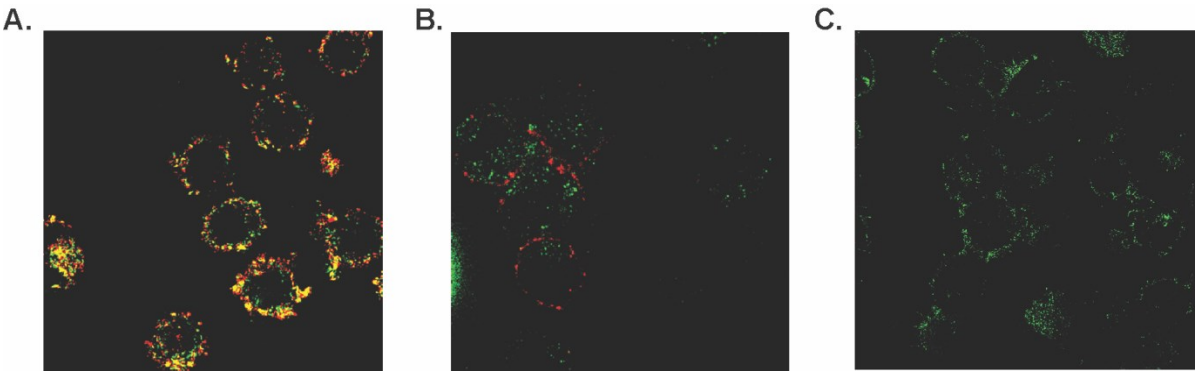

Figure 2.3. Two-color indirect staining of CD22 and BCR on A-BCL cells. A-BCL cells were washed and re-suspended in PBS. Cells were then attached onto coverslips and fixed using 2% glutaraldehyde for 2 h at 4 °C and stained with (A) α-CD22-AF488 and α-IgM-TRITC, or (B) α-CD22-AF488 and α-IgM-AF647, or (C) no receptor staining. Coverslips were transferred to microscopy slides and imaged using confocal microscopy. Green: CD22 stain; Red: IgM stain.

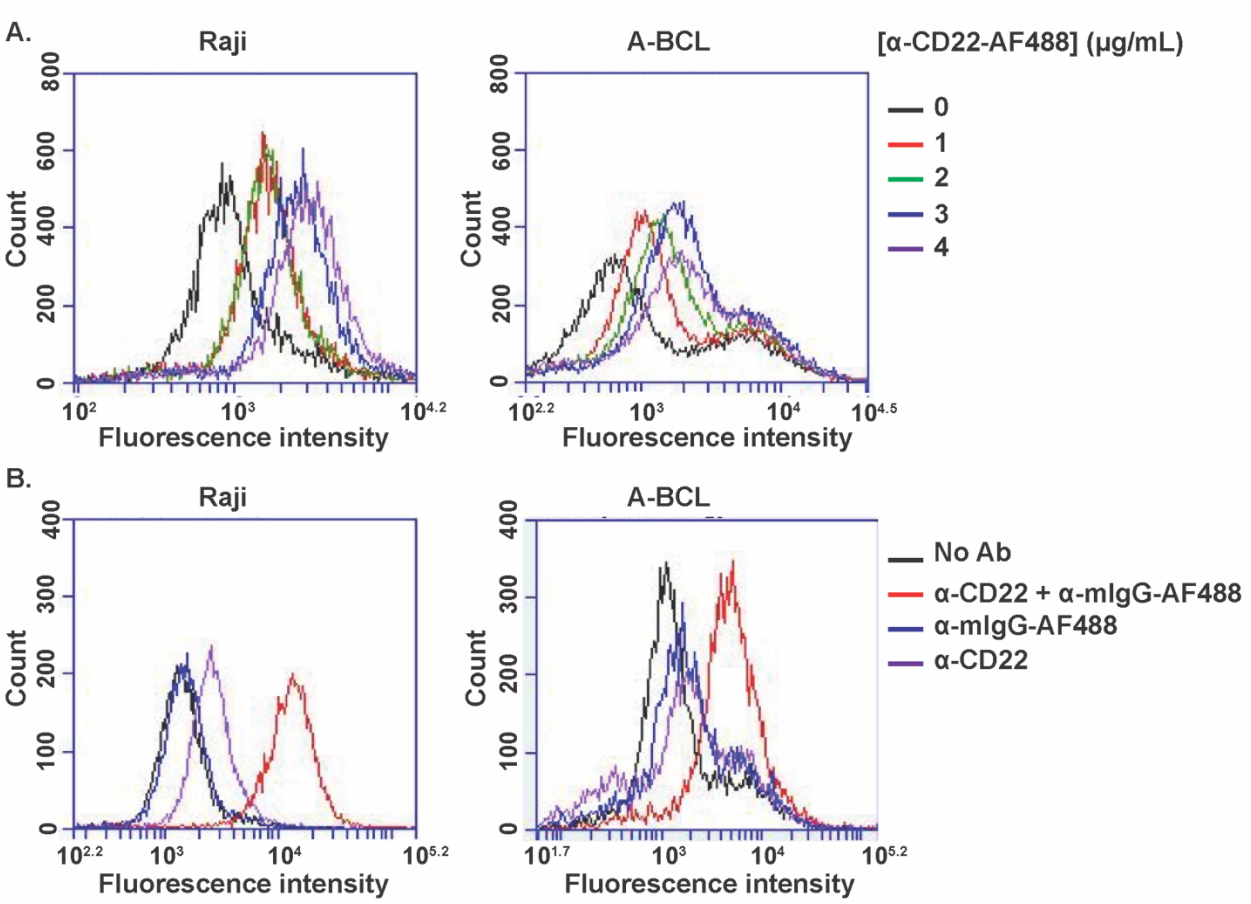

Figure 2.4. Expression and staining of CD22 receptors by flow cytometry. A-BCL cells were washed and resuspended in PBS buffer. Cells were then treated with (A) different concentrations of mouse α-CD22 antibody conjugated with AF488 (0, 1, 2, 3, or 4 μg/mL) or (B) mouse α-CD22 antibody and goat α-mouse IgG conjugated with AF488. Analysis of staining was performed by Flow Cytometry on a BD Acuri C6.

2.3.3 Cell attachment to coverslips

Suspension cells, like lymphocytes, are typically free-floating and must be attached to a surface for observation in microscopy. Some of the common substrates used for coating coverslips include poly-L-Lysine (PLL), fibronectin, laminin, and collagen. Each of these substrates has

different mechanism to promote cell attachment. For instance, PLL is a commonly used substrate that contains poly-cation which can non-covalently bind to negatively charged nucleic acids and proteins on the cell.[53] On the other hand, fibronectin, laminin, and collagen are extracellular matrix proteins that can promote cell adherence via membrane proteins integrins. Since each cell type has different set of proteins, suitable substrate for each cell line has to be determined for each protocol. B lymphocytes are suspension cells in culture, thus they do not naturally adhere to glass surfaces. We tested several substrates including PLL, fibronectin, collagen, and cell-tak at different conditions. Initially, cells were added to substrate-treated coverslips before treatments, staining, and fixation which yielded very little to no cells on the coverslips in all conditions. We speculated that since adsorption of the cells onto coverslips is through weak interactions, substantial number of washing steps detached most of these cells. We revised the protocol to perform treatments and staining before adding cells to the coverslips, and this gave better results when fibronectin was used as the substrate (**Figure 2.5**). However, in our experiments, staining after fixation was more desirable because we wanted to avoid the re-distribution of the receptors after treatment. Thus, we once again revised the protocol to the following order: treatments, addition of the cells onto treated coverslips, fixation, and staining. We tested this protocol and compared the amount of cells on the slides with different substrates. In all the conditions, only cell-tak and PLL provided for attachment and a significant number of cells retained for imaging. Due to the lower cost of PLL compared to cell-tak while giving similar results, we selected PLL for future experiments.

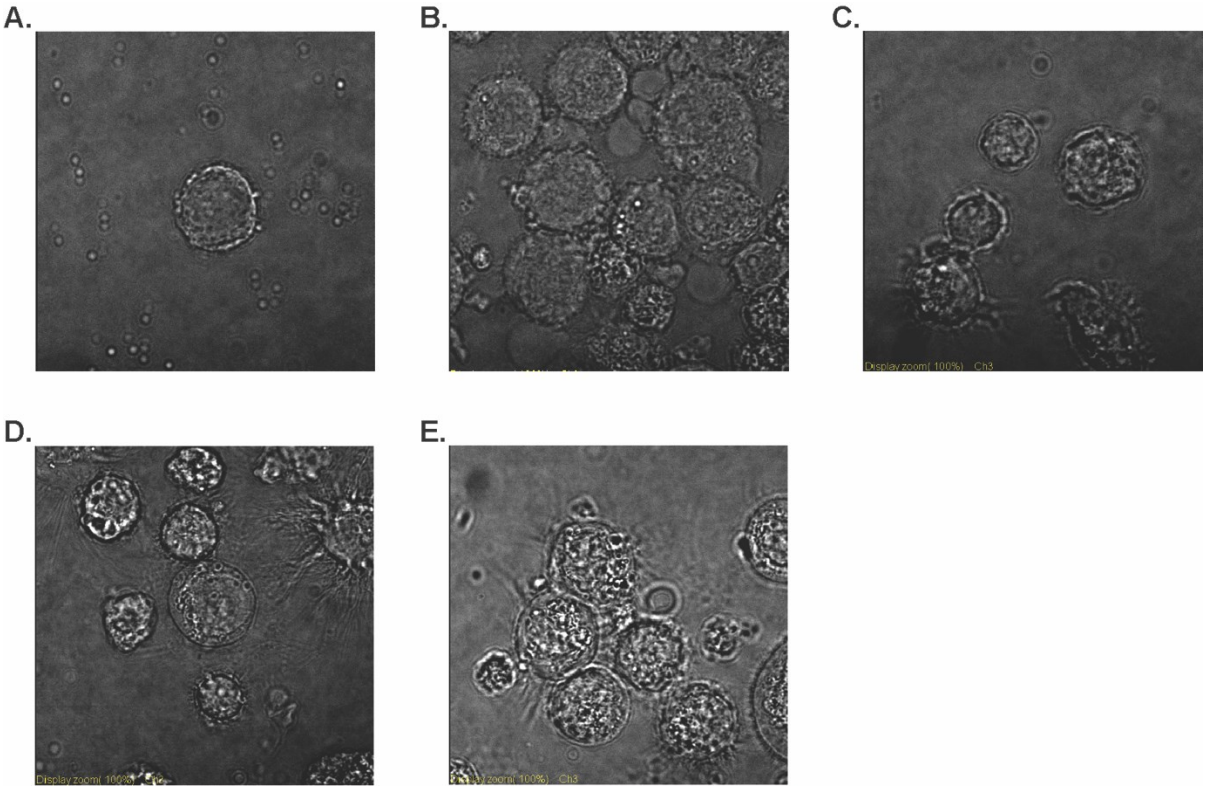

Figure 2.5. Attachment of A-BCL cells onto coverslips with different substrates. Cleaned coverslips were treated with (A) 5 μg/cm^2 rat tail collagen, (B) 10 μg/cm^2 rat tail collagen, (C) fibronectin, (D) Cell-tak, or (E) PLL overnight at 4 °C, washed with PBS and transferred to new wells in 24-well plates. A-BCL cells were washed and transferred to wells with coverslips, spun down at 300X for 15 min and DIC images were taken at 60X.

2.3.4 Imaging and cluster analysis

In order to obtain reliable microscopy data, it is necessary to obtain consistent image quality at high resolution which is dependent on number of factors. After optimization of sample preparation (vide supra), we turned our attention to acquisition of the fluorescence image and processing to analyze clustering. Resolution is defined as the shortest distance that two entities can be distinguished as distinct.[54] The image resolution is dependent on numerical aperture (NA),

wavelength of the light source, light diffraction, and refractive index of the mounting media.[55] We were interested in studying clustering of membrane receptors, and we expected the control of background fluorescence provided by confocal compared to widefield microscopy should provide consistent resolution.[26] This should allow for more detailed images and more accurate analysis of clusters. Although 100X optical lens has higher magnification, 60X was selected since this optical lens had higher numerical aperture giving better resolution of the images. We were able to image our membrane receptors in clusters, shown in **Figure 2.6A**, which is consistent with other findings.[42,56]

We were interested in comparing the CD22 clusters on B cell membrane in different conditions, and we tried measuring and drawing plots of fluorescence intensity for qualitative analysis (**Figure 2.6B**).[57] However, these data did not provide a basis for statistical analysis. Hence, we used the analyze particle function in imageJ. This function scans the binary thresholded image or selection for objects, which are then measured by counting the number of pixels in an object and then calculating the total area of those pixels. To ensure valid analysis of receptor distribution, individual cells were selected from a set of random fields collected for each condition (at least 10 per condition). From these images, individual cells were included in the analysis based on staining and morphology of the cells; with 1-2 cells per field. We accounted for background fluorescence by taking all the images with the same laser intensity and PMT, same z-coordinate, and same thresholding limits (**Figure 2.6C**) so that the contribution of background should be similar across conditions.

For a typical experiment, we analyzed clusters from 10 - 20 cells per condition allowing for statistical analysis of changes in average per-cluster size. Typical numbers of clusters ranged from 1-23 clusters on each individual cell, with each data point representing an individual cluster in μm^2

(not the total cluster area per cell). Conditions were compared using a Student's t-test or one-way ANOVA (**Figure 2.6D**). Cells were treated with either PBS (-) or with a glycoconjugate that was hypothesized to cluster CD22 receptors (+). To test the influence of sample size, we used a data set of 20 cells and randomly sampled to smaller numbers of replicates (n = 1, 5, 10, and 20) to evaluate the influence of sample size on the result. Data are shown for 1 cell (n = 35 clusters for PBS, n = 13 for treated), 5 cells (n = 106 clusters for PBS, n = 65 for treated), or 10 cells (n = 198 clusters for PBS, n = 115 for treated), and 20 cells (n = 371 clusters for PBS, n = 238 for treated). As shown in this figure, particle analysis from one cell could give statistically meaningful data, however using a larger sample showed a clearer distribution of particle size and increased statistical significance (lower p value). These data are represented as violin plots, where the dotted lines in the individual distributions represent the median and quartiles of each population. Representing our data this way gives us the advantage of showing all data points as a distribution.

It is also important to note that as we include more cells, we see thinner distribution; this is due to higher likelihood of including cells that have very large clusters or capping of receptors. This information is lost with lower cell numbers, although the change in cluster size was still captured. Above 10 cells, the distribution was unchanged, so we decided to analyze 20 cells for our subsequent studies. Hence, this method should allow reliable analyses of the receptor size. Overall, we concluded that this method provides a quantitative approach to standard capping experiments performed by fluorescence microscopy and could be used to study changes in receptor clustering.

It is also notable that previous work in our group has performed similar analyses of CD22 clustering using TIRFM which are in general agreement with our conclusions from this method (see Chapters 3 & 4). One disadvantage of using individual confocal images for this analysis is

that it cannot analyze the total number of receptors or clusters on the entire cell membrane. However, this analysis method allowed us to compare the degree of clustering between different conditions. Another drawback to our method is the diffraction limit of the confocal microscope, which in our experiments was 0.0235 μm^2 (Equation 4). We discuss the application of this method for determining changes in CD22 and BCR clustering on B cells in Chapters 3 & 4.

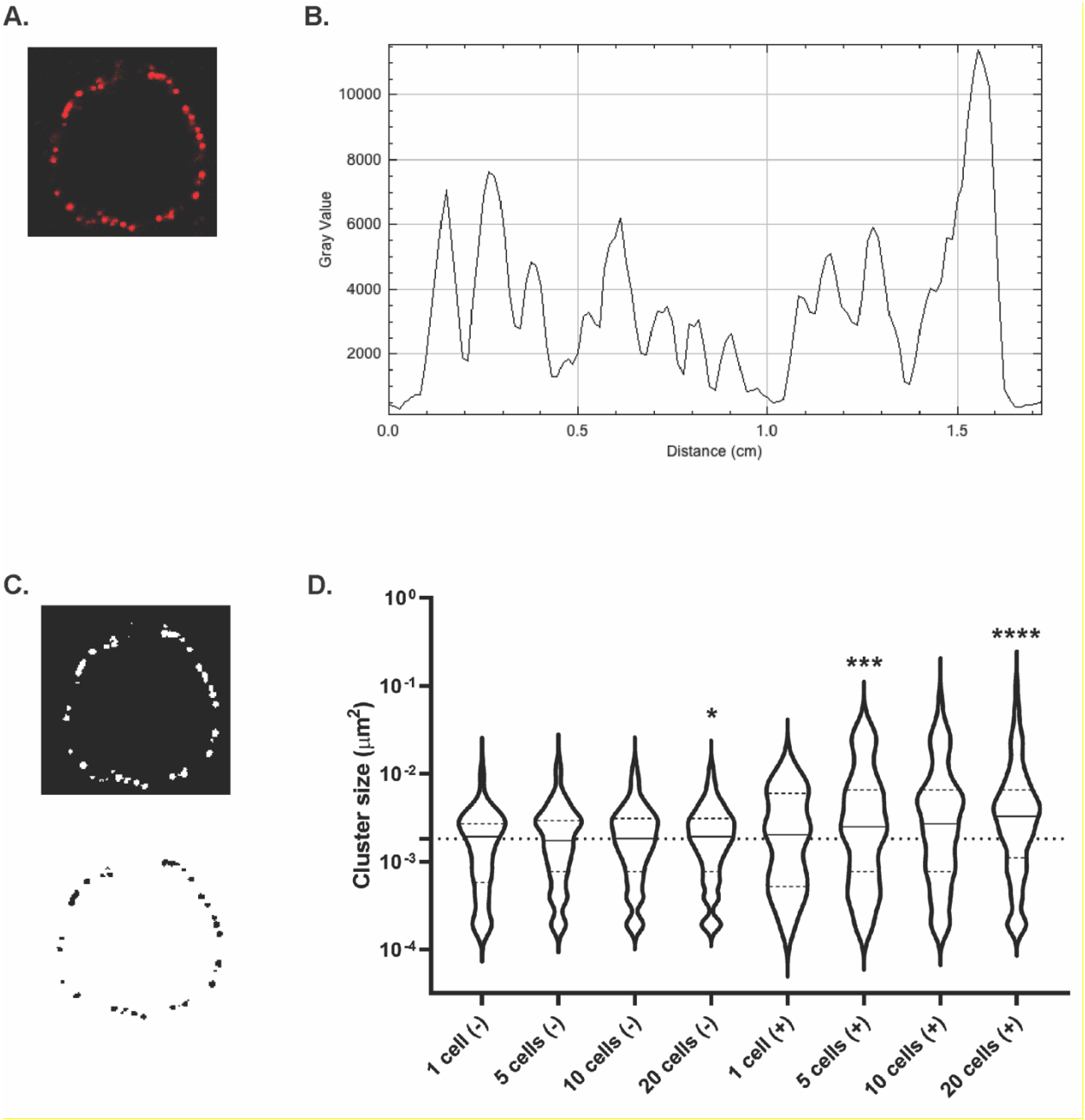

Figure 2.6. Statistical analysis of CD22 receptors on B cells. B cells were treated with either PBS (-) or with glycoconjugate. CD22 receptors were stained with mouse primary anti-CD22 antibody followed by anti-mouse secondary antibody conjugated with Alexa Fluor 647 and image was taken using confocal microscope (A). The fluorescent intensity profile of the receptors were drawn using image J in polar coordinates (B). The confocal images were also thresholded (C, top) and particle analysis of the receptors was performed to produce the masked images (C, bottom). The statistical analysis of CD22 receptors was performed using student's t-test and analyses of cluster sizes were drawn as violin plots on prism (D), using 1 cell, 5 cells, 10 cells, or 20 cells. Violin plots with diagonal lines are controls, and filled violin plots are treated conditions. The black thick dotted line within each population represents the median while top and bottom thin dotted lines are quartile 1 and 3, respectively.

2.4 CONCLUSIONS

We were able to develop a confocal microscope experiment to study changes in clustering of CD22 receptors on B cell membrane with simple sample preparation and data analysis. We optimized conditions for each step in the sample analysis, specifically: fixation, staining, attachment substrate, and microscope and analysis technique. We concluded that the optimal conditions for studying changes in CD22 clustering on B cells are gentle washes, PLL as the substrate for cells attachment onto coverslips, indirect antigen staining, and confocal microscopy for imaging. This protocol allows for quantitative comparison of changes to receptor microclusters on cells, and will be applied in Chapters 3 and 4.

REFERENCES

(1) Singer, S. J.; Nicolson, G. L. The Fluid Mosaic Model of the Structure of Cell Membranes. *Science* **1972**, *175* (4023), 720–731. https://doi.org/10.1126/science.175.4023.720.

(2) Fry, D. C. Protein–Protein Interactions as Targets for Small Molecule Drug Discovery. *Biopolymers* **2006**, *84* (6), 535–552. https://doi.org/10.1002/bip.20608.

(3) Haso, W.; Lee, D. W.; Shah, N. N.; Stetler-Stevenson, M.; Yuan, C. M.; Pastan, I. H.; Dimitrov, D. S.; Morgan, R. A.; FitzGerald, D. J.; Barrett, D. M.; Wayne, A. S.; Mackall, C. L.; Orentas, R. J. Anti-CD22–Chimeric Antigen Receptors Targeting B-Cell Precursor Acute Lymphoblastic Leukemia. *Blood* **2013**, *121* (7), 1165–1174. https://doi.org/10.1182/blood-2012-06-438002.

(4) Noble, M. E. M. Protein Kinase Inhibitors: Insights into Drug Design from Structure. *Science* **2004**, *303* (5665), 1800–1805. https://doi.org/10.1126/science.1095920.

(5) Cho, W.; Stahelin, R. V. Membrane-Protein Interactions in Cell Signaling and Membrane Trafficking. *Annu. Rev. Biophys. Biomol. Struct.* **2005**, *34* (1), 119–151. https://doi.org/10.1146/annurev.biophys.33.110502.133337.

(6) Barrera, N. P.; Zhou, M.; Robinson, C. V. The Role of Lipids in Defining Membrane Protein Interactions: Insights from Mass Spectrometry. *Trends Cell Biol.* **2013**, *23* (1), 1–8. https://doi.org/10.1016/j.tcb.2012.08.007.

(7) Vitrac, H.; MacLean, D. M.; Jayaraman, V.; Bogdanov, M.; Dowhan, W. Dynamic Membrane Protein Topological Switching upon Changes in Phospholipid Environment. *Proc. Natl. Acad. Sci.* **2015**, *112* (45), 13874–13879. https://doi.org/10.1073/pnas.1512994112.

(8) Bogdanov, M. A Polytopic Membrane Protein Displays a Reversible Topology Dependent on Membrane Lipid Composition. *EMBO J.* **2002**, *21* (9), 2107–2116. https://doi.org/10.1093/emboj/21.9.2107.

(9) Lenaz, G. Lipid Fluidity and Membrane Protein Dynamics. *Biosci. Rep.* **1987**, *7* (11), 823–837. https://doi.org/10.1007/BF01119473.

(10) Sezgin, E.; Levental, I.; Mayor, S.; Eggeling, C. The Mystery of Membrane Organization: Composition, Regulation and Roles of Lipid Rafts. *Nat. Rev. Mol. Cell Biol.* **2017**, *18* (6), 361–374. https://doi.org/10.1038/nrm.2017.16.

(11) Lingwood, D.; Simons, K. Lipid Rafts As a Membrane-Organizing Principle. *Science* **2010**, *327* (5961), 46–50. https://doi.org/10.1126/science.1174621.

(12) Tolar, P.; Hanna, J.; Krueger, P. D.; Pierce, S. K. The Constant Region of the Membrane Immunoglobulin Mediates B Cell-Receptor Clustering and Signaling in Response to

Membrane Antigens. *Immunity* **2009**, *30* (1), 44–55. https://doi.org/10.1016/j.immuni.2008.11.007.

(13) Wan, Z.; Liu, W. The Growth of B Cell Receptor Microcluster Is a Universal Response of B Cells Encountering Antigens with Different Motion Features. *Protein Cell* **2012**, *3*, 545–558.

(14) Nitschke, L. The Role of CD22 and Other Inhibitory Co-Receptors in B-Cell Activation. *Curr. Opin. Immunol.* **2005**, *17* (3), 290–297. https://doi.org/10.1016/j.coi.2005.03.005.

(15) Nitschke, L.; Carsetti, R.; Ocker, B.; Köhler, G.; Lamers, M. C. CD22 Is a Negative Regulator of B-Cell Receptor Signalling. *Curr. Biol.* **1997**, *7* (2), 133–143. https://doi.org/10.1016/S0960-9822(06)00057-1.

(16) Otipoby, K. L.; Draves, K. E.; Clark, E. A. CD22 Regulates B Cell Receptor-Mediated Signals via Two Domains That Independently Recruit Grb2 and SHP-1. *J. Biol. Chem.* **2001**, *276* (47), 44315–44322. https://doi.org/10.1074/jbc.M105446200.

(17) Cambi, A.; Lidke, D. S. Nanoscale Membrane Organization: Where Biochemistry Meets Advanced Microscopy. *ACS Chem. Biol.* **2012**, *7* (1), 139–149. https://doi.org/10.1021/cb200326g.

(18) Lang, T.; Rizzoli, S. O. Membrane Protein Clusters at Nanoscale Resolution: More Than Pretty Pictures. *Physiology* **2010**, *25* (2), 116–124. https://doi.org/10.1152/physiol.00044.2009.

(19) Paddock, S. W. Principles and Practices of Laser Scanning Confocal Microscopy. *Mol. Biotechnol.* **2000**, *16* (2), 127–150. https://doi.org/10.1385/MB:16:2:127.

(20) Damer, C. K.; O'Halloran, T. J. Spatially Regulated Recruitment of Clathrin to the Plasma Membrane during Capping and Cell Translocation□V. *Mol. Biol. Cell* **2000**, *11*, 9.

(21) Owen, D. M.; Williamson, D. J.; Magenau, A.; Gaus, K. Sub-Resolution Lipid Domains Exist in the Plasma Membrane and Regulate Protein Diffusion and Distribution. *Nat. Commun.* **2012**, *3* (1), 1256. https://doi.org/10.1038/ncomms2273.

(22) Rassam, P.; Copeland, N. A.; Birkholz, O.; Tóth, C.; Chavent, M.; Duncan, A. L.; Cross, S. J.; Housden, N. G.; Kaminska, R.; Seger, U.; Quinn, D. M.; Garrod, T. J.; Sansom, M. S. P.; Piehler, J.; Baumann, C. G.; Kleanthous, C. Supramolecular Assemblies Underpin Turnover of Outer Membrane Proteins in Bacteria. *Nature* **2015**, *523* (7560), 333–336. https://doi.org/10.1038/nature14461.

(23) Stuermer, C. A. O.; Langhorst, M. F.; Wiechers, M. F.; Legler, D. F.; Hanwehr, S. H. von; Guse, A. H.; Plattner, H. PrP ^{c} Capping in T Cells Promotes Its Association with the Lipid Raft Proteins Reggie-1 and Reggie-2 and Leads to Signal Transduction. *FASEB J.* **2004**, *18* (14), 1731–1733. https://doi.org/10.1096/fj.04-2150fje.

(24) Belyy, V.; Tran, N.-H.; Walter, P. Quantitative Microscopy Reveals Dynamics and Fate of Clustered IRE1α. *Proc. Natl. Acad. Sci.* **2020**, *117* (3), 1533–1542. https://doi.org/10.1073/pnas.1915311117.

(25) Blacutt, J.; Lan, Z.; Cosgriff-Hernandez, E. M.; Gordon, V. D. Quantitative Confocal Microscopy and Calibration for Measuring Differences in Cyclic-Di-GMP Signalling by Bacteria on Biomedical Hydrogels. *R. Soc. Open Sci.* **2021**, *8* (1), 201453. https://doi.org/10.1098/rsos.201453.

(26) Khiabani, K. T.; Stephenson, L. L.; Gabriel, A.; Nataraj, C.; Wang, W. Z.; Zamboni, W. A. A Quantitative Method for Determining Polarization of Neutrophil Adhesion Molecules Associated with Ischemia Reperfusion: *Plast. Reconstr. Surg.* **2004**, *114* (7), 1846–1850. https://doi.org/10.1097/01.PRS.0000143580.45631.DD.

(27) Ma, H.; Yankee, T. M.; Hu, J.; Asai, D. J.; Harrison, M. L.; Geahlen, R. L. Visualization of Syk-Antigen Receptor Interactions Using Green Fluorescent Protein: Differential Roles for Syk and Lyn in the Regulation of Receptor Capping and Internalization. *J. Immunol.* **2001**, *166* (3), 1507–1516. https://doi.org/10.4049/jimmunol.166.3.1507.

(28) Wu, Y.; Eghbali, M.; Ou, J.; Lu, R.; Toro, L.; Stefani, E. Quantitative Determination of Spatial Protein-Protein Correlations in Fluorescence Confocal Microscopy. *Biophys. J.* **2010**, *98* (3), 493–504. https://doi.org/10.1016/j.bpj.2009.10.037.

(29) Jaiswal, J. K.; Simon, S. M. Imaging Single Events at the Cell Membrane. *Nat. Chem. Biol.* **2007**, *3* (2), 92–98. https://doi.org/10.1038/nchembio855.

(30) Schermelleh, L.; Ferrand, A.; Huser, T.; Eggeling, C.; Sauer, M.; Biehlmaier, O.; Drummen, G. P. C. Super-Resolution Microscopy Demystified. *Nat. Cell Biol.* **2019**, *21* (1), 72–84. https://doi.org/10.1038/s41556-018-0251-8.

(31) Elson, E. L.; Magde, D. Fluorescence Correlation Spectroscopy. I. Conceptual Basis and Theory. *Biopolymers* **1974**, *13* (1), 1–27. https://doi.org/10.1002/bip.1974.360130102.

(32) Schwille, P.; Haupts, U.; Maiti, S.; Webb, W. W. Molecular Dynamics in Living Cells Observed by Fluorescence Correlation Spectroscopy with One- and Two-Photon Excitation. *Biophys. J.* **1999**, *77* (4), 2251–2265. https://doi.org/10.1016/S0006-3495(99)77065-7.

(33) Starr, T. E.; Thompson, N. L. Total Internal Reflection with Fluorescence Correlation Spectroscopy: Combined Surface Reaction and Solution Diffusion. *Biophys. J.* **2001**, *80* (3), 1575–1584. https://doi.org/10.1016/S0006-3495(01)76130-9.

(34) Fish, K. N. Total Internal Reflection Fluorescence (TIRF) Microscopy. *Curr. Protoc. Cytom.* **2009**, *50* (1). https://doi.org/10.1002/0471142956.cy1218s50.

(35) Moerner, W. E.; Fromm, D. P. Methods of Single-Molecule Fluorescence Spectroscopy and Microscopy. *Rev. Sci. Instrum.* **2003**, *74* (8), 3597–3619. https://doi.org/10.1063/1.1589587.

(36) Klar, T. A.; Jakobs, S.; Dyba, M.; Egner, A.; Hell, S. W. Fluorescence Microscopy with Diffraction Resolution Barrier Broken by Stimulated Emission. *Proc. Natl. Acad. Sci.* **2000**, *97* (15), 8206–8210. https://doi.org/10.1073/pnas.97.15.8206.

(37) Gustafsson, M. G. L. Surpassing the Lateral Resolution Limit by a Factor of Two Using Structured Illumination Microscopy. SHORT COMMUNICATION. *J. Microsc.* **2000**, *198* (2), 82–87. https://doi.org/10.1046/j.1365-2818.2000.00710.x.

(38) Rust, M. J.; Bates, M.; Zhuang, X. Sub-Diffraction-Limit Imaging by Stochastic Optical Reconstruction Microscopy (STORM). *Nat. Methods* **2006**, *3* (10), 793–796. https://doi.org/10.1038/nmeth929.

(39) Hess, S. T.; Girirajan, T. P. K.; Mason, M. D. Ultra-High Resolution Imaging by Fluorescence Photoactivation Localization Microscopy. *Biophys. J.* **2006**, *91* (11), 4258–4272. https://doi.org/10.1529/biophysj.106.091116.

(40) Schnell, U.; Dijk, F.; Sjollema, K. A.; Giepmans, B. N. G. Immunolabeling Artifacts and the Need for Live-Cell Imaging. *Nat. Methods* **2012**, *9* (2), 152–158. https://doi.org/10.1038/nmeth.1855.

(41) Suthipintawong, C.; Vinyuvat, S. Immunostaining of Cell Preparations: a comparative evaluation of common fixatives and protocols. *Diag. Cyto*. **1996**, 15(2), 167-174.

(42) Frick, M.; Schmidt, K.; Nichols, B. J. Modulation of Lateral Diffusion in the Plasma Membrane by Protein Density. *Curr. Biol.* **2007**, *17* (5), 462–467. https://doi.org/10.1016/j.cub.2007.01.069.

(43) Guigas, G.; Weiss, M. Effects of Protein Crowding on Membrane Systems. *Biochim. Biophys. Acta BBA - Biomembr.* **2016**, *1858* (10), 2441–2450. https://doi.org/10.1016/j.bbamem.2015.12.021.

(44) Lillemeier, B. F.; Pfeiffer, J. R.; Surviladze, Z.; Wilson, B. S.; Davis, M. M. Plasma Membrane-Associated Proteins Are Clustered into Islands Attached to the Cytoskeleton. *Proc. Natl. Acad. Sci.* **2006**, *103* (50), 18992–18997. https://doi.org/10.1073/pnas.0609009103.

(45) Kiernan, J. A. Formaldehyde, Formalin, Paraformaldehyde And Glutaraldehyde: What They Are And What They Do. *Microsc. Today* **2000**, *8* (1), 8–13. https://doi.org/10.1017/S1551929500057060.

(46) Eltoum, I.; Fredenburgh, J.; Myers, R. B.; Grizzle, W. E. Introduction to the Theory and Practice of Fixation of Tissues. *J. Histotechnol.* **2001**, *24* (3), 173–190. https://doi.org/10.1179/his.2001.24.3.173.

(47) Steinkamp, J. A.; Lehnert, N. M.; Keij, J. F.; Lehnert, B. E. Enhanced Immunofluorescence Measurement Resolution of Surface Antigens on Highly Autofluorescent, Glutaraldehyde-fixed Cells Analyzed by Phase-sensitive Flow Cytometry. *Cytometry*. **1999**, 37(4), 275-283.

(48) Tagliaferro, P.; Tandler, C. J.; Ramos, A. J.; Pecci Saavedra, J.; Brusco, A. Immunofluorescence and Glutaraldehyde Fixation. A New Procedure Based on the Schiff-Quenching Method. *J. Neurosci. Methods* **1997**, *77* (2), 191–197. https://doi.org/10.1016/S0165-0270(97)00126-X.

(49) Yavin, E.; Yavin, Z. ATTACHMENT AND CULTURE OF DISSOCIATED CELLS FROM RAT EMBRYO CEREBRAL HEMISPHERES ON POLYLYSINE-COATED SURFACE. *J. Cell Biol.* **1974**, *62* (2), 540–546. https://doi.org/10.1083/jcb.62.2.540.

(50) Jonkman, J. E. N.; Swoger, J.; Kress, H.; Rohrbach, A.; Stelzer, E. H. K. [18] Resolution in Optical Microscopy. In *Methods in Enzymology*; Elsevier, 2003; Vol. 360, pp 416–446. https://doi.org/10.1016/S0076-6879(03)60122-9.

(51) Gasparrini, F.; Feest, C.; Bruckbauer, A.; Mattila, P. K.; Müller, J.; Nitschke, L.; Bray, D.; Batista, F. D. Nanoscale Organization and Dynamics of the Siglec CD 22 Cooperate with the Cytoskeleton in Restraining BCR Signalling. *EMBO J.* **2016**, *35* (3), 258–280. https://doi.org/10.15252/embj.201593027.

(52) Wasim, L.; Buhari, F. H. M.; Yoganathan, M.; Sicard, T.; Ereño-Orbea, J.; Julien, J.-P.; Treanor, B. N-Linked Glycosylation Regulates CD22 Organization and Function. *Front. Immunol.* **2019**, *10*, 699. https://doi.org/10.3389/fimmu.2019.00699.

CHAPTER 3. ALTERING CD22 CLUSTERING ON B CELL MEMBRANE WITH SYNTHETIC GLYCOCONJUGATES

Portions of this chapter are included in the following publications:

Daskhan, G. C.; Tran, H.-T. T.; Meloncelli, P. J.; Lowary, T. L.; West, L. J.; Cairo, C. W. Construction of Multivalent Homo- and Heterofunctional ABO Blood Group Glycoconjugates Using a Trifunctional Linker Strategy. *Bioconjug. Chem.* **2018**, *29* (2), 343–362.

Dashkhan, G. C; Motyka, B.; Bascom, R.; Tran, H-T; Tao, K.; West, L, J.; Cairo, C. W. Extending the in vivo Persistence of Synthetic Glycoconjugates Using a Serum-Protein Binder. *RSC Chem. Biol.* **2022**.

Dashkhan, G. C.; Tran, H-T.; Cairo, C. W. Convergent Synthesis of Hexadecavalent Heterobifunctional ABO Blood Group Glycoconjugates. *Manuscript in preparation*.

Compounds **8**, **9**, **10**, **11**, **12**, **27**, **33**, **34**, **35**, **36** were prepared and characterized by Dr. G Daskhan.

3.1 INTRODUCTION

B cells are an important component of our immune system, and the B-cell receptor (BCR) is responsible for recognizing and binding to antigens and initiating cellular response. Upon binding with specific antigens BCRs form microclusters through interactions of the Cμ4 constant region and induce immune responses such as proliferation and antibody production after activation of the cell.[1,2] Proper functioning of BCR is important to health, and dysregulation can lead to issues such as autoimmune diseases,[3–5] immunodeficiencies,[6,7] and allergies.[8–10] Thus, a detailed understanding of the process of BCR activation may be crucial to a range of diseases.

The B cell membrane carries a number of co-receptors that are responsible for regulating B cell response. For instance, binding of Siglec-G and CD22 to α2,3-sialic acids or α2,6-sialic acids, respectively, is known to attenuate B cell response.[11,12] CD22 (Siglec-2) is a well-studied negative co-receptor of BCR and its expression is restricted to B lymphocytes.[13] CD22 is a transmembrane protein that is composed of an extracellular domain with 7 immunoglobulin (Ig) domains, the most

N-terminal domain binds to sialic acid, and 12 putative N-glycosylation sites. The cytoplasmic domain contains two immunoreceptor tyrosine-based inhibitory motifs (ITIMs) that recruit phosphatases to dephosphorylate BCRs upon binding of the ligand and co-clustering with BCRs.[14] This mechanism, and ligand specificity, are important for B cells to distinguish between self- and non-self antigens.

CD22 can bind to cis- or trans- ligands, however, they are basally masked by homotypic or heterotypic interactions on the cell surface.[15] Binding of Siglecs to their ligands is typically weak, but it is difficult to overcome this interaction due to competition with the dense array of cis ligands present at the membrane. Thus, disruption of sialosides on the cell membrane by sialic acid-cleaving sialidase (or neuraminidase) enzymes and periodate reduction have been used to enhance CD22 binding to trans ligands. An alternative way to compete with cis-ligand binding is through the use of high-avidity multivalent displays of CD22 ligands. Multivalent ligands, including liposomes,[16,17] polymers,[18,19] and synthetic scaffolds,[20] for CD22 have been investigated as B cell modulators based on their ability to engage and cluster the receptor. Indeed, glycans in biological systems are often heterogenous and multivalent, and can be important for protein stability, specificity, structure, and function.[21] Glycans on glycoconjugates are also essential for recognition of antigens by B cells,[22] thus synthetic glycoconjugates that mimic these glycans are used in vaccine development for antibody production against pathogens.[23] Furthermore, synthetic multivalent, bifunctional glycoconjugates which can bind to both BCR and siglecs can modulate immune responses. For example, multivalent glycoconjugates that display both BCR antigens and CD22 ligand have been found to induce B cell tolerance;[19,24] these types of molecules are also called tolerogens.[25]

As a negative regulator of BCR, CD22-targeting strategies hold promise to manipulate the immune response. For example, the ABH blood group antigens are a human antigen system critical for transfusion and transplantation. Incompatible ABH antigens can prevent successful tissue and blood product donation. Thus, inducing immune tolerance towards ABH blood group antigens by utilizing CD22 could provide a strategy for ABH-incompatible transplants and transfusions. The human ABH blood group system was first described by Karl Landsteiner in the early 20th century.[26] The ABH system is characterized by expression of ABO carbohydrate structures on human erythrocytes and other tissues generally derived from embryonic mesoderm. ABH-incompatibility is a major challenge for blood transfusion and organ transplantation due to pathologic effects of naturally occurring antibodies to non-self A/B antigens that are produced as a presumed immunologic cross-reaction to similar epitopes from the gut microbiome.[27,28] An important exception has been demonstrated in young children, who can safely receive ABH-incompatible heart transplants due to their normal developmental lag in production of anti-ABO antibodies.[29] Spontaneous development of immune tolerance to donor blood group A and B antigens has been observed after ABH-incompatible heart transplantation in children with immature immune systems. Thus, developing strategies to induce tolerance towards incompatible blood group antigens may allow for expansion of the donor pool for organ transplantation and blood transfusions.

Herein, we describe our studies on the ability of synthetic glycoconjugates to co-cluster BCR and CD22 using an A type-II specific B cell line with confocal microscopy. We further explored the effects of a serum protein-binding tag, GD10, and increased valency of the conjugates on clustering of CD22 and BCR.

3.2 MATERIALS AND METHODS

3.2.1 Cell culture and receptor expression

A-BCL cells were prepared and grown as described[22] and grown in R10 media supplemented with glutamax and 1% beta-mercaptoethanol added weekly in 12-well plates (Corning, Inc.). Plates were kept in a humidified incubator at 37 °C and 5% CO2. To confirm the expression of the receptors, one million cells were spun and washed three times with phosphate buffered saline (PBS) by spinning at 300 X g for 15 minutes. These cells were fixed by 1% paraformyldehyde (PFA) on ice for 20 minutes. Fixed cells were washed three times with PBS and re-suspended in 1 mL PBS, then treated with 1 μg/mL mouse anti-CD22 antibody (clone HIB22, BD Pharmingen) or 1 μg/mL rabbit anti-human IgM for one hour at room temperature. Cell were washed with PBS and treated with goat anti-mouse IgG (polyclonal, Sigma-Aldrich) conjugated with Alexa Fluor 647 or goat anti-rabbit IgG (polyclonal, Invitrogen) conjugated with Alexa Fluor 543 secondary antibodies for one hour at room temperature. Cells were washed and re-suspended in PBS, and were analyzed using BD Accuri C6 flow cytometer. Only the cells within passages 2-7 were used for analysis and cells were considered to express the receptors there is clear separation in fluorescence intensity between unstained cells and cells that were stained with specific antibodies.

3.2.2 One-color confocal microscopy

For single-color fluorescence microscopy experiments, 2 x10^6 A-BCL cells were washed and treated with 25 ng mL^{-1} of the indicated sample on ice for 1 h, then fixed using 1% PFA on ice for 20 min. Samples were treated with 1 μL mL^{-1} mouse anti-human IgM (clone IM260, Abcam) or mouse anti-human CD22 (clone HIB22, BD Pharmingen) at 4 °C overnight, washed, and stained with goat anti-mouse IgG (polyclonal, Sigma-Aldrich) conjugated with Alexa Flour 647 at room temperature for 1 h. The loading of the fluorophores was approximately 2 dye molecules per

protein as determined by spectrophotometry. After washing, samples were transferred to 24-well plates (Corning, Inc.) with 12 mm circular cover glass slides pre-treated with 0.001% poly-L-lysine and spun at 300 x g for 15 min. Cover glass slides with samples were washed, mounted onto microscopy slides with Slowfade Antifade (Thermo Fisher), and sealed with Cytoseal 60. Samples were imaged on a laser scanning confocal microscope (Olympus IX81) at 60X. Ten cells from each condition were chosen for analysis based on transmitted and fluorescence images, in which each image was subjected to similar thresholding levels, and each cluster was analyzed using the particle analysis function on ImageJ.[106] The area of a single pixel in these images was 0.053 μm^2. The areas of each cluster from the analyses were plotted using beanplot in the R statistical package.[107] Analysis of the means and Student's t-test were performed in Graphpad Prism.

3.2.3 Two-color confocal microscopy

For co-localization studies, A-BCL cells were prepared as above, and 2 x 10^6 cells were washed and treated with either 0 ng mL^{-1} or 25 ng mL^{-1} of conjugate **36** on ice for one hour, and then fixed with 1% PFA on ice for 20 min. Cells were then treated with 1 µL mL^{-1} mouse anti-human CD22 (clone HIB22, BD Pharmingen) and 1 µL mL^{-1} rabbit anti-human IgM (clone RM121, EMD Millipore) overnight at 4 °C. Samples were washed with PBS and stained with goat anti-mouse IgG (polyclonal, Sigma-Aldrich) conjugated with Alexa Fluor 647 and goat anti-rabbit IgG (polyclonal, Invitrogen) conjugated with Alexa Fluor 543 secondary antibodies for one hour at room temperature. Cells were washed with PBS and transferred to 12 mm circular coverslip slides pre-treated with 0.001% poly-L-lysine and spun at 300 x g for 15 min. Coverslip glass slides with samples were washed and mounted on microscopy slides with Slowfade Antifade (Thermo Fisher). Slides were imaged on a spinning disk confocal microscope (Olympus IX-81) at 60X. Ten cells from each condition were chosen for analysis based on transmitted and fluorescence images.

Background from each image was subtracted, and the degree of co-localization was analyzed using coloc2 function on ImageJ. Results were plotted and analyzed using Prism software.

3.3 RESULTS AND DISCUSSION

3.3.1 Clustering of CD22 receptors upon treatment with glycoconjugates

To investigate the ability of conjugates to interact with cell surface receptors, we synthesized a panel of bifunctional multi-valent compounds (**Table 3.1, Figure 3.1**), and we examined their ability to cluster the targeted receptors *in vitro* using confocal microscope. We chose an established cell line (A-BCL) previously used to characterize ABO-antigen coated nanoparticles.[30,31] A-BCL cells express a BCR complex that binds both A type I and A type II antigens, but not B antigens. We confirmed that these cells expressed both BCR and CD22 receptors using flow cytometry and proceeded to investigate if the conjugates could influence the distribution of CD22 and BCR receptors on the cell surface.

The glycoconjugates were synthesized on tetravalent PEG scaffold (**Figure 3.1A**). Each arm on the PEG scaffold carries two groups, R1 is BCR specific antigen and R2 is CD22 ligand. To test the specificity of the glycoconjuagtes, a panel of different groups were attached. Groups attached at R1 were D-lactose (lac, **Figure 3.1B**), specific antigen A type II antigen (AII, **Figure 3.1C**), or non-specific blood group antigen B type II (BII, **Figure 3.1D**). R2 groups were either sialic acid (SA, **Figure 3.1E**), 2,6-sialyllactose (6'SL, **Figure 3.1F**), or 2,3-sialyllactose (3'SL, **Figure 3.1G**). Since our model cell line, A-BCL cell is B lymphocytes with BCR specific to blood group A type II antigens, we only expected glycoconjuagtes with A type II antigens to cluster BCRs and those with 2,6-siallylactose to cluster CD22 receptors. For simplicity, the glycoconjugates were named using nomenclature x(Ag)y(CD22L), where x is number of BCR antigens and y is number of CD22 ligands.

Using a one-color confocal microscopy method, we analyzed the distribution of CD22 and BCRs cluster sizes. As we were interested in changes in individual clusters of CD22, we chose to analyze individual cluster size instead of total cluster size per cell since the latter may be influenced by total number of CD22 present on the membrane. These data were compiled and analyzed for changes in distribution of cluster sizes. As shown in **Table 3.1** and **Figure 3.2**, CD22 was evenly distributed as microclusters on the B cell membrane in untreated cells, which is consistent with other studies.[32,33] These microclusters form by homotypic interactions of CD22, which is the most prominent type of cis interactions.[34,35] The alpha-1 acidic glycoprotein (AGP)[36] was used as a control glycoprotein, and treatment of cells did not alter CD22 clustering. When A-BCL cells were treated with conjugate **36** (4(AII)4(6'SL)), clustering of CD22 increased, suggesting the ability of bifunctional multivalent ligand display to overcome cis-interactions. Notably, the co-presentation of CD22 ligands and BCR specific antigens was crucial, as treatment with conjugates **33** (4(Lac)4(6'SL), containing no BCR antigen) or conjugates **9** (4(AII), containing no CD22 ligands) showed no detectable changes in clustering. Indeed, many studies have used bifunctional glycoconjugates with co-presentation of BCR antigen and CD22 ligand as a high-affinity trans ligand for CD22.[24] Polyacrylic acid polymer (PAA) carrying sialic acids has been used as CD22's high-affinity probe, and when used as a positive control we observed that it clustered CD22 on A-BCL cells without BCR antigens.[37,38] Moreover, CD22 expression was visibly reduced on PAA-treated cells, potentially due to endocytosis of receptors upon clustering.

From these observations, we concluded that at low valency, BCR antigens are needed to cluster CD22 by 2,6-sialyllactose, but this requirement is overcome at higher presentation of CD22 ligands. These requirements are likely due to low-affinity nature of siglecs' ligand binding and high density of cis-ligands. High-valent presentation of the sialic acids compensates this by

offering higher overall concentration of the ligands, leading to more likelihood of CD22 receptors to bind to them and thus are able to compete with high prevalence of cis-ligand. On the other hand, lower presentation of CD22 ligands does not provide sufficient density of trans ligands compared to cis-ligands. Thus, co-presentation of BCR antigens were needed. They could increase the affinity of CD22's ligand binding by bringing the glycoconjugates into closer proximity to the cell membrane, making it easier for CD22 receptors to bind to them. BCRs are also known to diffuse to microdomains on the membrane upon antigen binding, bringing the antigens with them. If CD22 receptors reside within or are in close proximity with these microdomains, BCRs bring glycoconjugates to closer to CD22s, thus increasing their avidity towards the ligands. However, the mechanism by which BCR antigens do this remains to be investigated.

A.

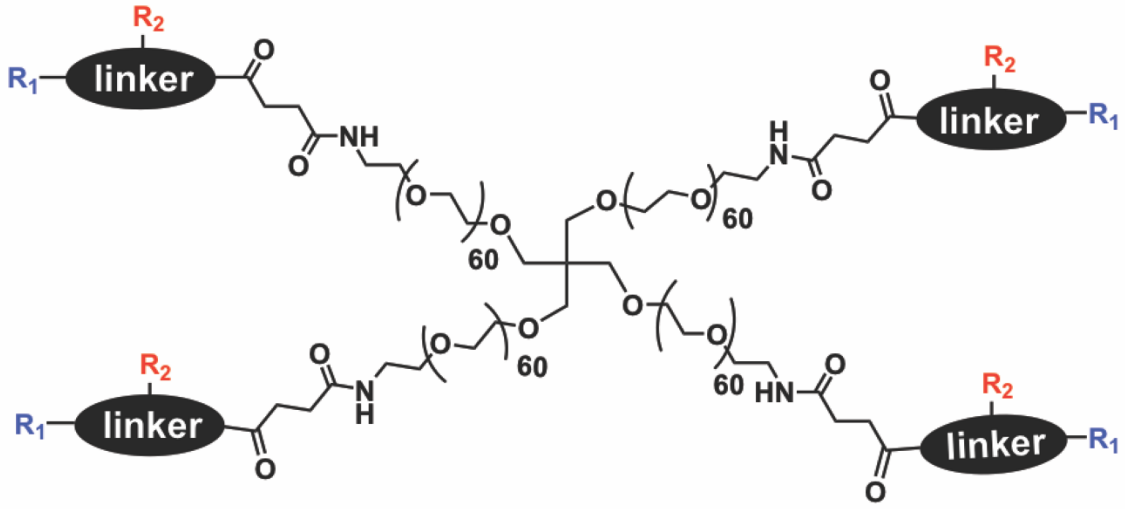

B.

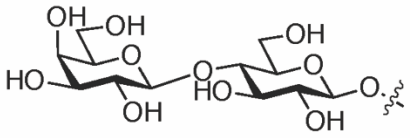

(D-lactose)

E.

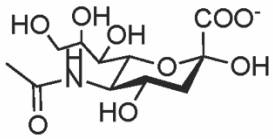

(sialic acid)

C.

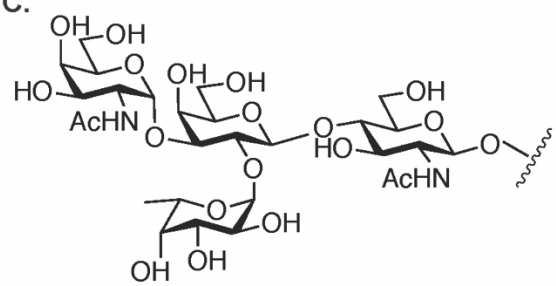

(A type II)

F.

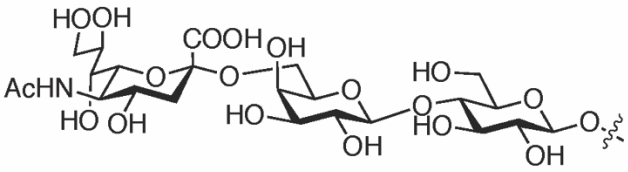

(2,6-sialyllactose)

D.

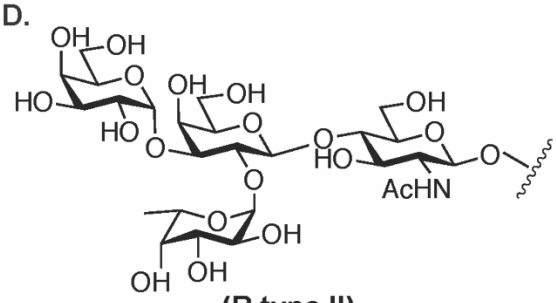

(B type II)

G.

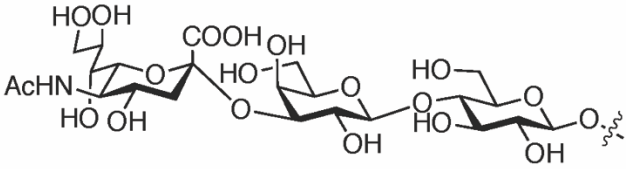

(2,3-sialyllactose)

Figure 3.1. Structures of ABO-glycoconjugates**.** Bi-functional tetravalent ABO-glycoconjugates were synthesized based on tetravalent PEG scaffold (A). R1 group was either sialic acid (B), 2,6-sialyllactose (C), 2,3-sialyllactose (D), or no group attached. R2 was either D-lactose (E), A type II (F), B type II (G), or no group attached. The nomenclature for the glycoconjugates is x(R1)y(R2), where x and y are number of valency of R1 and R2 groups, respectively.

Table 3.1: Clustering of BCR and CD22 receptors by conjugates and proteins

Compound	***Name/Antigen[a]***	***IgM[b]***	***n***	***cluster[c]***	***CD22[b]***	***n***	***cluster[c]***
-	control	0.32 ± 0.04	159	-	0.08 ± 0.004	127	-
-	AGP	0.36 ± 0.03	144	-	0.10 ± 0.01	56	-
-	PAA(SA)	0.29 ± 0.02	155	-	0.21 ± 0.06	84	+
8	4(Lac)	0.28 ± 0.02	143	-	0.11 ± 0.01	119	-
9	4(AII)	1.3 ± 0.2	55	+	0.10 ± 0.02	32	-
10	4(BII)	0.33 ± 0.03	194	-	0.11 ± 0.01	109	-
33	4(Lac)4(6'SL)	0.24 ± 0.02	139	-	0.07 ± 0.01	44	-
34	4(AII)4(SA)	0.93 ± 0.18	80	+	0.12 ± 0.01	161	-
35	4(AII)4(3'SL)	0.83 ± 0.13	98	+	0.13 ± 0.01	159	-
36	4(AII)4(6'SL)	2.2 ± 0.5	57	+	0.6 ± 0.2	45	+

a. Antigens on synthetic conjugates are listed in parenthesis, with the copy number preceding. Abbreviations used are: alpha-1 acid glycoprotein, AGP; sialic acid, SA; lactose, Lac; A-type II, AII; B-type II, BII; 6'-sialyllactose, 6'SL; 3'-sialyllactose, 3'SL.

b. Mean cluster size [μm^2] of the indicated receptor was determined as described in materials and methods.

c. The value of n refers to the number of individual clusters detected in the images from 10 cells for each condition. If the mean cluster size was statistically larger ($p < 0.0001$ by the Student's t-test) for the indicated receptor after treatment with a protein or conjugate, it is indicated with a "+".

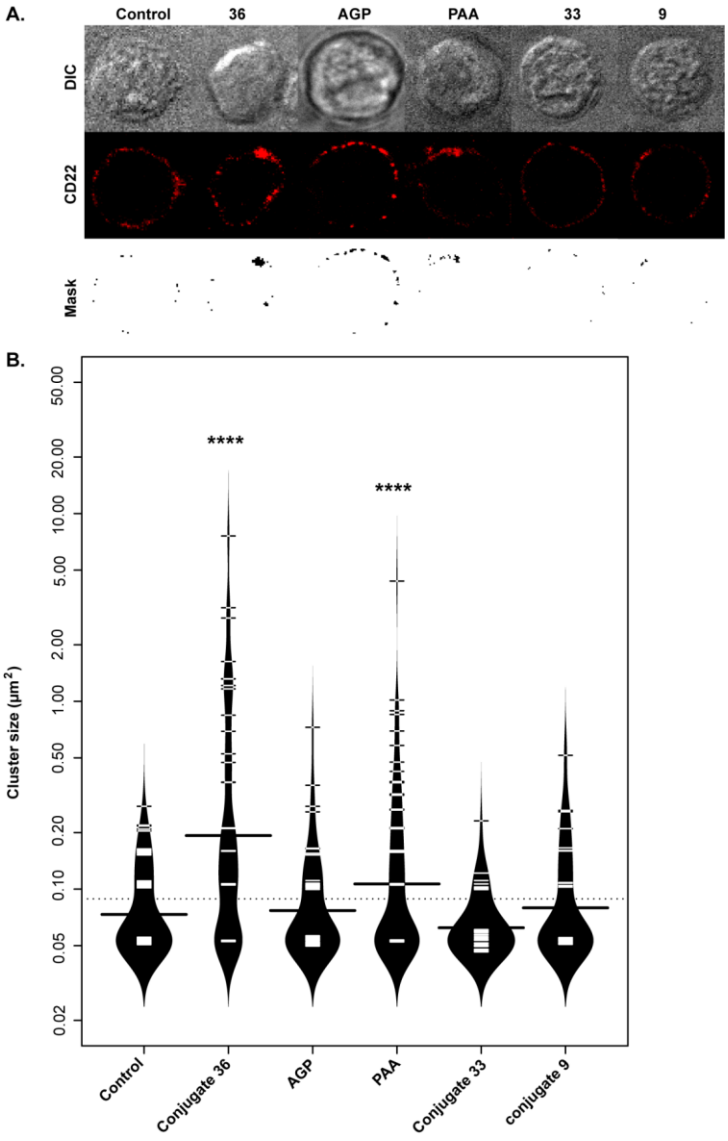

Figure 3.2. Clustering of CD22 receptors by glycoconjugates and glycoproteins. A-BCL cells were treated with 25 ng mL^{-1} PBS, **36**, AGP, PAA, **33**, or **9**, fixed and stained with mouse anti-human CD22, and visualized using confocal microscopy. (A) Representative cells are shown in transmitted (top), fluorescence (middle), and the mask showing identified pixels counted for the clustering analysis (bottom). (B) Cluster size on 10 individual cells was determined using particle analysis in ImageJ and plotted using the beanplot statistical package in R. Each individual white horizontal line within the beanplot represents one single data point, the black horizontal line indicates the geometric mean for each condition, and the dotted line indicates geometric mean of

all conditions within the plot. Populations which were statistically different from control by a Student's t-test are indicated where $p < 0.0001$ with ****, as calculated by GraphPad Prism software.

3.3.2 Clustering of CD22 receptors by control glycoconjugates

To confirm that receptor specificity was critical to regulation of cluster size, we proceeded to investigate the activity of glycoconjugates lacking CD22 ligands. Control cells showed CD22 as microclusters on the cell membrane, consistent with previous results (**Figure 3.3**). As shown in **Figure 3.3**, presentation of 4 copies of lactose alone in compound **8** (4(Lac)) or 4 copies or compound **10** having 4 copies of B type II antigen (4(BII)) did not affect CD22 clustering, ruling out the possibility of non-specific binding of CD22 to the scaffold. Moreover, the glycosidic linkage of the ligand was also important, as compound **35** (4(AII)4(3'SL)) did not cluster CD22; and having monohydrate sialic acids as CD22 ligand in compound **34** (4(AII)4(SA)) was not sufficient. This was predicted as human CD22's ligand binding is specific to α2,6-sialyllactose, thus specific linkage of glycans is an important aspect when designing high-affinity ligand for CD22 receptors. However, recall that PAA, which has high valency of sialic acids, clustered CD22. This suggests that although specific linkage is important at lower valency which is likely due to higher binding affinity, lower-affinity ligands on conjugates may also be able to cluster CD22 when presented at high density.

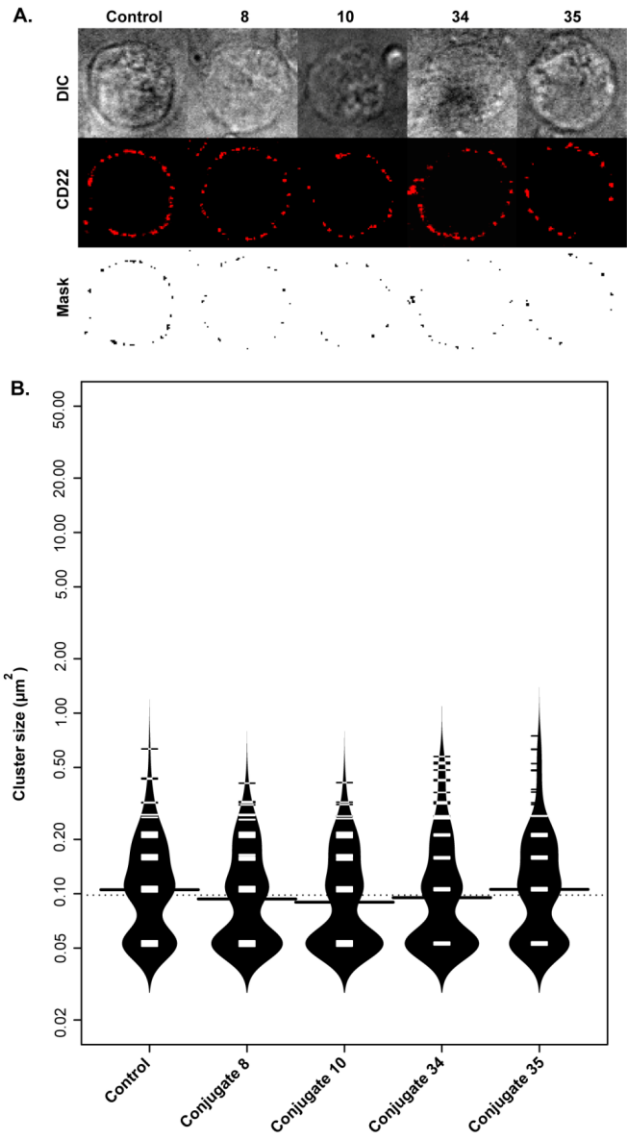

Figure 3.3. Clustering of CD22 receptors by glycoconjugates **8**, **10**, **34**, and **35**. A-BCL cells were treated with 25 ng mL^{-1} PBS, **8**, **10**, **34**, or **35**, fixed and stained with anti-CD22 (mouse), and were visualized using confocal microscopy. (A) Representative cells are shown in transmitted (top), fluorescence (middle), and the mask showing identified pixels counted for the clustering analysis (bottom). (B) Cluster size on 10 individual cells was determined using particle analysis in ImageJ and plotted using the beanplot statistical package in R. Each individual white horizontal line within the beanplot represents one single data point (size of one cluster), the black horizontal line indicates

the geometric mean for each condition, and the dotted line indicates geometric mean of all conditions within the plot.

3.3.3 Clustering of BCRs upon treatment with glycoconjugates

The BCR forms clusters in the presence of specific antigens, inducing cellular response against them. The B cell response is attenuated when CD22 is co-clustered in proximity with BCRs. For this reason, we also tested the ability of glycoconjugates to cluster BCRs. As seen in **Figure 3.3**, BCRs in untreated A-BCL cells are in microclusters on the cell membrane, which is already known for B lymphocytes. Compound **36** (4(AII)4(6'SL)) increased BCR clustering and, in some cases, all the receptors are cross-linked together in a single large cluster; this phenomenon is sometimes called capping.[39–41] Syk is responsible for the crosslinking and capping of BCRs,[42] and they are caused by the multi-valency of the antigen and the ability of BCR to bind to their antigens at two Fab chains, forming aggregates of receptors and antigens. Importantly, unlike CD22 which requires the presence of both BCR antigen and CD22 ligand for forming larger clusters, the presence of antigens alone was sufficient for BCR cross-linking and formation of large clusters. For instance, compound **9** (4(AII)) formed larger clusters and capped BCRs. These observations suggest that no mechanism for enhancing the avidity, such as bi-functional or high-valent antigen display was necessary for clustering the BCRs. Compound **33** (4(Lac)4(6'SL)) did not form larger BCR clusters, suggesting binding of BCRs on A-BCL cells was indeed specific to A type II antigens. As predicted, AGP and PAA did not have any effect on BCR as they do not carry antigens for BCRs. Similarly, in **Figure 3.5**, compounds **8**(4(Lac)) or **10**(4(BII)) did not change BCR clustering as they carry 4 copies of either Lactose or B type II antigens, further confirming the specificity of BCRs. Moreover, as seen previously, the presence of BCR specific antigens alone without CD22 specific ligand is adequate in promoting the clustering and capping

of BCRs as evident in treatment of A-BCL cells with compounds **34** (4(AII)4(SA)) and **35** (4(AII)4(3'SA)), which carry 4 copies of A(II) and 4 copies of either sialic acids or 3' sialosides, respectively, although they had no effects on CD22. These results suggest that generally, multivalent BCR antigens were able to form larger clusters or capping of BCRs regardless of presence or identity of CD22 ligands, while co-presentation of both specific BCR antigens and CD22 ligands is required to overcome CD22 cis ligands to promote clustering by trans interactions. This is possibly due to higher binding affinity of BCRs to their antigens compared to CD22's ligand binding, the presence of two Fab for antigen binding on BCRs, and absence of cis-binding partners to BCRs.

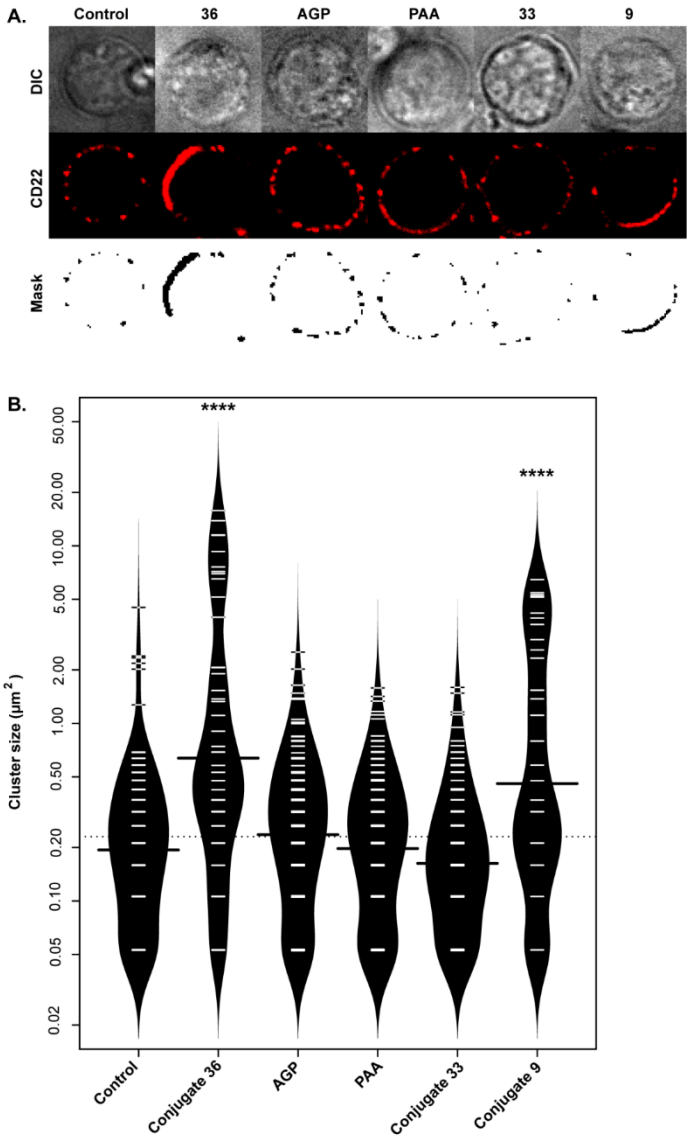

Figure 3.4. Clustering of BCR by glycoconjugates and glycoproteins. A-BCL cells were treated with 25 ng mL^{-1} PBS, **36**, AGP, PAA, **33**, or **9**, fixed and stained with anti-IgM (mouse), and visualized using confocal microscopy. (A) Representative cells are shown in transmitted (top), fluorescence (middle), and the mask showing identified pixels counted for the clustering analysis (bottom). (B) Cluster size on 10 individual cells was determined using particle analysis in ImageJ and plotted using the beanplot statistical package in R. Each individual white horizontal line within the beanplot represents one single data point, the black horizontal line indicates the geometric mean for each condition, and the dotted line indicates geometric mean of all conditions within the

plot. Populations which were statistically different from control by a Student's t-test are indicated where $p < 0.0001$ with ****, as calculated by GraphPad Prism software.

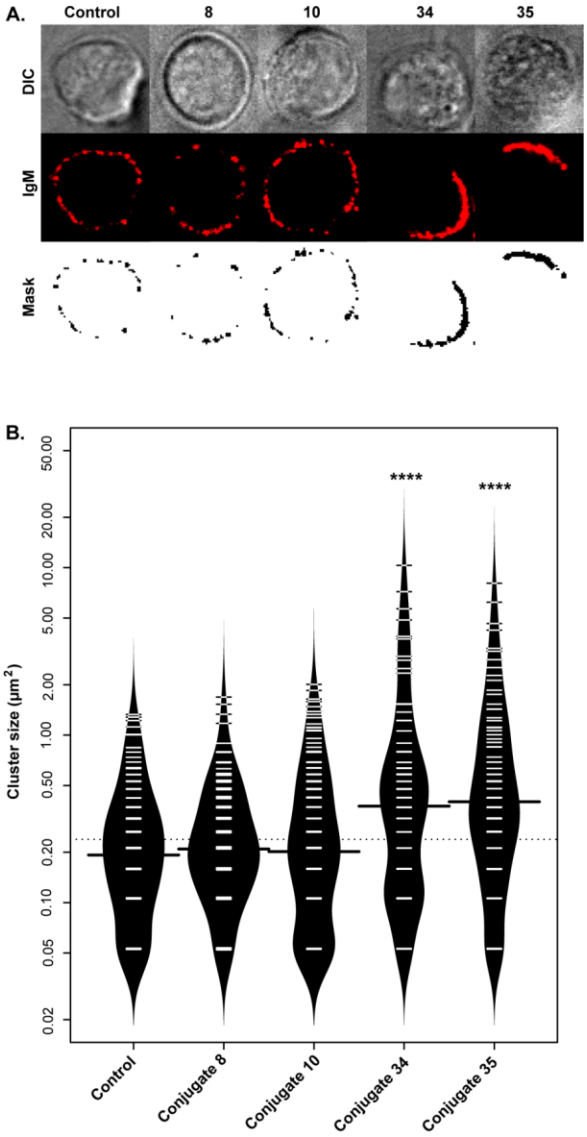

Figure 3.5. Clustering of BCR by glycoconjugates **8**, **10**, **34**, and **35**. A-BCL cells were treated with 25 ng mL^{-1} PBS, **8**, **10**, **34**, or **35**, fixed and stained with anti-IgM (mouse), and visualized using confocal microscopy. (A) Representative cells are shown in transmitted (top), fluorescence (middle), and the mask showing identified pixels counted for the clustering analysis (bottom). (B) Cluster size on 10 individual cells was determined using particle analysis in ImageJ and plotted using the beanplot statistical package in R. Each individual white horizontal line within the

beanplot represents one single data point, the black horizontal line indicates the geometric mean for each condition, and the dotted line indicates geometric mean of all conditions within the plot. Populations which were statistically different from control by a Student's t-test are indicated where $p < 0.0001$ with ****, as calculated by GraphPad Prism software.

3.3.4 Co-localization of CD22 and BCR by glycoconjugates

To attenuate the BCR response, the proximity of CD22 and BCRs is important for dephosphorylation of IgM by phosphatases recruited by CD22.[43] We observed that compound **36** was the only compound that clustered both CD22 and IgM in our previous studies due to the presence of both IgM antigen and CD22 ligand, hence it was important to investigate whether this glycoconjugate could co-cluster these receptors. To do this, two-color confocal microscopy was utilized. In **Figure 3.6**, it was clear that both CD22 and IgM formed microclusters as indicated by discrete islands on untreated cell membrane (**Figure 3.6A, 3.6B**). The co-clustering of the two receptors was analyzed both qualitatively and quantitatively. For qualitative analysis, we examined the yellow pixels on the merged image. There was little overlap between CD22 and IgM in untreated cells, while A-BCL cells treated with compound **36** showed larger clusters for both receptors and significant amount of overlap indicative by large yellow clusters. We also analyzed the co-clustering quantitatively by calculating Pearson's R-value in ImageJ,[44] with higher value indicating more overlapping pixels (**Figure 3.6C, 3.6D**). Compared to the untreated cells, A-BCL cells treated with compound **36** showed significantly higher overlap of the receptors. This supports the conclusion that tetravalent bifunctional glycoconjugates displaying both BCR antigen and CD22 ligand could co-cluster these receptors.

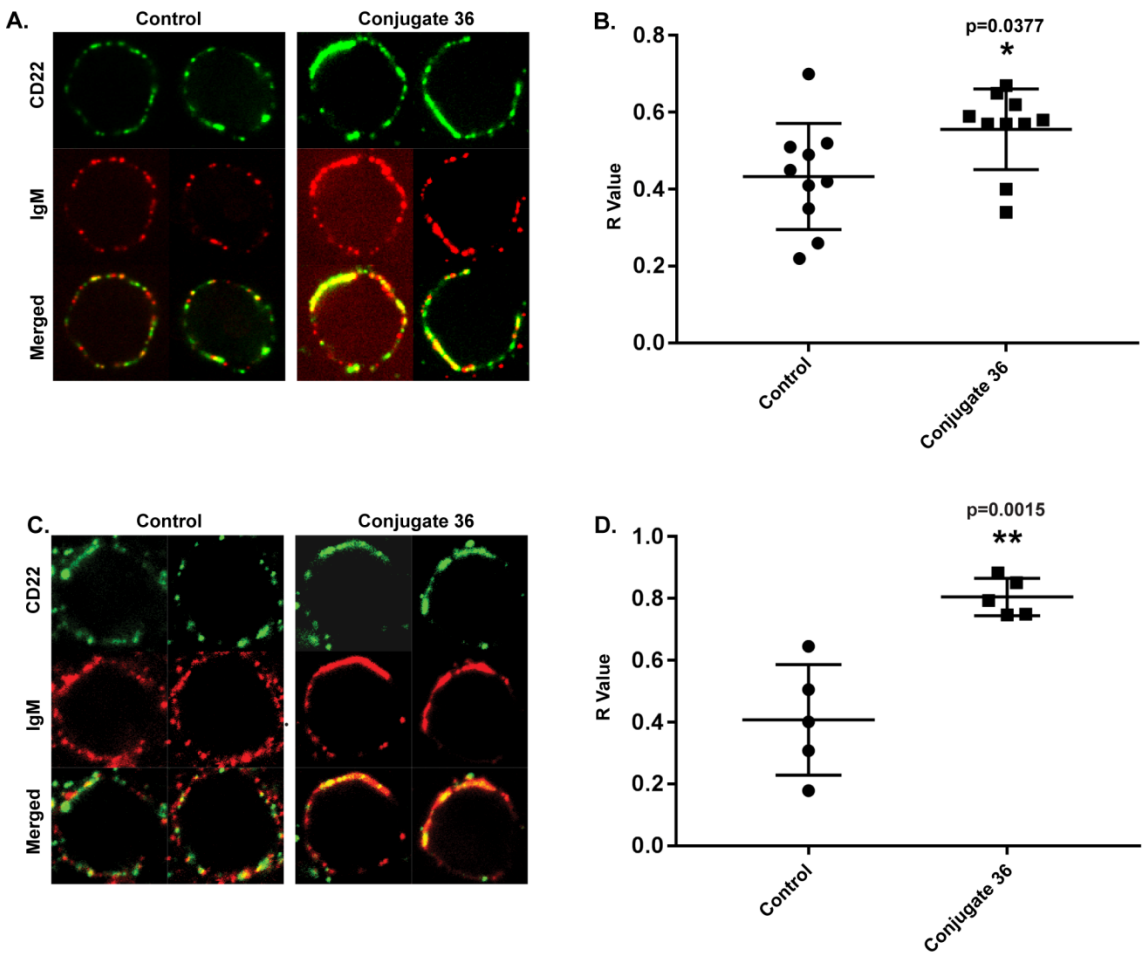

Figure 3.6. Co-localization of CD22 and BCR by glyconconjugate **36**. A-BCL cells were treated with 0 or 25 ng mL^{-1} of 36, stained and fixed, and then imaged by two-color confocal microscopy (CD22, green; IgM, red) (A and C). Two separate replicate experiments for each condition were performed, and multiple individual cells were analyzed in two separate runs and analyzed using the co-localization function (coloc2) in imageJ. Each dot in the analyses (B and C) represents one cell and the results were analyzed and plotted using GraphPad Prism (B and D). Populations were compared using a Student's t-test (*, $p < 0.05$; **, $p < 0.005$)

3.3.5 Clustering of CD22 receptors with GD10 multivalent glycoconjugates

Persistence in serum is an important aspect for therapeutic drugs, as clearance and half-life in serum can be critical determinants of activity. Different strategies are used to extend the half-life of conjugates. Among these, recent work has highlighted the application of small molecule serum-protein binders, which can non-covalently complex to serum proteins.[45] We hypothesized that the half-life of multivalent glyconconjugates could be significantly extended using this strategy. Previous reports had identified AG10 as a binder for protein serum protein transthyretin (TTR).[46,47] However, the AG10 group is challenging to synthesize and was not easily amenable to attachment to our conjugates. We developed a synthetic strategy to a related analog which we dubbed GD10, and conjugated this group to our glycoconjugates to test if we could alter their serum half-life. AG10 has been shown to extend half-lives of conjugates in serum due to high affinity to a protein serum transthyretin (TTR).[46,48] This multivalent glycoconjugate was synthesized on the tetravalent scaffold previously described, with addition of GD10 group on one of the branches on the scaffold (**Table 3.2**, **Figure 3.7**). On this branch, 2,6-sialyllactose is conjugated on the same PEG chain as the GD10 group, while A type II antigen is on another PEG chain of the same branch. Since GD10 is a relatively large group, it can potentially hinder the binding of the glycoconjugate to CD22, thus investigating the effects of this addition to receptor binding was necessary to ensure affinity is not compromised while extending serum half-life.

As shown in **Figure 3.8**, incubation of A-BCL cells with compound **27** formed fewer and significantly larger CD22 clusters, suggesting that addition of the GD10 analog onto glycoconjugate does not interfere with binding to its receptor. Additionally, since GD10 binds to TTR in serum to extend its half-life, it was important to investigate whether the presence of this protein has any effects on the ability of glycoconjugates to cluster CD22. To do this, we treated

A-BCL cells with glycoconjugates and TTR together. Confocal microscopy analysis of CD22 receptors also showed significant change in clustering, similar to treatment without TTR. The increased CD22 clustering by compound **36** was significant and similar to the change by compound **27**. Thus, we can conclude that addition of GD10 on glycoconjugates does not interfere with the binding to and clustering of CD22 in vitro. Although GD10 is a large group, this did not interfere with binding of glycoconjugate to CD22 receptors and cluster them. This could be due to the flexibility of the PEG scaffold and the linker, allowing sufficient binding to the receptors. Since A type II BCR-specific antigen was unchanged from compound **36** in the previous studies, we expected compound 27 to co-cluster BCR and CD22, potentially inhibiting B cell response.

Table 3.2: Clustering of BCR and CD22 receptors by GD10 conjugates

Compound	***Name/Antigen[a]***	***CD22[b]***	***n***	***cluster[c]***
-	control	0.14 ± 0.0002	638	-
27	4(AII)4(6'SL)1(GD10)	0.28 ± 0.0008	630	+
27 + TTR	4(AII)4(6'SL)1(GD10) + TTR	0.23 ± 0.0007	538	+
36	4(AII)4(6'SL)	0.21 ± 0.001	176	+

a. Antigens on synthetic conjugates are listed in parenthesis, with the copy number preceding. Abbreviations used are: lactose, Lac; A-type II, AII; 6'-sialyllactose, 6'SL; transthyretin, TTR.
b. Mean cluster size [μm^2] of the indicated receptor was determined as described in materials and methods.
c. The value of n refers to the number of individual clusters detected in the images from 20 cells for each condition. If the mean cluster size was statistically larger ($p < 0.0001$ by the Student's t-test) for the indicated receptor after treatment with a protein or conjugate, it is indicated with a "+".

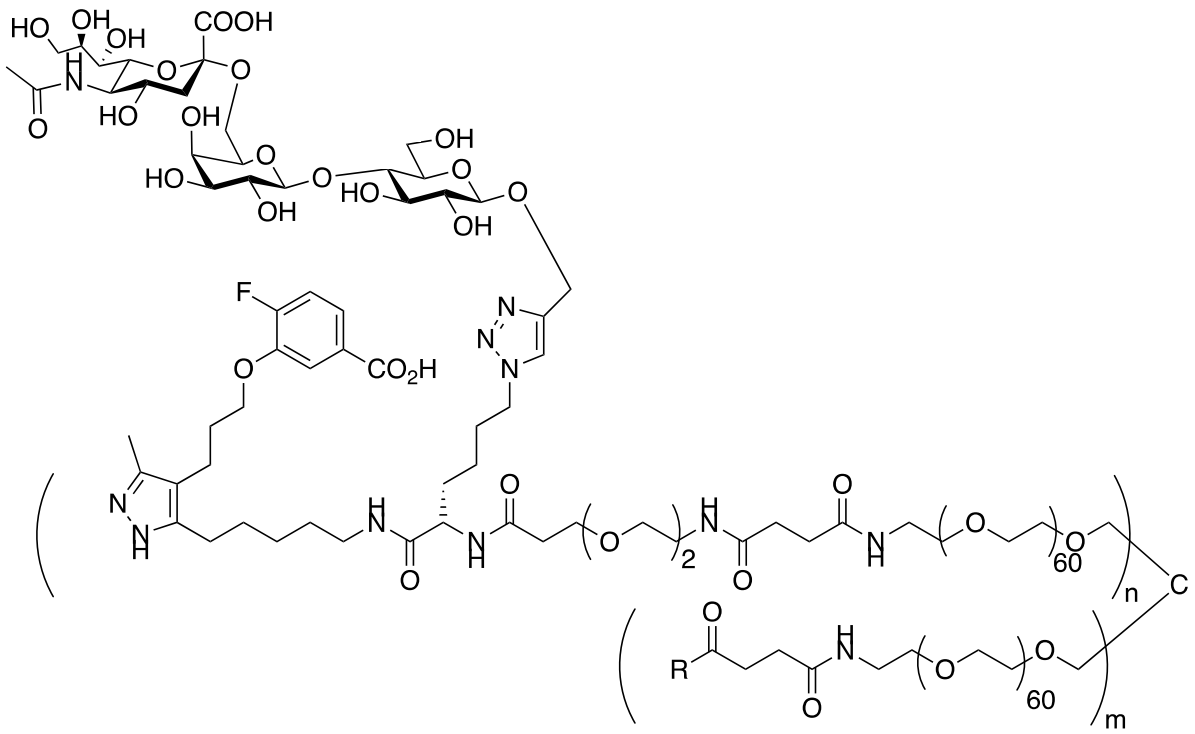

Figure 3.7. Structure of GD10 glycoconjugate **27** on one of the branches of PEG scaffold described previously; R = A type II antigens.

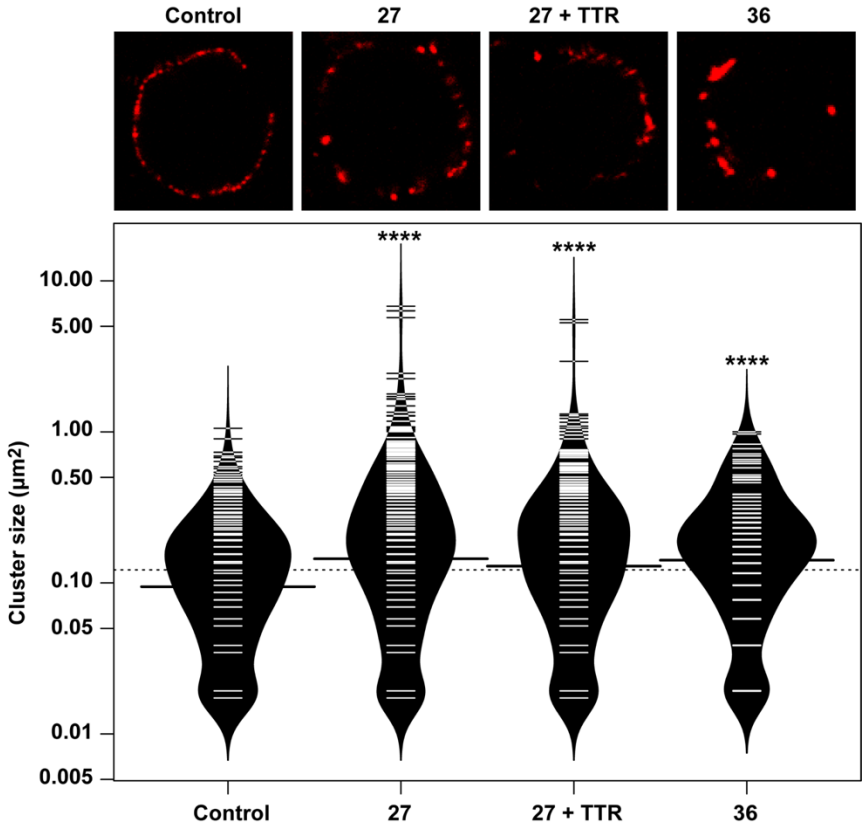

Figure 3.8. BCR clustering by high-valency glycoconjugates. A-BCL cells were treated with 25 ng mL-1 PBS, **27**, **27** with TTR, or **36 11**, then fixed and stained with anti-CD22 (mouse) and visualized using confocal microscopy. (**A**) Fluorescence images of representative cells are shown. (**B**) Cluster size on 20 individual cells was determined using particle analysis in ImageJ and plotted using the beanplot statistical package in R. Each individual short horizontal line within the beanplot represents one single data point, the longer black horizontal line indicates the mean for each condition, and the dotted line indicates mean of all conditions within the plot. Populations which were statistically different from control using a Student's t-test are indicated ($p < 0.0001$, ****) as calculated by GraphPad Prism software.

3.3.6 Clustering of CD22 and BCR with high-valent glycoconjugates

High affinity ligands are required to overcome cis-interactions of CD22 on B cell membrane. In our previous studies, we showed that the presence of BCR specific antigen and CD22 ligand

was required for clustering of CD22 receptors (4(Lac)4(6'SL)). However, we also showed that the presence of CD22 ligands alone clustered CD22 receptors if they were present in high valency (PAA). Thus, we speculated that increasing the copy numbers of CD22 ligands could cluster CD22 without the presence of BCR-specific antigens. To do this, glycoconjugate **11** (4(Lac)12(6'SL)) was synthesized (**Figure 3.3**, **Figure 3.9A, 3.9B**). These glycoconjugates were synthesized on the tetravalent scaffold as previously described, with each arm of the scaffold carrying 3 copies of 2,6-sialyllactose and one copy of antigen (**Figure 3.9A**). As shown in **Figure 3.10**, CD22 receptors are dispersed on cell membrane in microclusters on untreated A-BCL cells. Although compound **33** (4(Lac)4(6'SL)) was unable to cluster CD22 due to lack of BCR specific antigens, compound **11** (4(Lac)12(6'SL)) significantly increased CD22 cluster size. This suggests that even in the absence of specific antigen, CD22 ligand alone is sufficient to overcome cis interactions if they are present in high-valency. Having more copies of the CD22 ligand on glycoconjugates increased the affinity towards the receptors by presenting higher ligand density, thus increasing the probability of CD22 to bind to the ligand. Similarly, glycoconjugate **12** (4(AII)12(6'SL), **Figure 3.10C**) increased clustering, similar to conjugate **36** (4(AII)4(6'SL)). We hypothesized that increasing the valency of CD22 ligand could induce more clustering as each conjugate is able to bind to more CD22 molecules. However, although compound **12** increased CD22 cluster size, these clusters were not significantly different from compound **36**. This may be due receptor binding to the ligand is saturated with compound **36** and increasing number of ligands beyond this number cannot induce larger CD22 clusters.

We also investigated whether increasing the number of CD22 ligands on glycoconjugates has any influence on their ability of cluster BCR. In **Figure 3.11**, BCR is seen as being in microclusters on untreated cell membrane. When A-BCL cells were treated with compound **33** or

compound **11**, there was no significant change to the organization of the receptors, which was expected as no BCR specific antigens was present on these glycoconjugates, again confirming the specificity of BCR. When we treated A-BCL cells with compound **36** or compound **12**, BCR clustering significantly increased, but no difference was observed between these glycoconjugates. Since we only increased the valency of CD22 ligands on these glycoconjugates, it was expected to have no effect on BCR clustering. Although the tri-valent 2,6-sialyllactose group is relatively large, this did not interfere with clustering of BCR by their antigens, likely due to the flexible linkages which allowed sufficient binding of BCR antigens and CD22 ligands to their respective receptors. These results suggest that increasing the valency of the CD22 ligand does not influence BCR organization on cell membrane.

Table 3.3: Clustering of BCR and CD22 receptors by high-valent conjugates

Compound	***Name/Antigen[a]***	***IgM[b]***	***n***	***cluster[c]***	***CD22[b]***	***n***	***cluster[c]***
-	control	0.18 ± 0.0002	687	-	0.18 ± 0.0002	661	-
11	4 (Lac)12(6'SL)	0.17 ± 0.0002	739	-	0.21 ± 0.0003	831	+
12	4(AII)12(6'SL)	0.40 ± 0.001	633	+	0.38 ± 0.001	719	+
33	4(Lac)4(6'SL)	0.15 ± 0.0002	582	-	0.19 ± 0.0002	851	-
36	4(AII)6(6'SL)	0.45 ± 0.001	540	+	0.32 ± 0.001	498	+

a. Antigens on synthetic conjugates are listed in parenthesis, with the copy number preceding. Abbreviations used are: lactose, Lac; A-type II, AII; 6'-sialyllactose, 6'SL.

b. Mean cluster size [μm^2] of the indicated receptor was determined as described in materials and methods.

c. The value of n refers to the number of individual clusters detected in the images from 10 cells for each condition. If the mean cluster size was statistically larger ($p < 0.0001$ by the Student's t-test) for the indicated receptor after treatment with a protein or conjugate, it is indicated with a "+".

A.

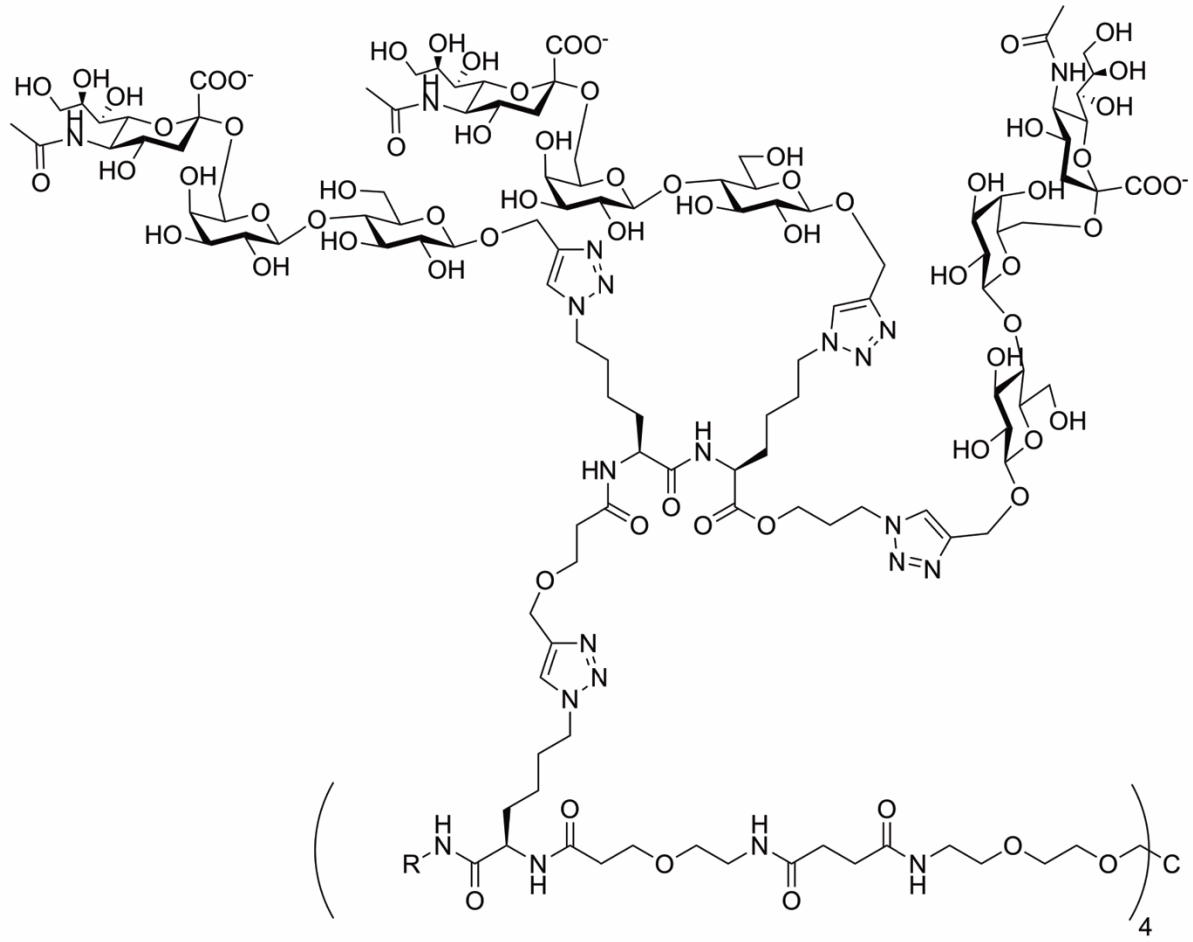

B.

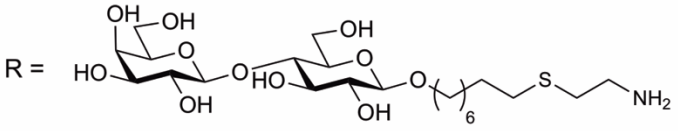

C.

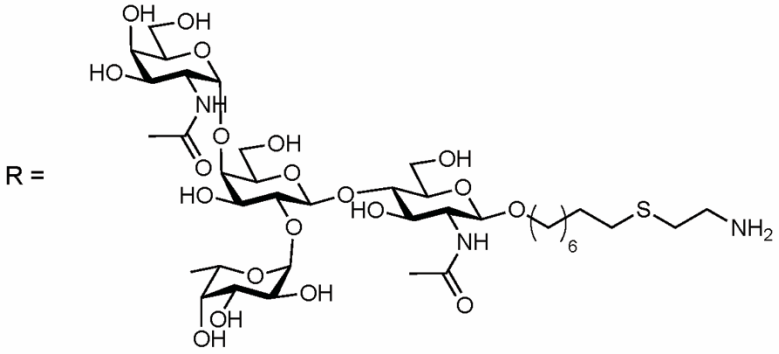

Figure 3.9. Structure of high-valency glycoconjugate. Structure of one arm of the PEG scaffold (**A**), each with 3 groups of 6'sialyllactose and R group. R group is either lactose (**B**) or A type II antigen (**C**).

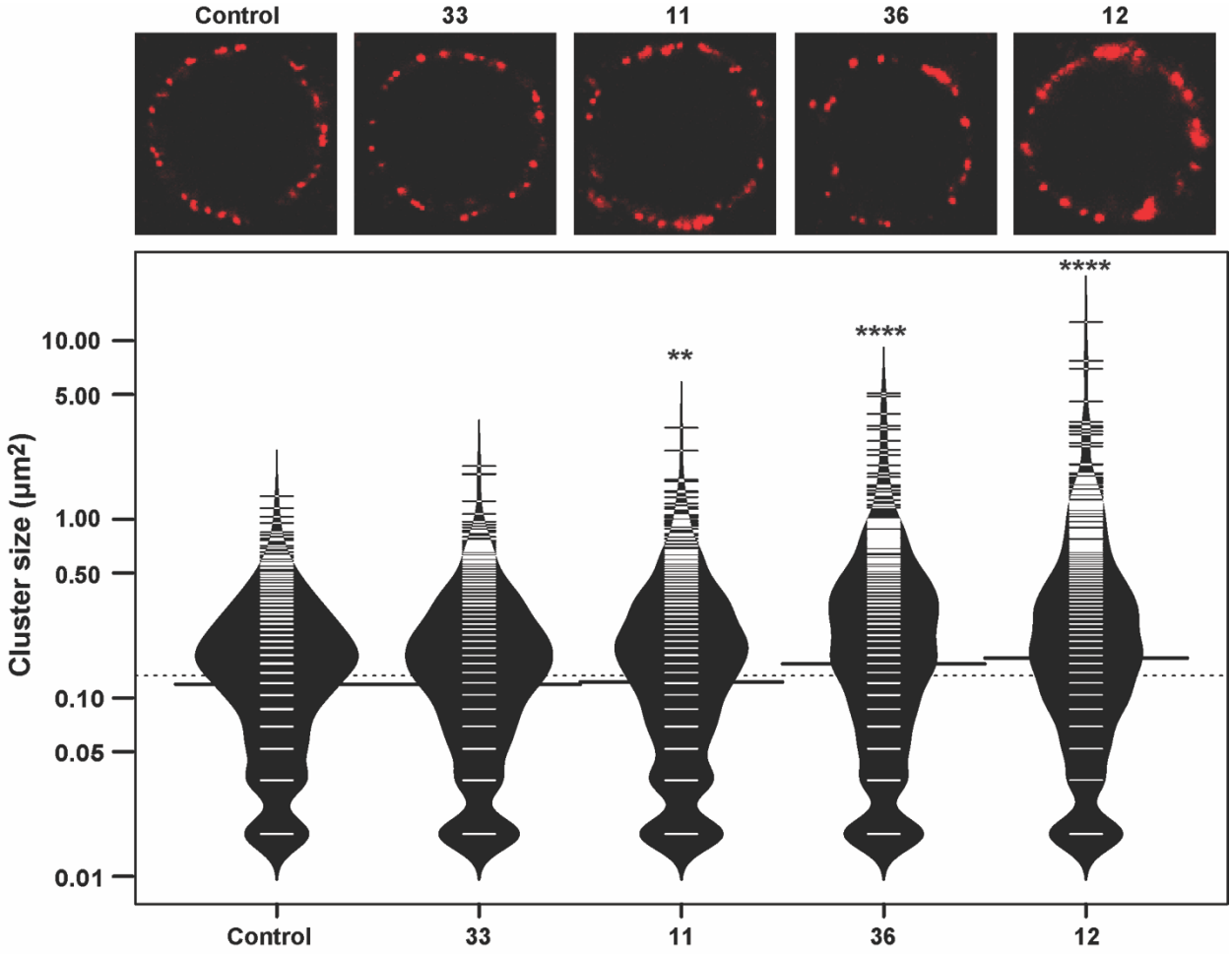

Figure 3.10. CD22 clustering by high-valency glycoconjugates. A-BCL cells were treated with 25 ng mL-1 PBS, **33**, **11**, **36**, or **12**, then fixed and stained with anti-CD22 (mouse), and visualized using confocal microscopy. (**A**) Fluorescence images of representative cells are shown. (**B**) Cluster size on 20 individual cells was determined using particle analysis in ImageJ and plotted using the beanplot statistical package in R. Each individual white horizontal line within the beanplot represents one single data point, the black horizontal line indicates the mean for each condition, and the dotted line indicates mean of all conditions within the plot. Populations which

were statistically different from control based on a Student's t-test are indicated ($p < 0.0001$, ****) as calculated by GraphPad Prism software. Data from three biological replicates experiments were pooled and analyzed.

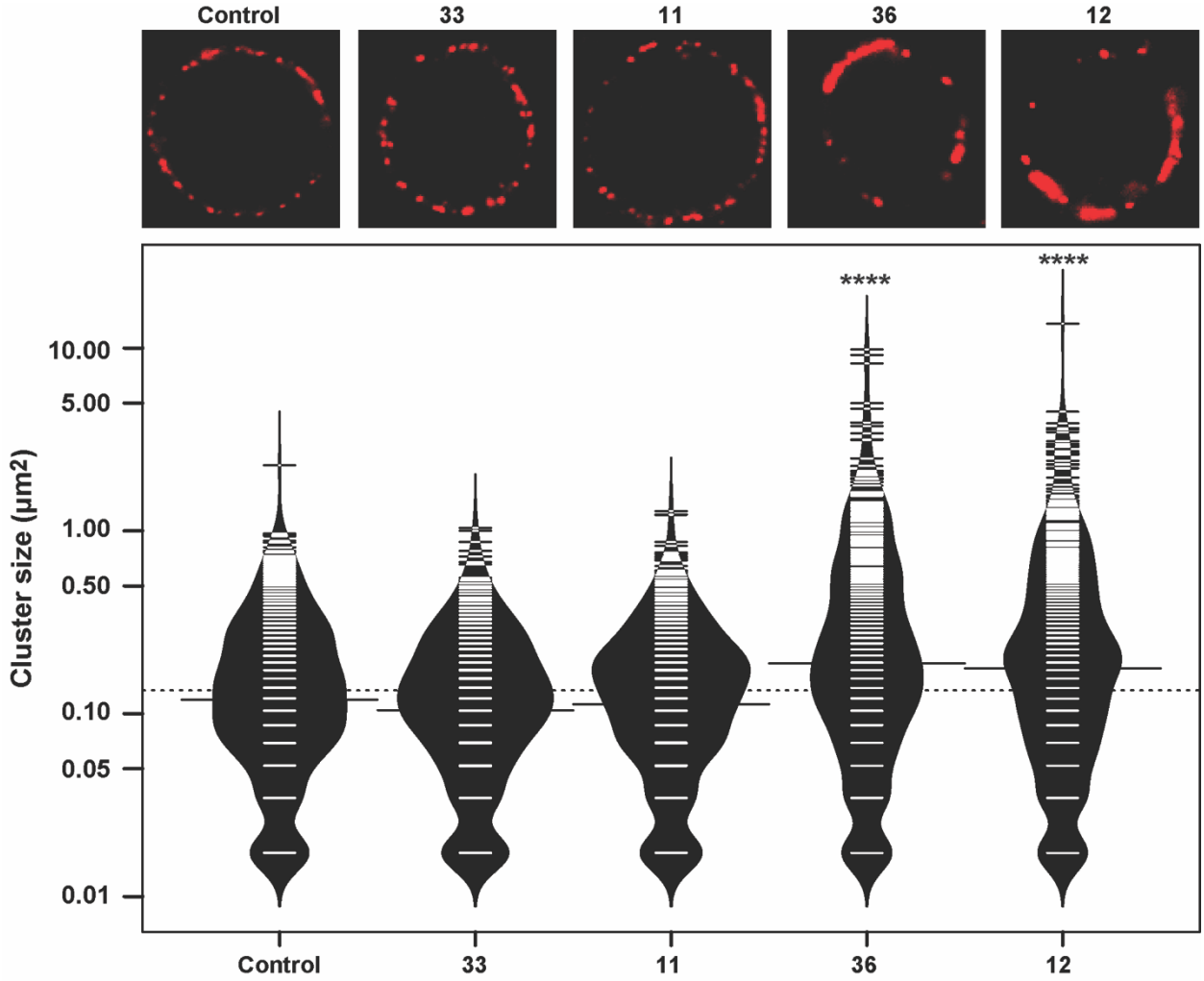

Figure 3.11. BCR clustering by high-valency glycoconjugates. A-BCL cells were treated with 25 ng mL-1 PBS, **33**, **11**, **3**6, or **12**, then fixed and stained with anti-IgM (mouse) and visualized using confocal microscopy. (**A**) Fluorescence images of representative cells are shown. (**B**) Cluster size on 20 individual cells was determined using particle analysis in ImageJ and plotted using the beanplot statistical package in R. Each individual white horizontal line within the beanplot represents one single data point, the black horizontal line indicates the mean for each condition,

and the dotted line indicates mean of all conditions within the plot. Data from three biological replicates were pooled and analyzed.

3.4 CONCLUSIONS

Using confocal microscopy to analyze the clustering of cell membrane receptors, we investigated the ability of synthetic mutivalent, bi-functional glycoconjugates to co-cluster BCR and CD22 on A type-II specific B cells (A-BCL cells). We found that glycoconjugate 4(AII)4(6'SL) was able to increase clustering of CD22 and BCR, and co-cluster these receptors. This points to the important roles of N-glycans on bringing CD22 and BCR into proximity for B cell signaling regulation. Recently, it has been found that galectin-9 (Gal-9) is involved mediating the inhibition of B cell response by co-clustering CD22 and BCR.[49] Consequently, mutation of glycan binding sites on CD22 disrupted this Gal-9 dependent inhibition of B cell signaling. Similarly, we speculate that if we mutate ligand binding domains on CD22, high-affinity ligands can no longer associate BCR and CD22, leading to elevated B cell response. Importantly, we also found that co-presentation of BCR antigen and CD22 ligand was important for CD22 clustering, as control glycoconjugate 4(Lac)4(6'SL) could not increase clustering in CD22 receptors. The conjugation of TTR binder GD10 had no influence on CD22 receptor binding of the glycoconjugates, suggesting that inclusion of this group will not disrupt targeting of CD22, and may help to prolong conjugates half-life in serum. We found that bifunctional conjugates were more effective at CD22 clustering by trans ligands at lower copy number of ligands. Conjugates with increased ligand valency, or that contained serum-protein binding elements, allowed CD22 clustering without BCR antigen. Together, these strategies may allow more approaches to manipulate B cell response by utilizing CD22 trans-ligands, for example expanding donor pool in blood transfusions and organ transplantations.

REFERENCES

(1) Tolar, P.; Hanna, J.; Krueger, P. D.; Pierce, S. K. The Constant Region of the Membrane Immunoglobulin Mediates B Cell-Receptor Clustering and Signaling in Response to Membrane Antigens. *Immunity* **2009**, *30* (1), 44–55. https://doi.org/10.1016/j.immuni.2008.11.007.

(2) Wan, Z.; Liu, W. The Growth of B Cell Receptor Microcluster Is a Universal Response of B Cells Encountering Antigens with Different Motion Features. *Protein Cell* **2012**, *3*, 545–558.

(3) Khare, S. D.; Sarosi, I.; Xia, X.-Z.; McCabe, S.; Miner, K.; Solovyev, I.; Hawkins, N.; Kelley, M.; Chang, D.; Van, G.; Ross, L.; Delaney, J.; Wang, L.; Lacey, D.; Boyle, W. J.; Hsu, H. Severe B Cell Hyperplasia and Autoimmune Disease in TALL-1 Transgenic Mice. **2000**, *PNAS 97* (7), 3370–3375.

(4) Petro, J. B.; Rahman, S. M. J.; Ballard, D. W.; Khan, W. N. Bruton's Tyrosine Kinase Is Required for Activation of I□B Kinase and Nuclear Factor □B in Response to B Cell Receptor Engagement. *J. Exp. Med.* **2000**, *191* (10), 1745–1753.

(5) Lipsky, P. E. Systemic Lupus Erythematosus: An Autoimmune Disease of B Cell Hyperactivity. *Nat. Immunol.* **2001**, *2* (9), 764–766. https://doi.org/10.1038/ni0901-764.

(6) Ammann, A. J.; Abrams, D. B-Cell Immunodeficiency in Acquired Immune Deficiency Syndrome. *J. Am. Med. Assoc.* **1984**, *251* (11), 1447–1449.

(7) Piqueras, B.; Lavenu-Bombled, C.; Galicier, L.; Cruyssen, F. B.-V. D.; Mouthon, L.; Chevret, S.; Debre, P.; Schmitt, C.; Oksenhendler, E. Common Variable Immunodeficiency Patient Classification Based on Impaired B Cell Memory Differentiation Correlates with Clinical Aspects. *J. Clin. Immunol.* **2003**, *23* (5), 385–400.

(8) Järvinen, K.-M.; Beyer, K.; Vila, L.; Chatchatee, P.; Busse, P. J.; Sampson, H. A. B-Cell Epitopes as a Screening Instrument for Persistent Cow's Milk Allergy. *J. Allergy Clin. Immunol.* **2002**, *110* (2), 293–297. https://doi.org/10.1067/mai.2002.126080.

(9) Li, X.-M.; Serebrisky, D.; Lee, S.-Y.; Huang, C.-K.; Bardina, L.; Schofield, B. H.; Stanley, J. S.; Burks, A. W.; Bannon, G. A.; Sampson, H. A. A Murine Model of Peanut Anaphylaxis: T- and B-Cell Responses to a Major Peanut Allergen Mimic Human Responses. *J. Allergy Clin. Immunol.* **2000**, *106* (1), 150–158. https://doi.org/10.1067/mai.2000.107395.

(10) Sánchez-Ruano, L.; de la Hoz, B.; Martínez-Botas, J. Clinical Utility of Microarray B-cell Epitope Mapping in Food Allergies: A Systematic Review. *Pediatr. Allergy Immunol.* **2020**, *31* (2), 175–185. https://doi.org/10.1111/pai.13141.

(11) Muller, J.; Obermeier, I.; Wohner, M.; Brandl, C.; Mrotzek, S.; Angermuller, S.; Maity, P. C.; Reth, M.; Nitschke, L. CD22 Ligand-Binding and Signaling Domains Reciprocally

Regulate B-Cell Ca2+ Signaling. *Proc. Natl. Acad. Sci.* **2013**, *110* (30), 12402–12407. https://doi.org/10.1073/pnas.1304888110.

(12) Jellusova, J.; Nitschke, L. Regulation of B Cell Functions by the Sialic Acid-Binding Receptors Siglec-G and CD22. *Front. Immunol.* **2012**, *2*. https://doi.org/10.3389/fimmu.2011.00096.

(13) Bou, R.; Lebien, T. W. Of CD22 in Acute Leukemia. *Blood* **1988**, *71* (5), 1480–1486.

(14) Doody, G.; Justement, L.; Delibrias, C.; Matthews, R.; Lin, J.; Thomas, M.; Fearon, D. A Role in B Cell Activation for CD22 and the Protein Tyrosine Phosphatase SHP. *Science* **1995**, *269* (5221), 242–244. https://doi.org/10.1126/science.7618087.

(15) Razi, N.; Varki, A. Masking and Unmasking of the Sialic Acid-Binding Lectin Activity of CD22 (Siglec-2) on B Lymphocytes. *Proc. Natl. Acad. Sci.* **1998**, *95* (13), 7469–7474. https://doi.org/10.1073/pnas.95.13.7469.

(16) Macauley, M. S.; Pfrengle, F.; Rademacher, C.; Nycholat, C. M.; Gale, A. J. Antigenic Liposomes Displaying CD22 Ligands Induce Antigen-Specific B Cell Apoptosis. *J. Clin. Invest.* **2013**, *123* (7), 3074–3083. https://doi.org/10.1172/JCI69187.

(17) Chen, W. C.; Completo, G. C.; Sigal, D. S.; Crocker, P. R.; Saven, A.; Paulson, J. C. In Vivo Targeting of B-Cell Lymphoma with Glycan Ligands of CD22. *Blood* **2010**, *115* (23), 4778–4786. https://doi.org/10.1182/blood-2009-12- 257386.

(18) Duong, B. H.; Tian, H.; Ota, T.; Completo, G.; Han, S.; Vela, J. L.; Ota, M.; Kubitz, M.; Bovin, N.; Paulson, J. C.; Nemazee, D. Decoration of T-Independent Antigen with Ligands for CD22 and Siglec-G Can Suppress Immunity and Induce B Cell Tolerance in Vivo. *J. Exp. Med.* **2010**, *207* (1), 173–187. https://doi.org/10.1084/jem.20091873.

(19) Courtney, A. H.; Puffer, E. B.; Pontrello, J. K.; Yang, Z.-Q.; Kiessling, L. L. Sialylated Multivalent Antigens Engage CD22 *in Trans* and Inhibit B Cell Activation. *Proc. Natl. Acad. Sci.* **2009**, *106* (8), 2500–2505. https://doi.org/10.1073/pnas.0807207106.

(20) Daskhan, G. C.; Tran, H.-T. T.; Meloncelli, P. J.; Lowary, T. L.; West, L. J.; Cairo, C. W. Construction of Multivalent Homo- and Heterofunctional ABO Blood Group Glycoconjugates Using a Trifunctional Linker Strategy. *Bioconjug. Chem.* **2018**, *29* (2), 343–362. https://doi.org/10.1021/acs.bioconjchem.7b00679.

(21) Varki, A. Biological Roles of Glycans. *Glycobiology* **2017**, *27* (1), 3–49. https://doi.org/10.1093/glycob/cww086.

(22) Doyle, H. A.; Mamula, M. J. Post-Translational Protein Modifications in Antigen Recognition and Autoimmunity. *Trends Immunol.* **2001**, *22* (8), 443–449. https://doi.org/10.1016/S1471-4906(01)01976-7.

(23) Avci, F. Y.; Li, X.; Tsuji, M.; Kasper, D. L. A Mechanism for Glycoconjugate Vaccine Activation of the Adaptive Immune System and Its Implications for Vaccine Design. *Nat. Med.* **2011**, *17* (12), 1602–1609. https://doi.org/10.1038/nm.2535.

(24) O'Reilly, M. K.; Collins, B. E.; Han, S.; Liao, L.; Rillahan, C.; Kitov, P. I.; Bundle, D. R.; Paulson, J. C. Bifunctional CD22 Ligands Use Multimeric Immunoglobulins as Protein Scaffolds in Assembly of Immune Complexes on B Cells. *J. Am. Chem. Soc.* **2008**, *130* (24), 7736–7745. https://doi.org/10.1021/ja802008q.

(25) Ferber, I.; Schonrich, G.; Schenkel, J.; Mellor, A.; Hammerling, G.; Arnold, B. Levels of Peripheral T Cell Tolerance Induced by Different Doses of Tolerogen. *Science* **1994**, *263* (5147), 674–676. https://doi.org/10.1126/science.8303275.

(26) Hosoi, E. Biological and Clinical Aspects of ABO Blood Group System. *J. Med. Invest.* **2008**, *55* (3,4), 174–182. https://doi.org/10.2152/jmi.55.174.

(27) Franchini, M.; Liumbruno, G. M. ABO Blood Group: Old Dogma, New Perspectives. *Clin. Chem. Lab. Med.* **2013**, *51* (8), 1545–1553. https://doi.org/10.1515/cclm-2013-0168.

(28) Rydberg, L. ABO-Incompatibility in Solid Organ Transplantation. *Transfus. Med.* **2001**, *11* (4), 325–342. https://doi.org/10.1046/j.1365-3148.2001.00313.x.

(29) West, L. J.; Cardella, C. J. ABO-Incompatible Heart Transplantation in Infants. *N. Engl. J. Med.* **2001**, *344* (11), 793–800.

(30) Chung, B. K.; Tsai, K.; Allan, L. L.; Zheng, D. J.; Nie, J. C.; Biggs, C. M.; Hasan, M. R.; Kozak, F. K.; van den Elzen, P.; Priatel, J. J.; Tan, R. Innate Immune Control of EBV-Infected B Cells by Invariant Natural Killer T Cells. *Blood* **2013**, *122* (15), 2600–2608. https://doi.org/10.1182/blood-2013-01-480665.

(31) Slaney, A. M.; Dijke, I. E.; Jeyakanthan, M.; Li, C.; Zou, L.; Plaza-Alexander, P.; Meloncelli, P. J.; Bau, J. A.; Allan, L. L.; Lowary, T. L.; West, L. J.; Cairo, C. W.; Buriak, J. M. Conjugation of A and B Blood Group Structures to Silica Microparticles for the Detection of Antigen-Specific B Cells. *Bioconjug. Chem.* **2016**, *27* (3), 705–715. https://doi.org/10.1021/acs.bioconjchem.5b00672.

(32) Collins, B. E.; Smith, B. A.; Bengtson, P.; Paulson, J. C. Ablation of CD22 in Ligand-Deficient Mice Restores B Cell Receptor Signaling. *Nat. Immunol.* **2006**, *7* (2), 8.

(33) Gasparrini, F.; Feest, C.; Bruckbauer, A.; Mattila, P. K.; Müller, J.; Nitschke, L.; Bray, D.; Batista, F. D. Nanoscale Organization and Dynamics of the Siglec CD 22 Cooperate with the Cytoskeleton in Restraining BCR Signalling. *EMBO J.* **2016**, *35* (3), 258–280. https://doi.org/10.15252/embj.201593027.

(34) Alborzian Deh Sheikh, A.; Akatsu, C.; Imamura, A.; Abdu-Allah, H. H. M.; Takematsu, H.; Ando, H.; Ishida, H.; Tsubata, T. Proximity Labeling of Cis-Ligands of CD22/Siglec-2 Reveals Stepwise A2,6 Sialic Acid-Dependent and -Independent Interactions. *Biochem.*

Biophys. Res. Commun. **2018**, *495* (1), 854–859. https://doi.org/10.1016/j.bbrc.2017.11.086.

(35) Han, S.; Collins, B. E.; Bengtson, P.; Paulson, J. C. Homomultimeric Complexes of CD22 in B Cells Revealed by Protein-Glycan Cross-Linking. *Nat. Chem. Biol.* **2005**, *1* (2), 93–97. https://doi.org/10.1038/nchembio713.

(36) Fournier, T.; Medjoubi-N, N.; Porquet, D. Alpha-1-Acid Glycoprotein. *Biochim. Biophys. Acta* **2000**, *1482*, 157–171.

(37) Collins, B. E.; Blixt, O.; Bovin, N. V.; Danzer, C.-P.; Chui, D.; Marth, J. D.; Nitschke, L.; Paulson, J. C. Constitutively Unmasked CD22 on B Cells of ST6Gal I Knockout Mice: Novel Sialoside Probe for Murine CD22. *Glycobiology* **2002**, *12* (9), 563–571. https://doi.org/10.1093/glycob/cwf067.

(38) Collins, B. E.; Blixt, O.; Han, S.; Nathan, J. K.; Bovin, N.; Paulson, J. C. High-Affinity Ligand Probes of CD22 Overcome the Threshold Set by Cis Ligands to Allow for Binding, Endocytosis, and Killing of B Cells. *J. Immunol.* **2006**, *177* (5), 2994–3003. https://doi.org/10.4049/jimmunol.177.5.2994.

(39) Bourguignon, L. Y.; Singer, S. J. Transmembrane Interactions and the Mechanism of Capping of Surface Receptors by Their Specific Ligands. *Proc. Natl. Acad. Sci.* **1977**, *74* (11), 5031–5035. https://doi.org/10.1073/pnas.74.11.5031.

(40) Patterson, H. C. K.; Kraus, M.; Kim, Y.-M.; Ploegh, H.; Rajewsky, K. The B Cell Receptor Promotes B Cell Activation and Proliferation through a Non-ITAM Tyrosine in the Igα Cytoplasmic Domain. *Immunity* **2006**, *25* (1), 55–65. https://doi.org/10.1016/j.immuni.2006.04.014.

(41) Tanner, J.; Weis, J.; Fearon, D.; Whang, Y.; Kieff, E. Epstein-Barr Virus Gp350/220 Binding to the B Lymphocyte C3d Receptor Mediates Adsorption, Capping, and Endocytosis. *Cell* **1987**, *50* (2), 203–213. https://doi.org/10.1016/0092-8674(87)90216-9.

(42) Ma, H.; Yankee, T. M.; Hu, J.; Asai, D. J.; Harrison, M. L.; Geahlen, R. L. Visualization of Syk-Antigen Receptor Interactions Using Green Fluorescent Protein: Differential Roles for Syk and Lyn in the Regulation of Receptor Capping and Internalization. *J. Immunol.* **2001**, *166* (3), 1507–1516. https://doi.org/10.4049/jimmunol.166.3.1507.

(43) Sieger, N.; Fleischer, S. J.; Mei, H. E.; Reiter, K.; Shock, A.; Burmester, G. R.; Daridon, C.; Dörner, T. CD22 Ligation Inhibits Downstream B Cell Receptor Signaling and Ca^{2+} Flux upon Activation. *Arthritis Rheum.* **2013**, *65* (3), 770–779. https://doi.org/10.1002/art.37818.

(44) Manders, E. M. M.; Verbeek, F. J.; Aten, J. A. Measurement of Co-Localization of Objects in Dual-Colour Confocal Images. *J. Microsc.* **1993**, *169* (3), 375–382. https://doi.org/10.1111/j.1365-2818.1993.tb03313.x.

(45) Alhamadsheh, M. M.; Connelly, S.; Cho, A.; Reixach, N.; Powers, E. T.; Pan, D. W.; Wilson, I. A.; Kelly, J. W.; Graef, I. A. Potent Kinetic Stabilizers That Prevent

Transthyretin-Mediated Cardiomyocyte Proteotoxicity. *Sci. Transl. Med.* **2011**, *3* (97), 97ra81-97ra81. https://doi.org/10.1126/scitranslmed.3002473.

(46) Judge, D. P.; Heitner, S. B.; Falk, R. H.; Maurer, M. S.; Shah, S. J.; Witteles, R. M.; Grogan, M.; Selby, V. N.; Jacoby, D.; Hanna, M.; Nativi-Nicolau, J.; Patel, J.; Rao, S.; Sinha, U.; Turtle, C. W.; Fox, J. C. Transthyretin Stabilization by AG10 in Symptomatic Transthyretin Amyloid Cardiomyopathy. *J. Am. Coll. Cardiol.* **2019**, *74* (3), 285–295. https://doi.org/10.1016/j.jacc.2019.03.012.

(47) Fox, J. C.; Hellawell, J. L.; Rao, S.; O'Reilly, T.; Lumpkin, R.; Jernelius, J.; Gretler, D.; Sinha, U. First-in-Human Study of AG10, a Novel, Oral, Specific, Selective, and Potent Transthyretin Stabilizer for the Treatment of Transthyretin Amyloidosis: A Phase 1 Safety, Tolerability, Pharmacokinetic, and Pharmacodynamic Study in Healthy Adult Volunteers. *Clin. Pharmacol. Drug Dev.* **2020**, *9* (1), 115–129. https://doi.org/10.1002/cpdd.700.

(48) Penchala, S. C.; Connelly, S.; Wang, Y.; Park, M. S.; Zhao, L.; Baranczak, A.; Rappley, I.; Vogel, H.; Liedtke, M.; Witteles, R. M.; Powers, E. T.; Reixach, N.; Chan, W. K.; Wilson, I. A.; Kelly, J. W.; Graef, I. A.; Alhamadsheh, M. M. AG10 Inhibits Amyloidogenesis and Cellular Toxicity of the Familial Amyloid Cardiomyopathy-Associated V122I Transthyretin. *Proc. Natl. Acad. Sci.* **2013**, *110* (24), 9992–9997. https://doi.org/10.1073/pnas.1300761110.

(49) Wasim, L.; Buhari, F. H. M.; Yoganathan, M.; Sicard, T.; Ereno-Orbea, J.; Julien, J.; Treanor, B. N-Linked Glycosylation Regulates CD22 Organization and Function. *Front. in Immunol*. **2019**, 699(10).

CHAPTER 4. NEU1 AND NEU3 ENZYMES ALTER CD22 ORGANIZATION ON B CELLS

Glycolipid analysis (Figure S6) was performed by Radhika Chakraberty. Neuraminidase inhibitors were provided by Tianlin Guo (Figure 5).

Portions of this chapter are included in the following publications:

Tran, H-T.; Li, C.; Chakraberty, R.; Cairo, C. W. NEU1 and NEU3 enzymes alter CD22 organization on B cells. *Biophys. Rep.* **2022**, 2(3).

4.1 INTRODUCTION

B cell receptors (BCRs) are responsible for antigen recognition leading to B cell activation and proliferation in immune response. Regulation of B cell activation involves co-receptors that fine-tune BCR signaling. One widely studied negative regulator of BCR is CD22 (Siglec-2), a member of the sialic-acid binding Immunoglobulin-like lectin (Siglec) family.[1] The structure and organization of CD22 on the cell membrane plays a crucial role in its activity. CD22 is a transmembrane protein containing seven Immunoglobulin domains (Ig) that adopts a rod-like structure; the N-terminal Ig domain specifically recognizes terminal α2,6-sialic acids.[2] The cytoplasmic portion of CD22 contains Immunoreceptor Tyrosine Inhibitory Motifs (ITIMs) that dampen cellular response.[3] CD22's lectin domain can interact with sialosides from cis- or trans-ligands; however, the high density of cis sialosides on the membrane results in the formation of hetero- and homotypic clusters of CD22. The N-link glycans of CD22 allow for homotypic interactions,[4,5] while heterotypic cis-binding partners, including CD45,[6,7] are known. Although CD22's ligand binding is somewhat weak,[8] high-affinity trans-ligands can overcome cis-interactions despite their prevalence.[9,10] High-affinity multivalent displays of CD22 ligands

including liposomes,[11,12] polymers,[4,10,13] and synthetic scaffolds[14] have been proposed as modulators of B cell activation.

The complexity of CD22 interactions and organization on the B cell membrane remains an active area of investigation. Previous studies have observed nanoclusters of CD22, with a minor role for the actin cytoskeleton in lateral mobility.[15] In this study, they found that disrupting the cytoskeleton using LatA or CytoD did not change the CD22 clustering while diffusion increased suggesting the minimal role of cytoskeleton on CD22's dynamic behavior but not their global organization on B cell membrane. Additionally, CD22 on $CD45^{-/-}$ B cells had larger clusters and slowed diffusion. CD22 on these knocked-out cells did not change their dynamic or organization behaviors when cytoskeleton was disrupted, but there were more clusters when treated with bacterial sialidases. From their results, they suggested that CD22 organization on B cells is largely influenced by homotypic interactions and not by cytoskeleton. Despite the large number of sialylated glycoproteins on the membrane, only a limited number of these have been identified as *in situ* ligands.[5] This observation may indicate a role for membrane microdomains in enforcing specific interactions, as CD45 and IgM have close associations with lipid rafts.[16–19] A common strategy for investigating the role of CD22-sialoside interactions is to use sialic acid-cleaving enzymes: *neuraminidases* (NEUs, also called *sialidases*).[20] Recombinant NEU from bacteria have been used for this purpose as research tools. NEU from *Clostridium perfringens* (NanI) has substrate preference for α2,3- glycoproteins, while the sialidase of *Athrobacter ureafaciens* (siaAU) has a broader range of substrate specificity cleaving α2,3-, α2,6-, or α2,8-linked gangliosides or glycoproteins. Exogenous NEU reagents have helped establish the importance of CD22-sialoside interactions; however, there has been very little work to investigate the role of native NEU enzymes on this system. There are four human NEU isoenzymes (hNEU): NEU1,

NEU2, NEU3, and NEU4 and they have important cellular functions and roles in health and disease,[21] including atherosclerosis,[22] malignancy,[23–25] and neurodegenerative diseases.[26–29] Together with glycosyl transferase enzymes (GTs), NEU regulate sialic acid content in cells.[20] Thus, native NEU activity could act as a regulator of CD22 organization, B cell activation, and immune response.

Here we investigated the influence of the cytoskeleton and native NEU activity on the membrane organization and dynamics of CD22. By utilizing confocal microscopy and single-particle tracking, we found that clustering and diffusion of these receptors are dependant on both cytoskeletal structure and changes in glycosylation of B cells. We confirmed our findings by performing knockdown of hNEU expression in model B cells. Finally, we confirmed that native hNEU activity affects B cell calcium levels. We conclude that organization and diffusion of CD22 receptors is dependent on an intact cytoskeleton and the homeostasis of native sialoside ligands.

4.2 MATERIALS AND METHODS

4.2.1 Confocal microscopy

Cells were grown in R10 media and kept in a humidified incubator at 37 °C and 5% CO_2. For confocal microscopy experiments, 1 x 10^6 Raji cells were counted, centrifuged, and re-suspended in Hank's Balanced Salt Solution (HBSS). The cells were washed and treated with NanI (*Clostridium perfringens*), siaAU (*Athrobacter ureafaciens*), or NEU3 in HBSS, or CytoD or LatA in HBSS with 0.005 % DMSO at 37 °C for 1 hour, then fixed using 1% PFA on ice for 30 min. Samples were treated with 1 μL/mL mouse anti-human IgM (clone IM260, Abcam cat# ab200541) or mouse anti-human CD22 (clone HIB22, BD Pharmingen cat# 555423) at 4 °C overnight, and stained with goat anti-mouse IgG (polyclonal, Sigma-Aldrich cat# M8642) conjugated with Alexa Flour 647 (AF647) at room temperature for 1 h. The loading of the fluorophores was approximately

2 dyes/protein. After washing, samples were transferred to 24-well plates (Corning, Inc.) with circular cover glass slides pre-treated with poly-L-lysine (PLL), spun at 300 x g for 15 min, washed, and glass slides were mounted onto microscopy slides with Slowfade Antifade (Thermo Fisher, cat# S2828) and sealed using Cytoseal 60. Samples were imaged on a laser scanning confocal microscope (Olympus IX81 with 60X objectives). Twenty cells from each condition were chosen for analysis based on transmitted and fluorescence images, and each cluster was analyzed using the particle analysis function on ImageJ. The data were plotted using the beanplot plugin in R, and statistics were done using Graphpad Prism. Three runs were performed and analyzed, and one representative run is shown for each condition.

4.2.2 Single-Particle Tracking

Raji cells were grown in R10 media as previously described.[14] For each condition, 1 x 10^6 cells were counted and washed with HBSS buffer three times. The cells were then re-suspended in HBSS and treated with NanI (10 mU/mL), siaAU (5 mU/mL or 10 mU/mL), or NEU3 (10 mU/mL). For CytoD and LatA, the cells were re-suspended in 0.005 % DMSO and the compounds were added to a final concentration of 100 nM. For all conditions, the cells were incubated for 1 h at 37 °C and 5% CO_2. After incubation, the cells were centrifuged and washed three times with HBSS buffer at 200 x g for 15 min, re-suspended in HBSS and labelled with anti-CD22 conjugated with AF647 (1 h at room temperature). After labelling, the cells were washed three times in buffer then transferred to 24 well-plates with circular glass cover pre-treated with PLL. The plate was then spun at 300 x g for 15 min, and the cover glass was mounted to microscope slides with buffer and sealed with Cytoseal 60. To record the trajectories, TIRFM was performed on Nikon Ti microscope. The angle of incidence was set at ~1100, and videos were taken at 10 FPS for 10 seconds.[30] All the videos were taken within one hour of slide preparation. Trajectories were

analyzed using UTrack software in MATLAB, and the coefficient of diffusion was calculated using MATLAB.[30]

4.2.3 Transfection of Raji cells

Raji cells were grown as described and passaged 24 h prior to transfection.[14] Cells (24 x 10^6) were washed and re-suspended into 750 µL of electroporation buffer (PBS with no Ca^{2+} or Mg^{2+}). For each knock-down condition, 15 µL from the 20 µM stock siRNA solution was added, while 15 µL of siRNA buffer was added for the no-treatment control. Cells were mixed by pipet and transferred to a 2 mm electroporation cuvette. Cell samples were left on ice for 20 min, and electric shock was applied using a Bio-Rad electroporator (0.6 kV, 50 µF, and 350 Ω). The cuvettes were then immediately transferred and left on ice for 30 min. Transfected cells were transferred to T25 cell culture flasks and pre-warmed R10 growth medium was added so the final volume for each condition was 6 mL. Cells were kept in a humidified incubator at 37 °C with 5% CO_2 for 24 h.

4.2.4 Ca^{2+} activity assay of Raji cells

For each condition, Raji cells were counted and re-suspended to a final concentration of 1 x 10^6 cells/mL. Cells were then treated with NEU at a final concentration of 10 mU/mL or with 100 nM neuraminidase inhibitors. For treatments of enzyme with inhibitors, these were incubated together for 30 min before addition to cells. The cells were treated with indicated conditions for 1 h at 37 °C with 5% CO_2. For transfected cells, cells were transfected and grown 24 hours prior to Ca^{2+} experiments. Cells were washed three times with PBS and re-suspended at 5 x 10^6/mL in loading buffer (RPMI-1640 supplemented with 1% FBS, 10 mM HEPES, 1 mM $MgCl_2$, 1mM EGTA, and 5% penicillin-streptomycin) and treated with 1.5 µM Indo-1 dye in a 37 °C water bath for 30 min while protected from light. After loading, the cells were washed with loading buffer three times, then re-suspended in running buffer (HBSS supplemented with 1% FCS, 1 mM

$MgCl_2$ and 1 mM $CaCl_2$), after which they were stored on ice. Using a Fortessa X10 FACS machine, a plot of violet (379 nm) versus blue (450 nm) was created and voltages were adjusted so that a maximum of 5% of unstimulated cells lie within the violet gate. To measure the amount of Ca^{2+} flow into the cells, 500 μL of previously suspended cells from each condition were transferred to FACS tubes incubated in 37 °C water bath for 2 min before running the samples. Ten seconds after the acquisition was initiated to establish the background, the tube was quickly removed and either PBS (unstimulated condition) or anti-IgM (stimulated condition) was added and vortexed before placing the tube back. The total acquisition time was 3 min for each tube and the number of cells analyzed ranged from 150-400 thousand cells. From these data, the percentage of cells emitting violet light from each condition was normalized to that of control unstimulated cells, and a Student's t-test was performed with GraphPad Prism.

4.2.5 Western Blot of Raji cells

Transfected cells were centrifuged and supernatant was discarded. The cells were lysed using 100 μL of HEPA buffer with protease inhibitor on ice for 1 h. The lysate was sonicated and centrifuged at 12,000 x g for 20 min. Supernatant was collected and the amount of protein was determined using BCA assay. For each condition, 10 μg of protein was mixed with the same volume of 2X gel running buffer with 5% dithiothreitol, followed by 5 min incubation at 95 °C. After heating the samples, they were then transferred to 11% acrylamide gel and SDS-PAGE was run at 110 V for 70 min. After the gel was completed, it was washed with water, and transferred to a nitrocellulose membrane in 1X blotting buffer at 20V for 2.5 h. Once the transfer was completed, the transfer of proteins was confirmed by soaking the membrane in Ponceau S buffer for 5 min, washing the membrane with water, and checking for presence of bands on the membrane. The membrane was blocked in blocking buffer (5% non-fat milk in 1X TBST) on an

orbital shaker overnight at 4 °C. The membrane was then washed three times with TBST for 5 min each time. The membrane was stained using primary antibody in TBST with 1:1000 dilution for 1 h at room temperature. The membrane was washed 5 times with TBST, then stained using secondary antibody conjugated with horse radish peroxidase with 1:10000 dilution in TBST for 1 h at room temperature. The membrane was washed and developed using ECL substrate for western blotting and visualized. Percent knock-down was determined by analyzing the intensity of each band using ImageJ. The samples were normalized to the control, and a Student's t-test was implemented for analysis.

4.2.6 Lectin blots

CD22 proteins were purified from Raji cells using murine hybridoma cells expressing anti-CD22 antibodies (α-CD22:4213 (10F4.4.1)). The purified sample was validated by SDS-PAGE and the protein concentration were determined using a BCA assay. From the stock solution, 4.4 μg of protein was diluted to a final volume of 200 μL and enzyme concentration of 10 mU/mL, then the samples were incubated at 37 °C for 3 h. After treatment of the proteins with enzyme, each sample was mixed with the same volume of 2X PAGE sample buffer with SDS, then 40 μL from each sample was subjected to SDS-PAGE with 10% acrylamide at 110 V for 70 minutes. For each of the samples, three lanes were loaded together with control samples. Gels were then taken out, washed three times with water, and transferred to nitrocellulose membrane. The presence of proteins on the membrane was confirmed using Ponceau S, then they were cut so that a control and an enzyme-treated lane was retained. The membranes were washed with TBST and blocked with blocking buffer (5% non-fat milk in TBST) at 4 °C overnight. Membranes were washed three times with TBST, then treated with 1 μg/mL biotinylated lectins (PNA, SNA, MAL) at room temperature for 1 h. The treated membranes were washed 5 times with TBST and treated with

streptavidin-HRP for 1 h at 1:10000 dilution, followed by washing the membranes with TBST. The bands were detected using ECL substrate for western blotting under a visualizer. The analysis of the bands was conducted using ImageJ.

4.3 RESULTS

4.3.1 Cytoskeletal interactions of BCR

To study the effect of cytoskeletal contacts on BCR, we used Raji cells treated with cytoskeletal disruptors *cytochalasin D* (CytoD) and *latrunculin A* (LatA) as a model B cell system. We used Raji model B cells in our studies in opposed to A-BCL cells due to their ease in growing, maintenance, and transfection; there have also been several studies that used model human B cell lines to investigate CD22 receptors.[32-34] Microclusters of BCR are known to form when B cells are stimulated due to the association of the constant region Cμ4, followed by phosphorylation that induces cellular response.[31] Several studies have observed cytoskeletal interactions with BCR, and the effect of cytoskeletal disruption was increased BCR cluster size and cell activation.[35,36] Cells were treated, fixed, and imaged by confocal microscopy allowing quantitation of cluster size (**Figure 4.1, Table 4.1**).[14] CytoD and LatA were used to disrupt the cytoskeleton.[37-40] We observed a significant increase in clustering of BCR upon treatment with both inhibitors at all concentrations,[15] and there was significantly increased clustering at lower concentration as compared to higher concentrations (2.5 vs 7.5 μg/mL; $p < 0.05$). [41]

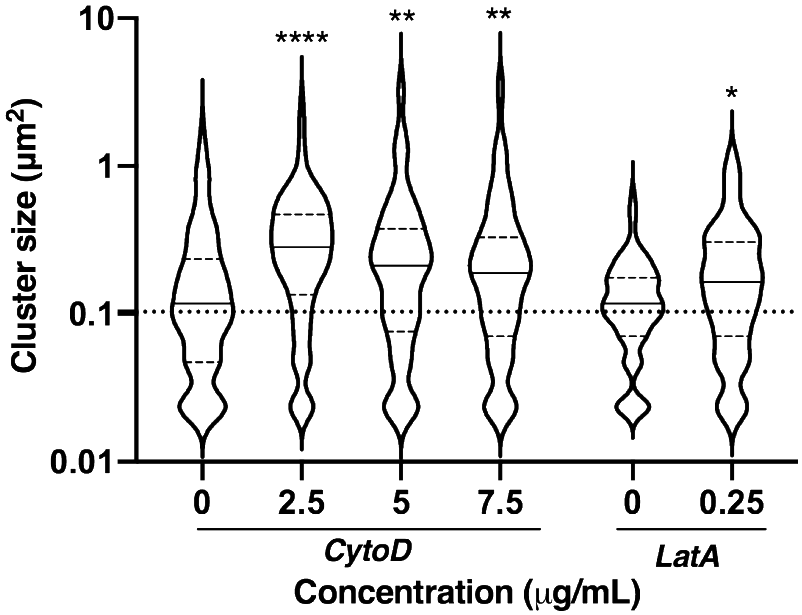

Figure 4.1. Cluster size of BCR after treatment with cytoskeletal disruptors. Raji cells were treated with cytochalasin D (CytoD) or latrunculin A (LatA) at 37 °C for 30 min. Cells were then fixed and stained with mouse anti-IgM and anti-mouse IgG-AF647 and imaged using confocal microscopy. Data shown are average from 30 cells among 3 biological replicates; cells were analyzed using imageJ and shown as beanplots.[14] Comparisons by student's t-test are shown relative to respective controls (****, $p < 0.0001$; **, $p < 0.01$; *, $p < 0.05$). Data shown are representative of three biological replicates.

Table 4.1. Cluster size of BCR after treatment with cytoskeleton disruptors

	Concentration (μg/mL)	Size	Error	n	p-value	Significance
CytoD	0	0.2079	0.0265	112	N/A	N/A
	2.5	0.3681	0.0358	122	0.0005	***
	5.0	0.3585	0.0427	168	0.0082	**
	7.5	0.3402	0.0432	165	0.0207	*
LatA	0	0.1386	0.0096	121	N/A	N/A
	0.25	0.2256	0.0240	93	0.0009	*

4.3.2 Cytoskeletal interactions of CD22

We next examined the cytoskeletal interactions of CD22 in a B cell model. Analysis of CD22 clustering after treatment with cytoskeletal disruptors is shown in **Figure 4.2** and **Table 4.2**. We observed that CD22 cluster size increased significantly when cells were treated with CytoD. Interestingly, the cluster size was increased at intermediate concentrations (2.5 – 7.5 μg/mL); however, this effect was lost at higher concentration (10 μg/mL). Similar trends have been observed in tight junctions, and may be attributed to different populations of actin within the cell.[41,42] Previous work has suggested that CytoD does not alter CD22 clustering or organization in the membrane; however, these studies were performed at higher drug concentrations (10 μM) and our results suggest that lower concentrations may be more appropriate in this system.[15] Treatment of cells with LatA showed no effect on the cluster size of CD22 at the concentrations tested (0.050 – 0.500 μg/mL). One explanation for this difference is the disparate mechanisms of actin disruption used by these two inhibitors.[40] Alternatively, the incubation time with LatA (30 min) may have been insufficient.[43-44] The significance of cluster size was tested using student's t-test, and the apparent larger clusters are largely due to presence of larger clusters and fewer smaller clusters. It is notable that there may be some overlaps in CD22 cluster sizes when looking at the bottom of the violin plots. However, it is important to pay attention to the shape of the plots, in which larger clusters are evident in drug-treated conditions. We speculate that this rearrangement in CD22 receptors ultimately lead to changes in B cell activation. Specifically, when there are more CD22 receptors that exist in larger homoclusters, they are kept away from BCR, leading to elevated B cell response.

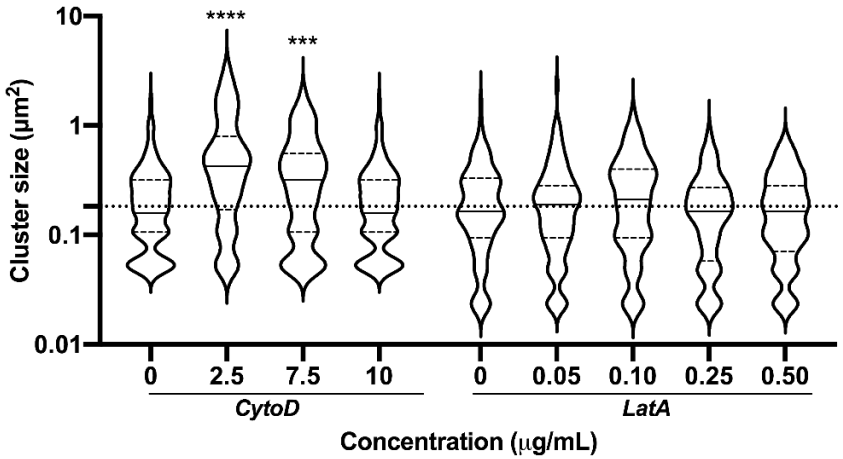

Figure 4.2. Cluster size of CD22 after treatment with cytoskeletal disruptors. Raji cells were treated with cytochalasin D (CytoD) or latrunculin A (LatA) at 37 °C for 30 min. Cells were then fixed and stained with mouse anti-CD22 and anti-mouse IgG-AF647 and imaged using confocal microscopy. Data shown are average from 30 cells among 3 biological replicates; cells were analyzed using imageJ and shown as beanplots.[14] Comparisons by student's t-test are shown relative to respective controls (****, $p < 0.0001$; ***, $p < 0.001$). Data shown are representative of three biological replicates.

Table 4.2. Cluster size of CD22 after treatment with cytoskeleton disruptors

	Concentration (μg/mL)	**Size (μm^2)**	**Error**	**n**	**p-value**	**Significance**
CytoD	0	0.2384	0.0200	132	N/A	N/A
	2.5	0.6567	0.0637	124	<0.0001	****
	7.5	0.4213	0.0368	125	0.0005	***
	10	0.2454	0.0221	117	0.4832	n.s
LatA	0	0.2361	0.0226	99	N/A	N/A
	0.05	0.2463	0.0271	111	0.2743	n.s
	0.10	0.2790	0.0210	145	0.1642	n.s
	0.25	0.1964	0.0141	141	0.0320	n.s
	0.50	0.2001	0.0128	164	0.1454	n.s

We next investigated if cytoskeletal interactions had a significant influence on the lateral mobility (diffusion) of CD22 in the membrane. We employed single-particle tracking (SPT) using Total Internal Fluorescence Microscopy (TIRFM) to measure changes in CD22 membrane

diffusion.[33] Raji cells were stained with minimal amounts of Alexa Flour 647 (AF647) - conjugated primary antibody to CD22. This sparse labelling allowed visualization of CD22 trajectories on live cells, which could be converted to rates of diffusion (**Figure 4.3**).[45] This method allowed us to compare lateral diffusion of proteins in control and cytoskeleton-disrupted conditions. Treatment with CytoD at low concentration (2.5 μg/mL) significantly decreased CD22 diffusion; however, at higher concentrations (10 μg/mL) this effect was lost. Treatment with LatA (0.25 μg/mL) also showed a significant decrease in lateral mobility of CD22.

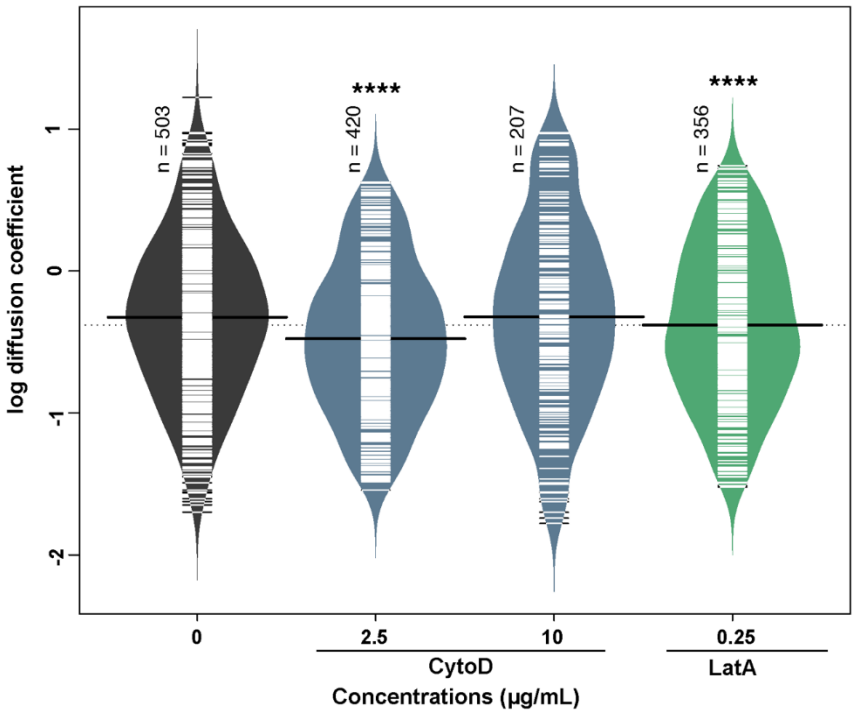

Figure 4.3. Lateral mobility of CD22 after treatment with cytoskeletal disruptors. Raji cells were treated at 37 °C for 30 min. Lateral mobility was analyzed using single-particle tracking with TIRFM videos recorded at 10 FPS for 10s.[30] Diffusion coefficients are given as log(D), where D is in units of $\times 10^{-10}$ [cm^2s^{-1}] or $\times 10^{-2}$ [μm^2s^{-1}]. 150 cells among 3 biological replicates were analyzed, and values were compared to control using a student's t-test (****, $p < 0.0001$). Beanplots were generated using R software. Individual data points are represented by short white

lines, a solid black line indicates the average for each condition, and the dotted line represents an average across all populations.

Table 4.3. Diffusion of CD22 after treatment with cytoskeleton disruptors

	Concentration (μg/mL)	Diffusion (x 10^{-10} cm^2s^{-1})	Error	n	p-value	Significance
DMSO		1.062	0.0744	503	N/A	N/A
CytoD	2.5	0.6664	0.0413	420	0.0005	n.s
	10	1.271	0.1367	207	<0.0001	****
LatA	0.25	0.8561	0.0565	356	<0.0001	****

4.3.3 NEU1 and NEU3 activity alter CD22 cluster size

Considering that the lectin activity of CD22 is dependent on sialylated cis ligands, we next investigated if native hNEU enzymes could alter CD22 membrane organization. CD22 is found in homotypic clusters,[5,46] and also has cis interactions with other sialylated proteins, including CD45.[47-49] We developed an siRNA knockdown protocol using electroporation for NEU1 and NEU3 enzymes,[50] as lymphocytes are often difficult to transfect using lipid-based methods. The reduced expression of NEU1 and NEU3 was confirmed by western blot of the transfected cells (**Figure 4.4A, 4.4B, 4.5**). We found that B cells treated with siRNA for *Neu1* or *Neu3* had expression of the enzymes reduced by approximately half. Viability of the cells by hemocytometer after treatment showed no significant decrease for *Neu1* siRNA, while *Neu3* siRNA did show a decrease in viability (**Figure 4.6**). We proceeded to determine if NEU1 and NEU3 knockdown (KD) cells showed evidence of changes to CD22 membrane organization. Analysis of clustering in these cells found a significant increase in CD22 cluster size in NEU1 KD cells while NEU3 KD cells had a significant decrease in cluster size, suggesting these two isoenzymes play different roles in regulating CD22 organization (**Figure 4.4B**). This observation can be partly attributed to the different substrate specificities of the two enzymes – with NEU1 known to prefer glycoprotein

substrates and NEU3 to prefer glycolipids.[20] Additionally, the expression levels of these two enzymes may vary in lymphoid cells, with NEU1 generally being found at higher expression in many cell types.[51,52]

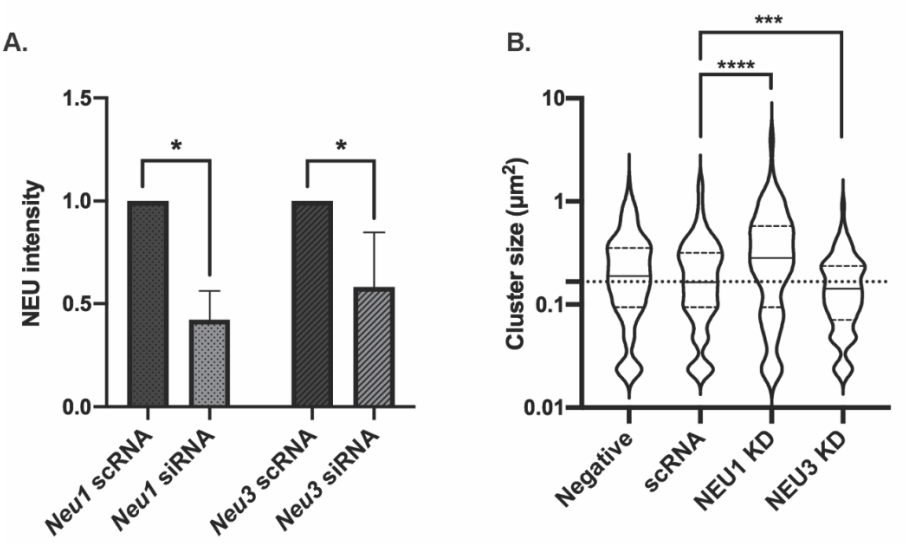

Figure 4.4. CD22 cluster size is altered by NEU1 and NEU3 knockdown. Raji cells were transfected with siRNA targeting *Neu1* or *Neu3* using electroporation and grown for 24 h. (**A**) Western blots confirmed reduced expression of NEU1 and NEU3. (**B**) After transfection, Raji cells were fixed and stained with mouse anti-CD22 and anti-mouse IgG-AF647 and imaged using confocal microscopy to determine the cluster size of CD22. Data shown are average from 30 cells among 3 biological replicates; cells were analyzed using imageJ and shown as beanplots.[14] Comparisons by student's t-test are shown relative to respective controls (****, $p < 0.001$; ***, $p < 0.005$).

Table 4.4. Cluster size of CD22 after NEU knock-down

	Size (μm^2)	**Error**	**n**	**p-value**	**Significance**
Negative	0.2628	0.0175	191	N/A	N/A
scRNA	0.2432	0.0160	245	0.6052	n.s
NEU1 KD	0.4280	0.0462	141	0.0001	****
NEU3 KD	0.1682	0.0112	160	0.0006	***

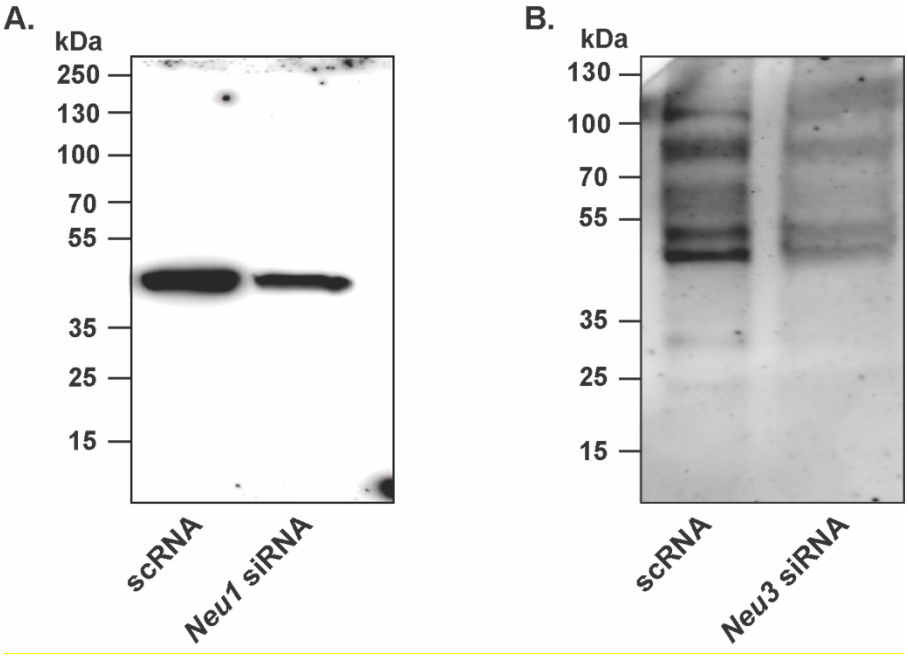

Figure 4.5. Western blots of NEU knockdowns. Raji cells were transfected with siRNA targeting Neu1 and Neu3 using electroporation and grown for 24 hours. Western blots show the reduction of expression of hNEU1 (A) and hNEU3 (B). Shown are representative blots of three replicates for each NEU.

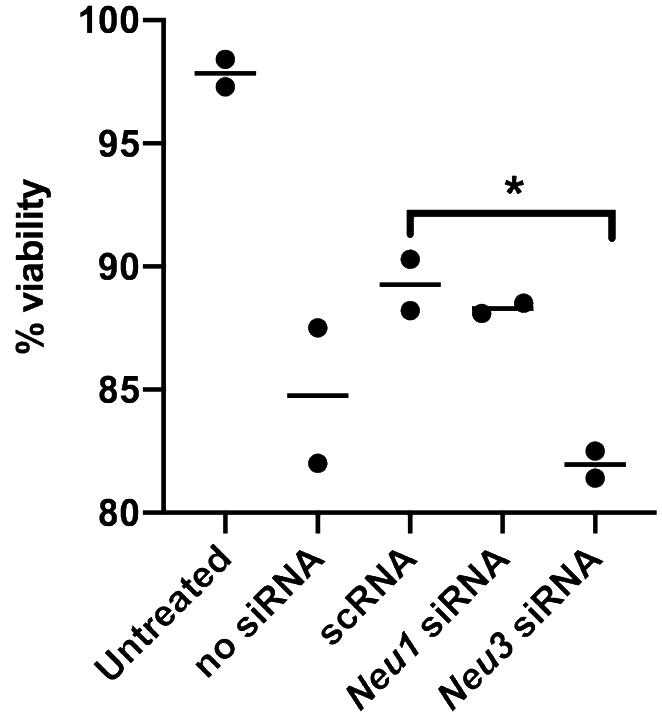

Figure 4.6. Raji cell viability after siRNA transfection. Raji cells were transfected with siRNA targeting Neu1, Neu3, or a scrambled control (scRNA) using electroporation and grown for 24 hours. The viability of cells from each condition was determined using trypan blue dye exclusion on a hemocytometer.

4.3.4 Native NEU modulate B cell activation

The CD22 receptor acts as a negative regulator of B cell activation and the organization and engagement of CD22 can alter B cell response.[54] We investigated the role of NEU1 and NEU3 in B cell activation using a calcium assay with Indo-1 dye.[51] We first asked if small molecule inhibitors of NEU enzymes had a measurable effect on B cell activation (**Figure 4.7**).[55] We used three different compounds: DANA, a pan-selective inhibitor of NEU enzymes; CG33300, a NEU1-selective inhibitor; and CG22600, a NEU3-selective inhibitor.[56-58] When all conditions were normalized to the control group, we observed that treating B cells with DANA increased

basal activation. Additionally, cells treated with DANA and anti-IgM showed a significant increase in activation relative to control. Although these observations are consistent with native NEU activity acting as a negative regulator of B cell activation, they did not indicate which enzymes were involved. The selective NEU1 inhibitor, CG33300, showed similar effects to DANA – increased B cell activation relative to unstimulated and stimulated controls (**Figure 4.7B**). A selective NEU3 inhibitor, CG22600, showed similar activity – enhancing cell activation in basal and stimulated cells (**Figure 4.7C**). From these experiments, we concluded that native human NEU enzymes, including NEU1 and NEU3, act as negative regulators of B cell activation. We sought to confirm the role of NEU1 and NEU3 on B cell activation using siRNA knockdown conditions. Transfected B cells were subjected to Ca^{2+} assay as described above after knockdown of NEU1 or NEU3 and compared to a scRNA control (**Figure 4.8**). We found that both NEU1 and NEU3 knockdowns had increased basal Ca^{2+} levels in cells, consistent with our inhibitor studies.

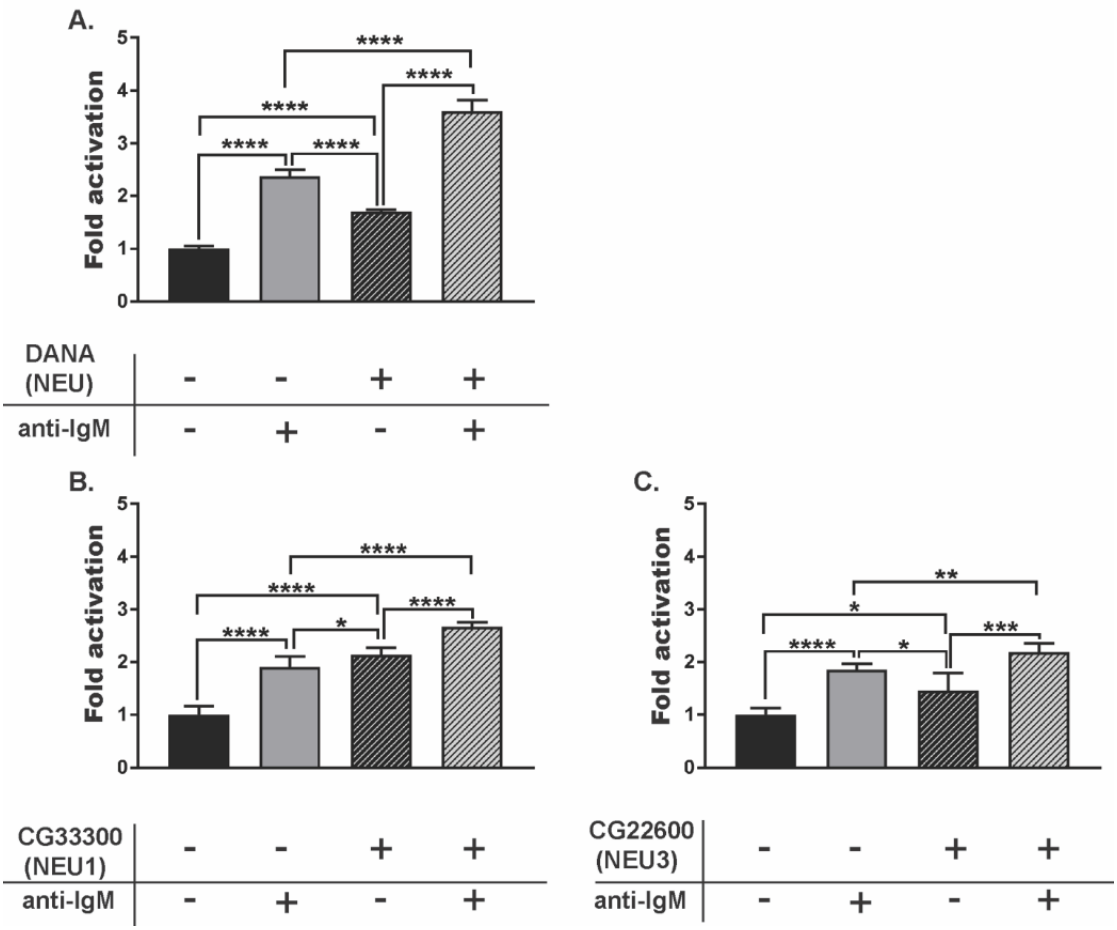

Figure 4.7. B cell response after treatment with NEU inhibitors. Raji cells were incubated at 37 °C for 30 min with NEU inhibitors: (**A**) DANA (100 μM), (**B**) CG33300, a NEU1 inhibitor (10 μM), or (**C**) CG22600, a NEU3 inhibitor (10 μM). Cells were either untreated (-, saline), or treated with inhibitor (+); followed by activation with anti-IgM. Activation of cells was monitored by observing Ca^{2+} levels by Indo-1 dye. For each treatment, 6 technical replicates from each of 3 biological replicates were performed. Responses were normalized to that of saline-treated, and unstimulated control groups and compared by student's t-test (****, $p < 0.001$; ***, $p < 0.005$; **, $p < 0.01$; *, $p < 0.05$).

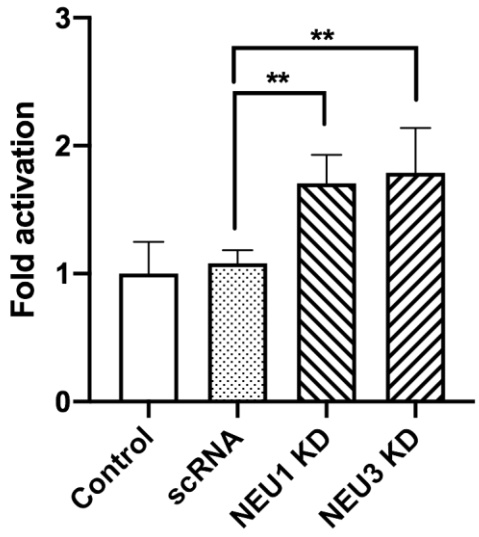

Figure 4.8. B cell calcium levels after NEU1 and NEU3 knockdown. Raji cells were transfected with siRNA targeting *Neu1, Neu3*, or a scrambled control (scRNA) using electroporation. Cells were grown for 24 h, and Ca^{2+} levels were monitored using Indo-1 dye. For each treatment, 2 technical replicates from each of 3 biological replicates were performed. Responses were normalized to that of saline-treated, and unstimulated control groups and compared by student's t-test (**, $p < 0.01$).

One possible explanation for changes to B cell activation after siRNA transfection is differences in CD22 expression after treatment. We tested for changes in CD22 expression using western blot following siRNA treatments (**Figure 4.9, 4.10**). We found no significant change in CD22 expression levels in scRNA and NEU1 KD samples. However, NEU3 KD showed an unexpected decrease in CD22 expression relative to the untreated and scRNA controls. NEU3 activity has been implicated in clathrin-dependent endocytosis and could influence transport and expression of CD22.[59-63]

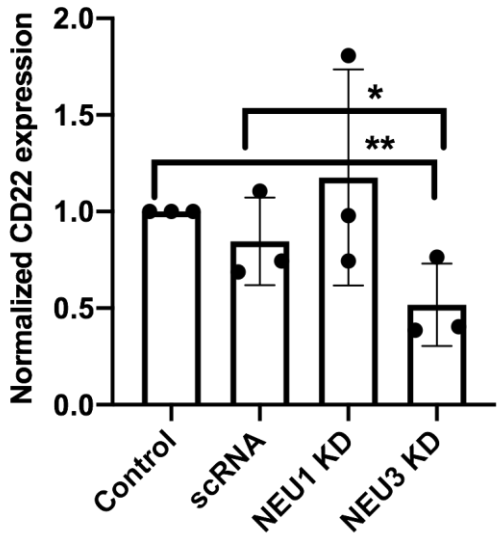

Figure 4.9. CD22 expression after NEU1 and NEU3 knockdown. Raji cells were transfected with siRNA targeting *Neu1, Neu3*, or a scrambled control (scRNA) using electroporation. Cells were allowed to grow for 24 h, and then harvested. A western blot was performed using anti-CD22 to compare expression levels and analyzed by densitometry using ImageJ (**, $p<0.01$; *, $p<0.05$).

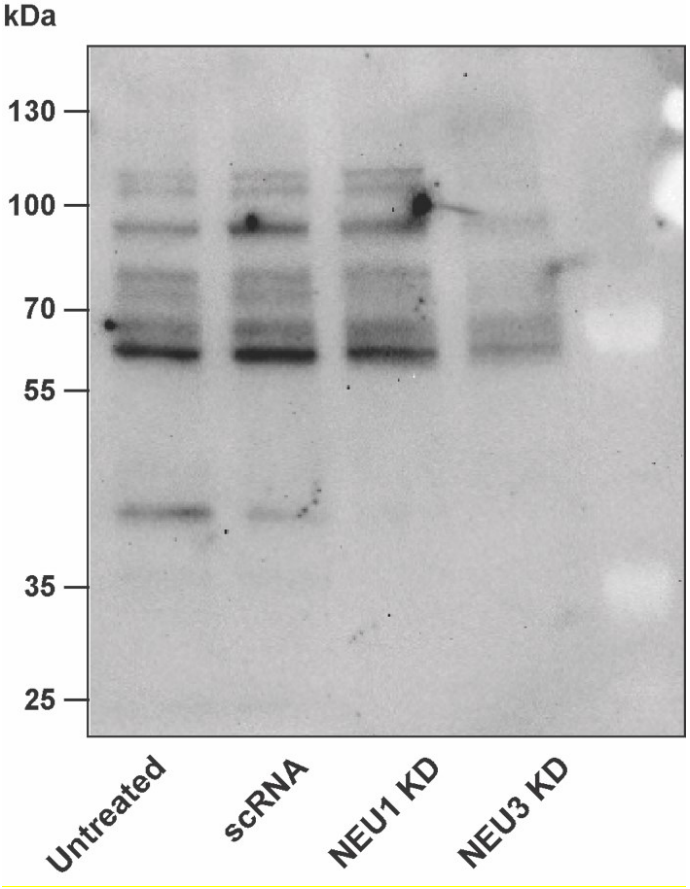

Figure 4.10. Western blot of CD22 expression after NEU1 and NEU3 knockdown. Raji cells were transfected with siRNA targeting Neu1, Neu3, or a scrambled control (scRNA) using electroporation. Cells were allowed to grow for 24 h, and then harvested. A western blot was performed using anti-CD22 to compare expression levels, and analyzed by densitometry using imageJ. Shown is representative blot of three replicates.

4.3.5 Exogenous NEU affect CD22 organization and B cell activation

A common strategy for probing the role of membrane sialosides in signaling is to treat cells with exogenous NEU enzymes. Typical examples include the sialidase from *Athrobacter ureafaciens* (siaAU) and NanI from *Clostridium perfringens*. These enzymes have different specificities, with siaAU having broad activity to cleave α2,3 and α2,6-linkages;[63,64] while the

latter prefers α2,3-linked sialosides.[65] It is worth noting that these enzymes have different substrate specificity from human NEU isoenzymes, and may not be good biochemical proxies for the native enzymes.[66] We found that treatment of B cells with NanI and siaAU generally increased clustering of CD22 (**Figure 4.11A, 4.11C**) but not BCR (**Figure 4.12**). We noted that the effect on CD22 cluster size was dependent on the activity of enzyme used – with high specific activity of siaAU (10 mU/mL) reversing significant increases seen at lower activity (5 mU/mL). Analysis of B cells treated with these enzymes by SPT found that CD22 lateral mobility was significantly reduced for both NanI and siaAU treatment (**Figure 4.13**). This result is similar to observations with CytoD treatment, where increased clustering of CD22 was coincident with decreased lateral mobility.

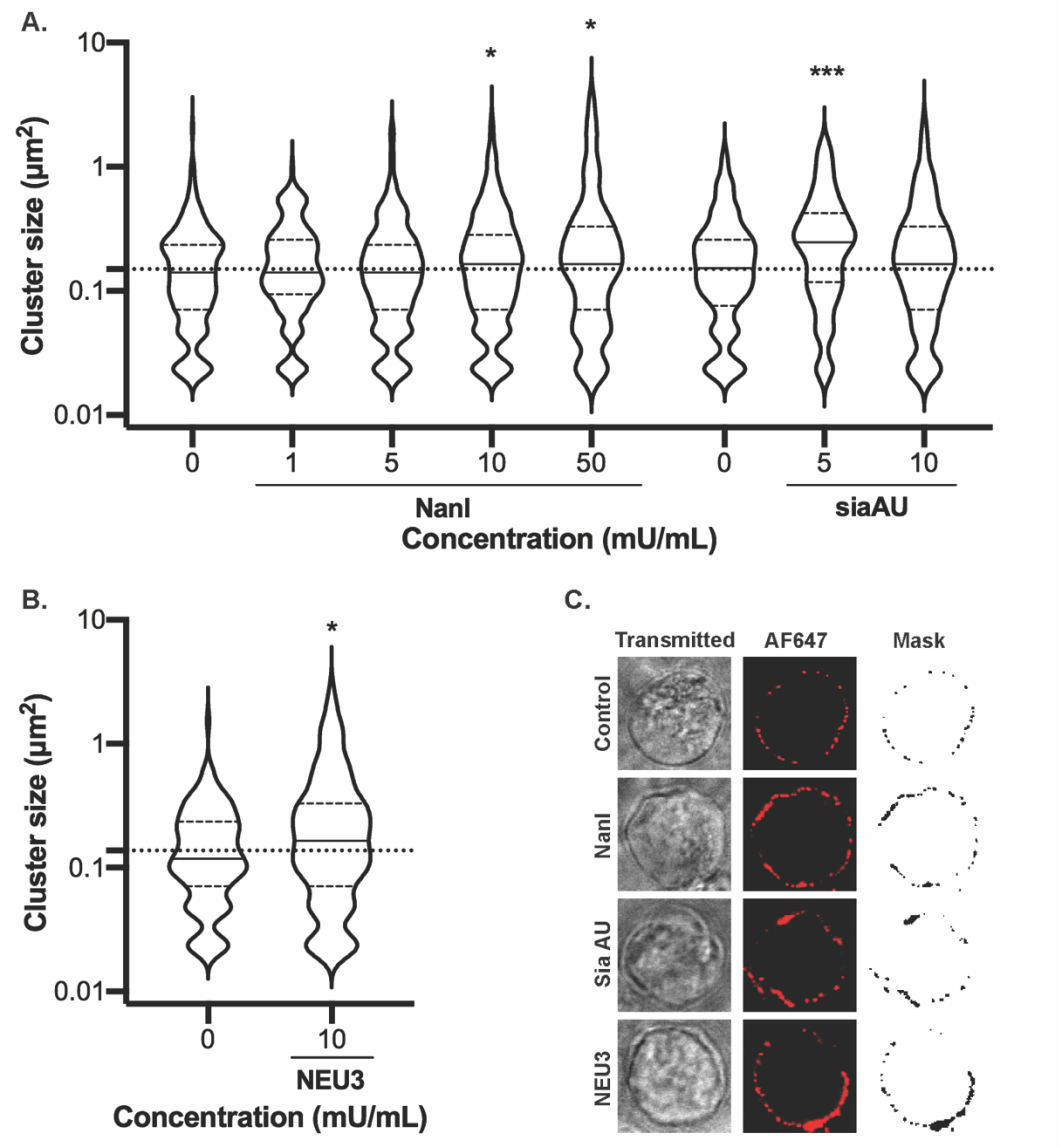

Figure 4.11. Cluster size of CD22 after treatment with NEU enzymes. Raji cells were treated with bacterial NEU (A) or human NEU enzymes (B) at the indicated concentrations at 37 °C for 30 min. Cells were then fixed and stained with mouse anti-IgM and anti-mouse IgG-AF647 and imaged using confocal microscopy (C). Ten cells from each condition were analyzed using ImageJ and are shown as beanplots. Bottom right: confocal images of Raji cells stained with anti-CD22 antibody. Comparisons by student's t-test are shown relative to respective controls (***, $p < 0.005$; *, $p < 0.05$).

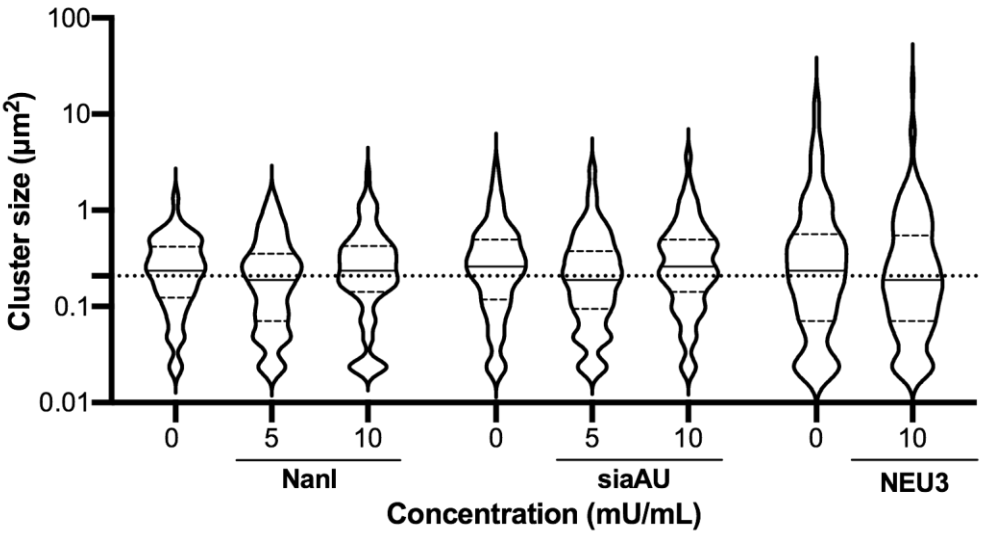

Figure 4.12. Cluster size of BCR after treatment with NEU enzymes. Raji cells were treated with NanI, siaAU, or NEU3 enzyme at 37 °C for 30 min. Cells were then fixed and stained with mouse anti-IgM and anti-mouse IgG-AF647 and imaged using confocal microscopy. Ten cells from each condition were analyzed using ImageJ and are shown as beanplots.

We next investigated if exogenous human NEU3 enzyme had similar effects to the bacterial NEU enzymes on clustering and diffusion of CD22. When B cells were treated with NEU3 (10 mU/mL) clustering of CD22 significantly increased, consistent with the effect of the bacterial enzymes (**Figure 4.11B**). Measurements of the lateral mobility of CD22 after NEU3 treatment showed an increase in diffusion (**Figure 4.13**). We performed an analysis of B cell glycosphingolipids after exogenous NEU treatment using LC-MS (**Figure 4.14**),[33] in which we observed no significant changes for any of the enzyme treatments. This may suggest that changes to glycosphingolipid composition are not the major factor in changes to CD22 organization, or that these changes in composition are below the detection limit of our assay. An alternative explanation for changes to CD22 organization is that exogenous NEU enzymes modify CD22 glycosylation, thus altering homotypic clustering. Using purified CD22, we confirmed that NanI and siaAU

reduced SNA staining and increased PNA staining for CD22, consistent with desialylation of the receptor in vitro (**Figure 4.15, 4.16**).

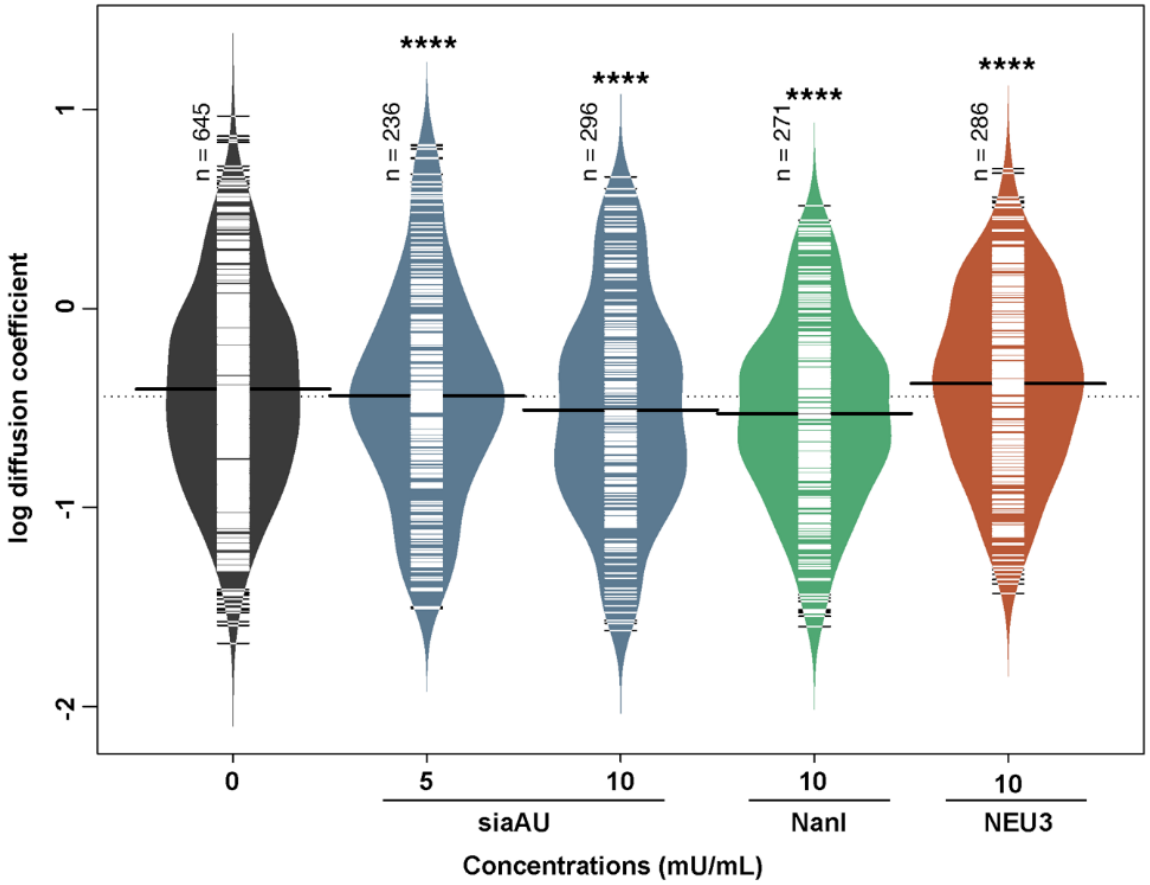

Figure 4.13. Lateral mobility of CD22 after treatment with NEU enzymes. Raji cells were treated at 37 °C for 30 min. Lateral mobility was analyzed using single-particle tracking with TIRFM videos recorded at 10 FPS for 10s.[30] Diffusion coefficients are given as log(D), where D is in units of $\times 10^{-10}$ [cm^2s^{-1}] or $\times 10^{-2}$ [μm^2s^{-1}]. 150 cells among 3 biological replicates were analyzed, and values were compared to control using a student's t-test (****, $p < 0.001$).

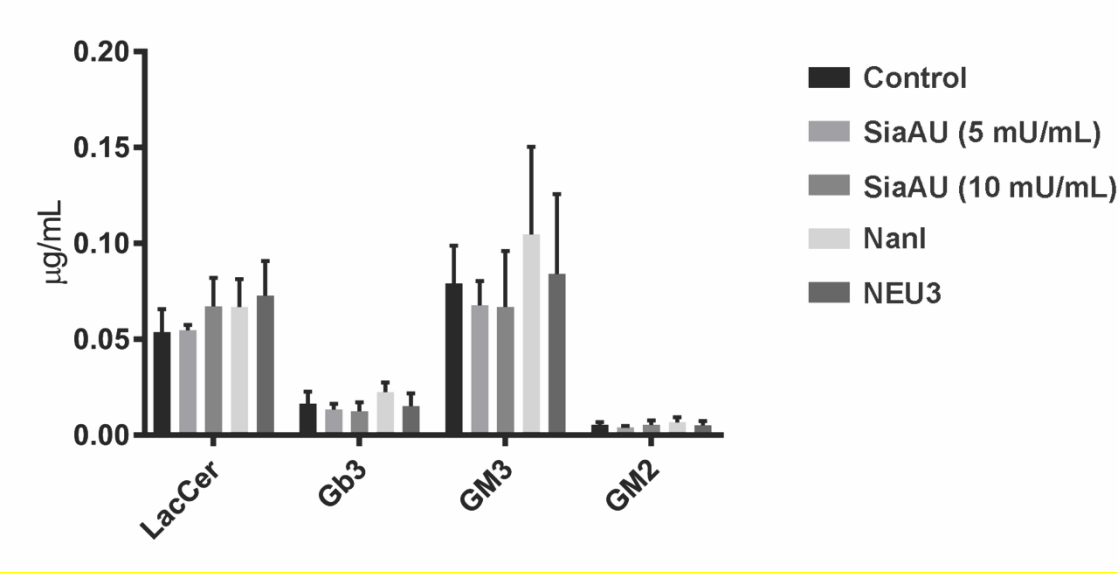

Figure 4.14. Glycolipid composition of Raji cells after NEU treatment. Raji cells were treated with saline, siaAU (5 mU/mL), siaAU (10 mU/mL), NanI (10 mU/mL), or NEU3 (10 mU/mL) for 30 min at 37 °C. Cells were then subjected to glycolipid analysis using LC-MS. Data shown are the average of four replicates.

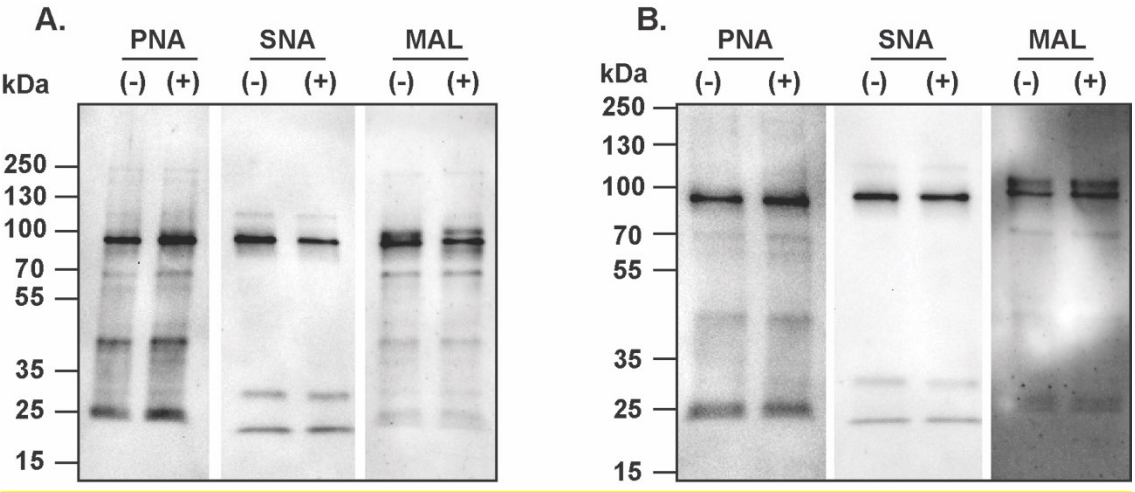

Figure 4.15. Lectin blots of purified CD22 protein treated with NEU enzymes. CD22 was purified from Raji cells using an immunoaffinity column. The protein was treated with (-) saline or (+) NEU enzymes (A) siaAU (5 mU/mL) or (B) NanI (10 mU/mL) for 30 minutes at 37 °C. Samples were then analyzed by lectin blotting with PNA, SNA, or MAL probes.

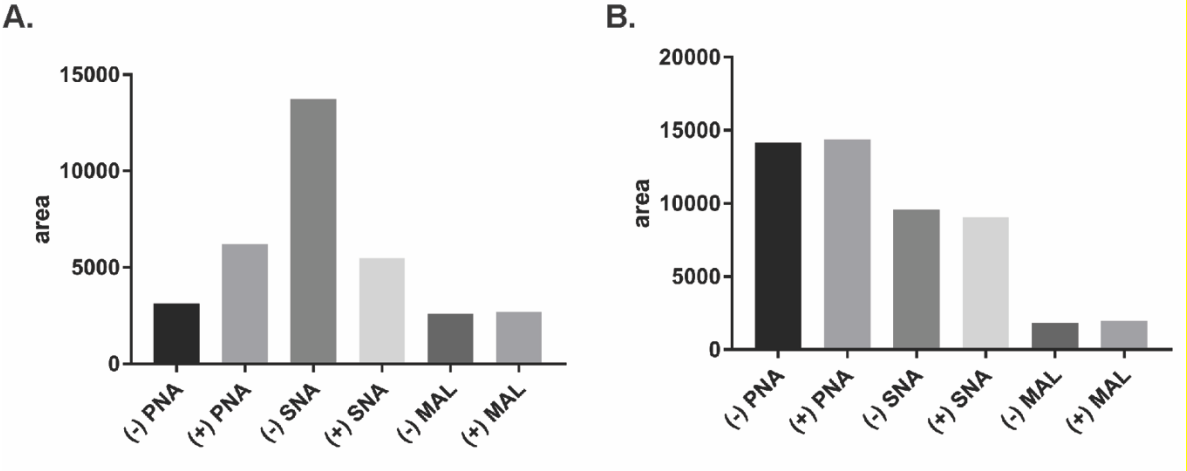

Figure 4.16. Quantification of NEU-treated CD22 protein. CD22 samples treated with (-) saline or (+) NEU enzymes (A) siaAU (5 mU/mL) or (B) NanI (10 mU/mL). Purified proteins were incubated with corresponding neuraminidase for 30 min at 37 °C. Samples were then analyzed by lectin blotting with PNA, SNA, or MAL probes, and images were quantified using densitometry.

During our studies, we encountered an issue that may complicate experiments which use exogenous bacterially-produced NEU. Exogenous enzymes from bacterial sources may contain lipopolysaccharide (LPS), and this contaminant may affect lymphocyte activation[67-69] or CD22 expression.[70] We found that samples of siaAU and NanI from commercial sources contained more than 1 EU/mL (EU = endotoxin units, 1 EU = 0.1 to 0.2 ng), with final LPS concentrations in our experiments of 0.0001 to 0.01 ng/mL. We tested whether these amounts of LPS alone could affect CD22 clustering (**Figure 4.17**). We observed a significant increase in CD22 clustering at 0.01 ng/mL of LPS in our assay, while higher concentrations attenuated this effect (0.1 ng/mL). Additionally, determinations of B cell activation using Ca^{2+} level assays after treatment with exogenous siaAU or NanI were ambiguous in our hands (**Figure 4.18**). For example, siaAU at lower concentrations had similar effects to treatment with DANA (**Figure S18A** versus **Figure 4.7**) despite the fact that these treatments should have opposite effects on sialic acid content on

cells. Higher concentrations of siaAU attenuated this effect (**Figure 4.18B**), while NanI treatment showed no significant differences from control (**Figure 4.18C**).

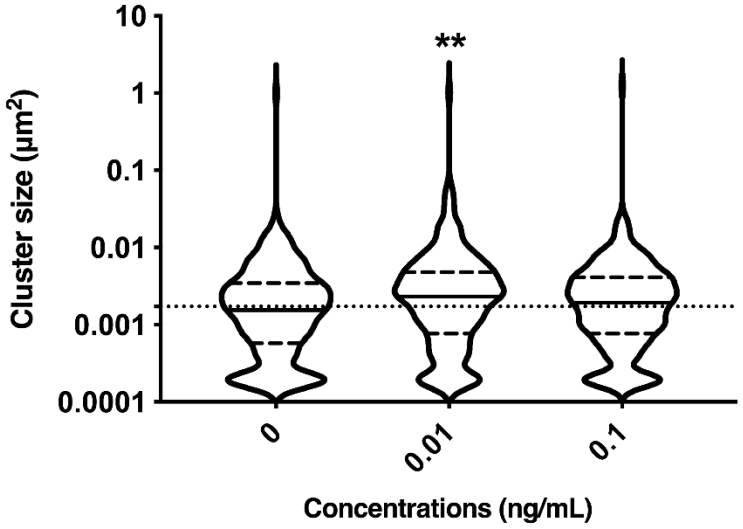

Figure 4.17. Cluster size of CD22 after treatment with LPS. Cluster size of CD22 using confocal microscopy. Raji cells were treated with LPS at 37 °C for 30 min. Cells were then fixed and stained with mouse anti-IgM and anti-mouse IgG-AF647 and imaged using confocal microscopy. Ten cells from each condition were analyzed using ImageJ and are shown as beanplots.22 Comparisons by student's t-test are shown relative to respective controls (*, $p < 0.5$).

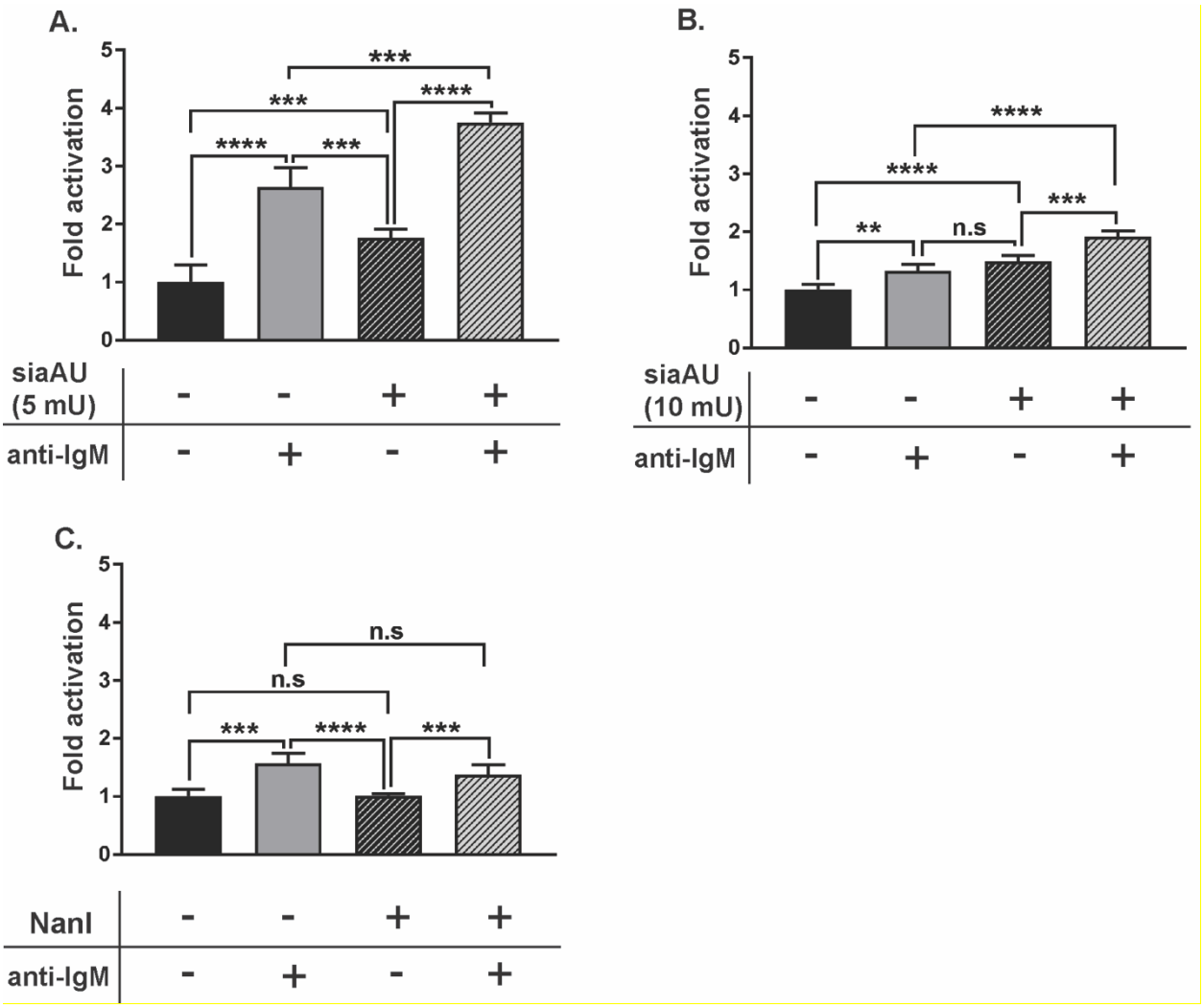

Figure 4.18. B cell response after treatment with NEU enzymes. Raji cells were incubated at 37 °C for 30 min with NEU enzymes: (A) sialidase from Athrobacter ureafaciens (siaAU) at 5 mU/mL, (B) siaAU at 10 mU/mL, or (C) NanI at 10 mU/mL. Cells were either untreated (-, saline), or treated with enzyme (+); followed by activation with anti-IgM. Activation of cells was monitored by observing Ca2+ influx monitored by Indo-1 dye. Responses were normalized to that of saline-treated, and unstimulated control groups and compared by student's t-test (****, $p < 0.001$; ***, $p < 0.005$; **, $p < 0.01$; *, $p < 0.05$).

4.4 DISCUSSION

The data described here provide critical insight into the effects of native and exogenous NEU enzymes on CD22 organization on B cells. The organization of CD22 on the membrane is dependent on the lectin activity of the receptor and the availability of sialoglycoproteins in the milieu of the plasma membrane. We set out to understand if native NEU enzymes, which help regulate levels of sialyation of glycolipids and glycoproteins, could influence CD22 organization. Using confocal microscopy and single-particle tracking we demonstrated that CD22 was influenced by disruption of cytoskeleton, though we did not resolve the nature of this interaction. We found that native NEU1 and NEU3 activity influenced both the size of CD22 clusters and their mobility within the membrane. Based on our results, we conclude that increased NEU1 activity led to smaller CD22 clusters. In contrast, increased NEU3 activity (both native or exogenous) generated larger CD22 clusters which had increased diffusion. Moreover, exogenous bacterial NEU activity generated larger CD22 clusters with decreased diffusion. These stark differences were likely the result of different substrate specificities for each enzyme. Importantly, we confirmed that LPS contamination in exogenous enzyme preparations influenced CD22 organization and could complicate attempts to use these reagents to understand the role of CD22 interactions with cis sialoside ligands. Furthermore, we confirmed that native NEU activity influenced B cell response to BCR clustering using a Ca^{2+} assay. Knockdown or chemical inhibition of both NEU1 and NEU3 enzymes resulted in increased basal activation of B cells, consistent with these enzymes acting as negative regulators of B cell stimulation. Our studies clearly support the involvement of the cytoskeleton and NEU enzymes in regulating CD22 organization and B cell activity.

Lateral mobility of immune cell receptors is complex and can be influenced by a number of factors[68] such as the lateral size of the protein,[72] cytoskeletal barriers,[73-76] the presence of membrane microdomains,[77] and crowding effects.[78] Studies have proposed CD22,[15] CD45,[79] and BCR[80,81] are associated with membrane microdomains in lymphocytes.[19,82] CD22 is not thought to have direct contacts to the cytoskeleton; though cis ligands could provide indirect contacts. In studies of CD22-cytoskeleton interactions, we found that SPT was more sensitive to changes in cluster size than confocal microscopy. We found an increase in CD22 diffusion on B cell membrane when the cytoskeleton was disrupted using *CytoD* or *LatA*. This is consistent with a previous study, as they did not find global change in CD22 clustering on B cell membrane using STORM but diffusion was found to be influenced by cytoskeleton disruption using SPT.[15] Furthermore, we examined CD22-cytoskeleton interactions using a range of CytoD concentrations (2.5 - 10 μg/mL), while previous studies tested only a single concentration and found no effect.[15] The interaction of CD22 with the cytoskeleton was complex, and our data indicated that with low concentrations of CytoD (2.5 μg/mL) CD22 was found in larger clusters with reduced lateral mobility. These data cannot resolve whether CD22-cytoskeleton contacts are direct or indirect, but it is well known that this receptor is found in homotypic clusters,[5] and has cis-binding interactions with sialoglycoproteins, such as CD45.[6,15,44,83] Notably, CD45 is associated with the cytoskeleton through a spectrin-ankyrin complex which regulates its lateral mobility, providing a likely explanation for these findings.[84-86] The previous study performed by another group concluded that disruption in cytoskeleton did not change the overall organization of CD22 on B cell membrane.[15] This difference could be due to differences in our methods including concentration of *CytoD* and microscopy techniques. However, similar to their results, we also observed diminished change in CD22 clustering at higher concentration of CD22. This behavior of CD22 clustering on B cell

membrane can be explained by a model (Figure 4.19). In our proposed model, CD22's binding partner, for example, CD45, is anchored to the cytoskeletal network, and CD22 forms clusters around these glycoproteins. When cytoskeletal network is only partially disrupted, it is not sufficient to free CD45 proteins, however, CD22 molecules are able to diffuse more freely to form larger clusters with other CD22 molecules by homotypic interactions. When cytoskeleton is further disrupted, CD45 becomes freed from the cytoskeleton, exposing more ligands for CD45, forming smaller clusters of CD22. Hence, our proposed model is able to explain the difference in our findings compared to previous study.

As a Siglec that engages cis ligands, CD22 organization could be expected to be influenced by mechanisms that regulate membrane sialoglycoproteins. Previous work has found changes to CD22 organization from altered sialyltransferase expression, CD45 expression, lectin activity of CD22, and altered glycosylation sites on CD22.[15,50,87,88] For example, CD45-knocked out mice had their CD22 clustering increased and their diffusion decreased, suggesting the important roles of ligands for CD22 organization. In these CD45-knocked out cells, treatment with LatA did not further change the CD22 diffusion, but exogenous sialidase treatment increased the clustering, and B cells with mutant form of CD22 decreased clustering and increased diffusion. Based on these findings, they concluded that cis-ligands are the main factors influencing CD22 organization and dynamic on B cells. Our work is the first to explore the role of native NEU enzymes in CD22 organization. We found that NEU1 and NEU3 had a role in CD22 clustering, and our data suggest that isoenzymes could play disparate roles in B cell regulation. There is growing recognition that native NEU enzymes may play important roles in inflammation and immune cells.[22,30,89,90] We propose that further investigation of the role of these enzymes in B cell regulation is needed.

A common strategy to perturb CD22-ligand interactions is to treat cells with exogenous NEU. Many examples have tested the effect of exogenous bacterial NEU enzymes on CD22 organization and activity.[15,53] While these reagents may reveal aspects of CD22-ligand interactions, they may not report on the role of native NEU isoenzymes. The substrate preferences of bacterial enzymes and native NEU are different. For example, enzymes like NanI prefer glycoprotein substrates, while NEU3 prefers glycolipids.[91,92] Glycosphingolipids are a major component of membrane microdomains, and these membrane components may be modulated by NEU3 activity.[93] Bacterially-produced enzymes may also be contaminated with LPS, which we observed could alter CD22 clustering. Thus, we suggest that results based on the use of bacterially-produced enzyme be interpreted with caution; and we favor the use of small molecule inhibitors or knockdown of NEU expression to avoid this complication.

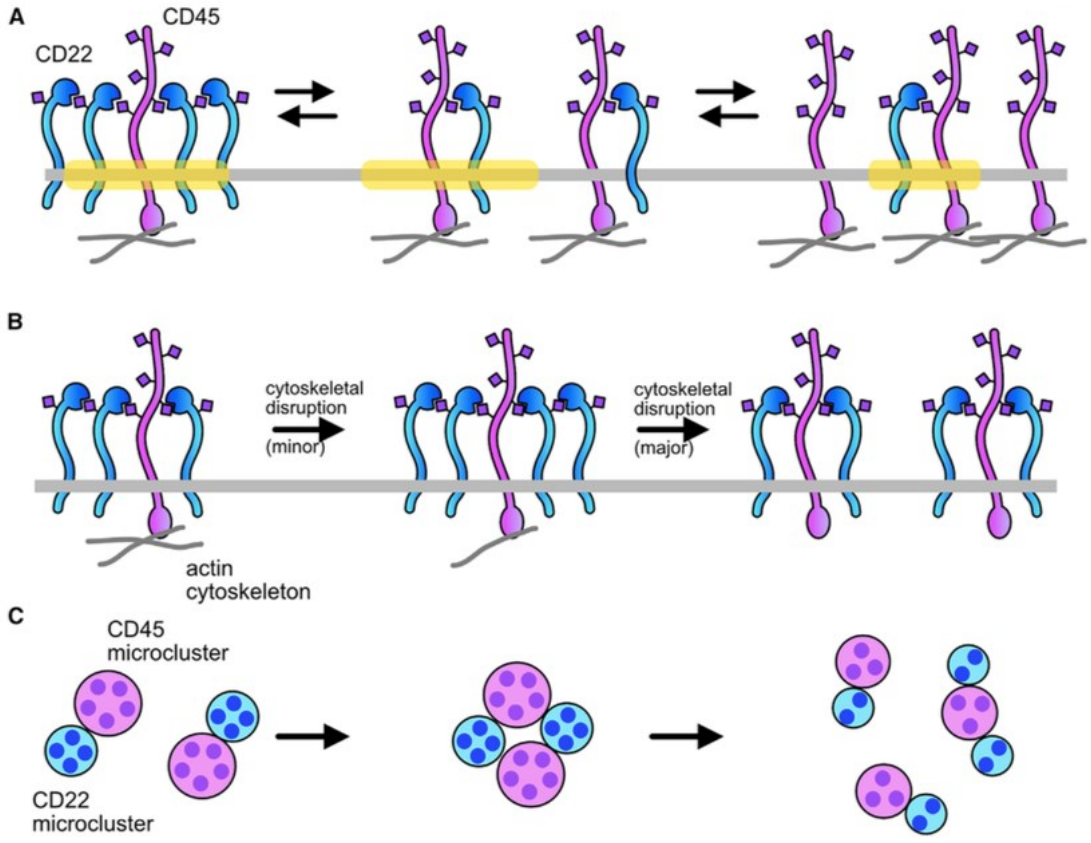

Figure 4.19. Model of changes in CD22 organization. (A) The size of the CD22 cluster formed is a result of interactions between CD22 and sialylated ligands, such as CD45, which can act as a bridge to homoclusters. A change in the stoichiometric ratio (with excess of the sialoside ligand or CD22) will result in smaller clusters at each extreme. Increased NEU activity could reduce the total number of sialylated ligands. (B) Cytoskeletal disruption allows microclusters of sialoglycoproteins to reorganize and act as a bridge to generate larger CD22 clusters. More extensive cytoskeletal disruption alters microclusters, leading to more diffuse clusters of both components. (C) A top-down representation of changes to cluster size due to cytoskeletal disruption.

REFERENCES

(1) Nitschke, L.; Carsetti, R.; Ocker, B.; Köhler, G.; Lamers, M. C. CD22 Is a Negative Regulator of B-Cell Receptor Signalling. *Curr. Biol.* **1997**, *7* (2), 133–143. https://doi.org/10.1016/S0960-9822(06)00057-1.

(2) Ereño-Orbea, J.; Sicard, T.; Cui, H.; Mazhab-Jafari, M. T.; Benlekbir, S.; Guarné, A.; Rubinstein, J. L.; Julien, J.-P. Molecular Basis of Human CD22 Function and Therapeutic Targeting. *Nat. Commun.* **2017**, *8* (764), 1–11. https://doi.org/10.1038/s41467-017-00836-6.

(3) Doody, G.; Justement, L.; Delibrias, C.; Matthews, R.; Lin, J.; Thomas, M.; Fearon, D. A Role in B Cell Activation for CD22 and the Protein Tyrosine Phosphatase SHP. *Science* **1995**, *269* (5221), 242–244. https://doi.org/10.1126/science.7618087.

(4) Razi, N.; Varki, A. Masking and Unmasking of the Sialic Acid-Binding Lectin Activity of CD22 (Siglec-2) on B Lymphocytes. *Proc. Natl. Acad. Sci.* **1998**, *95* (13), 7469–7474. https://doi.org/10.1073/pnas.95.13.7469.

(5) Han, S.; Collins, B. E.; Bengtson, P.; Paulson, J. C. Homomultimeric Complexes of CD22 in B Cells Revealed by Protein-Glycan Cross-Linking. *Nat. Chem. Biol.* **2005**, *1* (2), 93–97. https://doi.org/10.1038/nchembio713.

(6) Sgroi, D.; Koretzky, G. A.; Stamenkovic, I. Regulation of CD45 Engagement by the B-Cell Receptor CD22. *Proc. Natl. Acad. Sci.* **1995**, *92* (9), 4026–4030. https://doi.org/10.1073/pnas.92.9.4026.

(7) Law, C. L.; Aruffo, A.; Chandran, K. A.; Doty, R. T.; Clark, E. A. Ig Domains 1 and 2 of Murine CD22 Constitute the Ligand-Binding Domain and Bind Multiple Sialylated Ligands Expressed on B and T Cells. *1995 155* (7), 3368–3376.

(8) Nitschke, L. CD22 and Siglec-G: B-Cell Inhibitory Receptors with Distinct Functions. *Immunol. Rev.* **2009**, *230* (1), 128–143. https://doi.org/10.1111/j.1600-065X.2009.00801.x.

(9) Collins, B. E.; Blixt, O.; Han, S.; Nathan, J. K.; Bovin, N.; Paulson, J. C. High-Affinity Ligand Probes of CD22 Overcome the Threshold Set by Cis Ligands to Allow for Binding, Endocytosis, and Killing of B Cells. *J. Immunol.* **2006**, *177* (5), 2994–3003. https://doi.org/10.4049/jimmunol.177.5.2994.

(10) Courtney, A. H.; Puffer, E. B.; Pontrello, J. K.; Yang, Z.-Q.; Kiessling, L. L. Sialylated Multivalent Antigens Engage CD22 *in Trans* and Inhibit B Cell Activation. *Proc. Natl. Acad. Sci.* **2009**, *106* (8), 2500–2505. https://doi.org/10.1073/pnas.0807207106.

(11) Macauley, M. S.; Pfrengle, F.; Rademacher, C.; Nycholat, C. M.; Gale, A. J. Antigenic Liposomes Displaying CD22 Ligands Induce Antigen-Specific B Cell Apoptosis. *J. Clin. Invest.* **2013**, *123* (7), 3074–3083. https://doi.org/10.1172/JCI69187.

(12) Chen, W. C.; Completo, G. C.; Sigal, D. S.; Crocker, P. R.; Saven, A.; Paulson, J. C. In Vivo Targeting of B-Cell Lymphoma with Glycan Ligands of CD22. *Blood* **2010**, *115* (23), 4778–4786. https://doi.org/10.1182/blood-2009-12- 257386.

(13) Duong, B. H.; Tian, H.; Ota, T.; Completo, G.; Han, S.; Vela, J. L.; Ota, M.; Kubitz, M.; Bovin, N.; Paulson, J. C.; Nemazee, D. Decoration of T-Independent Antigen with Ligands for CD22 and Siglec-G Can Suppress Immunity and Induce B Cell Tolerance in Vivo. *J. Exp. Med.* **2010**, *207* (1), 173–187. https://doi.org/10.1084/jem.20091873.

(14) Daskhan, G. C.; Tran, H.-T. T.; Meloncelli, P. J.; Lowary, T. L.; West, L. J.; Cairo, C. W. Construction of Multivalent Homo- and Heterofunctional ABO Blood Group Glycoconjugates Using a Trifunctional Linker Strategy. *Bioconjug. Chem.* **2018**, *29* (2), 343–362. https://doi.org/10.1021/acs.bioconjchem.7b00679.

(15) Gasparrini, F.; Feest, C.; Bruckbauer, A.; Mattila, P. K.; Müller, J.; Nitschke, L.; Bray, D.; Batista, F. D. Nanoscale Organization and Dynamics of the Siglec CD 22 Cooperate with the Cytoskeleton in Restraining BCR Signalling. *EMBO J.* **2016**, *35* (3), 258–280. https://doi.org/10.15252/embj.201593027.

(16) He, X.; Woodford-Thomas, T. A.; Johnson, K. G.; Shah, D. D.; Thomas, M. L. Targeting of CD45 Protein Tyrosine Phosphatase Activity to Lipid Microdomains on the T Cell Surface Inhibits TCR Signaling. *Eur J Immunol* **2002**, *32*, 2578–2587. https://doi.org/10.1002/1521-4141(200209)32:9<2578::AID-IMMU2578>3.0.CO;2-3.

(17) Edmonds, S. D.; Ostergaard, H. L. Dynamic Association of CD45 with Detergent-Insoluble Microdomains in T Lymphocytes. *J. Immunol.* **2002**, *169* (9), 5036–5042. https://doi.org/10.4049/jimmunol.169.9.5036.

(18) Guo, B.; Kato, R. M.; Garcia-Lloret, M.; Wahl, M. I.; Rawlings, D. J. Engagement of the Human Pre-B Cell Receptor Generates a Lipid Raft–Dependent Calcium Signaling Complex. *Immunity* **2000**, *13* (2), 243–253. https://doi.org/10.1016/S1074-7613(00)00024-8.

(19) Gupta, N.; DeFranco, A. L. Visualizing Lipid Raft Dynamics and Early Signaling Events during Antigen Receptor-Mediated B-Lymphocyte Activation□V. *Mol. Biol. Cell* **2003**, *14* (2), 432–444. https://doi.org/www.molbiolcell.org/cgi/doi/10.1091/mbc.02– 05– 0078.

(20) Miyagi, T.; Yamaguchi, K. Mammalian Sialidases: Physiological and Pathological Roles in Cellular Functions. *Glycobiology* **2012**, *22* (7), 880–896.

(21) Glanz, V. Yu.; Myasoedova, V. A.; Grechko, A. V.; Orekhov, A. N. Sialidase Activity in Human Pathologies. *Eur. J. Pharmacol.* **2019**, *842*, 345–350. https://doi.org/10.1016/j.ejphar.2018.11.014.

(22) Demina Ekaterina P.; Smutova Victoria; Pan Xuefang; Fougerat Anne; Guo Tianlin; Zou Chunxia; Chakraberty Radhika; Snarr Brendan D.; Shiao Tze C.; Roy Rene; Orekhov Alexander N.; Miyagi Taeko; Laffargue Muriel; Sheppard Donald C.; Cairo Christopher W.; Pshezhetsky Alexey V. Neuraminidases 1 and 3 Trigger Atherosclerosis by

Desialylating Low-Density Lipoproteins and Increasing Their Uptake by Macrophages. *J. Am. Heart Assoc.* **2021**, *10* (4), e018756. https://doi.org/10.1161/JAHA.120.018756.

(23) Kato, T.; Wang, Y.; Yamaguchi, K.; Milner, C. M.; Shineha, R.; Satomi, S.; Miyagi, T. Overexpression of Lysosomal-Type Sialidase Leads to Suppression of Metastasis Associated with Reversion of Malignant Phenotype in Murine B16 Melanoma Cells. *Int. J. Cancer* **2001**, *92* (6), 797–804. https://doi.org/10.1002/ijc.1268.

(24) Sawada, M.; Moriya, S.; Saito, S.; Shineha, R.; Satomi, S.; Yamori, T.; Tsuruo, T.; Kannagi, R.; Miyagi, T. Reduced Sialidase Expression in Highly Metastatic Variants of Mouse Colon Adenocarcinoma 26 and Retardation of Their Metastatic Ability by Sialidase Overexpression. *Int. J. Cancer* **2002**, *97* (2), 180–185. https://doi.org/10.1002/ijc.1598.

(25) Silvestri, I.; Testa, F.; Zappasodi, R.; Cairo, C. W.; Zhang, Y.; Lupo, B.; Galli, R.; Di Nicola, M.; Venerando, B.; Tringali, C. Sialidase NEU4 Is Involved in Glioblastoma Stem Cell Survival. *Cell Death Dis.* **2014**, *5* (8), e1381. https://doi.org/10.1038/cddis.2014.349.

(26) Seyrantepe, V.; Demir, S. A.; Timur, Z. K.; Von Gerichten, J.; Marsching, C.; Erdemli, E.; Oztas, E.; Takahashi, K.; Yamaguchi, K.; Ates, N.; Dönmez Demir, B.; Dalkara, T.; Erich, K.; Hopf, C.; Sandhoff, R.; Miyagi, T. Murine Sialidase Neu3 Facilitates GM2 Degradation and Bypass in Mouse Model of Tay-Sachs Disease. *Exp. Neurol.* **2018**, *299*, 26–41. https://doi.org/10.1016/j.expneurol.2017.09.012.

(27) Seyrantepe, V.; Landry, K.; Trudel, S.; Hassan, J. A.; Morales, C. R.; Pshezhetsky, A. V. Neu4, a Novel Human Lysosomal Lumen Sialidase, Confers Normal Phenotype to Sialidosis and Galactosialidosis Cells. *J. Biol. Chem.* **2004**, *279* (35), 37021–37029. https://doi.org/10.1074/jbc.M404531200.

(28) Hasegawa, T.; Sugeno, N.; Takeda, A.; Matsuzaki-Kobayashi, M.; Kikuchi, A.; Furukawa, K.; Miyagi, T.; Itoyama, Y. Role of Neu4L Sialidase and Its Substrate Ganglioside GD3 in Neuronal Apoptosis Induced by Catechol Metabolites. *FEBS Lett.* **2007**, *581* (3), 406–412. https://doi.org/10.1016/j.febslet.2006.12.046.

(29) Igdoura, S. Sialidase-Mediated Depletion of GM2 Ganglioside in Tay-Sachs Neuroglia Cells. *Hum. Mol. Genet.* **1999**, *8* (6), 1111–1116. https://doi.org/10.1093/hmg/8.6.1111.

(30) Howlader, M. A.; Li, C.; Zou, C.; Chakraberty, R.; Ebesoh, N.; Cairo, C. W. Neuraminidase-3 Is a Negative Regulator of LFA-1 Adhesion. *Front. Chem.* **2019**, *7*. https://doi.org/10.3389/fchem.2019.00791.

(31) Tolar, P.; Hanna, J.; Krueger, P. D.; Pierce, S. K. The Constant Region of the Membrane Immunoglobulin Mediates B Cell-Receptor Clustering and Signaling in Response to Membrane Antigens. *Immunity* **2009**, *30* (1), 44–55. https://doi.org/10.1016/j.immuni.2008.11.007.

(32) Yang, Z.; Puffer, E. B.; Pontrello, J. K.; Kiessling, L. L. Synthesis of a multivalent display of a CD22-binding trisaccharide. Carbohydr. Res. 2002, 337, 1605-1613.

(33) Schneider, D.; Xiong, Y.; Wu, D.; Hu, P.; Alabanza, L.; Steimle, B.; Mahmud, H.; Anthony-Gonda, K.; Kruger, W.; Dropulic, B. Trispecific CD19-CD20-CD22-targeting duoCAR-T cells eliminate antigen-heterogeous B cell tumors in preclinical models. *Sci. Transl. Med*. **2021**, 13(586).

(34) Wasim, L.; Buhari, F. H. M.; Yoganatha, M.; Sicard, T.; Ereno-Orbea, J.; Julien, J-P.; Treanor, B. N-Linked Glycosylation Regulates CD22 Organization and Function. *Front. Immunol*. **2019**, 10(699).

(35) Harwood, N. E.; Batista, F. D. The Cytoskeleton Coordinates the Early Events of B-Cell Activation. *Cold Spring Harb. Perspect. Biol.* **2011**, *3* (2), a002360–a002360. https://doi.org/10.1101/cshperspect.a002360.

(36) Treanor, B.; Depoil, D.; Gonzalez-Granja, A.; Barral, P.; Weber, M.; Dushek, O.; Bruckbauer, A.; Batista, F. D. The Membrane Skeleton Controls Diffusion Dynamics and Signaling through the B Cell Receptor. *Immunity* **2010**, *32* (2), 187–199. https://doi.org/10.1016/j.immuni.2009.12.005.

(37) Schliwa, M. Action of Cytochalasin D on Cytoskeletal Networks. *J. Cell Biol.* **1982**, *92* (1), 79–91. https://doi.org/10.1083/jcb.92.1.79.

(38) Goddette, D. W.; Frieden, C. The Actin Polymerization. The Mechanism of Action of Cytochalasin D. *J. Biol. Chem.* **1986**, *261* (34), 15974–15980.

(39) Morton, W. M.; Ayscough, K. R.; McLaughlin, P. J. Latrunculin Alters the Actin-Monomer Subunit Interface to Prevent Polymerization. *Nat. Cell Biol.* **2000**, *2* (6), 376–378. https://doi.org/10.1038/35014075.

(40) Coué, M.; Brenner, S. L.; Spector, I.; Korn, E. D. Inhibition of Actin Polymerization by Latrunculin A. *FEBS Lett.* **1987**, *213* (2), 316–318. https://doi.org/10.1016/0014-5793(87)81513-2.

(41) Wakatsuki, T. Actin Polymerization and Cell Mechanics. *J. Cell Sci.* **2001**, *114* (Pt 5), 1025–1036.

(42) Stevenson, B. R.; Begg, D. A. Concentration-Dependent Effects of Cytochalasin D on Tight Junctions and Actin FIlaments in MDCK Epithelial Cells. *J. Cell Sci.* **1994**, *107* (3), 367–375.

(43) Cai, S.; Liu, X.; Glasser, A.; Volberg, T.; Filla, M.; Geiger, B.; Polansky, J. R.; Kaufman, P. L. Effect of Latrunculin-A on Morphology and Actin-Associated Adhe- Sions of Cultured Human Trabecular Meshwork Cells. *Mol. Vis.* **2000**, *6*, 132–143.

(44) Foissner, I.; Wasteneys, G. O. Wide-Ranging Effects of Eight Cytochalasins and Latrunculin A and B on Intracellular Motility and Actin Filament Reorganization in Characean Internodal Cells. *Plant Cell Physiol* **2007**, *48* (4), 587–597. https://doi.org/10.1093/pcp/pcm030.

(45) Jaqaman, K.; Loerke, D.; Mettlen, M.; Kuwata, H.; Grinstein, S.; Schmid, S. L.; Danuser, G. Robust Single-Particle Tracking in Live-Cell Time-Lapse Sequences. *Nat. Methods* **2008**, *5* (8), 695–702. https://doi.org/10.1038/nmeth.1237.

(46) Ramya, T. N. C.; Weerapana, E.; Liao, L.; Zeng, Y.; Tateno, H.; Liao, L.; Yates, J. R.; Cravatt, B. F.; Paulson, J. C. In Situ Trans Ligands of CD22 Identified by Glycan-Protein Photocross-Linking-Enabled Proteomics. *Mol. Cell. Proteomics MCP* **2010**, *9* (6), 1339–1351. https://doi.org/10.1074/mcp.m900461-mcp200.

(47) Zhang, M. Cell Surface Sialic Acids Do Not Affect Primary CD22 Interactions with CD45 and Surface IgM nor the Rate of Constitutive CD22 Endocytosis. *Glycobiology* **2004**, *14* (11), 939–949. https://doi.org/10.1093/glycob/cwh126.

(48) Coughlin, S.; Noviski, M.; Mueller, J. L.; Chuwonpad, A.; Raschke, W. C.; Weiss, A.; Zikherman, J. An Extracatalytic Function of CD45 in B Cells Is Mediated by CD22. *Proc. Natl. Acad. Sci.* **2015**, *112* (47), E6515. https://doi.org/10.1073/pnas.1519925112.

(49) Alborzian Deh Sheikh, A.; Akatsu, C.; Imamura, A.; Abdu-Allah, H. H. M.; Takematsu, H.; Ando, H.; Ishida, H.; Tsubata, T. Proximity Labeling of Cis-Ligands of CD22/Siglec-2 Reveals Stepwise A2,6 Sialic Acid-Dependent and -Independent Interactions. *Biochem. Biophys. Res. Commun.* **2018**, *495* (1), 854–859. https://doi.org/10.1016/j.bbrc.2017.11.086.

(50) Heiser, W. C. Optimizing Electroporation Conditions for the Transformation of Mammalian Cells. In *Transcription Factor Protocols*; Tymms, M. J., Ed.; Humana Press: Totowa, NJ, 2000; pp 117–134. https://doi.org/10.1385/1-59259-686-X:117.

(51) Kaminuma, O.; Katoh, S.; Miyagi, T.; Watanabe, N.; Kitamura, N.; Nishimura, T.; Saeki, M.; Mori, A.; Hiroi, T. Contribution of Neuraminidase 3 to the Differentiation of Induced Regulatory T Cells. *Genes Cells* **2017**. https://doi.org/10.1111/gtc.12553.

(52) Nan, X.; Carubelli, I.; Stamatos, N. M. Sialidase Expression in Activated Human T Lymphocytes Influences Production of IFN-γ. *J. Leukoc. Biol.* **2007**, *81* (1), 284–296. https://doi.org/10.1189/jlb.1105692.

(53) Meyer, S. J.; Linder, A. T.; Brandl, C.; Nitschke, L. B Cell Siglecs–News on Signaling and Its Interplay With Ligand Binding. *Front. Immunol.* **2018**, *9*, 2820. https://doi.org/10.3389/fimmu.2018.02820.

(54) Grynkiewicz, G.; Poenie, M.; TsienB, R. Y. A New Generation of Ca2+ Indicatorswith Greatly Improved Fluorescence Properties. *J. Biol. Chem.* **1985**, *260* (6), 3440–3450. https://doi.org/10.1016/S0021-9258(19)83641-4.

(55) Cairo, C. W. Inhibitors of the Human Neuraminidase Enzymes. *MedChemComm* **2014**, *5* (8), 1067–1074. https://doi.org/10.1039/C4MD00089G.

(56) Richards, M. R.; Guo, T.; Hunter, C. D.; Cairo, C. W. Molecular Dynamics Simulations of Viral Neuraminidase Inhibitors with the Human Neuraminidase Enzymes: Insights into

Isoenzyme Selectivity. *Bioorg. Med. Chem.* **2018**, *26* (19), 5349–5358. https://doi.org/10.1016/j.bmc.2018.05.035.

(57) Guo, T.; Dätwyler, P.; Demina, E.; Richards, M. R.; Ge, P.; Zou, C.; Zheng, R.; Fougerat, A.; Pshezhetsky, A. V.; Ernst, B.; Cairo, C. W. Selective Inhibitors of Human Neuraminidase 3. *J. Med. Chem.* **2018**, *61* (5), 1990–2008. https://doi.org/10.1021/acs.jmedchem.7b01574.

(58) Guo, T.; Héon-Roberts, R.; Zou, C.; Zheng, R.; Pshezhetsky, A. V.; Cairo, C. W. Selective Inhibitors of Human Neuraminidase 1 (NEU1). *J. Med. Chem.* **2018**, *61* (24), 11261–11279. https://doi.org/10.1021/acs.jmedchem.8b01411.

(59) Rodriguez-Walker, M.; Daniotti, J. L. Human Sialidase Neu3 Is S-Acylated and Behaves Like an Integral Membrane Protein. *Sci. Rep.* **2017**, *7* (1), 4167. https://doi.org/10.1038/s41598-017-04488-w.

(60) Wada, T.; Hata, K.; Yamaguchi, K.; Shiozaki, K.; Koseki, K.; Moriya, S.; Miyagi, T. A Crucial Role of Plasma Membrane-Associated Sialidase in the Survival of Human Cancer Cells. *Oncogene* **2007**, *26* (17), 2483–2490. https://doi.org/10.1038/sj.onc.1210341.

(61) Papini, N.; Anastasia, L.; Tringali, C.; Croci, G.; Bresciani, R.; Yamaguchi, K.; Miyagi, T.; Preti, A.; Prinetti, A.; Prioni, S.; Sonnino, S.; Tettamanti, G.; Venerando, B.; Monti, E. The Plasma Membrane-Associated Sialidase MmNEU3 Modifies the Ganglioside Pattern of Adjacent Cells Supporting Its Involvement in Cell-to-Cell Interactions. *J. Biol. Chem.* **2004**, *279* (17), 16989–16995. https://doi.org/10.1074/jbc.M400881200.

(62) Kakugawa, Y.; Wada, T.; Yamaguchi, K.; Yamanami, H.; Ouchi, K.; Sato, I.; Miyagi, T. Up-Regulation of Plasma Membrane-Associated Ganglioside Sialidase (Neu3) in Human Colon Cancer and Its Involvement in Apoptosis Suppression. *Proc. Natl. Acad. Sci.* **2002**, *99* (16), 10718–10723. https://doi.org/10.1073/pnas.152597199.

(63) Uchida, Y.; Tsukada, Y.; Sugimori, T. Enzymatic Properties of Neuraminidases from Arthrobacter Ureafaciens. *J. Biochem. (Tokyo)* **1979**, *86* (5), 1573–1585. https://doi.org/10.1093/oxfordjournals.jbchem.a132675.

(64) Ohta, Y.; Tsukada, Y.; Sugimori, T. Purification and Properties of Neuraminidase Isozymes in Arthrobacter Ureafaciens Mutant. *J. Biochem. (Tokyo)* **1989**, *106* (6), 1086–1089. https://doi.org/10.1093/oxfordjournals.jbchem.a122969.

(65) Wang, Y. Sialidases From Clostridium Perfringens and Their Inhibitors. *Front. Cell. Infect. Microbiol.* **2020**, *9* (462), 11. https://doi.org/0.3389/fcimb.2019.00462.

(66) Miyagi, T.; Yamaguchi, K. Mammlian Sialidases: Physiological and Pathological Roles in Cellular Functions. *Glycobiology* **2012**, *22* (7), 880–896. https://doi.org/10.1093/glycob/cws057.

(67) Sato, S.; Miller, A. S.; Inaoki, M.; Bock, C. B.; Jansen, P. J.; Tang, M. L. K.; Tedder, T. F. CD22 Is Both a Positive and Negative Regulator of B Lymphocyte Antigen Receptor Signal

Transduction: Altered Signaling in CD22-Deficient Mice. *Immunity* **1996**, *5* (6), 551–562. https://doi.org/10.1016/S1074-7613(00)80270-8.

(68) Rahman, H.; Qasim, M.; Schultze, F. C.; Oellerich, M.; R Asif, A. Fetal Calf Serum Heat Inactivation and Lipopolysaccharide Contamination Influence the Human T Lymphoblast Proteome and Phosphoproteome. *Proteome Sci.* **2011**, *9* (1), 71. https://doi.org/10.1186/1477-5956-9-71.

(69) Koenig, S.; Hoffmann, M. K. Bacterial Lipopolysaccharide Activates Suppressor B Lymphocytes. *Proc. Natl. Acad. Sci.* **1979**, *76* (9), 4608–4612. https://doi.org/10.1073/pnas.76.9.4608.

(70) Lajaunias, F.; Nitschke, L.; Moll, T.; Martinez-Soria, E.; Semac, I.; Chicheportiche, Y.; Parkhouse, R. M. E.; Izui, S. Differentially Regulated Expression and Function of CD22 in Activated B-1 and B-2 Lymphocytes. *J. Immunol.* **2002**, *168* (12), 6078. https://doi.org/10.4049/jimmunol.168.12.6078.

(71) Cairo, C. W.; Golan, D. E. T Cell Adhesion Mechanisms Revealed by Receptor Lateral Mobility. *Biopolymers* **2008**, *89* (5), 409–419.

(72) Ramadurai, S.; Holt, A.; Krasnikov, V.; van den Bogaart, G.; Killian, J. A.; Poolman, B. Lateral Diffusion of Membrane Proteins. *J. Am. Chem. Soc.* **2009**, *131* (35), 12650–12656. https://doi.org/10.1021/ja902853g.

(73) Auth, T.; Gov, N. S. Diffusion in a Fluid Membrane with a Flexible Cortical Cytoskeleton. *Biophys. J.* **2009**, *96* (3), 818–830. https://doi.org/10.1016/j.bpj.2008.10.038.

(74) Saha, S.; Lee, I.-H.; Polley, A.; Groves, J. T.; Rao, M.; Mayor, S. Diffusion of GPI-Anchored Proteins Is Influenced by the Activity of Dynamic Cortical Actin. *Mol. Biol. Cell* **2015**, *26* (22), 4033–4045. https://doi.org/10.1091/mbc.E15-06-0397.

(75) Gómez-Llobregat, J.; Buceta, J.; Reigada, R. Interplay of Cytoskeletal Activity and Lipid Phase Stability in Dynamic Protein Recruitment and Clustering. *Sci. Rep.* **2013**, *3* (1), 2608. https://doi.org/10.1038/srep02608.

(76) Koppel, D. E.; Sheetz, M. P.; Schindler, M. Matrix Control of Protein Diffusion in Biological Membranes. *Proc. Natl. Acad. Sci.* **1981**, *78* (6), 3576–3580. https://doi.org/10.1073/pnas.78.6.3576.

(77) Lenne, P.-F.; Wawrezinieck, L.; Conchonaud, F.; Wurtz, O.; Boned, A.; Guo, X.-J.; Rigneault, H.; He, H.-T.; Marguet, D. Dynamic Molecular Confinement in the Plasma Membrane by Microdomains and the Cytoskeleton Meshwork. *EMBO J.* **2006**, *25* (14), 3245–3256. https://doi.org/10.1038/sj.emboj.7601214.

(78) Javanainen, M.; Martinez-Seara, H.; Metzler, R.; Vattulainen, I. Diffusion of Integral Membrane Proteins in Protein-Rich Membranes. *J. Phys. Chem. Lett.* **2017**, *8* (17), 4308–4313. https://doi.org/10.1021/acs.jpclett.7b01758.

(79) Zhang, M.; Moran, M.; Round, J.; Low, T. A.; Patel, V. P.; Tomassian, T.; Hernandez, J. D.; Miceli, M. C. CD45 Signals Outside of Lipid Rafts to Promote ERK Activation, Synaptic Raft Clustering, and IL-2 Production. *J. Immunol.* **2005**, *174* (3), 1479–1490. https://doi.org/10.4049/jimmunol.174.3.1479.

(80) Mielenz, D.; Vettermann, C.; Hampel, M.; Lang, C.; Avramidou, A.; Karas, M.; Jäck, H.-M. Lipid Rafts Associate with Intracellular B Cell Receptors and Exhibit a B Cell Stage-Specific Protein Composition. *J. Immunol.* **2005**, *174* (6), 3508–3517. https://doi.org/10.4049/jimmunol.174.6.3508.

(81) Gupta, N.; Wollscheid, B.; Watts, J. D.; Scheer, B.; Aebersold, R.; DeFranco, A. L. Quantitative Proteomic Analysis of B Cell Lipid Rafts Reveals That Ezrin Regulates Antigen Receptor–Mediated Lipid Raft Dynamics. *Nat. Immunol.* **2006**, *7* (6), 625–633. https://doi.org/10.1038/ni1337.

(82) Kabouridis, P. S.; Jury, E. C. Lipid Rafts and T-Lymphocyte Function: Implications for Autoimmunity. *FEBS Lett.* **2008**, *582* (27), 3711–3718. https://doi.org/10.1016/j.febslet.2008.10.006.

(83) Bakker, T. R.; Piperi, C.; Davies, E. A. Comparison of CD22 Binding to Native CD45 and Synthetic Oligosaccharide. *Eur J Immunol* **2002**, *32* (7), 1924–1932. https://doi.org/10.1002/1521-4141(200207)32:7<1924::AID-IMMU1924>3.0.CO;2-N.

(84) Cairo, C. W.; Das, R.; Albohy, A.; Baca, Q. J.; Pradhan, D.; Morrow, J. S.; Coombs, D.; Golan, D. E. Dynamic Regulation of CD45 Lateral Mobility by the Spectrin-Ankyrin Cytoskeleton of T Cells. *J. Biol. Chem.* **2010**, *285* (15), 11392–11401. https://doi.org/10.1074/jbc.M109.075648.

(85) Pradhan, D.; Morrow, J. S. The Spectrin-Ankyrin Skeleton Controls CD45 Surface Display and Interleukin-2 Production. *Immunity* **2002**, *17* (3), 303–315. https://doi.org/10.1016/S1074-7613(02)00396-5.

(86) Lokeshwar, V. B.; Bourguignon, L. Y. Tyrosine Phosphatase Activity of Lymphoma CD45 (GP180) Is Regulated by a Direct Interaction with the Cytoskeleton. *J. Biol. Chem.* **1992**, *267* (30), 21551–21557. https://doi.org/10.1016/S0021-9258(19)36645-1.

(87) Collins, B. E.; Blixt, O.; Bovin, N. V.; Danzer, C.-P.; Chui, D.; Marth, J. D.; Nitschke, L.; Paulson, J. C. Constitutively Unmasked CD22 on B Cells of ST6Gal I Knockout Mice: Novel Sialoside Probe for Murine CD22. *Glycobiology* **2002**, *12* (9), 563–571. https://doi.org/10.1093/glycob/cwf067.

(88) Wasim, L.; Buhari, F. H. M.; Yoganathan, M.; Sicard, T.; Ereño-Orbea, J.; Julien, J.-P.; Treanor, B. N-Linked Glycosylation Regulates CD22 Organization and Function. *Front. Immunol.* **2019**, *10*, 699. https://doi.org/10.3389/fimmu.2019.00699.

(89) Gadhoum, S. Z.; Sackstein, R. CD15 Expression in Human Myeloid Cell Differentiation Is Regulated by Sialidase Activity. *Nat. Chem. Biol.* **2008**, *4* (12), 751–757. https://doi.org/10.1038/nchembio.116.

(90) Luzina, I. G.; Lillehoj, E. P.; Lockatell, V. K.; Hyun, S. W.; Lugkey, K. N.; Imamura, A.; Ishida, H.; Cairo, C. W.; Atamas, S. P.; Goldblum, S. E. Therapeutic Effect of Neuraminidase-1-Selective Inhibition in Mouse Models of Bleomycin-Induced Pulmonary Inflammation and Fibrosis. *J. Pharmacol. Exp. Ther.* **2020**. https://doi.org/10.1124/jpet.120.000223.

(91) Roggentin, P.; Kleineidam, R. G.; Schauer, R. Diversity in the Properties of Two Sialidase Isoenzymes Produced by Clostridium Perfringens Spp. *Biol. Chem. HOPPE SEYLER* **1995**, *376*, 569–569.

(92) Wang, Y.; Yamaguchi, K.; Shimada, Y.; Zhao, X. J.; Miyagi, T. Site-Directed Mutagenesis of Human Membrane-Associated Ganglioside Sialidase - Identification of Amino-Acid Residues Contributing to Substrate Specificity. *Eur. J. Biochem.* **2001**, *268* (8), 2201–2208.

(93) Simons, K.; Toomre, D. Lipid Rafts and Signal Transduction. *Nat. Rev. Mol. Cell Biol.* **2000**, *1* (1), 31–39. https://doi.org/10.1038/35036052.

CHAPTER 5. CONCLUSIONS

5.1 OVERVIEW

In Chapter 2, we developed a confocal microscope method to study clustering of membrane receptors. Using this developed method, we were able to visualize, quantitate, and compare clustering size of BCRs and CD22.

In Chapter 3, we found that bi-functional tetravalent glycoconjugates carrying BCR specific antigens (A type II antigens) and 2,6-sialosides on PEG scaffold could co-cluster BCR and CD22. Our results also suggested the bi-functional display was important for bigger clusters of CD22 but not BCR, however, increasing the valency of CD22 ligands can also cluster these receptors to the same extent. Additionally, adding a protein binder AG10 to the conjugates did not alter the ability of the conjugates to cluster CD22. It is possible to develop similar glycoconjugates bearing CD22 ligand and specific antigen for the BCR to negatively regulate B cell responses. Furthermore, the method that was developed in this thesis can be used as a simple, quick, and versatile tool to determine the efficiency of the glycoconjugates for their ability to co-cluster CD22 and BCR before proceeding with further studies.

In Chapter 4, we found that cytoskeleton has direct or indirect influence on organization and diffusion of CD22. Using NEU1 and NEU3 knocked down Raji cells, we also showed that NEU1 and NEU3 has opposite effects on receptor organization and expression; NEU1 activity seemed to be responsible for smaller CD22 clusters and lower protein expression while NEU3 activity leads to larger clusters and higher expression. Thus, human NEU enzymes may have important roles in regulating CD22 receptors, which in turn can modulate B cell activity.

The results from this thesis enabled us to develop and utilize methods that allowed us to study the organization of CD22 receptors on human B cell model. We found that CD22 receptors

on B cell membrane are associated with CD22 and CD45 proteins, which is in line with previous models.[1] In our proposed model, ligand proteins such as CD45 acts as the bridge to which CD22 can form homo-clusters. As opposed to previous models, which suggested minimal effects of cytoskeleton or cis-ligands on CD22 organization, our results can be explained by effects of changes on stoichiometry of cis ligands. Specifically, when number of sialoside ligands are increased, there are more binding partners for CD22, resulting in smaller clusters. This thesis, for the first time, examined the relationship between CD22 organization on B cells and human NEU enzymes.

We showed that CD22 organization and dynamics are influenced by cytoskeletal disruption and human NEU enzymes for the first time, however, their exact mechanism still needs further investigation. By understanding the effects of human NEU enzymes on CD22 organization and its function, this may enable us to potentially tune the B cell activation in autoimmune diseases. We hypothesize that by modifying the abundance of sialosides on B cell membrane by controlling the activity or expression of NEU enzymes or sialyltransferase, we are able to control the degree of clustering of CD22 receptors, thereby modulate the immune responses in autoimmune diseases.

5.2 FUTURE DIRECTIONS

5.2.1 Interaction of CD22 with cytoskeleton

In our study, we showed that disrupting the cytoskeleton increased clustering of CD22 while decreasing their diffusion. This suggests the interaction of CD22 with cytoskeleton, however, it was unclear whether this interaction was direct or indirect. We speculated indirect association because CD22's major binding partner, CD45, is known to have direct contact with the cytoskeleton.[1–3]

We can test whether CD45 is required for CD22 interactions with the cytoskeleton by knocking out CD45 proteins and disrupting cytoskeleton components using drugs like CytoD or LatA to observe changes in CD22 clustering and/or diffusion. This will likely give clues on whether our observed changes are due to CD22 alone or they are influenced by CD45 receptors. Alternatively, we can also examine CD22's interactions with underlying cytoskeletal components. Co-localization studies using confocal microscope is also a useful method for this purpose. Co-immunoprecipitation is widely used for studying protein-protein interactions, however, this method cannot discriminate between direct and indirect interactions.[4] Pull-down assays,[5,6] far-western blot,[7,8] protein microarrays,[9,10] and surface plasmon resonance[11,12] are some other techniques which can be employed to study this protein-protein interaction.

5.2.2 Association of CD22 in lipid rafts

Our results also suggested that CD22 may reside within or in proximity with the lipid rafts, since B cells with NEU3 knocked down had smaller cluster size while exogenous NEU3 enzyme increased the cluster size and their diffusion. Human NEU3 prefers glycolipids, so we speculated that lipid contents of the cell membrane plays a role in organization of the CD22. Lipid rafts are microdomains on the cell membrane enriched in cholesterol, glycosphingolipids, and raft-associated proteins.[13,14] Cis-binding partners of CD22 include BCR and CD45,[15,16] and associations of BCR and CD45 with lipid rafts have previously been reported.[17–20]

Lipid rafts are known to be insoluble in cold non-ionic detergents.[21] These domains can be enriched by applying a low concentration of detergents using an established protocol[22] followed by western blotting using CD22 specific antibodies. Moreover, since microdomains are important recruiting signalling receptors, it is also crucial to investigate localization of CD22 relatively to

lipid domains on activated and resting B cells to understand the forces that govern organizations of these receptors.

5.2.3 Mechanism of NEU enzyme on B cell response

Our investigations clearly suggested the roles of NEU enzymes in regulating CD22 organization, expression, and B cell activity, however, the mechanism was still unclear. Our findings also showed differential roles of NEU1 and NEU3 in regulating CD22, perhaps due to the differences in their substrate specificities; NEU1 prefers glycoproteins while NEU3 prefers glycolipids.[23] Since CD22 organization is influenced by binding to their cis-ligands,[24] changes glycosylations on the cell membrane and on their binding partners may affect their organization and their inhibitory functions.

Our data did not show significant changes in glycolipid content when we treated the cells with exogenous bacterial enzymes or NEU3 using LC-MS, but have not tested changes in glycosylations in NEU KD cells. Moreover, since NEU1 cleaves terminal sialic acids on glycoproteins, we can also potentially look into changes in glycosylation on CD22's common binding partners when we knock down NEU1 enzymes, including CD22, CD45, and IgM. Lectin blotting can be utilized to examine changes in proteins' glycosylation or total changes in glycosylation.

B cell activation involves phosphorylation of ITAM motifs of BCRs, leading to downstream cellular signalling; CD22 inhibits this by de-phophorylation of these ITAM following phosphorylation of their intracellular ITIM motifs.[25–27] We have confirmed that NEU enzymes changes the clustering of CD22, and we can further confirm degree of phosphprylation on CD22 following B cell activation in NEU1 or NEU3 knock-down, which can be performed using Western

Blot or ELISA. The results can give insights into whether observed elevated B cell activation in both NEU1 and NEU3 KD cells are correlated with changes in CD22 phosphorylation.

5.2.4 Testing in primary B lymphocytes

Although our investigation on the effects of human NEU enzymes activity on CD22 gave insights into possible roles of NEU1 and NEU3 in regulating CD22 and B cell activity, further studies are needed in primary B cells. Raji cells were originally derived by B lymphocytes from a Burkitt's lymphoma male patient,[28] hence they may not be entirely representative of B cells in healthy individuals. Primary B cells are derived directly from the peripheral blood (peripheral blood mononuclear cells, or PBMC), thus are more characteristic of normal B cells.

5.2.5 Roles of NEU in CD22 in vivo

To further confirm the findings related to roles of NEU in regulating CD22 functions, studies can also be performed in vivo. A significant number of CD22 research have been done on mice, however, it is important to note that the specificities of human CD22 and mouse CD22 are different; the former binds to α2,6'-sialosides while the latter is specific to α2,3'-sialosides. To circumvent this potential challenge, transgenic mouse model expressing human CD22 have been reported.[29] The B cells from theses mice showed similar activity as wild-type B cells expressing murine B cells, as shown by Ca^{2+} flux assay. Thus, although challenging, it is possible to study B cells from these transgenic mice with sialidases knocked down to investigate CD22 receptors organization, expression, and B cell activity.

REFERENCES

(1) Shao, J. Y.; Hochmuth, R. M. Mechanical Anchoring Strength of L-Selectin, B2 Integrins, and CD45 to Neutrophil Cytoskeleton and Membrane. *Biophys. J.* **1999**, *77* (1), 587–596. https://doi.org/10.1016/S0006-3495(99)76915-8.

(2) Cairo, C. W.; Das, R.; Albohy, A.; Baca, Q. J.; Pradhan, D.; Morrow, J. S.; Coombs, D.; Golan, D. E. Dynamic Regulation of CD45 Lateral Mobility by the Spectrin-Ankyrin Cytoskeleton of T Cells. *J. Biol. Chem.* **2010**, *285* (15), 11392–11401. https://doi.org/10.1074/jbc.M109.075648.

(3) Lokeshwar, V. B.; Bourguignon, L. Y. W. Tyrosine Phosphatase Activity of Lymphoma CD45 (GP180) Is Regulated by a Direct Interaction with the Cytoskeleton. *J. Biol. Chem.* **1992**, *267* (30), 21551–21557. https://doi.org/10.1016/s0021-9258(19)36645-1.

(4) Lin, J.-S.; Lai, E.-M. Protein–Protein Interactions: Co-Immunoprecipitation BT - Bacterial Protein Secretion Systems: Methods and Protocols; Journet, L., Cascales, E., Eds.; Springer New York: New York, NY, 2017; pp 211–219. https://doi.org/10.1007/978-1-4939-7033-9_17.

(5) Louche, A.; Salcedo, S. P.; Bigot, S. Protein–Protein Interactions: Pull-down Assays. *Methods Mol. Biol.* **2017**, *1615*, 247–255. https://doi.org/10.1007/978-1-4939-7033-9_20.

(6) Jain, A.; Liu, R.; Xiang, Y. K.; Ha, T. Single-Molecule Pull-down for Studying Protein Interactions. *Nat. Protoc.* **2012**, *7* (3), 445–452. https://doi.org/10.1038/nprot.2011.452.

(7) Hall, R. A. Studying Protein-Protein Interactions via Blot Overlay or Far Western Blot BT - Protein-Protein Interactions: Methods and Applications; Fu, H., Ed.; Humana Press: Totowa, NJ, 2004; pp 167–174. https://doi.org/10.1385/1-59259-762-9:167.

(8) Wu, Y.; Li, Q.; Chen, X. Z. Detecting Protein-Protein Interactions by Far Western Blotting. *Nat. Protoc.* **2007**, *2* (12), 3278–3284. https://doi.org/10.1038/nprot.2007.459.

(9) Templin, M. F.; Stoll, D.; Schwenk, J. M.; Pötz, O.; Kramer, S.; Joos, T. O. Protein Microarrays: Promising Tools for Proteomic Research. *Proteomics* **2003**, *3* (11), 2155–2166. https://doi.org/10.1002/pmic.200300600.

(10) Kodadek, T. Protein Microarrays: Prospects and Problems. *Chem. Biol.* **2001**, *8* (2), 105–115. https://doi.org/10.1016/S1074-5521(00)90067-X.

(11) Douzi, B. Protein–Protein Interactions: Surface Plasmon Resonance BT - Bacterial Protein Secretion Systems: Methods and Protocols; Journet, L., Cascales, E., Eds.; Springer New York: New York, NY, 2017; pp 257–275. https://doi.org/10.1007/978-1-4939-7033-9_21.

(12) Karlssonz, R.; Fält, A. Experimental Design for Kinetic Analysis of Protein-Protein Interactions with Surface Plasmon Resonance Biosensors. *J. Immunol. Methods* **1997**, *200* (1–2), 121–133. https://doi.org/10.1016/S0022-1759(96)00195-0.

(13) Lingwood, D.; Simons, K. Lipid Rafts as a Membrane-Organizing Principle. *Science (80-.).* **2010**, *327* (5961), 46–50. https://doi.org/10.1126/science.1174621.

(14) Rauch, S.; Fackler, O. T. Viruses, Lipid Rafts and Signal Transduction. *Signal Transduct.* **2007**, *7* (1), 53–63. https://doi.org/10.1002/sita.200600113.

(15) Han, S.; Collins, B. E.; Bengtson, P.; Paulson, J. C. Homomultimeric Complexes of CD22 in B Cells Revealed by Protein-Glycan Cross-Linking. *Nat. Chem. Biol.* **2005**, *1* (2), 93–97. https://doi.org/10.1038/nchembio713.

(16) Ramya, T. N. C.; Weerapana, E.; Liao, L.; Zeng, Y.; Tateno, H.; Liao, L.; Yates, J. R.; Cravatt, B. F.; Paulson, J. C. In Situ Trans Ligands of CD22 Identified by Glycan-Protein Photocross-Linking-Enabled Proteomics. *Mol. Cell. Proteomics* **2010**, *9* (6), 1339–1351. https://doi.org/10.1074/mcp.M900461-MCP200.

(17) Gupta, N.; DeFranco, A. L. Visualizing Lipid Raft Dynamics and Early Signaling Events during Antigen Receptor-Mediated B-Lymphocyte Activation. *Mol. Biol. Cell* **2002**, *14* (2), 432–444. https://doi.org/10.1091/mbc.02-05-0078.

(18) Guo, B.; Kato, R. M.; Garcia-Lloret, M.; Wahl, M. I.; Rawlings, D. J. Engagement of the Human Pre-B Cell Receptor Generates a Lipid Raft-Dependent Calcium Signaling Complex. *Immunity* **2000**, *13* (2), 243–253. https://doi.org/10.1016/S1074-7613(00)00024-8.

(19) Edmonds, S. D.; Ostergaard, H. L. Dynamic Association of CD45 with Detergent-Insoluble Microdomains in T Lymphocytes. *J. Immunol.* **2002**, *169* (9), 5036–5042. https://doi.org/10.4049/jimmunol.169.9.5036.

(20) Zhang, M.; Moran, M.; Round, J.; Low, T. A.; Patel, V. P.; Tomassian, T.; Hernandez, J. D.; Miceli, M. C. CD45 Signals Outside of Lipid Rafts to Promote ERK Activation, Synaptic Raft Clustering, and IL-2 Production. *J. Immunol.* **2005**, *174* (3), 1479–1490. https://doi.org/10.4049/jimmunol.174.3.1479.

(21) Brown, D. A. Lipid Rafts, Detergent-Resistant Membranes, and Raft Targeting Signals. *Physiology* **2006**, *21* (6), 430–439. https://doi.org/10.1152/physiol.00032.2006.

(22) Chamberlain, L. H. Detergents as Tools for the Purification and Classification of Lipid Rafts. *FEBS Lett.* **2004**, *559* (1–3), 1–5. https://doi.org/10.1016/S0014-5793(04)00050-X.

(23) Miyagi, T.; Yamaguchi, K. Mammalian Sialidases: Physiological and Pathological Roles in Cellular Functions. *Glycobiology* **2012**, *22* (7), 880–896. https://doi.org/10.1093/glycob/cws057.

(24) Wasim, L.; Buhari, F. H. M.; Yoganathan, M.; Sicard, T.; Ereño-Orbea, J.; Julien, J. P.; Treanor, B. N-Linked Glycosylation Regulates CD22 Organization and Function. *Front. Immunol.* **2019**, *10* (APR), 1–16. https://doi.org/10.3389/fimmu.2019.00699.

(25) Smith, K. G. C.; Tarlinton, D. M.; Doody, G. M.; Hibbs, M. L.; Fearon, D. T. Inhibition of

the B Cell by CD22: A Requirement for Lyn. *J. Exp. Med.* **1998**, *187* (5), 807–811. https://doi.org/10.1084/jem.187.5.807.

(26) Courtney, A. H.; Puffer, E. B.; Pontrello, J. K.; Yang, Z. Q.; Kiessling, L. L. Sialylated Multivalent Antigens Engage CD22 in Trans and Inhibit B Cell Activation. *Proc. Natl. Acad. Sci. U. S. A.* **2009**, *106* (8), 2500–2505. https://doi.org/10.1073/pnas.0807207106.

(27) Kelm, S.; Gerlach, J.; Brossmer, R.; Danzer, C. P.; Nitschke, L. The Ligand-Binding Domain of CD22 Is Needed for Inhibition of the B Cell Receptor Signal, as Demonstrated by a Novel Human CD22-Specific Inhibitor Compound. *J. Exp. Med.* **2002**, *195* (9), 1207–1213. https://doi.org/10.1084/jem.20011783.

(28) Karpova, M. B.; Schoumans, J.; Ernberg, J.; Henter, J. I.; Nordenskjöld, M.; Fadeel, B. Raji Revisited: Cytogenetics of the Original Burkitt's Lymphoma Cell Line [12]. *Leukemia* **2005**, *19* (1), 159–161. https://doi.org/10.1038/sj.leu.2403534.

(29) Bednar, K. J.; Shanina, E.; Ballet, R.; Connors, E. P.; Duan, S.; Juan, J.; Arlian, B. M.; Kulis, M. D.; Butcher, E. C.; Fung-Leung, W.; Rao, T. S.; Paulson, J. C.; Macauley, M. S. Human CD22 Inhibits Murine B Cell Receptor Activation in a Human CD22 Transgenic Mouse Model. *J. Immunol*. **2017**, 199(9), 3116-3128.

Bibliography

Adamczyk, B.; Tharmalingam, T.; Rudd, P. M. Glycans as Cancer Biomarkers. Biochim. Biophys. Acta BBA - Gen. Subj. 2012, 1820 (9), 1347–1353. https://doi.org/10.1016/j.bbagen.2011.12.001.

Albohy, A.; Li, M. D.; Zheng, R. B.; Zou, C.; Cairo, C. W. Insight into Substrate Recognition and Catalysis by the Human Neuraminidase 3 (NEU3) through Molecular Modeling and Site-Directed Mutagenesis. Glycobiology 2010, 20 (9), 1127–1138. https://doi.org/10.1093/glycob/cwq077.

Alborzian Deh Sheikh, A.; Akatsu, C.; Imamura, A.; Abdu-Allah, H. H. M.; Takematsu, H.; Ando, H.; Ishida, H.; Tsubata, T. Proximity Labeling of Cis-Ligands of CD22/Siglec-2 Reveals Stepwise A2,6 Sialic Acid-Dependent and -Independent Interactions. Biochem. Biophys. Res. Commun. 2018, 495 (1), 854–859. https://doi.org/10.1016/j.bbrc.2017.11.086.

Alcor, D.; Gouzer, G.; Triller, A. Single-Particle Tracking Methods for the Study of Membrane Receptors Dynamics. Eur. J. Neurosci. 2009, 30 (6), 987–997. https://doi.org/10.1111/j.1460-9568.2009.06927.x.

Alhamadsheh, M. M.; Connelly, S.; Cho, A.; Reixach, N.; Powers, E. T.; Pan, D. W.; Wilson, I. A.; Kelly, J. W.; Graef, I. A. Potent Kinetic Stabilizers That Prevent Transthyretin-Mediated Cardiomyocyte Proteotoxicity. Sci. Transl. Med. 2011, 3 (97), 97ra81-97ra81. https://doi.org/10.1126/scitranslmed.3002473.

Ammann, A. J.; Abrams, D. B-Cell Immunodeficiency in Acquired Immune Deficiency Syndrome. J. Am. Med. Assoc. 1984, 251 (11), 1447–1449.

Annunziata, I.; Patterson, A.; Helton, D.; Hu, H.; Moshiach, S.; Gomero, E.; Nixon, R.; d'Azzo, A. Lysosomal NEU1 Deficiency Affects Amyloid Precursor Protein Levels and Amyloid-β Secretion via Deregulated Lysosomal Exocytosis. Nat. Commun. 2013, 4 (1), 2734. https://doi.org/10.1038/ncomms3734.

Auth, T.; Gov, N. S. Diffusion in a Fluid Membrane with a Flexible Cortical Cytoskeleton. Biophys. J. 2009, 96 (3), 818–830. https://doi.org/10.1016/j.bpj.2008.10.038.

Avci, F. Y.; Li, X.; Tsuji, M.; Kasper, D. L. A Mechanism for Glycoconjugate Vaccine Activation of the Adaptive Immune System and Its Implications for Vaccine Design. Nat. Med. 2011, 17 (12), 1602–1609. https://doi.org/10.1038/nm.2535.

Axelrod, D.; Koppel, D. E.; Schlessinger, J.; Elson, E.; Webb, W. W. Mobility Measurement by Analysis of Fluorescence Photobleaching Recovery Kinetics. Biophys. J. 1976, 16 (9), 1055–1069. https://doi.org/10.1016/S0006-3495(76)85755-4.

Bagatolli, L. A. To See or Not to See: Lateral Organization of Biological Membranes and Fluorescence Microscopy. Biochim. Biophys. Acta BBA - Biomembr. 2006, 1758 (10), 1541–1556. https://doi.org/10.1016/j.bbamem.2006.05.019.

Bakker, T. R.; Piperi, C.; Davies, E. A. Comparison of CD22 Binding to Native CD45 and Synthetic Oligosaccharide. Eur J Immunol 2002, 32 (7), 1924–1932. https://doi.org/10.1002/1521-4141(200207)32:7<1924::AID-IMMU1924>3.0.CO;2-N.

Barr, T. A.; Shen, P.; Brown, S.; Lampropoulou, V.; Roch, T.; Lawrie, S.; Fan, B.; O'Connor, R. A.; Anderton, S. M.; Bar-Or, A.; Fillatreau, S.; Gray, D. B Cell Depletion Therapy Ameliorates Autoimmune Disease through Ablation of IL-6–Producing B Cells. J. Exp. Med. 2012, 209 (5), 1001–1010. https://doi.org/10.1084/jem.20111675.

Barrera, N. P.; Zhou, M.; Robinson, C. V. The Role of Lipids in Defining Membrane Protein Interactions: Insights from Mass Spectrometry. Trends Cell Biol. 2013, 23 (1), 1–8. https://doi.org/10.1016/j.tcb.2012.08.007.

Bednar, K. J.; Shanina, E.; Ballet, R.; Connors, E. P.; Duan, S.; Juan, J.; Arlian, B. M.; Kulis, M. D.; Butcher, E. C.; Fung-Leung, W.; Rao, T. S.; Paulson, J. C.; Macauley, M. S. Human CD22 Inhibits Murine B Cell Receptor Activation in a Human CD22 Transgenic Mouse Model. J. Immunol. 2017, 199(9), 3116-3128.

Belyy, V.; Tran, N.-H.; Walter, P. Quantitative Microscopy Reveals Dynamics and Fate of Clustered IRE1α. Proc. Natl. Acad. Sci. 2020, 117 (3), 1533–1542. https://doi.org/10.1073/pnas.1915311117.

Bigi, A.; Morosi, L.; Pozzi, C.; Forcella, M.; Tettamanti, G.; Venerando, B.; Monti, E.; Fusi, P. Human Sialidase NEU4 Long and Short Are Extrinsic Proteins Bound to Outer Mitochondrial Membrane and the Endoplasmic Reticulum, Respectively. Glycobiology 2010, 20 (2), 148–157. https://doi.org/10.1093/glycob/cwp156.

Birchmeier, W. Cytoskeleton Structure and Function. Trends Biochem. Sci. 1984, 9 (4), 192–195. https://doi.org/10.1016/0968-0004(84)90137-3.

Blacutt, J.; Lan, Z.; Cosgriff-Hernandez, E. M.; Gordon, V. D. Quantitative Confocal Microscopy and Calibration for Measuring Differences in Cyclic-Di-GMP Signalling by Bacteria on Biomedical Hydrogels. R. Soc. Open Sci. 2021, 8 (1), 201453. https://doi.org/10.1098/rsos.201453.

Bogdanov, M. A Polytopic Membrane Protein Displays a Reversible Topology Dependent on Membrane Lipid Composition. EMBO J. 2002, 21 (9), 2107–2116. https://doi.org/10.1093/emboj/21.9.2107.

Bonilla, F. A.; Oettgen, H. C. Adaptive Immunity. J. Allergy Clin. Immunol. 2010, 125 (2), S33–S40. https://doi.org/10.1016/j.jaci.2009.09.017.

Bonten, E. J.; Campos, Y.; Zaitsev, V.; Nourse, A.; Waddell, B.; Lewis, W.; Taylor, G.; d'Azzo, A. Heterodimerization of the Sialidase NEU1 with the Chaperone Protective Protein/Cathepsin A Prevents Its Premature Oligomerization. J. Biol. Chem. 2009, 284 (41), 28430–28441. https://doi.org/10.1074/jbc.M109.031419.

Bou, R.; Lebien, T. W. Of CD22 in Acute Leukemia. Blood 1988, 71 (5), 1480–1486.

Bourguignon, L. Y.; Singer, S. J. Transmembrane Interactions and the Mechanism of Capping of Surface Receptors by Their Specific Ligands. Proc. Natl. Acad. Sci. 1977, 74 (11), 5031–5035. https://doi.org/10.1073/pnas.74.11.5031.

Braeckmans, K.; Peeters, L.; Sanders, N. N.; De Smedt, S. C.; Demeester, J. Three-Dimensional Fluorescence Recovery after Photobleaching with the Confocal Scanning Laser Microscope. Biophys. J. 2003, 85 (4), 2240–2252. https://doi.org/10.1016/S0006-3495(03)74649-9.

Brooks, D. G.; Qiu, W. Q.; Luster, A. D.; Ravetch, J. V. Structure and Expression of Human IgG FcRII(CD32). Functional Heterogeneity Is Encoded by the Alternatively Spliced Products of Multiple Genes. J. Exp. Med. 1989, 170 (4), 1369–1385. https://doi.org/10.1084/jem.170.4.1369.

Brown, D. A. Lipid Rafts, Detergent-Resistant Membranes, and Raft Targeting Signals. Physiology 2006, 21 (6), 430–439. https://doi.org/10.1152/physiol.00032.2006.

Bugaj, L. J.; Choksi, A. T.; Mesuda, C. K.; Kane, R. S.; Schaffer, D. V. Optogenetic Protein Clustering and Signaling Activation in Mammalian Cells. Nat. Methods. 2013, 10(3).

Büll, C.; Heise, T.; Adema, G. J.; Boltje, T. J. Sialic Acid Mimetics to Target the Sialic Acid–Siglec Axis. Trends Biochem. Sci. 2016, 41 (6), 519–531. https://doi.org/10.1016/j.tibs.2016.03.007.

Cai, S.; Liu, X.; Glasser, A.; Volberg, T.; Filla, M.; Geiger, B.; Polansky, J. R.; Kaufman, P. L. Effect of Latrunculin-A on Morphology and Actin-Associated Adhe- Sions of Cultured Human Trabecular Meshwork Cells. Mol. Vis. 2000, 6, 132–143.

Cairo, C. W. Inhibitors of the Human Neuraminidase Enzymes. MedChemComm 2014, 5 (8), 1067–1074. https://doi.org/10.1039/C4MD00089G.

Cairo, C. W.; Das, R.; Albohy, A.; Baca, Q. J.; Pradhan, D.; Morrow, J. S.; Coombs, D.; Golan, D. E. Dynamic Regulation of CD45 Lateral Mobility by the Spectrin-Ankyrin Cytoskeleton of T Cells. J. Biol. Chem. 2010, 285 (15), 11392–11401. https://doi.org/10.1074/jbc.M109.075648.

Cairo, C. W.; Golan, D. E. T Cell Adhesion Mechanisms Revealed by Receptor Lateral Mobility. Biopolymers 2008, 89 (5), 409–419.

Cairo, C. W.; Golan, D. E. T Cell Adhesion Mechanisms Revealed by Receptor Lateral Mobility. Biopolymers 2008, 89 (5), 409–419. https://doi.org/10.1002/bip.20898.

Cambi, A.; Lidke, D. S. Nanoscale Membrane Organization: Where Biochemistry Meets Advanced Microscopy. ACS Chem. Biol. 2012, 7 (1), 139–149. https://doi.org/10.1021/cb200326g.

Cantarel, B. L.; Coutinho, P. M.; Rancurel, C.; Bernard, T.; Lombard, V.; Henrissat, B. The Carbohydrate-Active EnZymes Database (CAZy): An Expert Resource for Glycogenomics. Nucleic Acids Res. 2009, 37 (Database issue), D233–D238. https://doi.org/10.1093/nar/gkn663.

Cao, A.; Alluqmani, N.; Buhari, F. H. M.; Wasim, L.; Smith, L. K.; Quaile, A.; Shannon, M.; Hakim, Z.; Furmli, H.; Owen, D. M.; Savchenko, A.; Treanor, B. Galectin-9 binds IgM-BCR to regulate B cell siganlling. Nat. Comm. 2018, 9, 3288.

Cepok, S.; Rosche, B.; Grummel, V.; Vogel, F.; Zhou, D.; Sayn, J.; Sommer, N.; Hartung, H.-P.; Hemmer, B. Short-Lived Plasma Blasts Are the Main B Cell Effector Subset during the Course of Multiple Sclerosis. Brain 2005, 128 (7), 1667–1676. https://doi.org/10.1093/brain/awh486.

Chamberlain, L. H. Detergents as Tools for the Purification and Classification of Lipid Rafts. FEBS Lett. 2004, 559 (1–3), 1–5. https://doi.org/10.1016/S0014-5793(04)00050-X.

Chang, L.; Goldman, R. D. Intermediate Filaments Mediate Cytoskeletal Crosstalk. Nat. Rev. Mol. Cell Biol. 2004, 5 (8), 601–613. https://doi.org/10.1038/nrm1438.

Chen, J.; McLean, P. A.; Neel, B. G.; Okunade, G.; Shull, G. E.; Wortis, H. H. CD22 attenuates calcium signaling by potentiating plasma membrane calcium-ATPase activity. Nat. Immunol. 2004, 6(5).

Chen, J.; Wang, H.; Xu, W.; Wei, S.; Li, H. J.; Mei, Y.; Li, Y.; Wang, Y. Oncotarget. 2016. 35(7).

Chen, M.-P.; Chung, F.-M.; Chang, D.-M.; Tsai, J. C.-R.; Huang, H.-F.; Shin, S.-J.; Lee, Y.-J. Elevated Plasma Level of Visfatin/Pre-B Cell Colony-Enhancing Factor in Patients with Type 2 Diabetes Mellitus. J. Clin. Endocrinol. Metab. 2006, 91 (1), 295–299. https://doi.org/10.1210/jc.2005-1475.

Chen, W. C.; Completo, G. C.; Sigal, D. S.; Crocker, P. R.; Saven, A.; Paulson, J. C. In Vivo Targeting of B-Cell Lymphoma with Glycan Ligands of CD22. Blood 2010, 115 (23), 4778–4786. https://doi.org/10.1182/blood-2009-12- 257386.

Chen, W. C.; Sigal, D. S.; Saven, A.; Paulson, J. C. Targeting B Lymphoma with Nanoparticles Bearing Glycan Ligands of CD22. Leuk. Lymphoma 2012, 53 (2), 208–210. https://doi.org/10.3109/10428194.2011.604755.

Chichili, G. R. Clustering of Membrane Raft Proteins by the Actin Cytoskeleton. J. Biol. Chem. 2007, 282 (50), 10.

Cho, W.; Stahelin, R. V. Membrane-Protein Interactions in Cell Signaling and Membrane Trafficking. Annu. Rev. Biophys. Biomol. Struct. 2005, 34 (1), 119–151. https://doi.org/10.1146/annurev.biophys.33.110502.133337.

Chugh, P.; Clark, A. G.; Smith, M. B.; Cassani, D. A. D.; Dierkes, K.; Ragab, A.; Roux, P. P.; Charras, G.; Salbreux, G.; Paluch, E. K. Actin Cortex Architecture Regulates Cell Surface Tension. Nat. Cell Biol. 2017, 19 (6), 689–697. https://doi.org/10.1038/ncb3525.

Chung, B. K.; Tsai, K.; Allan, L. L.; Zheng, D. J.; Nie, J. C.; Biggs, C. M.; Hasan, M. R.; Kozak, F. K.; van den Elzen, P.; Priatel, J. J.; Tan, R. Innate Immune Control of EBV-Infected B Cells by Invariant Natural Killer T Cells. Blood 2013, 122 (15), 2600–2608. https://doi.org/10.1182/blood-2013-01-480665.

Clark, A. G.; Dierkes, K.; Paluch, E. K. Monitoring Actin Cortex Thickness in Live Cells. Biophys. J. 2013, 105 (3), 570–580. https://doi.org/10.1016/j.bpj.2013.05.057.

Clark, E. A.; Giltiay, N. CD22: A Regulator of Innate and Adaptive B Cell Responses and Autoimmunity. Frontiers in Immunol. 2018, 2235 (9).

Collins, B. E.; Blixt, O.; Bovin, N. V.; Danzer, C.-P.; Chui, D.; Marth, J. D.; Nitschke, L.; Paulson, J. C. Constitutively Unmasked CD22 on B Cells of ST6Gal I Knockout Mice: Novel Sialoside Probe for Murine CD22. Glycobiology 2002, 12 (9), 563–571. https://doi.org/10.1093/glycob/cwf067.

Collins, B. E.; Blixt, O.; DeSieno, A. R.; Bovin, N.; Marth, J. D.; Paulson, J. C. Masking of CD22 by Cis Ligands Does Not Prevent Redistribution of CD22 to Sites of Cell Contact. Proc. Natl. Acad. Sci. 2004, 101 (16), 6104–6109. https://doi.org/10.1073/pnas.0400851101.

Collins, B. E.; Blixt, O.; Han, S.; Nathan, J. K.; Bovin, N.; Paulson, J. C. High-Affinity Ligand Probes of CD22 Overcome the Threshold Set by Cis Ligands to Allow for Binding, Endocytosis, and Killing of B Cells. J. Immunol. 2006, 177 (5), 2994–3003. https://doi.org/10.4049/jimmunol.177.5.2994.

Collins, B. E.; Smith, B. A.; Bengtson, P.; Paulson, J. C. Ablation of CD22 in Ligand-Deficient Mice Restores B Cell Receptor Signaling. Nat. Immunol. 2006, 7 (2), 8.

Coué, M.; Brenner, S. L.; Spector, I.; Korn, E. D. Inhibition of Actin Polymerization by Latrunculin A. FEBS Lett. 1987, 213 (2), 316–318. https://doi.org/10.1016/0014-5793(87)81513-2.

Coughlin, S.; Noviski, M.; Mueller, J. L.; Chuwonpad, A.; Raschke, W. C.; Weiss, A.; Zikherman, J. An Extracatalytic Function of CD45 in B Cells Is Mediated by CD22. Proc. Natl. Acad. Sci. 2015, 112 (47), E6515. https://doi.org/10.1073/pnas.1519925112.

Coughlin, S.; Noviski, M.; Mueller, J. L.; Chuwonpad, A.; Raschke, W.; Weiss, A.; Zikherman, J. An extracatalytic function of CD45 in B cells is mediated by CD22. PNAS. 2015, 112(47), E6515-E6524.

Courtney, A. H.; Puffer, E. B.; Pontrello, J. K.; Yang, Z. Q.; Kiessling, L. L. Sialylated Multivalent Antigens Engage CD22 in Trans and Inhibit B Cell Activation. Proc. Natl. Acad. Sci. U. S. A. 2009, 106 (8), 2500–2505. https://doi.org/10.1073/pnas.0807207106.

Courtney, A. H.; Puffer, E. B.; Pontrello, J. K.; Yang, Z.-Q.; Kiessling, L. L. Sialylated Multivalent Antigens Engage CD22 in Trans and Inhibit B Cell Activation. Proc. Natl. Acad. Sci. 2009, 106 (8), 2500–2505. https://doi.org/10.1073/pnas.0807207106.

Damer, C. K.; O'Halloran, T. J. Spatially Regulated Recruitment of Clathrin to the Plasma Membrane during Capping and Cell Translocation□V. Mol. Biol. Cell 2000, 11, 9.

Daskhan, G. C.; Tran, H.-T. T.; Meloncelli, P. J.; Lowary, T. L.; West, L. J.; Cairo, C. W. Construction of Multivalent Homo- and Heterofunctional ABO Blood Group Glycoconjugates Using a Trifunctional Linker Strategy. Bioconjug. Chem. 2018, 29 (2), 343–362. https://doi.org/10.1021/acs.bioconjchem.7b00679.

De Geest, N. Systemic and Neurologic Abnormalities Distinguish the Lysosomal Disorders Sialidosis and Galactosialidosis in Mice. Hum. Mol. Genet. 2002, 11 (12), 1455–1464. https://doi.org/10.1093/hmg/11.12.1455.

Demina Ekaterina P.; Smutova Victoria; Pan Xuefang; Fougerat Anne; Guo Tianlin; Zou Chunxia; Chakraberty Radhika; Snarr Brendan D.; Shiao Tze C.; Roy Rene; Orekhov Alexander N.; Miyagi Taeko; Laffargue Muriel; Sheppard Donald C.; Cairo Christopher W.; Pshezhetsky Alexey V. Neuraminidases 1 and 3 Trigger Atherosclerosis by Desialylating Low-Density Lipoproteins and Increasing Their Uptake by Macrophages. J. Am. Heart Assoc. 2021, 10 (4), e018756. https://doi.org/10.1161/JAHA.120.018756.

Dinic, J.; Ashrafzadeh, P.; Parmryd, I. Actin Filaments Attachment at the Plasma Membrane in Live Cells Cause the Formation of Ordered Lipid Domains. Biochim. Biophys. Acta BBA - Biomembr. 2013, 1828 (3), 1102–1111. https://doi.org/10.1016/j.bbamem.2012.12.004.

Dogterom, M.; Koenderink, G. H. Actin–Microtubule Crosstalk in Cell Biology. Nat. Rev. Mol. Cell Biol. 2019, 20 (1), 38–54. https://doi.org/10.1038/s41580-018-0067-1.

Doody, G.; Justement, L.; Delibrias, C.; Matthews, R.; Lin, J.; Thomas, M.; Fearon, D. A Role in B Cell Activation for CD22 and the Protein Tyrosine Phosphatase SHP. Science 1995, 269 (5221), 242–244. https://doi.org/10.1126/science.7618087.

Douzi, B. Protein–Protein Interactions: Surface Plasmon Resonance BT - Bacterial Protein Secretion Systems: Methods and Protocols; Journet, L., Cascales, E., Eds.; Springer New York: New York, NY, 2017; pp 257–275. https://doi.org/10.1007/978-1-4939-7033-9_21.

Downing, K. H.; Nogales, E. Tubulin and Microtubulue Structure. Curr. Opin. Cell Biol. 1998, 10, 16–22.

Doyle, H. A.; Mamula, M. J. Post-Translational Protein Modifications in Antigen Recognition and Autoimmunity. Trends Immunol. 2001, 22 (8), 443–449. https://doi.org/10.1016/S1471-4906(01)01976-7.

Duncan, A. L.; Reddy, T.; Koldsø, H.; Hélie, J.; Fowler, P. W.; Chavent, M.; Sansom, M. S. P. Protein Crowding and Lipid Complexity Influence the Nanoscale Dynamic Organization of Ion Channels in Cell Membranes. Sci. Rep. 2017, 7 (1), 16647. https://doi.org/10.1038/s41598-017-16865-6.

Duong, B. H.; Tian, H.; Ota, T.; Completo, G.; Han, S.; Vela, J. L.; Ota, M.; Kubitz, M.; Bovin, N.; Paulson, J. C.; Nemazee, D. Decoration of T-Independent Antigen with Ligands for CD22 and Siglec-G Can Suppress Immunity and Induce B Cell Tolerance in Vivo. J. Exp. Med. 2010, 207 (1), 173–187. https://doi.org/10.1084/jem.20091873.

Durisic, N. Quantitative Super-Resolution Microscopy: Pitfalls and Strategies for Image Analysis. Curr. Opin. Chem. Biol. 2014, 20, 22-28.

Dustin, M. L.; Springer, T. A. T-Cell Receptor Cross-Linking Transiently Stimulates Adhesiveness through LFA-1. Nature 1989, 341 (6243), 619–624. https://doi.org/10.1038/341619a0.

Edmonds, S. D.; Ostergaard, H. L. Dynamic Association of CD45 with Detergent-Insoluble Microdomains in T Lymphocytes. J. Immunol. 2002, 169 (9), 5036–5042. https://doi.org/10.4049/jimmunol.169.9.5036.

Edward, J. T. Molecular Volumes and the Stokes-Einstein Equation. J. Chem. Educ. 1970, 47(4), 261.

Edwards, J. C. W.; Szechinski, J.; Emery, P.; Shaw, T. Efficacy of B-Cell–Targeted Therapy with Rituximab in Patients with Rheumatoid Arthritis. N. Engl. J. Med. 2004, 10.

Elson, E. L.; Magde, D. Fluorescence Correlation Spectroscopy. I. Conceptual Basis and Theory. Biopolymers 1974, 13 (1), 1–27. https://doi.org/10.1002/bip.1974.360130102.

Eltoum, I.; Fredenburgh, J.; Myers, R. B.; Grizzle, W. E. Introduction to the Theory and Practice of Fixation of Tissues. J. Histotechnol. 2001, 24 (3), 173–190. https://doi.org/10.1179/his.2001.24.3.173.

Enterina, J. R.; Jung, J.; Macauley, M. S. Coordinated roles for glycans in regulating the inhibitory function of CD22 on B cells. Biomed. J. 2019, 42, 218-232.

Enterina, J. R.; Sarkar, S.; Streith, L.; Jung, J.; Arlian, B. M.; Meyer, S. J.; Takematsu, H.; Xiao, C.; Baldwin, T. A.; Nitschke, L.; Shlomchick, M. J.; Paulson, J. C.; Macauley, M. S. Cell Reports. 2022, 38(11).

Ereño-Orbea, J.; Sicard, T.; Cui, H.; Mazhab-Jafari, M. T.; Benlekbir, S.; Guarné, A.; Rubinstein, J. L.; Julien, J.-P. Molecular Basis of Human CD22 Function and Therapeutic Targeting. Nat. Commun. 2017, 8 (764), 1–11. https://doi.org/10.1038/s41467-017-00836-6.

Fanzani, A.; Colombo, F.; Giuliani, R.; Preti, A.; Marchesini, S. Cytosolic Sialidase Neu2 Upregulation during PC12 Cells Differentiation. FEBS Lett. 2004, 566 (1–3), 178–182. https://doi.org/10.1016/j.febslet.2004.03.115.

Fanzani, A.; Giuliani, R.; Colombo, F.; Zizioli, D.; Presta, M.; Preti, A.; Marchesini, S. Overexpression of Cytosolic Sialidase Neu2 Induces Myoblast Differentiation in C2C12 Cells. FEBS Lett. 2003, 547 (1–3), 183–188. https://doi.org/10.1016/S0014-5793(03)00709-9.

Feigenson, G. W. Phase Diagrams and Lipid Domains in Multicomponent Lipid Bilayer Mixtures. Biochim. Biophys. Acta BBA - Biomembr. 2009, 1788 (1), 47–52. https://doi.org/10.1016/j.bbamem.2008.08.014.

Ferber, I.; Schonrich, G.; Schenkel, J.; Mellor, A.; Hammerling, G.; Arnold, B. Levels of Peripheral T Cell Tolerance Induced by Different Doses of Tolerogen. Science 1994, 263 (5147), 674–676. https://doi.org/10.1126/science.8303275.

Firestein, G. S. Evolving Concepts of Rheumatoid Arthritis. Nature 2003, 423 (6937), 356–361. https://doi.org/10.1038/nature01661.

Fish, K. N. Total Internal Reflection Fluorescence (TIRF) Microscopy. Curr. Protoc. Cytom. 2009, 50 (1). https://doi.org/10.1002/0471142956.cy1218s50.

Foissner, I.; Wasteneys, G. O. Wide-Ranging Effects of Eight Cytochalasins and Latrunculin A and B on Intracellular Motility and Actin Filament Reorganization in Characean Internodal Cells. Plant Cell Physiol 2007, 48 (4), 587–597. https://doi.org/10.1093/pcp/pcm030.

Fornasiero, E. F.; Opazo, F. Super-resolution Imaging for Cell Biologists. Bioessays. 2015, 37(4), 436-451.

Fournier, T.; Medjoubi-N, N.; Porquet, D. Alpha-1-Acid Glycoprotein. Biochim. Biophys. Acta 2000, 1482, 157–171.

Fox, J. C.; Hellawell, J. L.; Rao, S.; O'Reilly, T.; Lumpkin, R.; Jernelius, J.; Gretler, D.; Sinha, U. First-in-Human Study of AG10, a Novel, Oral, Specific, Selective, and Potent Transthyretin Stabilizer for the Treatment of Transthyretin Amyloidosis: A Phase 1 Safety, Tolerability, Pharmacokinetic, and Pharmacodynamic Study in Healthy Adult Volunteers. Clin. Pharmacol. Drug Dev. 2020, 9 (1), 115–129. https://doi.org/10.1002/cpdd.700.

Franchini, M.; Liumbruno, G. M. ABO Blood Group: Old Dogma, New Perspectives. Clin. Chem. Lab. Med. 2013, 51 (8), 1545–1553. https://doi.org/10.1515/cclm-2013-0168.

Frick, M.; Schmidt, K.; Nichols, B. J. Modulation of Lateral Diffusion in the Plasma Membrane by Protein Density. Curr. Biol. 2007, 17 (5), 462–467. https://doi.org/10.1016/j.cub.2007.01.069.

Fry, D. C. Protein–Protein Interactions as Targets for Small Molecule Drug Discovery. Biopolymers 2006, 84 (6), 535–552. https://doi.org/10.1002/bip.20608.

Fujiwara, T.; Ritchie, K.; Murakoshi, H.; Jacobson, K.; Kusumi, A. Phospholipids Undergo Hop Diffusion in Compartmentalized Cell Membrane. J. Cell Biol. 2002, 157 (6), 1071–1082. https://doi.org/10.1083/jcb.200202050.

Gadhoum, S. Z.; Sackstein, R. CD15 Expression in Human Myeloid Cell Differentiation Is Regulated by Sialidase Activity. Nat. Chem. Biol. 2008, 4 (12), 751–757. https://doi.org/10.1038/nchembio.116.

Galbraith, C. G.; Galbraith, J. A. Super-Resolution Microscopy at a Glance. J. Cell Sci. 2011, 124 (10), 1607–1611. https://doi.org/10.1242/jcs.080085.

Gambin, Y.; Lopez-Esparza, R.; Reffay, M.; Sierecki, E.; Gov, N. S.; Genest, M.; Hodges, R. S.; Urbach, W. Lateral Mobility of Proteins in Liquid Membranes Revisited. Proc. Natl. Acad. Sci. 2006, 103 (7), 2098–2102. https://doi.org/10.1073/pnas.0511026103.

Gasparrini, F.; Feest, C.; Bruckbauer, A.; Mattila, P. K.; Müller, J.; Nitschke, L.; Bray, D.; Batista, F. D. Nanoscale Organization and Dynamics of the Siglec CD 22 Cooperate with the Cytoskeleton in Restraining BCR Signalling. EMBO J. 2016, 35 (3), 258–280. https://doi.org/10.15252/embj.201593027.

Gee, K.; Kozlowski, M.; Kumar, A. Tumor Necrosis Factor-Alpha Induces Functionally Active Hyaluronan-Adhesive CD44 by Activating Sialidase through P38 Mitogen-Activated Protein Kinase in Lipopolysaccharide-Stimulated Human Monocytic Cells. J. Biol. Chem. 2003, 278 (39), 37275–37287.

Glanz, V. Yu.; Myasoedova, V. A.; Grechko, A. V.; Orekhov, A. N. Sialidase Activity in Human Pathologies. Eur. J. Pharmacol. 2019, 842, 345–350. https://doi.org/10.1016/j.ejphar.2018.11.014.

Goddette, D. W.; Frieden, C. The Actin Polymerization. The Mechanism of Action of Cytochalasin D. J. Biol. Chem. 1986, 261 (34), 15974–15980.

Gómez-Llobregat, J.; Buceta, J.; Reigada, R. Interplay of Cytoskeletal Activity and Lipid Phase Stability in Dynamic Protein Recruitment and Clustering. Sci. Rep. 2013, 3 (1), 2608. https://doi.org/10.1038/srep02608.

Goñi, F. M. The Basic Structure and Dynamics of Cell Membranes: An Update of the Singer–Nicolson Model. Biochim. Biophys. Acta BBA - Biomembr. 2014, 1838 (6), 1467–1476. https://doi.org/10.1016/j.bbamem.2014.01.006.

Goode, B. L.; Drubin, D. G.; Barnes, G. Functional Cooperation between the Microtubule and Actin Cytoskeletons. Curr. Opin. Cell Biol. 2000, 12(1), 63-71.

Grammer, A. C.; Lipsky, P. E. [No Title Found]. Arthritis Res. Ther. 2003, 5 (Suppl 4), S22. https://doi.org/10.1186/ar1009.

Grynkiewicz, G.; Poenie, M.; TsienB, R. Y. A New Generation of Ca2+ Indicatorswith Greatly Improved Fluorescence Properties. J. Biol. Chem. 1985, 260 (6), 3440–3450. https://doi.org/10.1016/S0021-9258(19)83641-4.

Guigas, G.; Weiss, M. Effects of Protein Crowding on Membrane Systems. Biochim. Biophys. Acta BBA - Biomembr. 2016, 1858 (10), 2441–2450. https://doi.org/10.1016/j.bbamem.2015.12.021.

Guo, B.; Kato, R. M.; Garcia-Lloret, M.; Wahl, M. I.; Rawlings, D. J. Engagement of the Human Pre-B Cell Receptor Generates a Lipid Raft-Dependent Calcium Signaling Complex. Immunity 2000, 13 (2), 243–253. https://doi.org/10.1016/S1074-7613(00)00024-8.

Guo, B.; Kato, R. M.; Garcia-Lloret, M.; Wahl, M. I.; Rawlings, D. J. Engagement of the Human Pre-B Cell Receptor Generates a Lipid Raft–Dependent Calcium Signaling Complex. Immunity 2000, 13 (2), 243–253. https://doi.org/10.1016/S1074-7613(00)00024-8.

Guo, T.; Dätwyler, P.; Demina, E.; Richards, M. R.; Ge, P.; Zou, C.; Zheng, R.; Fougerat, A.; Pshezhetsky, A. V.; Ernst, B.; Cairo, C. W. Selective Inhibitors of Human Neuraminidase 3. J. Med. Chem. 2018, 61 (5), 1990–2008. https://doi.org/10.1021/acs.jmedchem.7b01574.

Guo, T.; Héon-Roberts, R.; Zou, C.; Zheng, R.; Pshezhetsky, A. V.; Cairo, C. W. Selective Inhibitors of Human Neuraminidase 1 (NEU1). J. Med. Chem. 2018, 61 (24), 11261–11279. https://doi.org/10.1021/acs.jmedchem.8b01411.

Gupta, N.; DeFranco, A. L. Visualizing Lipid Raft Dynamics and Early Signaling Events during Antigen Receptor-Mediated B-Lymphocyte Activation. Mol. Biol. Cell 2002, 14 (2), 432–444. https://doi.org/10.1091/mbc.02-05-0078.

Gupta, N.; DeFranco, A. L. Visualizing Lipid Raft Dynamics and Early Signaling Events during Antigen Receptor-Mediated B-Lymphocyte Activation□V. Mol. Biol. Cell 2003, 14 (2), 432–444. https://doi.org/www.molbiolcell.org/cgi/doi/10.1091/mbc.02– 05– 0078.

Gupta, N.; Wollscheid, B.; Watts, J. D.; Scheer, B.; Aebersold, R.; DeFranco, A. L. Quantitative Proteomic Analysis of B Cell Lipid Rafts Reveals That Ezrin Regulates Antigen Receptor–Mediated Lipid Raft Dynamics. Nat. Immunol. 2006, 7 (6), 625–633. https://doi.org/10.1038/ni1337.

Gustafsson, M. G. L. Surpassing the Lateral Resolution Limit by a Factor of Two Using Structured Illumination Microscopy. SHORT COMMUNICATION. J. Microsc. 2000, 198 (2), 82–87. https://doi.org/10.1046/j.1365-2818.2000.00710.x.

Hall, R. A. Studying Protein-Protein Interactions via Blot Overlay or Far Western Blot BT - Protein-Protein Interactions: Methods and Applications; Fu, H., Ed.; Humana Press: Totowa, NJ, 2004; pp 167–174. https://doi.org/10.1385/1-59259-762-9:167.

Hamaguchi, Y.; Xiu, Y.; Komura, K.; Nimmerjahn, F.; Tedder, T. F. Antibody Isotype-Specific Engagement of Fcγ Receptors Regulates B Lymphocyte Depletion during CD20 Immunotherapy. J. Exp. Med. 2006, 203 (3), 743–753. https://doi.org/10.1084/jem.20052283.

Han, S.; Collins, B. E.; Bengtson, P.; Paulson, J. C. Homomultimeric Complexes of CD22 in B Cells Revealed by Protein-Glycan Cross-Linking. Nat. Chem. Biol. 2005, 1 (2), 93–97. https://doi.org/10.1038/nchembio713.

Hardy, R. R.; Hayakawa, K. B cell development pathways. Annu. Rev. Immunol. 2001, 19 (1), 595–621. https://doi.org/10.1146/annurev.immunol.19.1.595.

Hartwig, J. H.; DeSisto, M. The Cytoskeleton of the Resting Human Blood Platelet: Structure of the Membrane Skeleton and Its Attachment to Actin Filaments. J. Cell Biol. 1991, 112 (3), 407–425. https://doi.org/10.1083/jcb.112.3.407.

Harwood, N. E.; Batista, F. D. The Cytoskeleton Coordinates the Early Events of B-Cell Activation. Cold Spring Harb. Perspect. Biol. 2011, 3 (2), a002360–a002360. https://doi.org/10.1101/cshperspect.a002360.

Hasegawa, T.; Sugeno, N.; Takeda, A.; Matsuzaki-Kobayashi, M.; Kikuchi, A.; Furukawa, K.; Miyagi, T.; Itoyama, Y. Role of Neu4L Sialidase and Its Substrate Ganglioside GD3 in Neuronal Apoptosis Induced by Catechol Metabolites. FEBS Lett. 2007, 581 (3), 406–412. https://doi.org/10.1016/j.febslet.2006.12.046.

Haso, W.; Lee, D. W.; Shah, N. N.; Stetler-Stevenson, M.; Yuan, C. M.; Pastan, I. H.; Dimitrov, D. S.; Morgan, R. A.; FitzGerald, D. J.; Barrett, D. M.; Wayne, A. S.; Mackall, C. L.; Orentas, R. J. Anti-CD22–Chimeric Antigen Receptors Targeting B-Cell Precursor Acute Lymphoblastic Leukemia. Blood 2013, 121 (7), 1165–1174. https://doi.org/10.1182/blood-2012-06-438002.

Hass, K. M.; Johnson, K. L.; Phipps, J. P.; Do, C. CD22 promotes B-1b Cell Responses to T Cell-Independent Type 2 Antigens. J. Immunol. 2018, 200, 1671-1681.

He, X.; Woodford-Thomas, T. A.; Johnson, K. G.; Shah, D. D.; Thomas, M. L. Targeting of CD45 Protein Tyrosine Phosphatase Activity to Lipid Microdomains on the T Cell Surface Inhibits TCR Signaling. Eur J Immunol 2002, 32, 2578–2587. https://doi.org/10.1002/1521-4141(200209)32:9<2578::AID-IMMU2578>3.0.CO;2-3.

Heiser, W. C. Optimizing Electroporation Conditions for the Transformation of Mammalian Cells. In Transcription Factor Protocols; Tymms, M. J., Ed.; Humana Press: Totowa, NJ, 2000; pp 117–134. https://doi.org/10.1385/1-59259-686-X:117.

Hess, S. T.; Girirajan, T. P. K.; Mason, M. D. Ultra-High Resolution Imaging by Fluorescence Photoactivation Localization Microscopy. Biophys. J. 2006, 91 (11), 4258–4272. https://doi.org/10.1529/biophysj.106.091116.

Hohmann, T.; Dehghani, F. The Cytoskeleton - a Complex Interacting Meshwork. Cells. 2019, 8(4), 362.

Hosoi, E. Biological and Clinical Aspects of ABO Blood Group System. J. Med. Invest. 2008, 55 (3,4), 174–182. https://doi.org/10.2152/jmi.55.174.

Hou, G.; Liu, G.; Yang, Y.; Li, Y.; Yuan, S.; Zhao, L.; Wu, M.; Liu, L.; Zhou, W. Neuraminidase 1 (NEU1) Promotes Proliferation and Migration as a Diagnostic and Prognostic Biomarker of Hepatocellular Carcinoma. Oncotarget 2016, 7 (40), 64957–64966. https://doi.org/10.18632/oncotarget.11778.

Howlader, M. A.; Li, C.; Zou, C.; Chakraberty, R.; Ebesoh, N.; Cairo, C. W. Neuraminidase-3 Is a Negative Regulator of LFA-1 Adhesion. Front. Chem. 2019, 7. https://doi.org/10.3389/fchem.2019.00791.

Howlader, Md. A.; Li, C.; Zou, C.; Chakraberty, R.; Ebesoh, N.; Cairo, C. W. Neuraminidase-3 Is a Negative Regulator of LFA-1 Adhesion. Front. Chem. 2019, 7, 791. https://doi.org/10.3389/fchem.2019.00791.

Igdoura, S. Sialidase-Mediated Depletion of GM2 Ganglioside in Tay-Sachs Neuroglia Cells. Hum. Mol. Genet. 1999, 8 (6), 1111–1116. https://doi.org/10.1093/hmg/8.6.1111.

Jacobson, K.; Derzko, Z.; Wu, E.-S.; Hou, Y.; Poste, G. Measurement of the Lateral Mobility of Cell Surface Components in Single Living Cells by Fluorescence Recovery after Photobleaching. J. Supramol. Struct. 1976, 5 (4), 565–576. https://doi.org/10.1002/jss.400050411.

Jacobson, K.; Sheets, E.; Simson, R. Revisiting the Fluid Mosaic Model of Membranes. Science 1995, 268 (5216), 1441–1442. https://doi.org/10.1126/science.7770769.

Jain, A.; Liu, R.; Xiang, Y. K.; Ha, T. Single-Molecule Pull-down for Studying Protein Interactions. Nat. Protoc. 2012, 7 (3), 445–452. https://doi.org/10.1038/nprot.2011.452.

Jaiswal, J. K.; Simon, S. M. Imaging Single Events at the Cell Membrane. Nat. Chem. Biol. 2007, 3 (2), 92–98. https://doi.org/10.1038/nchembio855.

Jaqaman, K.; Loerke, D.; Mettlen, M.; Kuwata, H.; Grinstein, S.; Schmid, S. L.; Danuser, G. Robust Single-Particle Tracking in Live-Cell Time-Lapse Sequences. Nat. Methods 2008, 5 (8), 695–702. https://doi.org/10.1038/nmeth.1237.

Järvinen, K.-M.; Beyer, K.; Vila, L.; Chatchatee, P.; Busse, P. J.; Sampson, H. A. B-Cell Epitopes as a Screening Instrument for Persistent Cow's Milk Allergy. J. Allergy Clin. Immunol. 2002, 110 (2), 293–297. https://doi.org/10.1067/mai.2002.126080.

Javanainen, M.; Martinez-Seara, H.; Metzler, R.; Vattulainen, I. Diffusion of Integral Membrane Proteins in Protein-Rich Membranes. J. Phys. Chem. Lett. 2017, 8 (17), 4308–4313. https://doi.org/10.1021/acs.jpclett.7b01758.

Jellusova, J.; Nitschke, L. Regulation of B Cell Functions by the Sialic Acid-Binding Receptors Siglec-G and CD22. Front. Immunol. 2012, 2. https://doi.org/10.3389/fimmu.2011.00096.

Jonkman, J. E. N.; Swoger, J.; Kress, H.; Rohrbach, A.; Stelzer, E. H. K. [18] Resolution in Optical Microscopy. In Methods in Enzymology; Elsevier, 2003; Vol. 360, pp 416–446. https://doi.org/10.1016/S0076-6879(03)60122-9.

Judge, D. P.; Heitner, S. B.; Falk, R. H.; Maurer, M. S.; Shah, S. J.; Witteles, R. M.; Grogan, M.; Selby, V. N.; Jacoby, D.; Hanna, M.; Nativi-Nicolau, J.; Patel, J.; Rao, S.; Sinha, U.; Turtle, C. W.; Fox, J. C. Transthyretin Stabilization by AG10 in Symptomatic Transthyretin Amyloid Cardiomyopathy. J. Am. Coll. Cardiol. 2019, 74 (3), 285–295. https://doi.org/10.1016/j.jacc.2019.03.012.

Kabouridis, P. S.; Jury, E. C. Lipid Rafts and T-Lymphocyte Function: Implications for Autoimmunity. FEBS Lett. 2008, 582 (27), 3711–3718. https://doi.org/10.1016/j.febslet.2008.10.006.

Kakugawa, Y.; Wada, T.; Yamaguchi, K.; Yamanami, H.; Ouchi, K.; Sato, I.; Miyagi, T. Up-Regulation of Plasma Membrane-Associated Ganglioside Sialidase (Neu3) in Human Colon Cancer and Its Involvement in Apoptosis Suppression. Proc. Natl. Acad. Sci. 2002, 99 (16), 10718–10723. https://doi.org/10.1073/pnas.152597199.

Kaminuma, O.; Katoh, S.; Miyagi, T.; Watanabe, N.; Kitamura, N.; Nishimura, T.; Saeki, M.; Mori, A.; Hiroi, T. Contribution of Neuraminidase 3 to the Differentiation of Induced Regulatory T Cells. Genes Cells 2017. https://doi.org/10.1111/gtc.12553.

Karhadkar, T. R.; Chen, W.; Gomer, R. H. Attenuated Pulmonary Fibrosis in Sialidase-3 Knockout (Neu3 −/−) Mice. Am. J. Physiol.-Lung Cell. Mol. Physiol. 2020, 318 (1), L165–L179. https://doi.org/10.1152/ajplung.00275.2019.

Karlssonz, R.; Fält, A. Experimental Design for Kinetic Analysis of Protein-Protein Interactions with Surface Plasmon Resonance Biosensors. J. Immunol. Methods 1997, 200 (1–2), 121–133. https://doi.org/10.1016/S0022-1759(96)00195-0.

Karpova, M. B.; Schoumans, J.; Ernberg, J.; Henter, J. I.; Nordenskjöld, M.; Fadeel, B. Raji Revisited: Cytogenetics of the Original Burkitt's Lymphoma Cell Line [12]. Leukemia 2005, 19 (1), 159–161. https://doi.org/10.1038/sj.leu.2403534.

Kasumi, A.; Sako, Y. Cell Surface Organization by the Membrane Cytoskeleton. Curr. Opin. Cell Biol. 1996, 8, 566–574.

Kato, T.; Wang, Y.; Yamaguchi, K.; Milner, C. M.; Shineha, R.; Satomi, S.; Miyagi, T. Overexpression of Lysosomal-Type Sialidase Leads to Suppression of Metastasis Associated with Reversion of Malignant Phenotype in Murine B16 Melanoma Cells. Int. J. Cancer 2001, 92 (6), 797–804. https://doi.org/10.1002/ijc.1268.

Kelm, S.; Gerlach, J.; Brossmer, R.; Danzer, C. P.; Nitschke, L. The Ligand-Binding Domain of CD22 Is Needed for Inhibition of the B Cell Receptor Signal, as Demonstrated by a Novel Human CD22-Specific Inhibitor Compound. J. Exp. Med. 2002, 195 (9), 1207–1213. https://doi.org/10.1084/jem.20011783.

Kelm, S.; Gerlach, J.; Brossmer, R.; Danzer, C.-P.; Nitschke, L. The Ligand-Binding Domain of CD22 Is Needed for Inhibition of the B Cell Receptor Signal, as Demonstrated by a Novel Human CD22-Specific Inhibitor Compound. J. Exp. Med. 2002, 195 (9), 1207–1213. https://doi.org/10.1084/jem.20011783.

Khare, S. D.; Sarosi, I.; Xia, X.-Z.; McCabe, S.; Miner, K.; Solovyev, I.; Hawkins, N.; Kelley, M.; Chang, D.; Van, G.; Ross, L.; Delaney, J.; Wang, L.; Lacey, D.; Boyle, W. J.; Hsu, H. Severe B Cell Hyperplasia and Autoimmune Disease in TALL-1 Transgenic Mice. 2000, PNAS 97 (7), 3370–3375.

Khiabani, K. T.; Stephenson, L. L.; Gabriel, A.; Nataraj, C.; Wang, W. Z.; Zamboni, W. A. A Quantitative Method for Determining Polarization of Neutrophil Adhesion Molecules Associated with Ischemia Reperfusion: Plast. Reconstr. Surg. 2004, 114 (7), 1846–1850. https://doi.org/10.1097/01.PRS.0000143580.45631.DD.

Kiernan, J. A. Formaldehyde, Formalin, Paraformaldehyde And Glutaraldehyde: What They Are And What They Do. Microsc. Today 2000, 8 (1), 8–13. https://doi.org/10.1017/S1551929500057060.

Kimble, M.; Kuriyama, R. Functional Components Of Microtubule-Organizing Centers. In International Review of Cytology; Elsevier, 1992; Vol. 136, pp 1–50. https://doi.org/10.1016/S0074-7696(08)62049-5.

Kinnunen, T.; Chamberlain, N.; Morbach, H.; Cantaert, T.; Lynch, M.; Preston-Hurlburt, P.; Herold, K. C.; Hafler, D. A.; O'Connor, K. C.; Meffre, E. Specific Peripheral B Cell Tolerance Defects in Patients with Multiple Sclerosis. J. Clin. Invest. 2013, 123 (6), 2737–2741. https://doi.org/10.1172/JCI68775.

Klar, T. A.; Jakobs, S.; Dyba, M.; Egner, A.; Hell, S. W. Fluorescence Microscopy with Diffraction Resolution Barrier Broken by Stimulated Emission. Proc. Natl. Acad. Sci. 2000, 97 (15), 8206–8210. https://doi.org/10.1073/pnas.97.15.8206.

Kodadek, T. Protein Microarrays: Prospects and Problems. Chem. Biol. 2001, 8 (2), 105–115. https://doi.org/10.1016/S1074-5521(00)90067-X.

Koenig, S.; Hoffmann, M. K. Bacterial Lipopolysaccharide Activates Suppressor B Lymphocytes. Proc. Natl. Acad. Sci. 1979, 76 (9), 4608–4612. https://doi.org/10.1073/pnas.76.9.4608.
Koldsø, H.; Sansom, M. S. P. Organization and Dynamics of Receptor Proteins in a Plasma Membrane. J. Am. Chem. Soc. 2015, 137 (46), 14694–14704. https://doi.org/10.1021/jacs.5b08048.

Koppel, D. E.; Sheetz, M. P.; Schindler, M. Matrix Control of Protein Diffusion in Biological Membranes. Proc. Natl. Acad. Sci. 1981, 78 (6), 3576–3580. https://doi.org/10.1073/pnas.78.6.3576.

Korlach, J.; Schwille, P.; Webb, W. W.; Feigenson, G. W. Characterization of Lipid Bilayer Phases by Confocal Microscopy and Fluorescence Correlation Spectroscopy. Proc. Natl. Acad. Sci. 1999, 96 (15), 8461–8466. https://doi.org/10.1073/pnas.96.15.8461.

Koseki, K.; Wada, T.; Hosono, M.; Hata, K.; Yamaguchi, K.; Nitta, K.; Miyagi, T. Human Cytosolic Sialidase NEU2-Low General Tissue Expression but Involvement in PC-3 Prostate Cancer Cell Survival. Biochem. Biophys. Res. Commun. 2012, 428 (1), 142–149. https://doi.org/10.1016/j.bbrc.2012.10.028.

Kozyrev, S. V.; Abelson, A.-K.; Wojcik, J.; Zaghlool, A.; Linga Reddy, M. V. P.; Sanchez, E.; Gunnarsson, I.; Svenungsson, E.; Sturfelt, G.; Jönsen, A.; Truedsson, L.; Pons-Estel, B. A.; Witte, T.; D'Alfonso, S.; Barizzone, N.; Danieli, M. G.; Gutierrez, C.; Suarez, A.; Junker, P.; Laustrup, H.; González-Escribano, M. F.; Martin, J.; Abderrahim, H.; Alarcón-Riquelme, M. E. Functional Variants in the B-Cell Gene BANK1 Are Associated with Systemic Lupus Erythematosus. Nat. Genet. 2008, 40 (2), 211–216. https://doi.org/10.1038/ng.79.

Kusumi, A.; Fujiwara, T. K.; Chadda, R.; Xie, M.; Tsunoyama, T. A.; Kalay, Z.; Kasai, R. S.; Suzuki, K. G. N. Dynamic Organizing Principles of the Plasma Membrane That Regulate Signal Transduction: Commemorating the Fortieth Anniversary of Singer and Nicolson's Fluid-Mosaic Model. 2012, 39.

Kusumi, A.; Nakada, C.; Ritchie, K.; Murase, K.; Suzuki, K.; Murakoshi, H.; Kasai, R. S.; Kondo, J.; Fujiwara, T. Paradigm Shift of the Plasma Membrane Concept from the Two-Dimensional Continuum Fluid to the Partitioned Fluid: High-Speed Single-Molecule Tracking of Membrane Molecules. Annu. Rev. Biophys. Biomol. Struct. 2005, 34 (1), 351–378. https://doi.org/10.1146/annurev.biophys.34.040204.144637.

Kusumi, A.; Sako, Y.; Yamamoto, M. Confined Lateral Diffusion of Membrane Receptors as Studied by Single Particle Tracking (Nanovid Microscopy). Effects of Calcium-Induced Differentiation in Cultured Epithelial Cells. Biophys. J. 1993, 65 (5), 2021–2040. https://doi.org/10.1016/S0006-3495(93)81253-0.

Kusumi, A.; Suzuki, K. G. N.; Kasai, R. S.; Ritchie, K.; Fujiwara, T. K. Hierarchical Mesoscale Domain Organization of the Plasma Membrane. Trends Biochem. Sci. 2011, 36 (11), 604–615. https://doi.org/10.1016/j.tibs.2011.08.001.

Lajaunias, F.; Nitschke, L.; Moll, T.; Martinez-Soria, E.; Semac, I.; Chicheportiche, Y.; Parkhouse, R. M. E.; Izui, S. Differentially Regulated Expression and Function of CD22 in Activated B-1 and B-2 Lymphocytes. J. Immunol. 2002, 168 (12), 6078. https://doi.org/10.4049/jimmunol.168.12.6078.

Lambert, T. J.; Waters, J. C. Navigating Challenges in the Application of Superresolution Microscopy. J. Cell Biol. 2017, 216(1), 53-63.

Lang, T.; Rizzoli, S. O. Membrane Protein Clusters at Nanoscale Resolution: More Than Pretty Pictures. Physiology 2010, 25 (2), 116–124. https://doi.org/10.1152/physiol.00044.2009.

Law, C. L.; Aruffo, A.; Chandran, K. A.; Doty, R. T.; Clark, E. A. Ig Domains 1 and 2 of Murine CD22 Constitute the Ligand-Binding Domain and Bind Multiple Sialylated Ligands Expressed on B and T Cells. 1995 155 (7), 3368–3376.

Lenaz, G. Lipid Fluidity and Membrane Protein Dynamics. Biosci. Rep. 1987, 7 (11), 823–837. https://doi.org/10.1007/BF01119473.

Lenne, P.-F.; Wawrezinieck, L.; Conchonaud, F.; Wurtz, O.; Boned, A.; Guo, X.-J.; Rigneault, H.; He, H.-T.; Marguet, D. Dynamic Molecular Confinement in the Plasma Membrane by Microdomains and the Cytoskeleton Meshwork. EMBO J. 2006, 25 (14), 3245–3256. https://doi.org/10.1038/sj.emboj.7601214.

Li, R.; Rezk, A.; Miyazaki, Y.; Hilgenberg, E.; Touil, H.; Shen, P.; Moore, C. S.; Michel, L.; Althekair, F.; Rajasekharan, S.; Gommerman, J. L.; Prat, A.; Fillatreau, S.; Bar-Or, A.; on behalf of the Canadian B cells in MS Team. Proinflammatory GM-CSF–Producing B Cells in Multiple Sclerosis and B Cell Depletion Therapy. Sci. Transl. Med. 2015, 7 (310), 310ra166-310ra166. https://doi.org/10.1126/scitranslmed.aab4176.

Li, X.-M.; Serebrisky, D.; Lee, S.-Y.; Huang, C.-K.; Bardina, L.; Schofield, B. H.; Stanley, J. S.; Burks, A. W.; Bannon, G. A.; Sampson, H. A. A Murine Model of Peanut Anaphylaxis: T- and B-Cell Responses to a Major Peanut Allergen Mimic Human Responses. J. Allergy Clin. Immunol. 2000, 106 (1), 150–158. https://doi.org/10.1067/mai.2000.107395.

Liang, F.; Seyrantepe, V.; Landry, K.; Ahmad, R.; Ahmad, A.; Stamatos, N. M.; Pshezhetsky, A. V. Monocyte Differentiation Up-Regulates the Expression of the Lysosomal Sialidase, Neu1, and Triggers Its Targeting to the Plasma Membrane via Major Histocompatibility Complex Class II-Positive Compartments. J. Biol. Chem. 2006, 281 (37), 27526–27538. https://doi.org/10.1074/jbc.M605633200.

Lillemeier, B. F.; Pfeiffer, J. R.; Surviladze, Z.; Wilson, B. S.; Davis, M. M. Plasma Membrane-Associated Proteins Are Clustered into Islands Attached to the Cytoskeleton. Proc. Natl. Acad. Sci. 2006, 103 (50), 18992–18997. https://doi.org/10.1073/pnas.0609009103.

Lin, J.-S.; Lai, E.-M. Protein–Protein Interactions: Co-Immunoprecipitation BT - Bacterial Protein Secretion Systems: Methods and Protocols; Journet, L., Cascales, E., Eds.; Springer New York: New York, NY, 2017; pp 211–219. https://doi.org/10.1007/978-1-4939-7033-9_17.

Lindner, R.; Naim, H. Y. Domains in Biological Membranes. Exp. Cell Res. 2009, 315 (17), 2871–2878. https://doi.org/10.1016/j.yexcr.2009.07.020.

Lingwood, D.; Simons, K. Lipid Rafts as a Membrane-Organizing Principle. Science (80-.). 2010, 327 (5961), 46–50. https://doi.org/10.1126/science.1174621.

Lingwood, D.; Simons, K. Lipid Rafts As a Membrane-Organizing Principle. Science 2010, 327 (5961), 46–50. https://doi.org/10.1126/science.1174621.

Lipsky, P. E. Systemic Lupus Erythematosus: An Autoimmune Disease of B Cell Hyperactivity. Nat. Immunol. 2001, 2 (9), 764–766. https://doi.org/10.1038/ni0901-764.

Lleo, A.; Invernizzi, P.; Gao, B.; Podda, M.; Gershwin, M. E. Definition of Human Autoimmunity — Autoantibodies versus Autoimmune Disease. Autoimmun. Rev. 2010, 9 (5), A259–A266. https://doi.org/10.1016/j.autrev.2009.12.002.

Lokeshwar, V. B.; Bourguignon, L. Y. Tyrosine Phosphatase Activity of Lymphoma CD45 (GP180) Is Regulated by a Direct Interaction with the Cytoskeleton. J. Biol. Chem. 1992, 267 (30), 21551–21557. https://doi.org/10.1016/S0021-9258(19)36645-1.

Lokeshwar, V. B.; Bourguignon, L. Y. W. Tyrosine Phosphatase Activity of Lymphoma CD45 (GP180) Is Regulated by a Direct Interaction with the Cytoskeleton. J. Biol. Chem. 1992, 267 (30), 21551–21557. https://doi.org/10.1016/s0021-9258(19)36645-1.

Lommerse, P. H. M.; Spaink, H. P.; Schmidt, T. In Vivo Plasma Membrane Organization: Results of Biophysical Approaches. Biochim. Biophys. Acta BBA - Biomembr. 2004, 1664 (2), 119–131. https://doi.org/10.1016/j.bbamem.2004.05.005.

Louche, A.; Salcedo, S. P.; Bigot, S. Protein–Protein Interactions: Pull-down Assays. Methods Mol. Biol. 2017, 1615, 247–255. https://doi.org/10.1007/978-1-4939-7033-9_20.

Luu, A. R.; Wong, C.; Agrawal, V.; Wise, N.; Handyside, B.; Lo, M. J.; Pacheco, G.; Felix, J. B.; Giaramita, A.; d'Azzo, A.; Vincelette, J.; Bullens, S.; Bunting, S.; Christianson, T. M.; Hague, C. M.; LeBowitz, J. H.; Yogalingam, G. Intermittent Enzyme Replacement Therapy with Recombinant Human β-Galactosidase Prevents Neuraminidase 1 Deficiency. J. Biol. Chem. 2020, 295 (39), 13556–13569. https://doi.org/10.1074/jbc.RA119.010794.

Luzina, I. G.; Lillehoj, E. P.; Lockatell, V. K.; Hyun, S. W.; Lugkey, K. N.; Imamura, A.; Ishida, H.; Cairo, C. W.; Atamas, S. P.; Goldblum, S. E. Therapeutic Effect of Neuraminidase-1-Selective Inhibition in Mouse Models of Bleomycin-Induced Pulmonary Inflammation and Fibrosis. J. Pharmacol. Exp. Ther. 2020. https://doi.org/10.1124/jpet.120.000223.

Ma, H.; Yankee, T. M.; Hu, J.; Asai, D. J.; Harrison, M. L.; Geahlen, R. L. Visualization of Syk-Antigen Receptor Interactions Using Green Fluorescent Protein: Differential Roles for Syk and Lyn in the Regulation of Receptor Capping and Internalization. J. Immunol. 2001, 166 (3), 1507–1516. https://doi.org/10.4049/jimmunol.166.3.1507.

Macauley, M. S.; Pfrengle, F.; Rademacher, C.; Nycholat, C. M.; Gale, A. J. Antigenic Liposomes Displaying CD22 Ligands Induce Antigen-Specific B Cell Apoptosis. J. Clin. Invest. 2013, 123 (7), 3074–3083. https://doi.org/10.1172/JCI69187.

Macauley, M.; Paulson, J. Siglecs induce tolerance to cell surface antigens by BIM-dependent deletion of the antigen-reactive B cells. J. Immunol. 2014, 193(9), 4312-4321.

Maity, P.C .; Yang, J.; Klaesener, K.; Reth, M. The nanoscale organization of the B lymphocyte membrane. Biochimica et Biophys. Acta. 2015, 1853, 830-840.

Manders, E. M. M.; Verbeek, F. J.; Aten, J. A. Measurement of Co-Localization of Objects in Dual-Colour Confocal Images. J. Microsc. 1993, 169 (3), 375–382. https://doi.org/10.1111/j.1365-2818.1993.tb03313.x.

Mattila, P. K.; Batista, F. D.; Treanor, B. Dynamics of the actin cytosketon mediates receptor cross talk: An emerging concept in tuning receptor signaling. J. Cell Biol. 2016, 212 (3), 267-180.
McInnes, I. B. The Pathogenesis of Rheumatoid Arthritis. N. Engl. J. Med. 2011, 15.
Meilhac, N.; Le Guyader, L.; Salomé, L.; Destainville, N. Detection of Confinement and Jumps in Single-Molecule Membrane Trajectories. Phys. Rev. E 2006, 73 (1), 011915. https://doi.org/10.1103/PhysRevE.73.011915.

Meyer, S. J.; Boser, A.; Korn, M. A.; Koller, C.; Bertocci, B.; Reimann, L.; Warscheid, B.; Nitschke, L. Cullin 3 Is Crucial for Pro-B Cell Proliferation, Interacts with CD22, and Controls CD22 Internalization on B cells. J. Immunol. 2020, 204, 3360-3374.

Meyer, S. J.; Linder, A. T.; Brandl, C.; Nitschke, L. B Cell Siglecs–News on Signaling and Its Interplay With Ligand Binding. Front. Immunol. 2018, 9, 2820. https://doi.org/10.3389/fimmu.2018.02820.

Meyer, S. J.; Steffensen, M.; Acs, A.; Wesenburger, T.; Wadewitz, C.; Winkler, T. H.; Nitschke, L. J. Immunol. 2021, 207(4), 1018-1032.

Mielenz, D.; Vettermann, C.; Hampel, M.; Lang, C.; Avramidou, A.; Karas, M.; Jäck, H.-M. Lipid Rafts Associate with Intracellular B Cell Receptors and Exhibit a B Cell Stage-Specific Protein Composition. J. Immunol. 2005, 174 (6), 3508–3517. https://doi.org/10.4049/jimmunol.174.6.3508.

Miyagi, T.; Wada, T.; Yamaguchi, K. Roles of Plasma Membrane-Associated Sialidase NEU3 in Human Cancers. Biochim. Biophys. Acta BBA - Gen. Subj. 2008, 1780 (3), 532–537. https://doi.org/10.1016/j.bbagen.2007.09.016.

Miyagi, T.; Yamaguchi, K. Mammalian Sialidases: Physiological and Pathological Roles in Cellular Functions. Glycobiology 2012, 22 (7), 880–896.

Miyagi, T.; Yamaguchi, K. Mammalian Sialidases: Physiological and Pathological Roles in Cellular Functions. Glycobiology 2012, 22 (7), 880–896. https://doi.org/10.1093/glycob/cws057.
Miyagi, T.; Yamaguchi, K. Mammlian Sialidases: Physiological and Pathological Roles in Cellular Functions. Glycobiology 2012, 22 (7), 880–896. https://doi.org/10.1093/glycob/cws057.
Moerner, W. E.; Fromm, D. P. Methods of Single-Molecule Fluorescence Spectroscopy and Microscopy. Rev. Sci. Instrum. 2003, 74 (8), 3597–3619. https://doi.org/10.1063/1.1589587.

Monti, E.; Bassi, M. T.; Bresciani, R.; Civini, S.; Croci, G. L.; Papini, N.; Riboni, M.; Zanchetti, G.; Ballabio, A.; Preti, A.; Tettamanti, G.; Venerando, B.; Borsani, G. Molecular Cloning and Characterization of NEU4, the Fourth Member of the Human Sialidase Gene Family. Genomics 2004, 83 (3), 445–453. https://doi.org/10.1016/j.ygeno.2003.08.019.

Monti, E.; Bassi, M. T.; Papini, N.; Riboni, M.; Manzoni, M.; Venerando, B.; Croci, G.; Preti, A.; Ballabio, A.; Tettamanti, G.; Borsani, G. Identification and Expression of NEU3, a Novel Human Sialidase Associated to the Plasma Membrane. Biochem. J. 2000, 349(1), 343-351.

Morton, W. M.; Ayscough, K. R.; McLaughlin, P. J. Latrunculin Alters the Actin-Monomer Subunit Interface to Prevent Polymerization. Nat. Cell Biol. 2000, 2 (6), 376–378. https://doi.org/10.1038/35014075.

Mukherjee, S.; Maxfield, F. R. MEMBRANE DOMAINS. Annu. Rev. Cell Dev. Biol. 2004, 20 (1), 839–866. https://doi.org/10.1146/annurev.cellbio.20.010403.095451.

Muller, J.; Obermeier, I.; Wohner, M.; Brandl, C.; Mrotzek, S.; Angermuller, S.; Maity, P. C.; Reth, M.; Nitschke, L. CD22 Ligand-Binding and Signaling Domains Reciprocally Regulate B-Cell Ca2+ Signaling. Proc. Natl. Acad. Sci. 2013, 110 (30), 12402–12407. https://doi.org/10.1073/pnas.1304888110.

Murase, K.; Fujiwara, T.; Umemura, Y.; Suzuki, K.; Iino, R.; Yamashita, H.; Saito, M.; Murakoshi, H.; Ritchie, K.; Kusumi, A. Ultrafine Membrane Compartments for Molecular Diffusion as Revealed by Single Molecule Techniques. Biophys. J. 2004, 86 (6), 4075–4093. https://doi.org/10.1529/biophysj.103.035717.

Nan, X.; Carubelli, I.; Stamatos, N. M. Sialidase Expression in Activated Human T Lymphocytes Influences Production of IFN-γ. J. Leukoc. Biol. 2007, 81 (1), 284–296. https://doi.org/10.1189/jlb.1105692.

Naparstekt, Y. The Role of Autoantibodies in Autoimmune Disease. Ann. Rev. Immunol. 1993, 11(1), 79-104.

Nicolau, D. V.; Burrage, K.; Parton, R. G.; Hancock, J. F. Identifying Optimal Lipid Raft Characteristics Required To Promote Nanoscale Protein-Protein Interactions on the Plasma Membrane. Mol. Cell. Biol. 2006, 26 (1), 313–323. https://doi.org/10.1128/MCB.26.1.313-323.2006.

Nicolson, G. L. The Fluid—Mosaic Model of Membrane Structure: Still Relevant to Understanding the Structure, Function and Dynamics of Biological Membranes after More than 40years. Biochim. Biophys. Acta 1838, 16.

Nicolson, G. L. Update of the 1972 Singer-Nicolson Fluid-Mosaic Model of Membrane Structure. 14.

Niemela, P. S.; Ollila, S.; Hyvonen, M. T.; Kattunen, M.; Vattulainen, I. Assessing the Nature of Lipid Raft Membranes. PLOS Comp. Biol. 2007, 3(2), 34.

Nitschke, L. CD22 and Siglec-G: B-Cell Inhibitory Receptors with Distinct Functions. Immunol. Rev. 2009, 230 (1), 128–143. https://doi.org/10.1111/j.1600-065X.2009.00801.x.

Nitschke, L. The Role of CD22 and Other Inhibitory Co-Receptors in B-Cell Activation. Curr. Opin. Immunol. 2005, 17 (3), 290–297. https://doi.org/10.1016/j.coi.2005.03.005.

Nitschke, L.; Carsetti, R.; Ocker, B.; Köhler, G.; Lamers, M. C. CD22 Is a Negative Regulator of B-Cell Receptor Signalling. Curr. Biol. 1997, 7 (2), 133–143. https://doi.org/10.1016/S0960-9822(06)00057-1.

Noble, M. E. M. Protein Kinase Inhibitors: Insights into Drug Design from Structure. Science 2004, 303 (5665), 1800–1805. https://doi.org/10.1126/science.1095920.

O'Keefe, T. L.; Williams, G. T.; Davies, S. L.; Neuberger, M. S. Hyperresponsive B Cells in CD22-Deficient Mice. Science 1996, 274 (5288), 798–801. https://doi.org/10.1126/science.274.5288.798.

O'Reilly, M. K.; Collins, B. E.; Han, S.; Liao, L.; Rillahan, C.; Kitov, P. I.; Bundle, D. R.; Paulson, J. C. Bifunctional CD22 Ligands Use Multimeric Immunoglobulins as Protein Scaffolds in Assembly of Immune Complexes on B Cells. J. Am. Chem. Soc. 2008, 130 (24), 7736–7745. https://doi.org/10.1021/ja802008q.

Ohta, Y.; Tsukada, Y.; Sugimori, T. Purification and Properties of Neuraminidase Isozymes in Arthrobacter Ureafaciens Mutant. J. Biochem. (Tokyo) 1989, 106 (6), 1086–1089. https://doi.org/10.1093/oxfordjournals.jbchem.a122969.

Ondee, T.; Surawut, S.; Taratummarat, S.; Hirankarn, N.; Palaga, T.; Pisitkun, P.; Pisitkun, T.; Leelahavanichkul, A. Fc Gamma Receptor IIB Deficient Mice: A Lupus Model with Increased Endotoxin Tolerance-Related Sepsis Susceptibility. Shock 2017, 47 (6), 743–752. https://doi.org/10.1097/SHK.0000000000000796.

Ono, S. Mechanism of Depolymerization and Severing of Actin Filaments and Its Significance in Cytoskeletal Dynamics. In International Review of Cytology; Elsevier, 2007; Vol. 258, pp 1–82. https://doi.org/10.1016/S0074-7696(07)58001-0.

Otipoby, K. L.; Draves, K. E.; Clark, E. A. CD22 Regulates B Cell Receptor-Mediated Signals via Two Domains That Independently Recruit Grb2 and SHP-1. J. Biol. Chem. 2001, 276 (47), 44315–44322. https://doi.org/10.1074/jbc.M105446200.

Owen, D. M.; Magenau, A.; Williamson, D.; Gaus, K. The Lipid Raft Hypothesis Revisited - New Insights on Raft Composition and Function from Super-Resolution Fluorescence Microscopy. BioEssays 2012, 34 (9), 739–747. https://doi.org/10.1002/bies.201200044.

Owen, D. M.; Williamson, D. J.; Magenau, A.; Gaus, K. Sub-Resolution Lipid Domains Exist in the Plasma Membrane and Regulate Protein Diffusion and Distribution. Nat. Commun. 2012, 3 (1), 1256. https://doi.org/10.1038/ncomms2273.

Paddock, S. W. Principles and Practices of Laser Scanning Confocal Microscopy. Mol. Biotechnol. 2000, 16 (2), 127–150. https://doi.org/10.1385/MB:16:2:127.

Paladino, S.; Sarnataro, D.; Pillich, R.; Tivodar, S.; Nitsch, L.; Zurzolo, C. Protein Oligomerization Modulates Raft Partitioning and Apical Sorting of GPI-Anchored Proteins. J. Cell Biol. 2004, 167 (4), 699–709. https://doi.org/10.1083/jcb.200407094.

Papini, N.; Anastasia, L.; Tringali, C.; Croci, G.; Bresciani, R.; Yamaguchi, K.; Miyagi, T.; Preti, A.; Prinetti, A.; Prioni, S.; Sonnino, S.; Tettamanti, G.; Venerando, B.; Monti, E. The Plasma Membrane-Associated Sialidase MmNEU3 Modifies the Ganglioside Pattern of Adjacent Cells Supporting Its Involvement in Cell-to-Cell Interactions. J. Biol. Chem. 2004, 279 (17), 16989–16995. https://doi.org/10.1074/jbc.M400881200.

Parton, D. L.; Klingelhoefer, J. W.; Sansom, M. S. P. Aggregation of Model Membrane Proteins, Modulated by Hydrophobic Mismatch, Membrane Curvature, and Protein Class. Biophys. J. 2011, 101 (3), 691–699. https://doi.org/10.1016/j.bpj.2011.06.048.

Patterson, H. C. K.; Kraus, M.; Kim, Y.-M.; Ploegh, H.; Rajewsky, K. The B Cell Receptor Promotes B Cell Activation and Proliferation through a Non-ITAM Tyrosine in the Igα Cytoplasmic Domain. Immunity 2006, 25 (1), 55–65. https://doi.org/10.1016/j.immuni.2006.04.014.

Pattison, S.; Pankarican, M.; Rupar, C. A.; Graham, F. L.; Igdoura, S. A. Five Novel Mutations in the Lysosomal Sialidase Gene (NEU1) in Type II Sialidosis Patients and Assessment of Their Impact on Enzyme Activity and Intracellular Targeting Using Adenovirus-Mediated Expression. Hum. Mutat. 2004, 23 (1), 32–39. https://doi.org/10.1002/humu.10278.

Penchala, S. C.; Connelly, S.; Wang, Y.; Park, M. S.; Zhao, L.; Baranczak, A.; Rappley, I.; Vogel, H.; Liedtke, M.; Witteles, R. M.; Powers, E. T.; Reixach, N.; Chan, W. K.; Wilson, I. A.; Kelly, J. W.; Graef, I. A.; Alhamadsheh, M. M. AG10 Inhibits Amyloidogenesis and Cellular Toxicity of the Familial Amyloid Cardiomyopathy-Associated V122I Transthyretin. Proc. Natl. Acad. Sci. 2013, 110 (24), 9992–9997. https://doi.org/10.1073/pnas.1300761110.

Peng, W.; Paulson, J. C. CD22 Ligands on a Natural N -Glycan Scaffold Efficiently Deliver Toxins to B-Lymphoma Cells. J. Am. Chem. Soc. 2017, 139 (36), 12450–12458. https://doi.org/10.1021/jacs.7b03208.

Petro, J. B.; Rahman, S. M. J.; Ballard, D. W.; Khan, W. N. Bruton's Tyrosine Kinase Is Required for Activation of I□B Kinase and Nuclear Factor □B in Response to B Cell Receptor Engagement. J. Exp. Med. 2000, 191 (10), 1745–1753.

Piqueras, B.; Lavenu-Bombled, C.; Galicier, L.; Cruyssen, F. B.-V. D.; Mouthon, L.; Chevret, S.; Debre, P.; Schmitt, C.; Oksenhendler, E. Common Variable Immunodeficiency Patient Classification Based on Impaired B Cell Memory Differentiation Correlates with Clinical Aspects. J. Clin. Immunol. 2003, 23 (5), 385–400.

Pradhan, D.; Morrow, J. S. The Spectrin-Ankyrin Skeleton Controls CD45 Surface Display and Interleukin-2 Production. Immunity 2002, 17 (3), 303–315. https://doi.org/10.1016/S1074-7613(02)00396-5.

Pritchard, N. R.; Smith, K. G. C. B Cell Inhibitory Receptors and Autoimmunity. Immunology 2003, 108 (3), 263–273. https://doi.org/10.1046/j.1365-2567.2003.01592.x.

Pshezhetsky, A. V.; Richard, C.; Michaud, L.; Igdoura, S.; Wang, S.; Elsliger, M.-A.; Qu, J.; Leclerc, D.; Gravel, R.; Dallaire, L.; Potier, M. Cloning, Expression and Chromosomal Mapping of Human Lysosomal Sialidase and Characterization of Mutations in Sialidosis. Nat. Genet. 1997, 15 (3), 316–320. https://doi.org/10.1038/ng0397-316.

Qian, H.; Sheetz, M. P.; Elson, E. L. Single Particle Tracking. Analysis of Diffusion and Flow in Two-Dimensional Systems. Biophys. J. 1991, 60 (4), 910–921. https://doi.org/10.1016/S0006-3495(91)82125-7.

Rahman, H.; Qasim, M.; Schultze, F. C.; Oellerich, M.; R Asif, A. Fetal Calf Serum Heat Inactivation and Lipopolysaccharide Contamination Influence the Human T Lymphoblast Proteome and Phosphoproteome. Proteome Sci. 2011, 9 (1), 71. https://doi.org/10.1186/1477-5956-9-71.

Ramadurai, S.; Holt, A.; Krasnikov, V.; van den Bogaart, G.; Killian, J. A.; Poolman, B. Lateral Diffusion of Membrane Proteins. J. Am. Chem. Soc. 2009, 131 (35), 12650–12656. https://doi.org/10.1021/ja902853g.

Ramya, T. N. C.; Weerapana, E.; Liao, L.; Zeng, Y.; Tateno, H.; Liao, L.; Yates, J. R.; Cravatt, B. F.; Paulson, J. C. In Situ Trans Ligands of CD22 Identified by Glycan-Protein Photocross-Linking-Enabled Proteomics. Mol. Cell. Proteomics 2010, 9 (6), 1339–1351. https://doi.org/10.1074/mcp.M900461-MCP200.

Ramya, T. N. C.; Weerapana, E.; Liao, L.; Zeng, Y.; Tateno, H.; Liao, L.; Yates, J. R.; Cravatt, B. F.; Paulson, J. C. In Situ Trans Ligands of CD22 Identified by Glycan-Protein Photocross-Linking-Enabled Proteomics. Mol. Cell. Proteomics MCP 2010, 9 (6), 1339–1351. https://doi.org/10.1074/mcp.m900461-mcp200.

Rassam, P.; Copeland, N. A.; Birkholz, O.; Tóth, C.; Chavent, M.; Duncan, A. L.; Cross, S. J.; Housden, N. G.; Kaminska, R.; Seger, U.; Quinn, D. M.; Garrod, T. J.; Sansom, M. S. P.; Piehler, J.; Baumann, C. G.; Kleanthous, C. Supramolecular Assemblies Underpin Turnover of Outer Membrane Proteins in Bacteria. Nature 2015, 523 (7560), 333–336. https://doi.org/10.1038/nature14461.

Rauch, S.; Fackler, O. T. Viruses, Lipid Rafts and Signal Transduction. Signal Transduct. 2007, 7 (1), 53–63. https://doi.org/10.1002/sita.200600113.

Rawlings, D. J.; Metzler, G.; Wray-Dutra, M.; Jackson, S. W. Altered B cells signaling and autoimmunity. Immunol. 2017, 17, 421-436.

Razi, N.; Varki, A. Masking and Unmasking of the Sialic Acid-Binding Lectin Activity of CD22 (Siglec-2) on B Lymphocytes. Proc. Natl. Acad. Sci. 1998, 95 (13), 7469–7474. https://doi.org/10.1073/pnas.95.13.7469.

Reff, M.; Carner, K.; Chambers, K.; Chinn, P.; Leonard, J.; Raab, R.; Newman, R.; Hanna, N.; Anderson, D. Depletion of B Cells in Vivo by a Chimeric Mouse Human Monoclonal Antibody to CD20. Blood 1994, 83 (2), 435–445. https://doi.org/10.1182/blood.V83.2.435.435.

Reth, M.; Hombach, J.; Wienands, J.; Campbell, K. S.; Chien, N.; Justement, L. B.; Cambier, J. C. The B-Cell Antigen Receptor Complex. Immunol. Today 1991, 12 (6), 196–201. https://doi.org/10.1016/0167-5699(91)90053-V.

Richards, M. R.; Guo, T.; Hunter, C. D.; Cairo, C. W. Molecular Dynamics Simulations of Viral Neuraminidase Inhibitors with the Human Neuraminidase Enzymes: Insights into Isoenzyme Selectivity. Bioorg. Med. Chem. 2018, 26 (19), 5349–5358. https://doi.org/10.1016/j.bmc.2018.05.035.

Rillahan, C. D.; Macauley, M. S.; Schwartz, E.; He, Y.; McBride, R.; Arlian, B. M.; Rangarajan, J.; Fokin, V. V.; Paulson, J. C. Disubstituted Sialic Acid Ligands Targeting Siglecs CD33 and CD22 Associated with Myeloid Leukaemias and B Cell Lymphomas. Chem. Sci. 2014, 5 (6), 2398. https://doi.org/10.1039/c4sc00451e.

Ritchie, K.; Iino, R.; Fujiwara, T.; Murase, K.; Kusumi, A. The Fence and Picket Structure of the Plasma Membrane of Live Cells as Revealed by Single Molecule Techniques (Review). Mol. Membr. Biol. 2003, 20 (1), 13–18. https://doi.org/10.1080/0968768021000055698.

Rodriguez, O. C.; Schaefer, A. W.; Mandato, C. A.; Forscher, P.; Bement, W. M.; Waterman-Storer, C. M. Conserved Microtubule–Actin Interactions in Cell Movement and Morphogenesis. Nat. Cell Biol. 2003, 5 (7), 599–609. https://doi.org/10.1038/ncb0703-599.

Rodriguez-Walker, M.; Daniotti, J. L. Human Sialidase Neu3 Is S-Acylated and Behaves Like an Integral Membrane Protein. Sci. Rep. 2017, 7 (1), 4167. https://doi.org/10.1038/s41598-017-04488-w.

Roggentin, P.; Kleineidam, R. G.; Schauer, R. Diversity in the Properties of Two Sialidase Isoenzymes Produced by Clostridium Perfringens Spp. Biol. Chem. HOPPE SEYLER 1995, 376, 569–569.

Roggentin, P.; Schauer, R.; Hoyer, L. L.; Vimr, E. R. The Sialidase Superfamily and Its Spread by Horizontal Gene Transfer. Mol. Microbiol. 1993, 9 (5), 915–921. https://doi.org/10.1111/j.1365-2958.1993.tb01221.x.

Royer, B.; Cazals-Hatem, D.; Sibilia, J.; Agbalika, F.; Cayuela, J.-M.; Soussi, T.; Maloisel, F.; Clauvel, J.-P.; Brouet, J.-C.; Mariette, X. Lymphomas in Patients With Sjögren's Syndrome Are Marginal Zone B-Cell Neoplasms, Arise in Diverse Extranodal and Nodal Sites, and Are Not Associated With Viruses. Blood 1997, 90 (2), 766–775. https://doi.org/10.1182/blood.V90.2.766.

Rust, M. J.; Bates, M.; Zhuang, X. Sub-Diffraction-Limit Imaging by Stochastic Optical Reconstruction Microscopy (STORM). Nat. Methods 2006, 3 (10), 793–796. https://doi.org/10.1038/nmeth929.

Rydberg, L. ABO-Incompatibility in Solid Organ Transplantation. Transfus. Med. 2001, 11 (4), 325–342. https://doi.org/10.1046/j.1365-3148.2001.00313.x.

Saeki, K. The B Cell-Specific Major Raft Protein, Raftlin, Is Necessary for the Integrity of Lipid Raft and BCR Signal Transduction. EMBO J. 2003, 22 (12), 3015–3026. https://doi.org/10.1093/emboj/cdg293.

Saffman, P. G.; Delbruck, M. Brownian Motion in Biological Membranes. Proc. Natl. Acad. Sci. 1975, 72 (8), 3111–3113. https://doi.org/10.1073/pnas.72.8.3111.

Saha, S.; Lee, I.-H.; Polley, A.; Groves, J. T.; Rao, M.; Mayor, S. Diffusion of GPI-Anchored Proteins Is Influenced by the Activity of Dynamic Cortical Actin. Mol. Biol. Cell 2015, 26 (22), 4033–4045. https://doi.org/10.1091/mbc.E15-06-0397.

Sánchez-Ruano, L.; de la Hoz, B.; Martínez-Botas, J. Clinical Utility of Microarray B-cell Epitope Mapping in Food Allergies: A Systematic Review. Pediatr. Allergy Immunol. 2020, 31 (2), 175–185. https://doi.org/10.1111/pai.13141.

Sato, S.; Miller, A. S.; Inaoki, M.; Bock, C. B.; Jansen, P. J.; Tang, M. L. K.; Tedder, T. F. CD22 Is Both a Positive and Negative Regulator of B Lymphocyte Antigen Receptor Signal Transduction: Altered Signaling in CD22-Deficient Mice. Immunity 1996, 5 (6), 551–562. https://doi.org/10.1016/S1074-7613(00)80270-8.

Sawada, M.; Moriya, S.; Saito, S.; Shineha, R.; Satomi, S.; Yamori, T.; Tsuruo, T.; Kannagi, R.; Miyagi, T. Reduced Sialidase Expression in Highly Metastatic Variants of Mouse Colon Adenocarcinoma 26 and Retardation of Their Metastatic Ability by Sialidase Overexpression. Int. J. Cancer 2002, 97 (2), 180–185. https://doi.org/10.1002/ijc.1598.

Saxton, M. J. Single-Particle Tracking: The Distribution of Diffusion Coefficients. Biophys. J. 1997, 72 (4), 1744–1753. https://doi.org/10.1016/S0006-3495(97)78820-9.

Saxton, M. J.; Jacobson, K. SINGLE-PARTICLE TRACKING:Applications to Membrane Dynamics. Annu. Rev. Biophys. Biomol. Struct. 1997, 26 (1), 373–399. https://doi.org/10.1146/annurev.biophys.26.1.373.

Scaringi, R.; Piccoli, M.; Papini, N.; Cirillo, F.; Conforti, E.; Bergante, S.; Tringali, C.; Garatti, A.; Gelfi, C.; Venerando, B.; Menicanti, L.; Tettamanti, G.; Anastasia, L. NEU3 Sialidase Is Activated under Hypoxia and Protects Skeletal Muscle Cells from Apoptosis through the Activation of the Epidermal Growth Factor Receptor Signaling Pathway and the Hypoxia-Inducible Factor (HIF)-1α. J. Biol. Chem. 2013, 288 (5), 3153–3162. https://doi.org/10.1074/jbc.M112.404327.

Schermelleh, L.; Ferrand, A.; Huser, T.; Eggeling, C.; Sauer, M.; Biehlmaier, O.; Drummen, G. P. C. Super-Resolution Microscopy Demystified. Nat. Cell Biol. 2019, 21 (1), 72–84. https://doi.org/10.1038/s41556-018-0251-8.

Schliwa, M. Action of Cytochalasin D on Cytoskeletal Networks. J. Cell Biol. 1982, 92 (1), 79–91. https://doi.org/10.1083/jcb.92.1.79.

Schneider, D.; Xiong, Y.; Wu, D.; Hu, P.; Alabanza, L.; Steimle, B.; Mahmud, H.; Anthony-Gonda, K.; Kruger, W.; Dropulic, B. Trispecific CD19-CD20-CD22-targeting duoCAR-T cells eliminate antigen-heterogeous B cell tumors in preclinical models. Sci. Transl. Med. 2021, 13(586).

Schnell, U.; Dijk, F.; Sjollema, K. A.; Giepmans, B. N. G. Immunolabeling Artifacts and the Need for Live-Cell Imaging. Nat. Methods 2012, 9 (2), 152–158. https://doi.org/10.1038/nmeth.1855.

Schwille, P.; Haupts, U.; Maiti, S.; Webb, W. W. Molecular Dynamics in Living Cells Observed by Fluorescence Correlation Spectroscopy with One- and Two-Photon Excitation. Biophys. J. 1999, 77 (4), 2251–2265. https://doi.org/10.1016/S0006-3495(99)77065-7.

Scofield, R. H. Autoantibodies as Predictors of Disease. THE LANCET 2004, 363, 3.

Seyrantepe, V.; Canuel, M.; Carpentier, S.; Landry, K.; Durand, S.; Liang, F.; Zeng, J.; Caqueret, A.; Gravel, R. A.; Marchesini, S.; Zwingmann, C.; Michaud, J.; Morales, C. R.; Levade, T.; Pshezhetsky, A. V. Mice Deficient in Neu4 Sialidase Exhibit Abnormal Ganglioside Catabolism and Lysosomal Storage. Hum. Mol. Genet. 2008, 17 (11), 1556–1568. https://doi.org/10.1093/hmg/ddn043.

Seyrantepe, V.; Demir, S. A.; Timur, Z. K.; Von Gerichten, J.; Marsching, C.; Erdemli, E.; Oztas, E.; Takahashi, K.; Yamaguchi, K.; Ates, N.; Dönmez Demir, B.; Dalkara, T.; Erich, K.; Hopf, C.; Sandhoff, R.; Miyagi, T. Murine Sialidase Neu3 Facilitates GM2 Degradation and Bypass in Mouse Model of Tay-Sachs Disease. Exp. Neurol. 2018, 299, 26–41. https://doi.org/10.1016/j.expneurol.2017.09.012.

Seyrantepe, V.; Landry, K.; Trudel, S.; Hassan, J. A.; Morales, C. R.; Pshezhetsky, A. V. Neu4, a Novel Human Lysosomal Lumen Sialidase, Confers Normal Phenotype to Sialidosis and Galactosialidosis Cells. J. Biol. Chem. 2004, 279 (35), 37021–37029. https://doi.org/10.1074/jbc.M404531200.

Seyrantepe, V.; Poupetova, H.; Froissart, R.; Zabot, M.-T.; Maire, I.; Pshezhetsky, A. V. Molecular Pathology of NEU1 Gene in Sialidosis. Hum. Mutat. 2003, 22 (5), 343–352. https://doi.org/10.1002/humu.10268.

Sezgin, E.; Levental, I.; Mayor, S.; Eggeling, C. The Mystery of Membrane Organization: Composition, Regulation and Roles of Lipid Rafts. Nat. Rev. Mol. Cell Biol. 2017, 18 (6), 361–374. https://doi.org/10.1038/nrm.2017.16.

Sgroi, D.; Koretzky, G. A.; Stamenkovic, I. Regulation of CD45 Engagement by the B-Cell Receptor CD22. Proc. Natl. Acad. Sci. 1995, 92 (9), 4026–4030. https://doi.org/10.1073/pnas.92.9.4026.

Shao, J. Y.; Hochmuth, R. M. Mechanical Anchoring Strength of L-Selectin, B2 Integrins, and CD45 to Neutrophil Cytoskeleton and Membrane. Biophys. J. 1999, 77 (1), 587–596. https://doi.org/10.1016/S0006-3495(99)76915-8.

Shaw, A. S. Lipid Rafts: Now You See Them, Now You Don't. Nat. Immunol. 2006, 7 (11), 1139–1142. https://doi.org/10.1038/ni1405.

Shen, L.; Gao, C.; Suresh, L.; Xian, Z.; Song, N.; Chaves, L. D.; Yu, M.; Ambrus, J. L. Central Role for Marginal Zone B Cells in an Animal Model of Sjogren's Syndrome. Clin. Immunol. 2016, 168, 30–36. https://doi.org/10.1016/j.clim.2016.04.008.

Sieger, N.; Fleischer, S. J.; Mei, H. E.; Reiter, K.; Shock, A.; Burmester, G. R.; Daridon, C.; Dörner, T. CD22 Ligation Inhibits Downstream B Cell Receptor Signaling and Ca 2+ Flux upon Activation. Arthritis Rheum. 2013, 65 (3), 770–779. https://doi.org/10.1002/art.37818.

Silvestri, I.; Testa, F.; Zappasodi, R.; Cairo, C. W.; Zhang, Y.; Lupo, B.; Galli, R.; Di Nicola, M.; Venerando, B.; Tringali, C. Sialidase NEU4 Is Involved in Glioblastoma Stem Cell Survival. Cell Death Dis. 2014, 5 (8), e1381. https://doi.org/10.1038/cddis.2014.349.

Silvestri, I.; Testa, F.; Zappasodi, R.; Cairo, C. W.; Zhang, Y.; Lupo, B.; Galli, R.; Di Nicola, M.; Venerando, B.; Tringali, C. Sialidase NEU4 Is Involved in Glioblastoma Stem Cell Survival. Cell Death Dis. 2014, 5 (8), e1381–e1381. https://doi.org/10.1038/cddis.2014.349.

Simons, K.; Toomre, D. Lipid Rafts and Signal Transduction. Nat. Rev. Mol. Cell Biol. 2000, 1 (1), 31–39. https://doi.org/10.1038/35036052.

Singer, S. J.; Nicolson, G. L. The Fluid Mosaic Model of the Structure of Cell Membranes. Science 1972, 175 (4023), 720–731. https://doi.org/10.1126/science.175.4023.720.

Slaney, A. M.; Dijke, I. E.; Jeyakanthan, M.; Li, C.; Zou, L.; Plaza-Alexander, P.; Meloncelli, P. J.; Bau, J. A.; Allan, L. L.; Lowary, T. L.; West, L. J.; Cairo, C. W.; Buriak, J. M. Conjugation of A and B Blood Group Structures to Silica Microparticles for the Detection of Antigen-Specific B Cells. Bioconjug. Chem. 2016, 27 (3), 705–715. https://doi.org/10.1021/acs.bioconjchem.5b00672.

Smith, K. G. C.; Tarlinton, D. M.; Doody, G. M.; Hibbs, M. L.; Fearon, D. T. Inhibition of the B Cell by CD22: A Requirement for Lyn. J. Exp. Med. 1998, 187 (5), 807–811. https://doi.org/10.1084/jem.187.5.807.

Song, W.; Liu, C.; Upadhyaya, A. The pivotal position of the actin cytoskeleton in the initiation and regulation of B cell receptor activation. Biochim. Biophysic. Acta. 2014, 1838, 569-578.

Starr, T. E.; Thompson, N. L. Total Internal Reflection with Fluorescence Correlation Spectroscopy: Combined Surface Reaction and Solution Diffusion. Biophys. J. 2001, 80 (3), 1575–1584. https://doi.org/10.1016/S0006-3495(01)76130-9.

Steinert, P. M.; Steven, A. C.; Roop, D. R. The Molecular Biology of Intermediate Filaments. Cell 1985, 42 (2), 411–419. https://doi.org/10.1016/0092-8674(85)90098-4.

Steinkamp, J. A.; Lehnert, N. M.; Keij, J. F.; Lehnert, B. E. Enhanced Immunofluorescence Measurement Resolution of Surface Antigens on Highly Autofluorescent, Glutaraldehyde-fixed Cells Analyzed by Phase-sensitive Flow Cytometry. Cytometry. 1999, 37(4), 275-283.

Stevenson, B. R.; Begg, D. A. Concentration-Dependent Effects of Cytochalasin D on Tight Junctions and Actin FIlaments in MDCK Epithelial Cells. J. Cell Sci. 1994, 107 (3), 367–375.

Stuermer, C. A. O.; Langhorst, M. F.; Wiechers, M. F.; Legler, D. F.; Hanwehr, S. H. von; Guse, A. H.; Plattner, H. PrP c Capping in T Cells Promotes Its Association with the Lipid Raft Proteins Reggie-1 and Reggie-2 and Leads to Signal Transduction. FASEB J. 2004, 18 (14), 1731–1733. https://doi.org/10.1096/fj.04-2150fje.

Suthipintawong, C.; Vinyuvat, S. Immunostaining of Cell Preparations: a comparative evaluation of common fixatives and protocols. Diag. Cyto. 1996, 15(2), 167-174.

Tagliaferro, P.; Tandler, C. J.; Ramos, A. J.; Pecci Saavedra, J.; Brusco, A. Immunofluorescence and Glutaraldehyde Fixation. A New Procedure Based on the Schiff-Quenching Method. J. Neurosci. Methods 1997, 77 (2), 191–197. https://doi.org/10.1016/S0165-0270(97)00126-X.

Tanner, J.; Weis, J.; Fearon, D.; Whang, Y.; Kieff, E. Epstein-Barr Virus Gp350/220 Binding to the B Lymphocyte C3d Receptor Mediates Adsorption, Capping, and Endocytosis. Cell 1987, 50 (2), 203–213. https://doi.org/10.1016/0092-8674(87)90216-9.

Tedder, T. F.; Tuscano, J.; Sato, S.; Kehrl, J. H. CD22, A B LYMPHOCYTE–SPECIFIC ADHESION MOLECULE THAT REGULATES ANTIGEN RECEPTOR SIGNALING *. Annu. Rev. Immunol. 1997, 15 (1), 481–504. https://doi.org/10.1146/annurev.immunol.15.1.481.

Templin, M. F.; Stoll, D.; Schwenk, J. M.; Pötz, O.; Kramer, S.; Joos, T. O. Protein Microarrays: Promising Tools for Proteomic Research. Proteomics 2003, 3 (11), 2155–2166. https://doi.org/10.1002/pmic.200300600.

Tkachenko, E. Clustering Induces Redistribution of Syndecan-4 Core Protein into Raft Membrane Domains. J. Biol. Chem. 2002, 277(22), 19946-19951.

Tolar, P.; Hanna, J.; Krueger, P. D.; Pierce, S. K. The Constant Region of the Membrane Immunoglobulin Mediates B Cell-Receptor Clustering and Signaling in Response to Membrane Antigens. Immunity 2009, 30 (1), 44–55. https://doi.org/10.1016/j.immuni.2008.11.007.

Treanor, B. B-cell receptor: from resting state to activate. Immunol. 2012, 136, 21-27.

Treanor, B.; Depoil, D.; Gonzalez-Granja, A.; Barral, P.; Weber, M.; Dushek, O.; Bruckbauer, A.; Batista, F. D. The Membrane Skeleton Controls Diffusion Dynamics and Signaling through the B Cell Receptor. Immunity 2010, 32 (2), 187–199. https://doi.org/10.1016/j.immuni.2009.12.005.

Treanor, B.; Depoli, D.; Gonzalez-Granja, A.; Barral, P.; Weber, M.; Dushek, O.; Bruckbauer, A.; Batista, F. The Membrane Skeleton Controls Diffusion Dynamics and Signaling through the B Cell Receptor. Immunity. 2010, 32, 187-199.

Tridandapani, S.; Kelley, T.; Pradhan, M.; Cooney, D.; Justement, L. B.; Coggeshall, K. M. Recruitment and Phosphorylation of SH2-Containing Inositol Phosphatase and Shc to the B-Cell Fc Gamma Immunoreceptor Tyrosine-Based Inhibition Motif Peptide Motif. Mol. Cell. Biol. 1997, 17 (8), 4305–4311. https://doi.org/10.1128/MCB.17.8.4305.

Uchida, J.; Hamaguchi, Y.; Oliver, J. A.; Ravetch, J. V.; Poe, J. C.; Haas, K. M.; Tedder, T. F. The Innate Mononuclear Phagocyte Network Depletes B Lymphocytes through Fc Receptor–Dependent Mechanisms during Anti-CD20 Antibody Immunotherapy. J. Exp. Med. 2004, 199 (12), 1659–1669. https://doi.org/10.1084/jem.20040119.

Uchida, Y.; Tsukada, Y.; Sugimori, T. Enzymatic Properties of Neuraminidases from Arthrobacter Ureafaciens. J. Biochem. (Tokyo) 1979, 86 (5), 1573–1585. https://doi.org/10.1093/oxfordjournals.jbchem.a132675.

Uemura, T.; Shiozaki, K.; Yamaguchi, K.; Miyazaki, S.; Satomi, S.; Kato, K.; Sakuraba, H.; Miyagi, T. Contribution of Sialidase NEU1 to Suppression of Metastasis of Human Colon Cancer Cells through Desialylation of Integrin B4. 12.

Ueno, S.; Saito, S.; Wada, T.; Yamaguchi, K.; Satoh, M.; Arai, Y.; Miyagi, T. Plasma Membrane-Associated Sialidase Is Up-Regulated in Renal Cell Carcinoma and Promotes Interleukin-6-Induced Apoptosis Suppression and Cell Motility. J. Biol. Chem. 2006, 281 (12), 7756–7764. https://doi.org/10.1074/jbc.M509668200.

Varki, A. Biological Roles of Glycans. Glycobiology 2017, 27 (1), 3–49. https://doi.org/10.1093/glycob/cww086.

Vaz, W. L.; Almeida, P. F. Microscopic versus Macroscopic Diffusion in One-Component Fluid Phase Lipid Bilayer Membranes. Biophys. J. 1991, 60 (6), 1553–1554. https://doi.org/10.1016/S0006-3495(91)82190-7.

Vitrac, H.; MacLean, D. M.; Jayaraman, V.; Bogdanov, M.; Dowhan, W. Dynamic Membrane Protein Topological Switching upon Changes in Phospholipid Environment. Proc. Natl. Acad. Sci. 2015, 112 (45), 13874–13879. https://doi.org/10.1073/pnas.1512994112.

Wada, T.; Hata, K.; Yamaguchi, K.; Shiozaki, K.; Koseki, K.; Moriya, S.; Miyagi, T. A Crucial Role of Plasma Membrane-Associated Sialidase in the Survival of Human Cancer Cells. Oncogene 2007, 26 (17), 2483–2490. https://doi.org/10.1038/sj.onc.1210341.

Wakatsuki, T. Actin Polymerization and Cell Mechanics. J. Cell Sci. 2001, 114 (Pt 5), 1025–1036.

Wallrabe, H.; Elangovan, M.; Burchard, A.; Periasamy, A.; Barroso, M. Confocal FRET Microscopy to Measure Clustering of Ligand-Receptor Complexes in Endocytic Membranes. Biophys. J. 2003, 85 (1), 559–571. https://doi.org/10.1016/S0006-3495(03)74500-7.

Wan, C.; Kiessling, V.; Tamm, L. K. Coupling of Cholesterol-Rich Lipid Phases in Asymmetric Bilayers. Biochemistry 2008, 47 (7), 2190–2198. https://doi.org/10.1021/bi7021552.

Wan, Z.; Liu, W. The Growth of B Cell Receptor Microcluster Is a Universal Response of B Cells Encountering Antigens with Different Motion Features. Protein Cell 2012, 3, 545–558.

Wang, D.; Zaitsev, S.; Taylor, G.; d'Azzo, A.; Bonten, E. Protective Protein/Cathepsin A Rescues N-Glycosylation Defects in Neuraminidase-1. Biochim. Biophys. Acta BBA - Gen. Subj. 2009, 1790 (4), 275–282. https://doi.org/10.1016/j.bbagen.2009.01.006.

Wang, Y. Sialidases From Clostridium Perfringens and Their Inhibitors. Front. Cell. Infect. Microbiol. 2020, 9 (462), 11. https://doi.org/0.3389/fcimb.2019.00462.

Wang, Y.; Yamaguchi, K.; Shimada, Y.; Zhao, X. J.; Miyagi, T. Site-Directed Mutagenesis of Human Membrane-Associated Ganglioside Sialidase - Identification of Amino-Acid Residues Contributing to Substrate Specificity. Eur. J. Biochem. 2001, 268 (8), 2201–2208.

Wasim, L.; Buhari, F. H. M.; Yoganatha, M.; Sicard, T.; Ereno-Orbea, J.; Julien, J-P.; Treanor, B. N-Linked Glycosylation Regulates CD22 Organization and Function. Front. Immunol. 2019, 10(699).

Wasim, L.; Buhari, F. H. M.; Yoganathan, M.; Sicard, T.; Ereño-Orbea, J.; Julien, J. P.; Treanor, B. N-Linked Glycosylation Regulates CD22 Organization and Function. Front. Immunol. 2019, 10 (APR), 1–16. https://doi.org/10.3389/fimmu.2019.00699.

Wasim, L.; Buhari, F. H. M.; Yoganathan, M.; Sicard, T.; Ereno-Orbea, J.; Julien, J.; Treanor, B. N-Linked Glycosylation Regulates CD22 Organization and Function. Front. in Immunol. 2019, 699(10).

Wasim, L.; Buhari, F. H. M.; Yoganathan, M.; Sicard, T.; Ereño-Orbea, J.; Julien, J.-P.; Treanor, B. N-Linked Glycosylation Regulates CD22 Organization and Function. Front. Immunol. 2019, 10, 699. https://doi.org/10.3389/fimmu.2019.00699.

West, L. J.; Cardella, C. J. ABO-Incompatible Heart Transplantation in Infants. N. Engl. J. Med. 2001, 344 (11), 793–800.

Wilson, T. Resolution and Optical Sectioning in the Confocal Microscope: PROPERTIES OF THE FLUORESCENT CONFOCAL MICROSCOPE. J. Microsc. 2011, 244 (2), 113–121. https://doi.org/10.1111/j.1365-2818.2011.03549.x.

Wu, Y.; Eghbali, M.; Ou, J.; Lu, R.; Toro, L.; Stefani, E. Quantitative Determination of Spatial Protein-Protein Correlations in Fluorescence Confocal Microscopy. Biophys. J. 2010, 98 (3), 493–504. https://doi.org/10.1016/j.bpj.2009.10.037.

Wu, Y.; Li, Q.; Chen, X. Z. Detecting Protein-Protein Interactions by Far Western Blotting. Nat. Protoc. 2007, 2 (12), 3278–3284. https://doi.org/10.1038/nprot.2007.459.

Yamaguchi, K.; Hata, K.; Koseki, K.; Shiozaki, K.; Akita, H.; Wada, T.; Moriya, S.; Miyagi, T. Evidence for Mitochondrial Localization of a Novel Human Sialidase (NEU4). Biochem. J. 2005, 390 (1), 85–93. https://doi.org/10.1042/BJ20050017.

Yamaguchi, K.; Koseki, K.; Shiozaki, M.; Shimada, Y.; Wada, T.; Miyagi, T. Regulation of Plasma-Membrane-Associated Sialidase NEU3 Gene by Sp1/Sp3 Transcription Factors. Biochem. J. 2010, 430 (1), 107–117. https://doi.org/10.1042/BJ20100350.

Yamanami, H.; Shiozaki, K.; Wada, T.; Yamaguchi, K.; Uemura, T.; Kakugawa, Y.; Hujiya, T.; Miyagi, T. Down-Regulation of Sialidase NEU4 May Contribute to Invasive Properties of Human Colon Cancers. Cancer Sci. 2007, 98 (3), 299–307. https://doi.org/10.1111/j.1349-7006.2007.00403.x.

Yang, S.-T.; Kreutzberger, A. J. B.; Lee, J.; Kiessling, V.; Tamm, L. K. The Role of Cholesterol in Membrane Fusion. Chem. Phys. Lipids 2016, 199, 136–143. https://doi.org/10.1016/j.chemphyslip.2016.05.003.

Yang, Z.; Puffer, E. B.; Pontrello, J. K.; Kiessling, L. L. Synthesis of a multivalent display of a CD22-binding trisaccharide. Carbohydr. Res. 2002, 337, 1605-1613.

Yavin, E.; Yavin, Z. ATTACHMENT AND CULTURE OF DISSOCIATED CELLS FROM RAT EMBRYO CEREBRAL HEMISPHERES ON POLYLYSINE-COATED SURFACE. J. Cell Biol. 1974, 62 (2), 540–546. https://doi.org/10.1083/jcb.62.2.540.

Yi, J.; Balagopalan, L.; Nguyen, T.; McIntire, K. M.; Samelson, L. E. TCR microclusters form spatially segregated domains and sequentially assemble in calcium- dependent kinetic steps. Nat. Comm. 2019, 10(277).

Yogalingam, G.; Bonten, E. J.; van de Vlekkert, D.; Hu, H.; Moshiach, S.; Connell, S. A.; d'Azzo, A. Neuraminidase 1 Is a Negative Regulator of Lysosomal Exocytosis. Dev. Cell 2008, 15 (1), 74–86. https://doi.org/10.1016/j.devcel.2008.05.005.

Yurasov, S.; Wardemann, H.; Hammersen, J.; Tsuiji, M.; Meffre, E.; Pascual, V.; Nussenzweig, M. C. Defective B Cell Tolerance Checkpoints in Systemic Lupus Erythematosus. J. Exp. Med. 2005, 201 (5), 703–711. https://doi.org/10.1084/jem.20042251.

Zhang, M. Cell Surface Sialic Acids Do Not Affect Primary CD22 Interactions with CD45 and Surface IgM nor the Rate of Constitutive CD22 Endocytosis. Glycobiology 2004, 14 (11), 939–949. https://doi.org/10.1093/glycob/cwh126.

Zhang, M.; Moran, M.; Round, J.; Low, T. A.; Patel, V. P.; Tomassian, T.; Hernandez, J. D.; Miceli, M. C. CD45 Signals Outside of Lipid Rafts to Promote ERK Activation, Synaptic Raft Clustering, and IL-2 Production. J. Immunol. 2005, 174 (3), 1479–1490. https://doi.org/10.4049/jimmunol.174.3.1479.

Zhou, X.-Y.; Willemsen, R.; Berry, G. T.; Strisciuglio, P.; Andria, G. Molecular and Biochemical Analysis of Protective Protein/Cathepsin A Mutations: Correlation with Clinical Severity in Galactosialidosis. 11.